Identification of novel therapeutic strtegies for Uveal Melanoma

Nabil Amirouchene-Angelozzi

UNIVERSITÉ PARIS-SUD

ÉCOLE DOCTORALE 418 :
DE CANCÉROLOGIE

Laboratoire : *Departement de transfertde l'Insitut Curie*
Équipe : Biophenics

THÈSE DE DOCTORAT

Aspects moléculaires et cellulaires de la biologie

par

Nabil AMIROUCHENE ANGELOZZI

Identification of novel therapeutic strategies in Uveal Melanoma

Date de soutenance : 26/11/2014

<u>Composition du jury</u> :

Directeur de thèse :	Sergio ROMAN ROMAN	PhD,HDR (DEpt. de transfert, Institut Curie, Paris)
Rapporteurs :	Fréderic MOURIAX	PU/PH (Dept ; d'Ophtalmologie CHU Rennes)
	Gérard MILANO	DR1 (Centre Antoine lacassagne, Nice)
Examinateurs :	Eric RAYMOND	PU/PH (CHUV,Lausanne, Suisse)
	Jean-Yves PIERGA	PU/PH (Dept. d'Oncologie, Institut Curie, Paris)
	Salem CHOUAIB	DR1 (UMR753, Institut Gustave Roussy, Villejuif)

Acknowledgements

This PhD had been a wonderful experience. I would like to thank the persons that made it possible.

The one who gave me the possibility to spend these 3 years in Paris and in Curie: Sergio, my thesis director, an exceptional person from a professional and human point of view, and Pr. F. Doz.

The members of the jury, who accepted the task of reading my manuscript: the “rapporteurs” Frédéric Mouriaux and Gérard Milano who accepted to review my work and come to Paris for my discussion, Salem Chouaib, Eric Raymond and Jean-Yves Pierga who accepted to be my “examinateurs”.

All the persons in the “Departement de transfert” of Institut Curie, in particular Fariba Nemati, who offered me constant support during working week-ends, Virginie Maire and Lynda Latreche whose friendship resulted also in important technical support for my thesis, Marie Schoumacher whose contributions had been essential for the second part of my project, the Affymetrix group for their precious help, all the members of the BCBG-RPPA and Biophenics team for providing me with company and support, Marc- Henri Stern, Olivier Lantz, Sophie Piperno-Neumann and the other clinicians and researchers of the Uveal Melanoma Group of Curie, who became the audience of my lab meetings, Dominique Gallier, one of the pillars of the department, Didier Decaudin and the LIP team who contributed to my thesis, and all the friends I met in the Institute, an essential and unforgettable component of my parisian life.

Foreword

Uveal Melanoma is a rare tumor; about half of the patients develop metastasic disease and are referred to specialized centers for treatment.

Unfortunately no therapy has yet been identified which can prolong survival in the metastatic setting.

During my PhD I aimed to establish preclinical models that reflect the molecular characteristics of this disease. Using these models I searched for therapeutic approaches that could guide clinical trials towards effective treatment for advanced Uveal Melanoma.

This manuscript starts with an introduction to Uveal Melanoma in which I underline the necessity of cellular models correspondent to our latest understanding of the disease and I present the treatment options currently proposed or under preclinical and clinical evaluation. Results are described in two sections : in the first a paper is presented describing the establishment of new, relevant, cell lines and showing the efficacy of mTOR inhibitor Everolimus in relevant preclinical models; the second section contains a manuscript which describes a drug association screening that led to the identification of the combination of Everolimus with PI3K inhibitor GDC0941 as a promising strategy to induce apoptotic death in a class of Uveal Melanomas. A chapter containing conclusions and future perspectives terminates the thesis. In the Appendix I included the paper presented in the first part of the Results in its original format as it was published in *Molecular Oncology.*

Abbreviations

ABL	Abelson murine leukemia viral oncogene homolog 1
ATCC	American Type Culture Collection
aCGH	Array Comparative Genome Hybridisation
AKT	Protein kinase B
AMOT	Angiomotin
EMBL-EBI	European Searchable tumor line database and cell bank
BAP1	RCA1 associated protein 1
BRAF	v-Raf murine sarcoma viral oncogene homolog B
BRCA2	Breast Cancer Type 1 susceptibility protein
CDKN2A	Cyclin-dependent kinase inhibitor 2A
CXCR4	Chemokine receptor type 4
DAPK	Death-associated protein kinase 1
DDEF1	Development and differentiation enhancing factor 1
EGFR	Epidermal growth factor receptor
EF1AX	Eukaryotic translation initiation factor 1A
EFS	Embryonal Fyn-associated substrate
EGFP	Enhanced green fluorescent protein
EMEA	European Medicines Agency
ERK	Extracellular signal-regulated kinase
FBS	Fetal bovine Serum
GNAQ	Guanine nucleotide binding protein (G protein), q polypeptide
GNA11	Guanine nucleotide binding protein (G protein), alpha 11 (Gq class)
HRAS	Harvey rat sarcoma viral oncoprotein homolog
HCF1	Host Cell Factor 1
HGF	Hepatocyte growth factor
HSP90	Heat shock protein 90

Abbreviations

hTERT	Human telomerase reverse transcriptase
IGF-1R	Insulin-like growth factor 1 receptor
IGF2	Insulin-like growth factor 2
INK4a	Cyclin Dependent Kinase inhibitor 4a
IRS	Insulin receptor substrates
JNK	c-Jun NH(2)-terminal kinase
KIT	v-kit Hardy-Zuckerman 4 feline sarcoma viral oncogene homolog
KRAS	Kirsten rat sarcoma viral oncogene homolog
LOH	Loss of heterozygosity
LZTS1	Leucine zipper, putative tumor suppressor 1
MAPK	Mitogen Activated Protein Kinase
MEK	Mitogen-Activated Protein Kinase Kinase Kinase , E3 Ubiquitin Protein
MGMT	O-6-methylguanine-DNA methyltransferase
MITF	Licrophtlmia-associated transcriptor factor
MYC	Avian Myelocytomatosis Viral Oncogene homolog
mTOR	Lammalian target of Rapamycin
NBS1	Nijmegen breakage syndrome1
NEUROG1	Neurogenin 1
NF1	Nerofibromin 1
NF-kB	Nuclear factor kB
PDGFR	Platelet-derived growth factor receptor beta
PDX	Patient Derived Xenograft
PKC	Phospholipase C
PI3K	Phosphatidylinositol-4,5-bisphosphate 3-kinase
PIP 2	Posphatidyllinositol (1,4)bis-phosphate
PIP 3	Posphatidylinositol (1,4,5)tris- phosphate

Abbreviations

PLC	Phospholipase C
PPP	Picrpopdophyllin
PR-DUB	Polycomb repressive deubiquitinase complex
PTEN	Phosphatase and tensin homolog
RAC	Ras-Related C3 Botulinum Toxin Substrate
RAF	Rapidly accelerated fibrosarcoma
RARB	Retinoic acid receptor, beta
RASEF	RAS and EF-hand domain containing
RASSF1A	Ras-association domain 1a
RHO	Rhodopsin
SF3B1	Splicing factor 3b, subunit 1
SCF	Stem cell factor
SMADD	Small mother against decapentaplegic
TAZ	Tafazzin
TEAD	TEA Domain Family Member 1 (SV40 Transcriptional Enhancer Factor)
TIMP3	TIMP metallopeptidase inhibitor 3
TRIO	Trio Rho guanine nucleotide exchange factor
UM	Uveal Melanoma
US	United states of America
YAP	Yes-associated protein 1

Table of contents

Table of contents

Table of contents

Table of contents

INTRODUCTION

A MELANOMA OF THE EYE

Uveal Melanoma, a primary malignant tumor of the eye has progressively been recognized as a unique pathological entity, quite different, from a clinical and biological point of view, from its cutaneous counterpart, skin Melanoma. The aim of this research thesis is to propose novel therapeutic strategies based on new preclinical models corresponding to our latest comprehensive knowledge of the disease.

I. EPIDEMIOLOGY OF UVEAL MELANOMA

1. Uveal melanoma is a rare cancer

Uveal Melanoma (UM) is a malignant tumor that arises from resident melanocytes of the Uvea, a pigmented vascular layer situated in the eye between sclera and retina.

It is the most frequent primary intraocular malignant tumor in adults and it accounts for 3% of all melanoma cases. Its age-adjusted incidence of 5 new cases per million per year (according to the american Surveillance, Epidemiology and End Results Database) has remained unchanged in the past 30 years (Singh and Topham, 2003; Singh et al., 2011). A similar incidence was obtained in European studies, where a country-related variation was reported (from a minimum of 2 per million in Spain and southern Italy to up to 8 per million in Norway and Denmark) (Virgili et al., 2007); this would suggest that fair-skinned subjects have a much higher risk of developing the disease than dark-skinned ones (Mouratova, 2012). Accordingly, ethnic variations in the annual age-adjusted incidence for UM were reported in the USA where 0,31 cases per million were accounted for Blacks; 0,38 for Asians; 1,67 for Hispanics and 6,02 for non-Hispanic Caucasians (Hu et al., 2005).

UM is usually diagnosed during the sixth decade of life (Papastefanou and Cohen, 2011). The most common site of primary tumors is the choroid (73.7-87,37 percent of cases), while ciliary body and iris are less frequently affected (13,2-21,1% and 2,3-5,3% respectively) (Mouratova, 2012).

Gender ratio approximates 1:1 with a slight increased prevalence of males in a series of reports (Desjardins et al., 2006; Mouratova, 2012; Singh and Topham, 2003).

2. Risk factors

No environmental risk factor/exposure has been identified so far, rendering prevention through large-scale screening impossible. A correlation between the incidence of the disease and the ethnicity or the geographical origin of the cases is suggested from epidemiological studies. Moreover, a meta-analysis on host susceptibility factors in UM has identified light eye color, fair skin color and ability to tan as statistically significant risk factors (Weis E et al., 2006). No clear evidence was found that proved sunlight or occupational exposure to be a risk factor for the developement of the disease, as it is in the case of cutaneous melanoma (Guénel et al., 2001; Lutz et al., 2005; Singh et al., 2004). Moreover, recent whole exome sequencing analysis failed to show any UV-induced DNA damage “signature”, which excludes sun exposure as a risk factor (Furney et al., 2013).

Beside environmental aspects, genetic alterations have been correlated with an increased risk of developing the disease in the context of familial cancer syndromes. However, they are estimated to represent only 0,6% of all UMs (Singh et al., 1996). UM has been reported to occur in the context of Xeroderma pigmentosa, Li-Fraumeni syndrome, familial breast and ovarian cancer, familial atypical mole and melanoma syndrome (van et al., 2013). Nevi of Ota are also risk factors (Singh et al., 1998) and germline mutations of the protein BAP1 (BRCA1 associated protein 1) had been recently identified in families displaying UM in the context of hereditary cancer syndromes (Abdel-Rahman et al., 2011). Studies discussing the occurrence of mutations in the CDKN2A locus and BRCA2 gene are quite controversial, probably suggesting a marginal role of these mutations in familial UM (Buecher et al., 2010; Goldstein et al., 2006; Soufir et al., 2000).

II. NATURAL HISTORY

1. Primary tumor

The Uvea is a highly pigmented layer because of the abundance of resident differentiated melanocytes derived from neural crest progenitors (fig.1). Even if melanocytes are fully differentiated cells, proliferation of melanocytes may still occur and results in benign neoplasms (uveal nevi) or in malignant melanoma. As for cutaneous melanoma, there is clinical and histopathological evidence suggesting that UM arises both from pre-existing and de novo nevi (Harbour et al., 2004; Singh et al., 2005a; Smith et al., 2007).

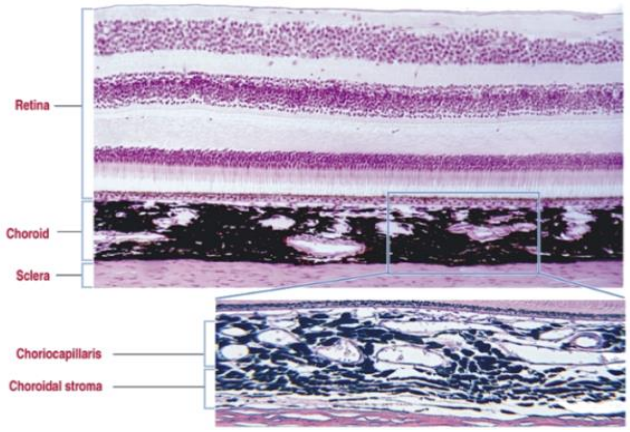

Figure 1. Picture of a human choroid showing the enrichment for melanocytes and the well developed network of blood vessels (choriocapillaris) (Adapted from Krierszenbaum and Tres; Histology and Cell Biology).

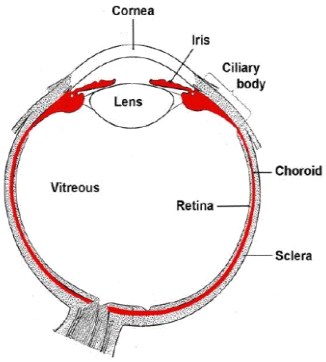

Figure 2. The 3 anatomical part of the Uvea (in red) (from Dan-Ning Hu; pathobiology of the Uveal tract)

Since the uvea can be anatomically divided into iris (the anterior part), the ciliary body, and choroid (posterior) (fig.2), UM can be classified into iris, ciliary body and choroidal UM.

UM grows initially with a discoid shape. According to its location, it might acquire a hemispheric shape, and obliterate the choriocapillaris. Because of the higher physical compliance of the inner part of the eye, UM invades the retina inward (choroidal melanomas) and spreads into the subretinal space with a collar button shape or mushroom configuration (for bigger tumors) (fig.3). Invasive tumors might also affect the lens and penetrate the posterior chamber (anterior tumors), leading to possible secondary glaucoma. Scleral infiltration is also quite frequent, with 30% of tumors presenting

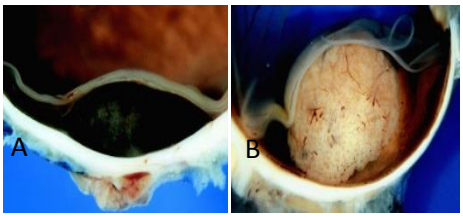

Figure 3. Highly pigmented Uveal melanoma with a discoid shape (A). Amelanotic Uveal Melanoma with a mushroom appearance (B) (from Ralph EJ; Intraocular tumors in adults)

invasion along ciliary vessels, the vortex veins and the ciliary nerves. Patterns of diffuse growth on the uvea plane or with circumferential spread along the iris root is reported in 5% of the cases.

2. Metastatic UM

The uveal tract is highly vascularized (fig.1), as a consequence of its primary function as a supplier for nutrition to the adjacent neuroepithelium and sclera and its lack of linfatic drainage. Hematogenous spread is thus the mechanism for metastatic dissemination.

Micrometastatic disease is thought to be present already at the time of diagnosis, as the different treatments for primary tumors show quite similar outcomes.

The liver is the most common affected organ (89%), lung and with decreasing frequencies bone, skin and lymph nodes might also be a site of metastatic spreading. Rare cases of metastatic disease in the central nervous system, adrenal gland, heart, kidney, spleen, colon and pancreas are also reported (Mouratova, 2012).

The reasons for the hepatic tropism of UM cells is still under debate. Different studies underlined the importance of HGF/c-Met signalling (Surriga et al., 2013a; Wu et al., 2012a), but also of the pathways downstream the receptors EGFR (Epidermal growth factor receptor), IGF-1R (Insulin-like growth factor 1 receptor) and CXCR4 (Chemokine receptor type 4) (Bakalian et al., 2008). Postmortem studies on the liver of patients with UM identified foci of nonproliferative and avascular micrometastasis (Borthwick et al., 2011; Grossniklaus HE, 2013), suggesting that UM cells might remain dormant and might respond to stimuli from the hepatic microenvironment to progress into clinically evident disease.

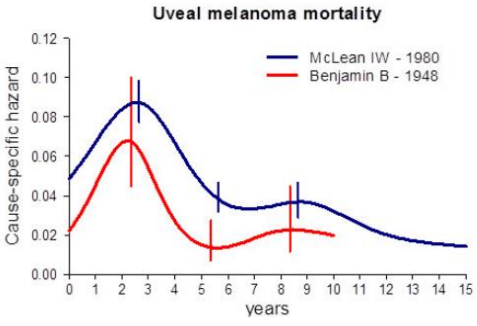

Figure 4. Bimodal mortality distribution as demonstrated in a meta-anlysis of different datasets might suggest the presence of two biologically distinct subtypes of metastatic UM (Demicheli et al., 2014).

Interestingly, a bimodal pattern of metastatic disease progression is suggested by the bimodal distribution of mortality (Demicheli et al., 2014) which presents a main peak 2-3 years after primary treatment and a second peak at about 8-9 years. These distributions

might correspond to two biologically distinct entities, one subtype UM metastasis with a rapidly course and one subtype with a slowler progressive evolution (fig.4).

3. The rapid evolution of metastatic disease is still unchallenged

Primary tumors are successfully treated with surgery and radiotherapy: local control is higher than 90% at five years with plaque radiotherapy (Desjardins et al., 2003), proton beam (Caujolle et al., 2013; Munzenrider et al., 1989) and enucleation (Diener-West et al., 2001; Sanke et al., 1981).

On the contrary, the 5-year mortality ranges between 16% and 53% depending on the size of the tumor (Singh et al., 2005b) and this is mainly due to distant recurrences. About 90% of the diagnosis of metastatic disease are made within 15 years after enucleation with a peak in the second and third year (Zimmerman et al., 1978). A study from Kujala and colleagues reports a cumulative incidence of patients developing metastases of 31% in 5 years, 45% of patients in 15 years, 50% in 25 years and 52% within 35 years (Kujala et al., 2003). The death rate following a report of melanoma metastasis is 80% at 1 year and 92% at 2 year (Singh and Borden, 2005). As a consequence, the median survival with metastatic disease is short: 2-6 months (Diener-West et al., 1992), while it rises at 19-28 months when the disease does not involve the liver (Woodman, 2012). This fact has not been significantly impacted up to now by medical treatment.

III. HISTOLOGICAL FEATURES

Histologically, under the standard Hematoxylin and Eosin staining, three types of primary or metastatic uveal melanoma are defined: (1) tumors with predominant spindle cell (with two subtypes A and B), (2) with predominant epithelioid cells and (3) with a mixt component of spindle and epithelioid cells. Spindle cells are characterized by elongated nuclei, finely dispersed chromatin and indistinct nucleoli (subtype A) or prominent nucleoli (subtype B). Epithelioid cells are large cells with round or polygonal shapes, large pleomorphic nuclei and prominent eosinophilic nucleoli. These cells, considered as poorly differentiated melanocytes, are sometimes flanked

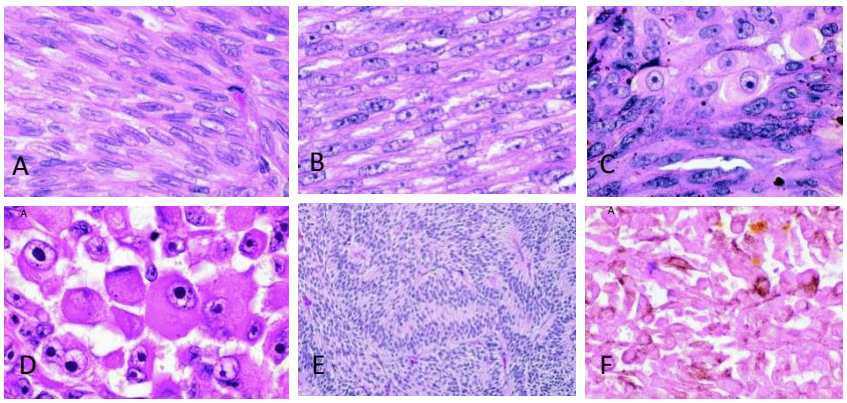

Figure 5. **The Callender classification of UM**: spindle cell subtype A (A), spindle cell subtype B (B) mixed (C), epithelioid (D) fasciular (E) and necrotic (F) subtypes (from from Ralph EJ; Intraocular tumors in adults).

by giant anaplastic tumor cells which may display a small-cell appearance (Fig. 5 A-D). UMs are classified as epithelioid (5% of the cases) when more than 50% of cells have an epithelioid appearance and classified as mixed cells when the epithelioid component accounts for less than 50% of the tumoral cells. About 30% of intraocular tumors UM are of the spindle cell type. This classification, proposed by MCLean and modified by Callender (McLean et al., 1983, 2004), originally included also a necrotic and a fascicular variants (fig.5 E,F). It has been highly regarded for its prognostic value: tumors exclusively composed of spindle cells have a better outcome than tumors with a component of epithelioid cells (Shields and Shields, 2008).

Another histologic characteristic often reported in UMs is the low mitotic index (fig.6). Some studies have reported a lower proliferation rate in tumors of the spindle cell type (in which the rate of cells in G2/M/S is 1,9-4,5%), than in tumors of the epithelioid or mixed type (proliferation rate 5,5-8,4%) (Hodge et al., 1995; Rennie et al., 1989). Therefore mitotic/proliferative index has been regarded as a prognostic factor (Gass, 1985; Karlsson et al., 1996; Lattman et al., 1995).

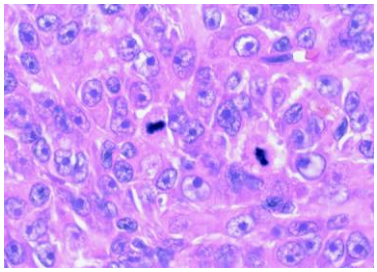

Figure 6. Paucity of Mitosis in UM histologic specimens (from from Ralph EJ; Intraocular tumors in adults).

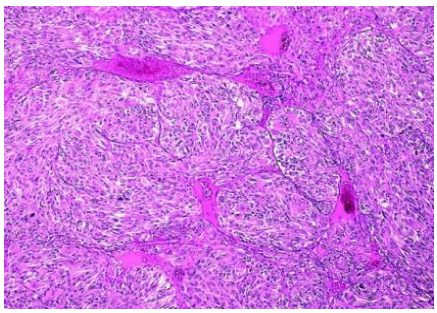

Figure 7. The presence of vascular loops has also been accounted as negative prognostic factor (from from Ralph EJ; Intraocular tumors in adults).

Another morphological criteria associated with survival is the nucleolar size (Gamel et al., 1982; Huntington et al., 1989). However, this parameter did not enter in daily practice because of its insufficient inter-observers reproducibility. Microvascular patterns characterized by back to back vascular

loops was also regarded as factor associated with metastatic spread (Folberg et al., 1993) although not as significant as the other histological criteria (McLean et al., 1997).

The density of the lymphocytic infiltrate might also be correlated with metastatic dissemination and poor outcome (De la Cruz et al., 1990; Whelchel et al., 1993).

These different morphological parameters have been combined with tumor size (width and thickness) (Shields et al., 2009) and scleral extension/local invasion (McLean et al., 1997; Mooy et al., 1995; Seddon et al., 1983) to constitute an histoprognostic index.

IV. MOLECULAR BIOLOGY OF UM

1. Cytogenetics

Genetic studies on frequent chromosomal alterations in Uveal Melanoma began in the early nineties following analogous studies carried on cutaneous Melanoma (Becher et al., 1983). Confirming early data concerning single case reports (Griffin et al., 1988; Horsman et al., 1990), Prescher and colleagues reported frequent non-random aberrations in primary UM involving **chromosome 3** in **43-65%** of cases (Prescher et al., 1990). Usually the entire copy of the chromosome is lost , in 5-10% of the cases a duplication of the remaining copy occur (**isodisomy**)(Aalto et al., 2001; Scholes et al., 2001); less frequently **partial deletions** occur (Diener-West et al., 2004). Monosomy of chromosome 3 was soon correlated with reduced survival by Presher and collegues, who showed that 57% of patients bearing tumors with monosomy 3 developed metastatic disease for a median follow up of 3,4 years while a control group bearing UMs disomic for chromosome 3 remained metastasis-free. Monosomy 3 also relates to histopathological parameters such as epitheliod cytology and ciliary body involvement (Prescher et al., 1995, 1995).

Loss of the entire chromosome 3 or of a part or the full short arm of it appears to be an early event in tumorigenesis of UM, since this aberration is usually found in all neoplastic cells (Prescher et al., 1990). A correlation with aberrations in chromosome

8 (gain of 8q) have also been assessed by cytogenetic studies (Prescher et al., 1995)

Numerous analysis have been performed in order to find a putative tumor suppressor gene whose inactivation could correlate with LOH (Loss of heterozygosity) of chromosome 3 (Blasi et al., 1999; Kilic et al., 2005; Scholes et al., 2001; Sisley et al., 1993; Tschentscher et al., 2001). Only recently, with an approach of high throughput sequencing of the whole chromosome 3 in tumors characterized by monosomy 3 the group of A. Bowcock was able to identify somatic mutations of the protein BAP1 as recurrent mutation in UM with monosomy 3 (Harbour et al., 2010).

Another recurrent chromosomal aberration in UM involves the **chromosome 8,** in 40-55% of cases. More frequently a **gain** of **8q** or an isochromosome 8q (associated with loss of 8p) are found, gain of the entire chromosome 8 are less frequently reported. Gain of 8q had also been showed to be an independent predictor of survival (Sisley et al., 1997). Indeed a study by Kilic et al. reported a loss of statistical significance after correction of the correlation for confounding variables, such as vascular pattern, cell type and 3p or 3q loss (Kilic et al., 2006). As for monosomy 3 gain of 8q correlates with ciliary body involvement (Sisley et al., 2000), and the two anomalies are often seen togather (Aalto et al., 2001; Horsman and White, 1993).

Indeed gain of 8q in tumors with concomitant loss of chromosome 3 seems to hold an important role in tumor progression, but appers to be secondary to the loss of chromosome 3, as subclones with different pattern of aberration of chromosome 8 were found in tumors with monosomy 3 (Prescher et al., 1994).

Copy number gain in the long arm of chromosome 8 might possibly influence UM growth through the overexpression of genes such as MYC (situated on 8q24), NBS1(8q21) whose expression was reported to correlate with cytologic severity and survival (Ehlers and Harbour, 2005), DDEF1, which was found to be overexpressed in UM with gain 8q and to increase motility in low-grade UM, (Ehlers et al., 2005), while a potential metastasis suppressor gene situated on the short arm of chromosome 8, LZTS1, was reported by the group of Harbour (Onken et al., 2008a).

Anomalies of **chromosome 6** (**gain** in **6p** and/or **loss** on **6q**) were recorded in 28-44% of samples (Prescher et al., 1990; Singh et al., 1994; Sisley et al., 1992). Loss

of 6p had been associated with low risk of developement of metastasis (White et al., 1998a) while loss of 6q was associated with poor overall survival. Aalto et al. found a strong enrichment of 6q gain in metastasizing tumors and metastasis compared to non metastasizing primary tumors (83%,40% and 7% respectively), while gain of 6p is more prevalent among low-risk tumors compared to metastasizing ones and to metastasis (29%,20%,17% respectively) (Aalto et al., 2001). Rearrangements of chromosome 6 are found more frequently in choroidal melanomas, and gain of 6p is relatively exclusive with monosomy 3 while it is associated with alterations of 8q, and probabely precedes it, as suggested by Parrella et al. on the basis of the strong association of 6p alterations with the other two anomalies (Parrella et al., 1999). Moreovoer loss of 6p is suggested to represent a separate branch of an evolutionary bifurcation in UM: tumors could progress towards a high metastatising phenotype characterized by LOH of chromosome 3 or to a more indolent type of metastasizing tumor characterized by alterations of chromosome 6 (Ehlers et al., 2008; McCannel TA et al., 2010; Parrella et al., 1999).

Approximately 30% of UM present **loss of 1p** and/or gain of 1q; in the analysis of Aalto et al. both anomalies were enriched in tumor metastasis and metastasizing tumors, and loss of 1p has been suggested to be a marker of worse prognosis (Trolet et al., 2009), however loss of 1p was not showed to be an independent marker of survival and it is not usually taken into account in DNA-based prognostic algorithms (Cassoux et al., 2014; Kilic et al., 2006).

Alterations on chromosome 9 (loss of 9p), loss of chromosome 10, loss of 11q23, gain in chromosome 7 and loss of 16q as well as loss of one the sexual chromosomes in 35-50% of cases have also been reported but lower frequencies and the absence of a clear correlation with prognosis and biological behaviour limited further analysis (Horsman and White, 1993; Horsthemke et al., 1992; Parrella et al., 1999; Prescher et al., 1990; Scholes et al., 2001; Sisley et al., 1992, 2000; Wiltshire et al., 1993).

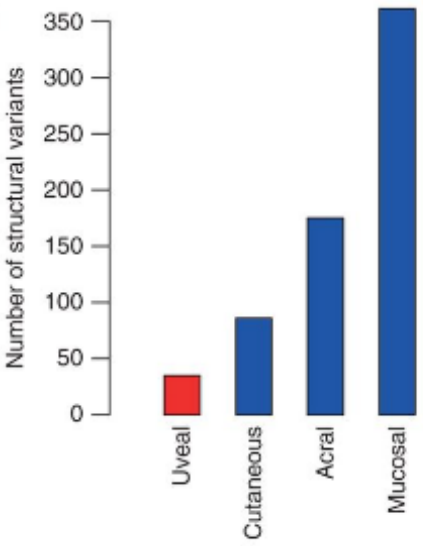

Figure 8. comparison of somatic structural variation in uveal, cutaneous, acral, and mucosal melanoma subtypes (Furney et al., 2013)

Finally it appears that UM is characterized by a low level of chromosomal instability compared to other tumors such as breast tumors (Papadopoulos et al., 2002) or other types of melanomas (Furney et al., 2013) (fig.8), which presumes mantainance of good regulation of mitosis during tumorigenesis.

Studies that aimed to compare chromosomal changes in high-risk primary tumors and metastasis are quite rare but it appears that the number of chromosomal alterations as well as the gross pattern of rearrangements remains the same during disease progression (Aalto et al., 2001; Singh et al., 2009).

2. Mutations

2.1 UM mutational status compared to cutaneous melanoma

Initial assessment of mutational status in Uveal Melanoma tumors followed again the path traced for Cutaneous Melanoma. N-Ras mutations are shown not to play a role in pathogenesis of Uveal Melanoma (Mooy et al., 1991). **HRas** and **Kras** were found to be **wild type** in Uveal Melanoma series (Soparker et al., 1993). **B-Raf** mutations is not a recurrent event in Uveal Melanoma either: reports on uveal melanomas harboring Braf **mutations** are **sporadical** (Malaponte et al., 2006), and the absence of BRaf mutations found in many tumor series suggests that BRaf mutations may arise sporadically in small distinct subgroups of uveal melanoma, such as iris melanomas (Hriquez et al., 2007) or in small subclones (Maat et al., 2008a). Therefore, they do not play a role in the vast majority of cases (Edmunds et al., 2003).

Mutations in p53 are an uncommon event (Kishore et al., 1996). Microdeletions of CDKN2A locus or promoter methylation are reported to increase the frequencies of inactivation of the locus (Merbs and Sidransky, 1999; van der Velden et al., 2001; Wang et al., 1996). However, recent studies are quite discordant on the role of

CDKN2A inactivations in UM (Edmunds et al., 2002; Lamperska et al., 2002). Finally, occasional mutations in NF1 have also been reported (Foster et al., 2003).

2.2 Identification of GNAQ/11 mutations

An approach of high throughput screening for new putative oncogenes in mice melanocytes (Van Raamsdonk et al., 2004) identified mutations in the **GNAQ** or **GNA11** genes as in the majority of UM, with a frequency of **83-96%** (Onken et al., 2008b; Piperno-Neumann et al., 2014a; Van Raamsdonk et al., 2008, 2010).

GNAQ and GNA11 encode members of the Gαq family of heterotrimeric G protein α, subunits of G proteins that mediate the cellular response to extracellular stimuli via interaction with membrane receptors (G protein coupled receptors). Mutations in GNAQ and GNA11 occur in a mutually exclusive manner at arginine 183 (**R183**) or glutamine 209 (**Q209**) and constitutively activate downstream signaling pathways. From a recent review of COSMIC database, this appear to be the case in approximately 5-6% of sequenced cancers (O'Hayre et al., 2013). High frequencies are found in eye melanomas, leptomeningeal melanocytic lesions (60%) and in a subset of skin melanomas (6%), while in other tumors such mutations are quite sporadical. Therefore, GNAQ and GNA11 mutations are thought to be driver mutations in melanocytic lesions and to occur early in UM. Indeed, mutations in these proteins had been found in most blue nevi of the skin (83%) (Van Raamsdonk et al., 2008), implying that these lesions might not be sufficient for malignant progression in UM. This hypothesis is supported by the fact that stable transfection of mutated GNAQ into normal melanocytes is not sufficient to transform cells (Van Raamsdonk et al., 2008).

Mutations in GNAQ are enriched in blue nevi (54,7%) and primary UMs (44,7%) compared to UM metastasis (21,7%), while GNA11 mutations are more prevalent in metastases (56,5%) compared to primary tumors and blue nevi (31,9% and 16,7% respectively) (Van Raamsdonk et al., 2010), an observation confirmed by Dono et al. (Dono et al., 2014). However, no significative correlation between GNA mutational status and patient survival has been proved (Koopmans et al., 2013; Van Raamsdonk et al., 2010). Studies to elucidate differences between GNAQ and

GNA11 roles are made difficult by the absence of selective pharmacological compounds targeting each type of Gαq mutation. Therefore, no proof of any biological difference between GNAQ vs. GNA11 mutated status has been found so far and the two proteins are thought to have redundant functions and activate same downstream pathways. Mutations at R183 and mutations at Q209 are mutually exclusive but interestingly the former seems to have much less oncogenic activity than the latter since mouse injected with melan-a cells transduced with GNA11 R183C variant developed tumors with increased latency compared to mice injected with cells bearing GNA11 Q209L variant. This fact might explain the lower prevalence of substitutions in R183 compared to Q209, and, possibly, also the selectivity observed in pharmacological response (Van Raamsdonk et al., 2010).

Gαq proteins are known to activate via Phospholipase C (PLC) and Protein Kinase C (PKC) the Mitogen Activated Protein Kinase (MAPK) pathway, that was ideed shown in several reports to be constitutively activated in UM bearing GNAQ/11 mutations (Chen et al., 2013a; Mitsiades et al., 2011; Van Raamsdonk et al., 2008, 2010). However recent studies show that GNA mutated proteins also activate an alternative pathway: GNAQ/11 mutations would cause, through Trio, a guanine nucleotide exchange factor, the overactivation of Rho and Rac GTPase, these proteins in turns would lead to nuclear localization of the protein YAP, a component of the Hippo pathway, and possibly JNK and p38 (Feng et al., 2014; Vaqué et al., 2013; Yu et al., 2014a)

2.3 BAP1, a tumor suppressor gene with a putative role in metastatic disease

Various studies attempted to identify a tumor suppressor gene in chromosome 3 in UM (Blasi et al., 1999; Parrella et al., 2003; Tschentscher et al., 2001). The increased accessibility and efficacy of sequencing technologies led to systematic analysis for mutations in UM characterized by monosomy 3. Exome sequencing of tumors with monosomy 3 identified BAP1 as a tumor suppressor gene coupled with LOH of chromosome 3 (Harbour et al., 2010).

BAP1 gene is located on chromosome region 3p21.1. Mutations in BAP1 are found in 47-58% of primary UMs (Koopmans et al., 2013; Shah et al., 2013). As chromosome 3 loss is strongly associated with metastatic risk, the rate of BAP1 mutations increases among aggressive metastasizing tumors, reaching 84% in this subset (Harbour et al., 2010). These mutations are inactivating mutations with mutation sites spread all along the *BAP1* gene. Coding sequences are the most affected regions, but splicing sites might also be mutated. The *BAP1* gene encodes for a protein with various functions. It was first reported to be a ubiquitin hydrolase which is capable to bind the BRCA1 protein and enhances BRCA1 mediated suppression of cell growth (Jensen et al., 1998). BAP1 was also shown to interact with ASXL to form the polycomb repressive deubiquitinase complex (PR-DUB). PR-DUB is a transcriptional modulator which cooperates with polycomb complexes to regulate the expression of a wide series of genes with roles in developmental processes, and stem cell properties (Carbone et al., 2013). BAP1 is able to deubiquitinate transcription factor HCF1, suggesting a role of BAP1 in transcription regulation (Yu et al., 2010). Interestingly, deubiquitination of Histone 2A by PR-DUB was shown to play a role in DNA damage repair by promoting the repair of double-strand breaks. (Ismail et al., 2014; Yu et al., 2014b). Since ubiquitination has been related to a wide range of cellular processes, such as labeling of proteins for degradation, DNA damage repair, gene transcription, cell membrane trafficking, progression through cell cyle, stress response, cell communication, differentiation and apoptosis (Carbone et al., 2013), the cellular interactions and functions of BAP1 are probably still largely uknown. In particular, the precise roles of BAP1 in UM tumorigenesis are unclear.

BAP1 mutations were initially reported to characterize UM tumors with a propensity to metastasize (Harbour et al., 2010). Indeed, since LOH of chromosome 3 negatively impacts on prognosis, and BAP1 mutations are found in presence of chromosome 3 LOH, the cytogenetic model supports the hypothesis of a role of BAP1 mutations in the metastatic progression of UM. In line with this assumption, Harbour and colleagues show that knock down of BAP1 in UM cells derived from primary tumors and wild-type for BAP1 induces in gene expression an enrichment of a set of transcripts associated with metastasis (Harbour et al., 2010). This result is in agreement with a previously published transcriptional signature that allow to separate low-risk non-metastasizing from high-risk metastasizing UM primary tumors (Onken

et al., 2004). Therefore the study of Harbour and colleagues suggests a central role of BAP1 in promoting UM metastasis. Again, such a statement remains an hypothesis due to a lack of reliable models for studying BAP1 role in the progression to metastatic disease.

Using a transcriptional analysis of knock down models, the group of Harbour explains the effects of BAP1 loss as a loss of differentiation and gain of stem-cell properties. However, transcriptional profiles do not correlate with the previously published signature of metastastic disease. This might imply that a knock down model is artificial and do not appropriately mimic UM metastastic tumor cells (Matatall et al., 2013). In vitro cellular effects of BAP1 knock down also slow down cell doubling times (Matatall et al., 2013), a notion that is hardly integrated with the concept of a more aggressive disease, and that has not been yet correlated with distinct cell cycle patterns in patient biopsies.

Finally BAP1 familial syndroms have been described where germline mutations of BAP1 increase the risk of development of melanocytic tumors, non melanocytic skin cancers, mesothelioma, clear cell renal carcinoma, meningioma, lung, ovarian, pancreatic and breast carcinoma. This fact suggests a role of BAP1 as a tumor suppressor gene and early driver of tumor progression rather than having a role specifically in advanced disease (Murali et (Abdel-Rahman et al., 2011; Goldstein, 2011; Murali et al., 2013; Testa et al., 2011; Wiesner et al., 2011, 2012).

On the other hand, somatic mutations of BAP1 have been reported in tumors other than Uveal Melanoma, such as mesothelioma and clear cell carcinoma (Peña-Llopis et al., 2012; Yoshikawa et al., 2012). Finally, genetically engineered mouse models of BAP1 developed myeloid proliferations, suggesting that this protein have a broad range of actions and the effects of BAP1 loss might differ in differnet tumor types .

Further studies on cellular functions of BAP1 and on the phenotype of the different molecular subtypes of UMs are needed to elucidate the role of BAP1 in the progression of this disease**.**

2.4 Other recurrent mutations identified in UM

Other recurrent mutations in subgroubs of primary Uveal Melanomas have also been reported.

In 2013 three independent studies (Furney et al., 2013; Harbour et al., 2013; Martin et al., 2013a) reported 15-20% mutations of the *SF3B1* gene (splicing factor 3b, subunit 1), enriched in the subgroup of UM characterized by disomy 3 and good prognosis. SF3B1 encodes for subunit 1 of splicing factor 3B, a component of the spliceosome, the cellular machinery that processes pre-mRNA into mature mRNA, and is reported to be mutated in myelodisplastic syndromes and myeloproliferative neoplasm (Papaemmanuil et al., 2011; Quesada et al., 2012; Rossi et al., 2011; Yoshida et al., 2011). SF3B1 was subsequently found mutated also in solid tumors such as bladder, lung, endometrial, pancreatic and breast carcinoma as well as in cutaneous melanoma (Scott and Rebel, 2013). Mutations in *SF3B1* occur in hot spots in functional regions called HEAT repeats, in a situation of heterozigosity where a wild type allele is preserved. In UM, they are more common at position R625 but mutations in other positions such as K666 and K700 (Furney et al., 2013), E622,Y623,E783, and the occurrence of indels and small deletions are also reported (Martin et al., 2013a).

SF3B1 mutations are associated with aberrant splicing in Chronic lymphocytic Leukemia and Myelodysplastic Syndrome (Wang et al., 2011; Yoshida et al., 2011). In line with these reports, Furney et al. shows that SF3B1 mutations in UM are associated with alternative splicing. Interestingly, the same splicing signature found in UM was could also be used to identify SF3B1 alterations in in Chronic lymphocytic Leukemia and Myelodysplastic Syndrome (Gentien et al., 2014), implying common features in RNA splicing pattern alterations caused by mutated SF3B1. On the other hand, in haematological malignancies, the relative frequence of SF3B1 mutations differs from UM, K700 mutation being the most prevalent. Martin et al. found that, in a small number of primary tumors that gave rise to metastasis, mutations in SF3B1 were located in positions other than R625 (Martin et al., 2013a), this suggests that different mutational hotspots have possibly different effects on tumor progression. This is also confirmed by the fact that while SF3B1 mutations are associated with a worse prognosis in haematological malignancies (Rossi et al., 2013), in UM the

strong correlation with disomy 3 and epithelioid histologic appearance, link SF3B1 alterations with good prognosis,and this is confirmed by survival analysis (Harbour et al., 2013). Consequently, SF3B1 mutations are mutually exclusive with BAP1 loss and very few tumors showing both mutations have been reported (Martin et al., 2013a) .

In addition to SF3B1 mutations, the same report from (Martin et al., 2013a) identifies also 24% of mutations in EF1AX among primary UMs enriched for chromosome 3 disomy, in a pattern of mutual exclusivity with SF3B1 mutations.

EF1AX (also EIF1A) located at Xp22 encodes the eukaryotic translation initiation factor 1A, which plays a role in the interaction between the ribosomal 40S subunit and the mRNA allowing the formation of a stable mRNA-ribosome complex and the initiation of translation (Pestova et al., 1998). Alterations in this gene are all located in exons 1 and 2 and are mostly missense mutations, although altered splicing sites leading to small deletions are also reported. In females only the active allele was targeted by mutations. Nonetheless, the protein is still expressed in mutated tumors. Studies on yeast eIF1A suggest that these mutations could impair the function of the protein by altering the balance of transcripts in neoplastic cells towards a pattern of gene expression favoring cell proliferation and survival (Martin et al., 2013b). Such hypothesis remains still to be assessed in pathologic situation such as UM.

The mutational pattern of SF3B1 and EIF1AX and the correlation with cytogenetical data suggest an evolutionary fork between High-risk BAP1 mutated tumors and tumors disomic for chromosome 3. The propensity to metastasize of tumors with disomy 3 and an average low risk for metastasis could vary according to SF3B1 or EF1AX mutational status (fig.9).

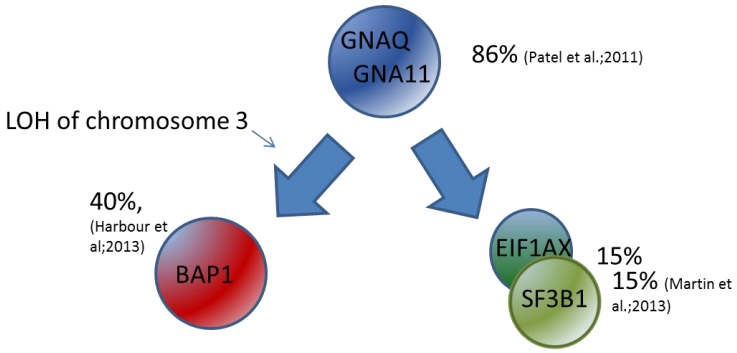

Figure 9. Evolutionary model of UM. GNAQ/11 are early driver mutations and have been reported in the vast majority of UM, conversely BAP1 (and LOH of chromosome 3),SF3B1 and EIF1AX are secondary driver mutations nad identify a class of UM characterized by bad prognosis (BAP1 mutated tumor, with LOH of chromosome 3) and a class with intermediate-good prognosis (EIF1AX or SF3B1 mutatedtumors), where the risk of metastasis is influenced by the type of mutation and by the cytogenetical pattern.

Other mutations are found sporadically in UM, such as mutations in EGFR (Daniels et al., 2012) and NF1 (Foster et al., 2003). But the rate of mutations detected in primary tumors remains overall quite low when compared with other types of tumors as well as with cutaneous and acral melanoma (fig.10). Uveal Melanoma has not been found to show phenomena of genetic instability as in tumors characterized by impaired DNA damage repair. Microsatellite stability has been reported (Cross et al., 2003) and even BAP1 mutated tumors do not show the caracteristics of genomic instability that might be induced by Homologous repair deficiency (Matatall et al., 2013). On the other hand, reports describing a role of BAP1 in DNA damage repair have indicated a selective sensitivity of BAP1 deficient cell lines to therapies targeting HR deficiency (Ismail et al., 2014; Peña-Llopis et al., 2012) , but the use of models different from UM where loss of BAP1 of

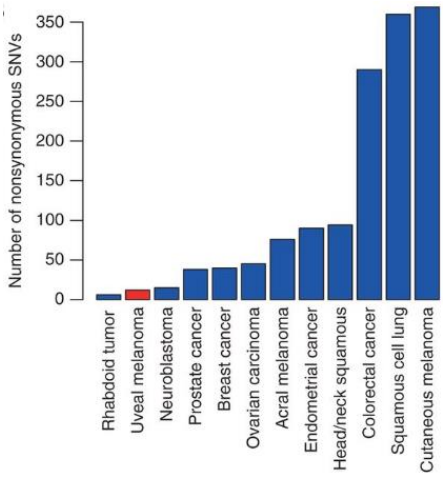

Figure 10. Comparison of non-synonymous point mutation rates identified from whole-genome and exome sequencing studies in various solid tumors (Furney et al., 2013).

function was artificially induced prevent any conclusion on a role of BAP1 on genetic stability in UM disease.

To resume

- The relative rate of mutaions in UM is very low
- Mutations in GNAQ and GNA11 are early drivers of tumorigenesis but other alterations might be necessary for the acquisition of the malignant phenotype.
- BAP1 mutations with LOH of chromosome 3 have a high tendancy for metastatic spread, while SF3B1 or EF1AX mutations in chromosome 3 disomic tumors are secondary events affecting distint UM subtypes and represent alternative branches of biological progression.

3. RNA expression based classifications

Analysis of RNA expression has been used as well as a tool to investigate and characterize UM. Unsupervised hierarchical cluster analysis of gene expression profiles in primary Uveal Melanoma defines two subgroups of tumors, which almost perfectly matches with copy number status of chromosome 3 (Tschentscher et al., 2003). No strong correlation was on the contrary found between molecular subgroups and chromosome 6 and 8q status. Interestingly, this classification stands the removal of chromosome 3 from the analysis, implying that these classes are not a mere consequence of the transcription of genes located on chromosome 3. A similar approach was used in the work by Onken and colleagues (Onken et al., 2004). Using an unsupervised analysis, this study confirms the biological basis of a classification of primary UMs into two transcriptional subgroups, caracterized repectively by a good (class I) or a bad prognosis (class II). Again the two classes strongly correlate with chromosome 3 monosomy but are not correlated with status of chromosome 6 and 8q. Both studies also depict an unbalaced pattern of transcriptional deregulation, where the molecular classes enriched in monosomy 3 present an overall profile of downregulation of the gene expression.

The analysis on a series of 25 tumors of a possible correlation between the molecular class and variables such as age, gender, tumor diameter, tumor thickness, local

invasion, ciliary body involvement and pigmentation rank demonstrated a significant association only for age, which is associated with class II profile (Onken et al., 2004). This has implication on prognosis and suggests that tumor diameter, tumor thickness, invasivity and location are independent prognostic factors with no or minimal impact on the biological phenotype of the disease.

Notably, the discriminant genes identified in the two studies minimally overlap, making difficult a further validation of other hypothesis on the biological meaning of these transcriptional profiles. Since both classifications are strongly correlated with the previously established cytogenetic classes, it is reasonable to think that the molecular classification might be more informative than cytogenetics for the phenotypical classification of the disease, as transcriptomics allows to take into account also epigenetic changes whose role in the disease is still not known. Indeed systematic studies on the epigenetics of UM that might complement genetic and transcriptional analyses have not been yet been published.

4. Epigenetic of UM

Almost all the studies on epigenetics in UM have focused on candidate genes, selected on the basis of analogies with cutaneous melanoma.

The pattern of promoter hypermethylation is the most frequently reported epigenetic change. Reduced expression of p16(INK4a) occur with frequencies ranging from 0% to 30% in different series (Edmunds et al., 2002; Merbs and Sidransky, 1999; Moulin et al., 2008; van der Velden et al., 2001; Zeschnigk et al., 2003) and was found also in Uveal Melanoma cell lines (Van der Velden et al., 2001). *RASSF1A*, a tumor suppressor gene adjacent to BAP1 locus, was found to be hypermethylated in 13-83% of UMs and might have a role in the early phases of tumorigenesis of UM (Calipel et al., 2011; Dratviman-Storobinsky et al., 2012; Maat et al., 2007; Merhavi et al., 2007; Moulin et al., 2008). Methylation of hTERT promoter is reported in 52% of samples analysed by Moulin et al. (Moulin et al., 2008), while other studies point out the methylation of the *EFS* gene (Neumann et al., 2011); *RASEF* was also found to be hypermethylated in a significant number of samples (Maat et al., 2008b), and sporadical hypermethylation of genes such as *MGMT*, *DAPK*, *IGF2*, *NEUROG1*

(Merhavi et al., 2007) *RARB* and *TIMP3* (Merhavi et al., 2007; Moulin et al., 2008; van der Velden et al., 2003) have also been reported. Systematic analysis of methylation by high-throughput technologies are expected to provide new understanding on the relevance of these epigenetic mechanisms in the development of the disease.

In the study of the possible roles of microRNA in the progression of disease, a more comprehensive approach has been attempted by the group of Harbour, who reports that unsupervised miRNA expression profiles shows a bimodal clustering completely concordant with the previously published classI-classII RNA-based classification (Onken et al., 2004; Worley et al., 2008). miRNA let-7b and miR-199a are the most significant discriminators of the two classes in this analysis, however these results are quite discordant with those issued from a similar analysis performed by Larsen and colleagues (Larsen et al., 2013). Only one study attempts to compare UM with is normal counterpart and reports a comparison of four UM with four normal choroid samples; the analysis pointed out that miRNA-20a, miRNA-106a, miRNA-17, miRNA-21 and miRNA-34a were upregulated while miRNA-145 and miRNA-204 were downregulated in tumoral samples (Yang and Wei, 2011). In vitro experiments in UM cell lines showed that miRNA-34a, miRNA34b/c and miR-137 inhibit cell growth and migration through downregulation of c-MET and MITF (Chen et al., 2011; Dong and Lou, 2012; Yan et al., 2009), while miR-9 suppression was involved with cell migration through activation of NF-kB (Liu et al., 2012). Other miRNAs whose downregulation has been associated with development and progression of UM are miR-182 (Yan et al., 2012) and miR-124a (Chen et al., 2013b). Independent validation in wider cohorts of samples is needed to prove the biological significance of these findings.

IV. MOLECULAR NETWORKS

Studies on biological samples and tumor-derived models had been conducted also at the protein level.

1. MAPK pathway

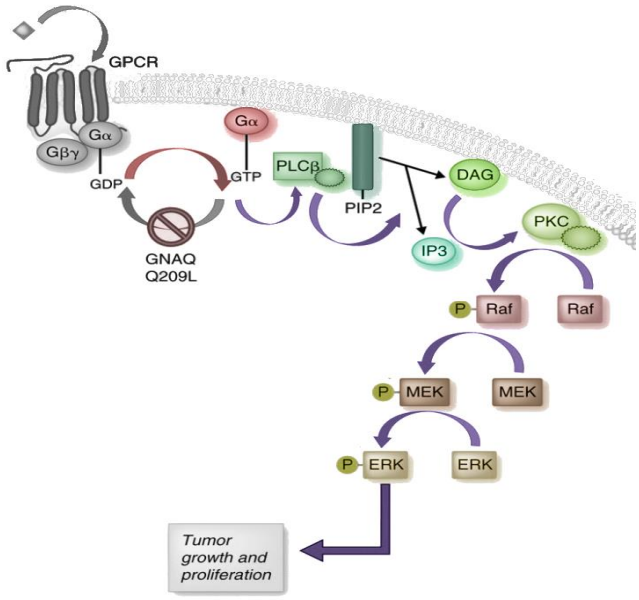

Figure 11: Constitutive activation of the PKC/MAPK pathway in GNAQ/11 mutated UM. Mutations in Gαq subunits stabilize the active Guanine triphosphate (GTP)-bound form. This constitutively activates the Phospholipase C β(PLCβ) which in turns promotes the clivage of phosphatidilynositol-(4,5) bisphosphate (PIP2) to inositol-triphosphate (IP3) and diacylglycerol (DAG). DAG activates ProteinKinase C (PKC) leading to the induction of the MAPK cascade. GPCR:G protein coupled receptor; modified from (Patel et al;2011).

Again in analogy with cutaneous melanoma, the MAPK pathway has been a privileged subject of analysis. This signaling cascade is activated in many different cancers, and mediates cell proliferation, survival, differentiation and prevention of apoptosis. Extracellular signals are transduced via multiple cell surface receptor tyrosine kinases to intracellular effectors, such as small GTPase like Ras and protein kinases such as Raf and MEK/ERK kinases. In cutaneous melanoma, constitutive MAPK singaling is a consequence of activated mutations in Ras and BRAF.

The MAPK kinase pathway is constitutively activated in the vast majority of UMs. Weber et al. identified constitutive activation of ERK in 86% of the samples tested, which was absent in normal uveal cells. Calipel et al. showed that UM cell lines possess an activated MAPK pathway, even in the absence of B-Raf mutations, that controls cell proliferation, probably through regulation of cyclin D1 expression (Calipel et al., 2006).

Different key proteins have been implicated in the deregulation of the MAPK pathway in UM.

First, mutations of GNAQ/11, found in about 90% of UM have been reported to promote constitutive MAPK activation through induction of PLCβ function and consequent activation of PKC. In vitro modeling confirmed these hypothesis: GNAQ Q209 transfected melanocytes show increased ERK phosphorylation compared to controls, and silencing of GNAQ or GNA11 reduces phospho-ERK levels, increases

number of resting cells, reduces overall cell number and decreases anchorage-independent growth (Van Raamsdonk et al., 2008, 2010). An indirect confirmation comes also from the differential activity of chemical inhibitiors: PKC and MEK inhibitors have been shown to be selective for UM with GNAQ and GNA11 mutations compared to WT cell lines (Khalili et al., 2012; Wu et al., 2012b).

Second, few other proteins appear to play roles in UM tumoral progression and have been suggested to cooperate in MAPK pathway activation. HSP90 chaperone protein has been shown to be important in the wild type form of BRaf activity specifically in UM, and HSP90 inhibition was shown to reduce viability specifically in UM cell lines (Babchia et al., 2008). C-kit activation, possibly through an autocrine SCF/c-Kit loop, has been assessed in UM cell lines and associated with constitutive ERK activation (Lefevre et al., 2004). Moreover, transcriptomic studies showed that *c-KIT* gene upregulation was associated with metastastic tumors (Onken et al., 2004), suggesting a possible role in in the progression of the disease.

2. PI3K pathway

PI3K pathway has been implicated in survival and proliferation of UM. PI3K converts posphatidylinositol(1,4)bis-phosphate (PIP2) to posphatidylinositol(1,4,5)tris- phosphate (PIP3) mediating its translocation to the plasma membrane. PIP3 in turns activates the AKT protein kinase, which is upstream of several patwhays that are essential in proliferation and cell survival (fig.12). PI3K activity is balanced by PTEN, a protein that converts PIP3 to PIP2. Deletions of *PTEN* have been suggested to have a role in the pathogenesis of UM with a correlation

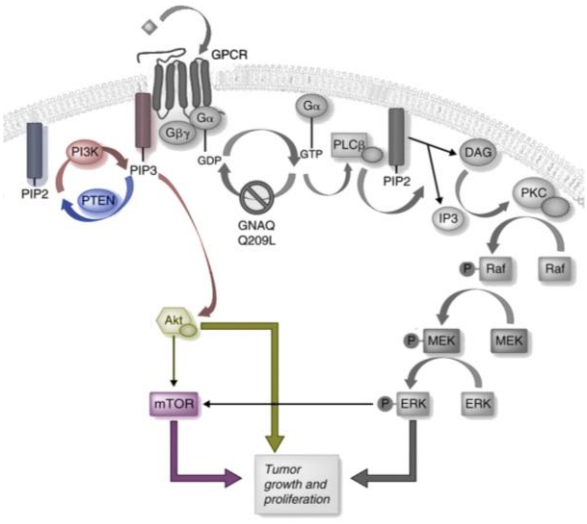

Figure 12. PI3K pathway plays a role in UM. PI3K convertes PIP2 to PI3 medating ist translocation to the plasma membrane and the consequent activation of AKT, AKT activates mTOR and other effectors supporting cell proliferation. PTEN antagonize the activity of PI3K restoring PIP in its biphosphorylated form (modified from Patel et al. 2011)

between lower PTEN expression in tumors and a correlation with reduced survival is reported (Abdel-Rahman et al., 2006). In this study, on 75 primary UM, 12% showed loss of PTEN expression, and another 42% showed a reduced immunostaining compared to internal control. Microdeletions of the PTEN gene were suggested to be the most important mechanism of PTEN insufficiency. However, PTEN loss does not seem to be a major cause of activation of PI3K pathway in UM, and mutations in the known key components of the pathway are rare (Babchia et al., 2010a; Daniels et al., 2012).

Still AKT phosphorylation was detected in more than half of the samples studied in (Saraiva et al., 2005) and (Babchia et al., 2010a), a finding that supports activation of the PI3K/AKT axis in UM.

However, the role of PI3K pathway downstream effector, mTOR, is controversial. mTOR associates with other proteins to form the mTORC1 complex, which is activated by PI3K/AKt pathway and has a central role in the regulation of protein synthesis. mTOR can also associate with other proteins to form the mTORC2 complex, which holds a function in cytoskeleton organization and is insensitive to the effets of the mTORC1 inhibitor Rapamycine. While Babchia et al. shows no role of mTOR in UM cell proliferation, a work from Ho et al. demonstrates a strong synergistic activity of a MEK inhibitor with two different mTOR inhibitors, Rapamycine and AZD8055, suggesting that the interconnection between PI3K and MAPK pathway is strong at the mTOR level as well (Babchia et al., 2010a; Ho et al., 2012a).

3. RTKs induced signaling pathways

Kit and IGFR1 are among the cell membrane receptors that are suggested to play a role in MAPK and PI3K pathway activation.

Kit is a receptor tyrosine kinase involved in differentiation, cell adhesion, migration and proliferation. A Role for c-Kit and its ligand SCF in the proliferation of choroidal melanocytes was suggested by Mouriaux et al. (Mouriaux et al., 2003). A search for activating mutations that could justify a constitutive signaling proved negative, but high expression of the receptor was detected by different groups in 63-87% of tumoral samples (All-Ericsson et al., 2004; Pache et al., 2003; Pereira et al., 2005). Moreover, inhibition of the autocrine loop SCF/c-Kit or treatment with STI571

(imatinib) an inhibitor of ABL, KIT and PDGFR, reduced proliferation and migration of UM cell lines (All-Ericsson et al., 2004; Lefevre et al., 2004; Pereira et al., 2005).

Kit signaling was suggested to contribute to the activation of MAPK and PI3K/AKT pathways because stimulation of melanocytes with SCF results in activation of ERK and AKT. In UM cell lines however, SCF stimulation led only to ERK activation (Pereira et al., 2005).

IGF1R (Insulin-like Growth Factor 1 Receptor) is a transmembrane receptor that transduces signals from IGF1, a soluble factor produced by the liver. Binding of IGF1 to IGF1R leads to phosphorylation of several intracellular proteins, including the family of insulin receptor substrates (IRS) (Baserga, 1995). Activation of IGF1R acts upstream of MAPK and PI3K/AKT signaling cascades (fig.13). Inhibition of IGF1R signaling in UM cell lines with a specific compound, picrpopdophyllin, decreases both phospho-AKT and phospho-ERK, resulting in decreased cell viability (Girnita et al., 2006).

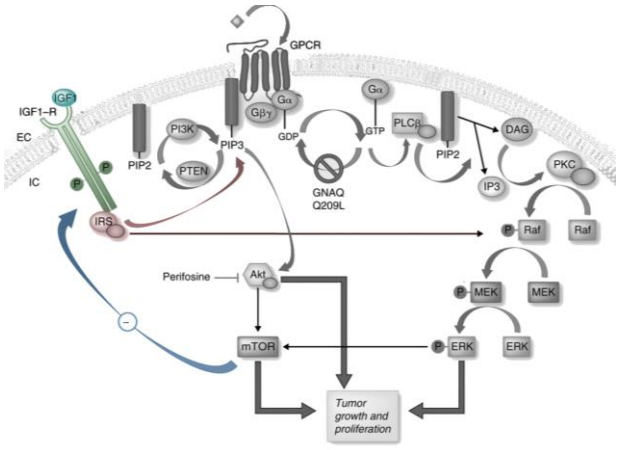

Figure 13. IGF1R cascade interacts in UM with the MAPK and PI3K pathways. IGF1 singals are transduced via the IGF1 Receptor which leads to the phosphorylation of soluble effectors allowing interaction with the MAPK and PI3K pathways. IRS: Insulin receptor substrates. PPP: Picropodophyllin (Modified from Patel et al. 2011)

IGF1R was also shown to be involved in tumor invasivity. IGFR1 is overexpressed in metastastic tumors. Importantly, liver is the most frequent site for UM metastatic spread and hepatocytes secrete high levels of IGF1, supporting a possible role of an IGF1R/IGF1 paracrine loop in metastatic growth. Several studies analyzed the expression of IGFR in primary UMs by immunohistochemistry and showed a correlation between the expression of the receptor and subsequent metastatic spread (All-Ericsson et al., 2002; Economou et al., 2005; Mallikarjuna et al., 2006). A trend towards higher serum levels of IGF1 in patients with locally advanced disease was also found (Topcu-Yilmaz et al., 2010), and a study on a small series confirms the correlation between IGF1R expression and liver metastasis and shows consequent activation of the AKT pathway (Bao et al., 2012a). In agreement with the previous finding, Yoshida et al. showed positive staining for IGF1R in UM hepatic metastatic samples, and that a long-term cell line derived from a liver metastasis had

reduced growth and decreased AKT-S347 phosphorylation upon IGF1R inhibition (Yoshida et al., 2014). Altogether, these studies suggested that IGF1R signaling might be involved in liver metastatic spread, with a possible link to AKT activity. One discordant study exists however, where an anticorrelation of IGF1R staining with extrascleral invasion and no association with survival on a series of 167 primary UMs was detected (Al-Jamal and Kivelä, 2011).

The specific liver tropism of UM metastases led to investigate the role of the hepatocyte growth factor (HGF) in the progression of the disease. Foci of metastatic melanoma in the liver stained diffusely for HGF, while primary tumors showed staining for HGF at the level of the choriocapillaris suggesting that HGF might regulate the invasion and migration of UM cells. Moreover, the HGF receptor c-MET was found to be selectively expressed in vimentin positive/keratin negative uveal melanoma cells and tumor samples, a phenotype found to correlate to extravasation and invasivity (Hendrix et al., 1998). In the study by Economou et al., c-MET expression correlated with metastatic spread, although less then IGFR1 and only in the univariate analysis (Economou et al., 2005). Another study reports as well a correlation between c-MET expression and metastatic death but found no HGF staining in tumors with liver metastases suggesting that c-Met contribution to tumoral progression could be ligand independent (Mallikarjuna et al., 2007). Another confirmation of a role of c-Met in metastatic spread comes from drug-response studies with the c-Met inhibitor Crizotinib whose administration led to reduced liver micrometastasis in an in vivo mouse model of UM (Surriga et al., 2013).

4. YAP signaling

Recently, genome-wide RNA interference approaches in Drosophila allowed the identification of an alternative signaling pathway downstream of GNAQ/11 (Vaqué et al., 2013; Yu et al., 2014). These two studies elegantly demonstrate that mutated GNAQ/11 trigger YAP dephosphorylation and nuclear localization, and thus activate YAP signaling activity independently of PLCβ signaling. YAP is a component of the Hippo pathway and, together with its homologue TAZ, is responsible for activation of different nuclear transcriptor factors including TEADs and SMADs. In nonproliferating cells, YAP activity is reduced and this can be done in two different ways. In the classical Hippo signaling cascade, YAP is phosphorylated and is either degraded or

retained in the cytoplasm. Alternatively, binding with the protein angiomotin (AMOT) sequesters YAP away from the nucleus. Mutants GNAQ/11 were shown to activate the guanine nucleotide exchange factor Trio, which in turns activates the small GTPases Rho and Rac1, inducing actin polymerization and dissociation of the protein AMOT from YAP. Unbound YAP can then enter the nucleus and induce cell proliferation (fig. 14).

In addition to the regulation of YAP signaling, activation of Trio by Gaq mutants is also suggested to play a role in the activation of the AP-1 transcription factor and possibly also of JNK and p38 dependent cascades (Vaqué et al., 2013).

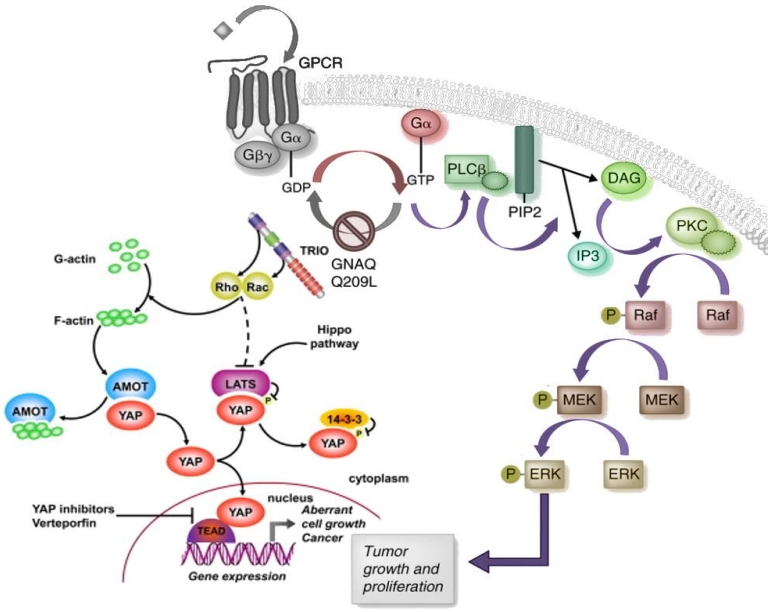

Figure 14. Nuclear localization and phosphorylation of YAP in a GNAQ/11 mutated dependent way contributes to tumorigenesis in UM. GNAQ/11 mutated GTPases activates Rho and Rac small GTPase through the mediation of Trio, independently from PLCβ. Rho and Rac in turns stimulate YAP nuclear localization an dephosphorilation by inducing Fibrillar actin formation which releaves YAP of the inhibitory effect of AMOT. Alternatively inhibition of LATS, which with 14-3-3 proteins is responsible of the phosphorylation and cytoplasmic sequestration of YAP, could also contribute to YAP activation. Nuclear dephosphorylated YAP interacts with transcription factor TEAD to promote gene expression (modified from Patel et al., 2011; and Yu et al., 2014)

The pattern of singaling network characteristic of UM reflects the peculiarity of the disease already seen at the genetic level , and the growth of knowledge on activated pathways had proved essential for the choice, at the preclinical and clinical level, of therapeutic strategies with targeted agents.

Table 1 shows the differences, in terms of frequent chromosomal aberrations and recurrent mutations, between uveal and cutaneous melanoma and displays the molecular pathways resulted to be alterated in these two types of disease.

UVEAL MELANOMA				CUTANEOUS MELANOMA				
MOST FREQUENT CHROMOSOMAL ABERRATIONS								
Gain		Loss		Gain		Loss		
1q	24%	1p	25%	1q	25-33%	1p	28%	
		3	43-65%					
6p	18-29%	6q	29%	6p	24-28%	6q	28-42%	
				7	50%			
8q	40%			8q	34%			
				18,20	40-60%	9(p)	80%	
						10	60%	
						14,15,16,17q, 21,22	20-40%	
		X ;Y	35-50%			X	20-40%	
MUTATIONS								
Activatory		Inactivatory		Activatory		Inactivatory		
GNAQ/11	80-90%	BAP1	50-60%	BRAF	60-70%	CDKN2A	infrequent	30–80% of familial cases
SF3B1	15-30%	EEF1AX	24%	NRAS	15-25%	PTEN	10%	
MAIN ALTERED DOWNSTREAM SIGNALING PATHWAYS								
MAPK PKC PTEN/PI3K YAP				MAPK PTEN PI3K CDK4/Rb MDM2/p53				

Table 1. Most frequent alterations found in Uveal Melanoma Compared to Cutaneous Melanoma. (Albert and Polans, 2003; Babchia et al., 2010 ; van den Bosch et al., 2010; Chen et al., 2013a; Feng et al., 2014 ; Haluska et al., 2006; Harbour et al., 2010; Kilic et al., 2006; Martin et al., 2013b; Nelson et al., 2000; Piperno-Neumann et al., 2014a; Prescher et al., 1990; Van Raamsdonk et al., 2008, 2010; Sisley et al., 1992).

V. PROGNOSTIC ALGORITHMS

The increase of knowledge in tumor characterization and subclassification derived from clinico-pathological and molecular studies has greatly implemented the prognostic algorithms for UM, but up to now, no general consensus has been reached on gold standard prognostic algorithms assessing the risk for primary tumors to evolve into disseminate disease.

While gene expression profile classification has been progressively more widely accepted in the United States of America (US) and Canada for prognostic purposes, a greater confidence on reproducibility and cost-effectiveness has pushed European centers to rely on algorithms based on clinical, histological and cytogenetic markers.

The prognostic algorithm widely used in the US, proposed by the group of Harbour, is completely based on gene expression profiles presented in (Onken et al., 2004) and relies on the analysis of the expression of 12 discriminating genes and 3 endogenous control genes (Onken et al., 2010). The test, named DecisionDx-UM test proposed in the US with the purpose of being the standard prognostic tool for clinical decisions, was validated in a clinical trial involving over 400 patients. A positive predictive value of 95% in predicting 4 years metastasis free survival and a negative predictive value of 80% resulted from the study (Onken et al., 2012). The test uses RNA extracted from fine needle aspiration biopsy samples as well as from formalin-fixed paraffin embedded enucleated or resected tumors (reported technical success is 97%). It is for the moment performed in a single accredited center in the US and is therefore still subjected to cost and reproducibility problems. This has probably impaired unbiased comparisons with the other prognostic algorithms.

European approaches rely on the evaluation of anatomopathological parameters such as tumor size at enuclation, local invasiveness, cell type and the cytogenetic evaluation of aberration of chromosome 8q and 3 using (Cassoux et al., 2014; Damato et al., 2009).

The approach is exemplified by an online algorithm proposed by Damato et al. that takes into account age, sex, TNM size category, ciliary body involvement, cytomorphology, closed loops, mitotic count, chromosome 3 loss and 8q gain as assessed by multiplex ligation-dependent probe amplification, presence of extraocular spread (Damato et al., 2011).

Trolet et al. uses DNA arrays, which allows deletion of partial chromosomal losses and isodisomies, to define a high-risk class of primary tumors. Statistical analysis of the predictive power of the different combinations of recurrent chromosomal alterations suggests that the combination of loss of chromosome 3, loss of 8p, loss of 16q, gain of 6p, gain of 8 showing a proximal breakpoint and evaluation of 8q logratio after the breakpoint permits prediction of metastatic evolution with a positive predictive value of 84,6% and a negative predictive value of 87,5%, a performance similar to DecisionDx test (Trolet et al., 2009). Indeed a validation study made in the same institution suggest that most robust prognostic information proposes is

provided by a classification based on 4 subgroups on the basis of chromosome 3 monosomy and 8q gain only (Cassoux et al., 2014).

A comparison of DecisionDx and different prognostic factors made by Harbour's group demonstrates better sensitivity, specificity, negative and positive predictive values obtained with the molecular classification compared to simple monosomy 3 detected by array Comparative Genome Hybridisation (aCGH) (Worley et al., 2007). However a study of the same group has indeed demonstrated a superiority of Single Nucleotide Polimorphism Arrays to aCGH in predicting metastasis (Onken et al., 2007). This demonstrate that a randomized comparison between DecisionDx and other cutting edge algorithms proposed by other Institution is still needed to fully validate a gold standard for prognosis of UM. An independent analysis was attempted by Gill and Char, who compared the different molecular tests proposed in Europe and the US on the basis of the relative frequencies of patients with positive test results and metastasis/mortality rates (Gill and Char, 2012). However, times of follow up are different in the different studies making a real comparison impossible.

The increase of knowledge on mutational and functional status of driver genes will urge a deeper understanding of the relationship between gene expression and genetic and epigenetic alterations. The prognostic value of BAP1 expression by immunohistochemistry was recently evaluated (Kalirai et al., 2014; Koopmans et al., 2014).And only one BAP1 deficient tumor clustered in class I in the series of 55 primary UM analysed by Harbour (Harbour et al., 2010). Methylation of BAP1 promoter or other epigenetics mechanisms could produce loss of the protein expression and induce to underestimation of the correlation between molecular class of risk and BAP1 expression, since this correlation has still to be assessed by non DNA-based methods such as immunohistochemistry. Recently, Harbour modified the molecular classification by defining a third group, class I-b, with intermediate prognosis, rendering this prognostic test more accurate and showing that multiple variables have to be taken into account to predict the phenotype of the disease (Harbour, 2012). Even if gene expression profiles, which represent an information integrated for tumoral heterogeneity, expression of drivers and regulatory tumoral alterations could be hardly be reduced to the dicotomic presence or absence of a single protein, for the routine practice the advantages of a test based on the immunohistochemistry for BAP1 are evident. Other markers easily detected by

immunodetection in tumoral samples might be integrated in such prognostic algorithms, like PTP4A3, which is reported by (Laurent et al., 2011) to be highly overexpressed in metastatic tumors. Moreover, the increase of experimental procedures that imply mutation detection for therapeutic purposes increase the value of testing also alternative diagnostic algorithm based on mutational profiles of a panel of genes (GNAQ/11,BAP1,EF1AX,SF3B1), and US academic centers are starting to assess the value of prognostic algorithm based on the integration of cytogenetics with mutational profile (Ewens et al., 2014).

VI. PRECLINICAL MODELS

1. *In vitro…*

> *"Human uveal melanoma cell lines are difficult to establish in vitro, particularly in contrast to their counterpart, cutaneous melanoma, for reasons that are unclear"*
>
> *June Kan-Mitchell and colleagues, 1989*

The first known report of established ocular melanoma cells lines is described by Daniel Kirby in 1929. The author was able to culture a portion of a patient-derived tumor. Out of six primary cultures, none survived more than 10 passages in vitro and the attempt to use chick embryo fibroblasts as feeder cells resulted in outgrowth of these cells at the expenses of melanoma cells. The author still concluded that "undoubtedly, with proper mediums they could be caused to divide and multiply indefinitely *in vitro*" (Kirby, 1929). Other attempts to grow UM cell lines in culture are reported only decades after (Barishak et al., 1960; Vrabec, 1948).

Eventually in 1984 Albert et al. described the establishment of 6 Uveal Melanoma cell lines, which were cultured for more than 100 passages (Albert et al., 1984). Irradiated MRC5 were successfully used as a feeder layer. Supplementation of Ham's F-12 medium with glucose, cholera toxin, epidermal growth factor, fetal bovine serum (FBS) (15%, v/v), and donor horse serum (5%, v/v) was necessary for the growth of these lines. The authors were able to identify three almost pure spindle cell lines, two spindle-shaped with a small component of epithelioid cells, and one predominantly

epithelioid cell line. Interestingly, Albert et al. reported a progressive loss of pigmentation in serial passages, described carefully the cytologic architecture using electron microscopy and concluded “that all the cell lines examined contained human chromosomes in diploid or near diploid numbers. Several types of chromosome abnormalities including breaks and rearrangements were noted “ (Albert et al., 1984).
The establishment of a stable and nowadays widely used cell line was described five years later by Kan-Mithcell J and colleagues. They derived the OCM-1 and OCM-2 cell lines from biopsied specimens of choroidal melanoma and for the first time injected them in the anterior chamber of immunosuppressed rabbits to produce a xenograft model of the UM disease (Kan-Mitchell et al., 1989). Culture medium was glutamine enriched RPMI164 supplemented with 10% FBS only, and no feeder layer was used. Colonies of growing melanoma cells were already seen after 3 weeks of culture. Karyotype analyses by chromosomal spreads showed that both cell lines were close to be tetraploid (a degree of aneuploidy quite uncommon in primary UMs), suggesting that strong selection might have already occurred.
In 1993, C Aubert reports the establishment of 5 Uveal Melanoma cell lines out of 29 ocular melanomas (Aubert et al., 1993). In 1995, the establishment from a primary tumor of the mixed spindle and epithelioid cell line 92.1 was reported by the group of M. J. Jager. Full karyotype of the 92.1 cell line revealed a tetrasomy of chromosome 8, a tetrasomy of 6p with translocation to a sex chromosome and to chromosome 17 with no cytogenetic anomalies reported on chromosome 3, showing this time a reasonable resemblance to cytogenetic profiles of low risk primary UM (De Waard-Siebinga et al., 1995). Overall, the success rate was 1/12 from freshly derived tumors over a period of 1,5 years, and an unspecified number of unsuccessful attempts to grow in vitro cell lines from frozen tumor tissues was also reported. In 1996, 2 primary (EOM-3, EOM29) and 3 metastatic uveal melanoma cell lines (OMM-1, OMM-2, OMM-3) were established. They showed, among other structural chromosomal aberrations, aneuploidy of chromosomes 3, 8 and 6. Several others cell lines have been subsequently established and widely used for in vitro and in vivo studies of UM.

In the laboratory practice, in most of cases UM cell lines are acquired directly from the group which has generated them or from laboratories that received them from another source. The majority of UM lines can not be purchased from institutional cell

banks such as the ATCC (American Type Culture Collection), and only 4 UM cell lines are registered in the EMBL-EBI (European Searchable tumor line database and cell bank) .

Importantly, the sharing those lines between different laboratories has drastically increased the number of impredictable variables of selection in culture conditions and multiplied the risk of contamination.Folberg et al. examined 7 UM cell lines obtained from original stocks. The study shows that one cell line (MUM2C) was genetically not related to the original patient but rather to cell lines C918 and M619, and that the lines OCM3 and OCM8 comes from the same patient (Folberg et al., 2008). With a similar intent of assessing the identity of UM cell lines, Griewank et al. published a systematic genetic and molecular characterization of UM cell lines. This study shows that a wide number of cell lines used by the scientific community display a genetic background not correspondent to the disease: 5 out of 19 cell lines listed present V600E BRAF mutations, among them OCM-1 and SP6.5 widely used in preclinical studies; only 3 cell lines present GNA11 and 8 GNAQ mutations, while 3 were negative for both Gαq (Griewank et al., 2012). These studies pinpoint the lack of good disease modeling, with for instance cell lines bearing BRAF mutations which are mostly absent in UM patients. Together, it underlines the necessity of increasing the number and diversification of our UM preclinical models. Having good and relevant models for UM is a prerequisite to allow more solid biology and also to avoid the risk of chosing a model on the basis of a phenotypical effects matching common lab work expectations (faster growth, better uptake in vivo, metastatic spread) that might not be fully representative of the disease.

2. *…in vivo*

During the past decade the growing availability of new therapeutic (“targeted”) molecules stimulated the characterization of in vivo models of the metastatic disease for preclinical drug studies.

The majority of the first UM animal models was originated from stable UM cell lines. Following the experience of Kan-Mitchell, Blanco P et al. describes in 2005 the characterisation of an orthotopic model issued from 92.1 cell line. Cells were injected in the suprachoroidal space of the eye of immunosuppressed rabbits. The model showed micrometastasis to the liver in 18% of the animals and macroscopic

metastasis to the lungs in 41%. Isolation of circulating tumor cells in 26% of sampled blood was also possible (Blanco et al., 2005; Kan-Mitchell et al., 1989).

A mouse xenograft model of UM was later presented by Yang et al., with, notably, the assesment of liver metastasis. The model was derived by the Mel290 cell line, a GNAQ/11 wt cell line originated from a primary tumor. Injections of cells in the posterior compartment of the eye or in the tail vein led, 4 weeks after inoculation, to the development of micrometastasis in the liver, in significantly higher numbers in case of posterior compartment injection (Yang et al., 2008a). In another study the authors developed a similar metastatic xenograft model with the *GNAQ*-mutant cell line Omm1.3 cell line (derived from a UM metastasis); cells were labeled with EGFP-luciferase allowing visualisation of distant spreading with positron emission tomography. 7 weeks after retro orbital injection of cells, metastatic sites were detected predominantely in the lungs and liver (Surriga et al., 2013a).

Syngenic models have not been so far of a significant use for preclinical modeling of UM. Sponateous UMs develop too sporadically (Folberg et al., 2008), and transgenic models do not match the histogenesis of the disease. (Crosby et al., 2011) presented a C57Bl/6 mouse model obtained with injection of B16-LS9 mouse melanoma cells in the eyes and showed metastatic spread to the liver. However, the B16-LS9 cell line is derived from a mouse skin melanoma which have been shown to be quite different from UM. Recently Shiffner et al. described uveal melanocytic neoplasia in one already established transgenic mouse model: a transgenic mouse in which the metabotropic glutamate receptor 1 transgene is under the control of the promoter of dopachrome tautomerase (Dct, Trp2), a gene involved in the production of melanin. This model developed highly pigmented nodular melanomas at the hairless skin regions of ear, tail and anus as well choroidal thickening and uveal melanocytic neoplasia, with the gistologic appearance of UM (Schiffner et al., 2014). However, it is uncertain if this model might represent a good model for UM, especially for the assessment of drug efficacy, since the murine neoplasia do not possess any already known genetic or epigenetic alterations found in UM. This model might however be helpful in addressing novel hypothesis on the biology of the disease at early stages.

The development of Patient Derived Xenografts (PDXs) offers a valuable model to study in vivo tumor biology and response to therapy. Nemati et al. describes the

establishment of 25 Uveal Melanoma mouse PDXs. Histology, molecular analyses by immunohistochemistry, genetic alteration analysis by single-nucleotide polymorphism and specific tumor antigen expression revealed strict resemblance to the original human tumors. An advantage of these models is thus that they present a genotype and phenotype very similar to the original tumors preserving also tumoral heterogeneity. The use of PDXs for in vivo modeling avoids the long in vitro culture, which reduces the original cellular variability and selects for phenotypes adapted to in vitro growth that are not necessarely the same as in the original tumor. In the PDXs developed at the Curie Institute 7 out of 15 analysed models have *BAP1* deleterious mutations, and 94% of the xenografted tumors display *GNAQ* or *GNA11* mutations depicting a situation quite adherent to our current knowledge of the disease. It is important to remember that one disadvantage in the age of raising interest and success of immunotherapies is that these models are unsuitable to studiy the role of the immune system in the phenotype of the tumors and the response to therapy. The development of Genetic engineered models based on known driver alterations in the disease might thus provide essential complementary information.

VI. THERAPY

1. Treatment of localized disease

While primary tumors are successfully treated with enucleation and radiotherapy (proton therapy and plaque brachytherapy) with successful local control rates of over 90% (Diener-West et al., 2001; Shields and Shields, 2004, 1993), no effective therapy has been yet identified for the metastatic disease.

1.1 Standard care

Primary disease is typically treated with enucleation or radiotherapy. The choice of treatment is guided by tumor characteristics and localization, visual acuity of the contralateral eye, age and health of the patient as well as by the acquaintance and technical experience of the ophthalmologist with the different procedures as well as by the possibility to access to an accelerator for the production of radioactive isotopes.

Enucleation, more common in the past, is today the treatment of choice for large tumors (tumor depth >= 12mm, tumor diameter >=18mm), when they are located around the optic disc, when they cause secondary glaucoma, when presenting extensive bleeding, retinal detachment or vitreous hemorrhage. Enucleation is usually accompanied by conventional radiotherapy in case of posterior extra-scleral invasion, while conjunctival resection is performed in case of anterior exteriorization of the tumoral mass.

Radiotherapy is usally delivered with external irradiators (external proton radiotherapy) but it might be performed also with implantable devices (plaque brachytherapy). Since radiotherapy based treatments allow to spare eye and vision, they have become the treatment of choice for small and medium size UMs and several groups consider them for larger tumors as well (Puusaari et al., 2004a; Shields et al., 2002) even if loss of visual acuity and other complications are increased in these cases (Puusaari et al., 2004b). Common side effects of ocular radiotherapy are cataract, optic neuropathy, maculopathy and neovascular glaucoma and depends on the type and dose of radiation and on the localization of the tumor. External proton radiotherapy offers the advantage of a more homogeneus delivery of the charged particles, and therefore a more homogeneus biological effect on the different areas of the tumor. Plaque brachytherapy present the advantage of being easily avaible in a major number of centers, requires less compliance from the patient and might be used when proton beam is discouraged by possible side effects, as in tumors located near the lacrimary gland.

External radiotherapy implies the delivery of charged particles, usually **protons**; helium and carbon ions being used as alternative in few centers. It is less invasive than surgical procedures and allows to focus collimated beams at the desired tissue depth, with theoretical sparing of surrounding tissues. Possible complications are retinal detachment, maculopathy, papillopathy, cataract, glaucoma, vitreous hemorrhage and dryness as well. Dendale et al. describes results of proton beam radiotherapy on a series of 1406 patients. 5-year control rate was 96% and complication rate was 7,7%(Dendale et al., 2006). Desjardins et al. reports, within an integrated analyisis of recent patient series from Insitut Curie and a review of the literature, a local recurrence rate at 10 years of 5% and a rate of secondary enucleation of 10-15%. Interestingly the study suggests that post-irradiation

treatment with endoresection or transpupillary therapy of the residual tumoral scar decreases the rates of complications, possibly reducing the level of cytokines or other soluble factors released by the residual tissue (Desjardins et al., 2012). Moreover proton beam might reveal particularly useful in selected cases, as for anterior lesions, like diffuse iris melanomas, many of which are unresectable (Konstantinidis et al., 2013) but epidemiological studies suggest a benefit also in the case of larger tumors or tumors near the optic disk. Proton therapy might be also used as salvage therapy for local tumor recurrence after plaque radiotherapy, phototherapy or surgical resection (Damato et al., 2013). Some centers advocate also its use as neoadjuvant treatment but an arm of the COMS (Collaborative Ocular Melanoma Study) showed that pre-enucleation external beam radiotherapy of large choroidal melanomas does not improve survival (Collaborative Ocular Melanoma Study Group ; 1998). On the contrary proton therapy should be possibly avoided in patients at higher risk of developing retinopathy, such as diabetic patients, or when long treatment and follow-up are more difficult, where surgery might be more appropriated.

Radiation therapy with **plaque brachytherapy** is a widely used alternative to proton beam irradiation since randomized trials showed no differences in survival comparing this modality of treatment with enucleation: the COMS showed that the mortality rates after Iodine-125 plaque therapy and enucleation are similar (Diener-West et al., 2001), cobalt plaque radiotherapy also proved non inferior to enucleation in patient survival (Augsburger et al., 1989, 1990) and similar findings were reported for ruthenium brachitherapy (Seregard, 1999) even if higher risk of tumor recurrences comparing iodine and ruthenium brachytherapy had been reported in a series of 597 patients (Wilson and Hungerford, 1999). A recent systematic review of observational studies found in the literature confirmed the absence of a significant difference with proton therapy in mortality or enucleation rates but found higher rates of retinopathy and cataract formation (Wang et al., 2013). A meta-analysis on 27 studies comparing the efficacy of charged particle therapy and plaque brachytherapy confirmed the absence of a significant difference in mortality, even if a rete of local recurrences was singnificantly inferior with proton beam therapy. The study also suggests that better autcomes might be possible with proton beam with respect to retinopathy and cataract formation rates (Wang et al., 2013). Therefore plaque therapy becomes the treatment of choice when proton beam therapy is not feasible, in case of lack of an

accelerator in the medical center or if the procedures needed for proton beam are hardly beared by the patient, and also for selected small anterior lesions. The different radioisotopes used, on the basis of their half-life and tissue penetration can be chosen in accordance to tumor size: Ruthenium 106 emits beta radiation which is a charged particle and has limited tissue penetration, while cobalt 60 and iodine 125 emits gamma radiations and might be more suitable for larger tumors . Higher tissue penetration, and higher doses are associated to increased damage to surrounding tissues. Correct positioning as eccentric placement for small tumors of the optic disk and the fovea and adapted devices as slotted plaques incorporating the optic nerve when the latter shows neoplastic invasion are important to reduce side effects and maximize the therapeutic effects. Loss of visual acuity , radiaition retinopathy, retinal hemorrhage, radiation maculopaty, optic neuropathy and retinal detachment are the main documented side effects of this treatment option (Jensen et al., 2005).

1.2 Other reported techniques

Local surgical resections might allow eye retention, with retinal detachment, vitreous hemorrhage, cataract and elevated ocular pression as possible complications; however the limited number of studies on this technique suggest higher rates of local recurrence as well as a low percentage of cases with residual tumor and are therefore not performed as sole therapeutic procedure but in addition to radiation therapy (Bechrakis et al., 2010).

Other less documented procedures are **stereotactic radiation therapy**, suggested as an option for centrally located choroidal tumors with recurrence rates comparable to brachytherapy, although high incidence of retinopathy and optic neuropathy is reported (Dunavoelgyi et al., 2011, 2012); combination of stereotatic radiation therapy and local surgery is suggested by a german study in order to reduce radiation complications (Suesskind et al., 2013).

A non ionizing radiative therapy option is represented by transpupillary **thermotherapy** a technique that allows to deliver infrared radiations to tumor cells through a dilated pupil, however the use of lower energy radiation doesn’t seem to diminish visual side effects compared to conventional radiotherapy, while local

control appears much reduced (Singh et al., 2008); another study suggest that an association with brachytherapy could provide similar results in terms of local and distant recurrences and side effects as brachyterhapy alone (Yarovoy et al., 2012).

Finally **photodynamic therapy** relies on the injection of compounds that are activated at the tumor level by visible light rays and generate reactive oxygen species that induce tumor cell death. This technique had been shown some efficacy in causing tumoral regression in selected cases (Barbazetto et al., 2003; Campbell and Pejnovic, 2012). Still strong proves of efficacy are lacking, and this procedure might be even less effective in highly pigmented lesions. However a photoactivated cytotoxic compound, Verteporfin, was recently proved to possess in its “inactive” form a “targeted effect” on molecular pathways important for the progression of UM (Feng et al., 2014; Yu et al., 2014a); Verteporfin proved in vivo to have an inhibitor effect on UM and could possibly have an efficacy not only in the treatment of the primary lesion but also as adjuvant therapy; still the association with a complementary therapeutic procedure would probably be necessary for the control of the primary tumor.

Therapeutic possibilities remain much more limited for up to 50% of patients, who will develop metastatic disease with only 0,5-20% of overall 5 years survival (Diener-West et al., 2005; Rietschel et al., 2005).

2. Adjuvant therapy

Adjuvant therapies have been tested in small non-randomized trials with the aim of preventing metastatic disease but **without any proof of efficacy**.

Adjuvant intra arterial hepatic **chemotherapy** with fotemustine had been tested by a swiss study on 22 high-risk patients. The comparison with a matched control group randomly selected from archives showed a non significant increase in median overall survival : 9 years [95% confidence interval (CI) 2.2-12.7] for the treated patients versus 7.4 years (95% CI 5.4-12.7; P=0.5) for the control group, with 5-year survival rates of 75 and 56% respectively (Voelter et al., 2008). Even if a trend that favors fotemustine treatment appears from this study the authours could not draw a clear conclusion on the real efficacy of the therapy; however a randomized multicentric

phase III trial with adjuvant intravenous (i.v.) fotemustine is ongoing (Piperno-Neumann, 2012). This trial had been designed in order to assess a significant 20% difference in 5-year overall survival in high risk patients (defined by clinical or genomic criteria: tumor diameter>18 mm or >15 mm associated with retinal detachment, monosomy 3 or partial deletion of 3p associated with 8q gain).

Similar approaches had been tested with molecules enhancing the immune response towards tumoral cells (cancer immunotherapy): **adjuvant** therapy with **Interferon 2 alfa**, which was shown in cutaneous melanoma to improve relapse-free survival, had been attempted but failed to show any significant survival advantage in 121 patients (Lane et al., 2009), while (NCT01585194) a clinical trial testing **ipilimumab**, an anti CTL4A antibody that enhance the activity of cytotoxic lymphocytes, will likely be closed for clinical and commercial reasons. Finally a trial on adjuvant **vaccine therapy** was started by the European Organisation for Research and Treatment of Cancer (EORTC) but no promising datas have yet been drawn from this study.

A different strategy in adjuvant treatment is represented by the administration of molecules that could **prevent metastatic spreading** rather than aiming to eliminate early non-detectable micrometastasis or circulating tumor cells.

Crizotinib, an inhibitor of c-Met, a cell membrane receptor that is reported to have a role in metastatic spread, showed to reduce and delay metastasis in an in vivo model of Uveal Melanoma (Surriga et al., 2013); similar results were reported for the IGFR1 inhibitor **Picropodophyllin** (Girnita et al., 2006). NCT02223819 clinical trial will assess the relapse-free survival (RFS) of adjuvant crizotinib in patients with uveal melanoma class II (high risk) according to molecular caracterisation (Harbour and Chen, 2013).

Another strategy proposed to prevent tumoral spread implies the administration of **HDAC** (Histone deacetylases) **inhibitors. These molecules** have been shown to revert the molecular signature of UM from class II (high metastatic risk) to class I (low risk); the highest efficacy was reported with valproic acid, an antiepileptic drug which was shown to inhibit the activity of HDAC (Gottlicher et al., 2001; Landreville et al., 2012); adjuvant therapy with valproic acid might therefore revert the metastatic phenotype of the primary tumor by altering their gene expression profile; following

this idea recently a clinical trial testing Adjuvant Sunitinib or Valproic Acid in High-Risk Patients with UM (NCT02068586) had been started. However Sunitinib efficacy tested in the metastatic setting was quite modest (see further). Moreover since HDAC inhibitors had only limited effects in delay tumoral growth in vivo (Landreville et al., 2012), to prevent any possibility of metastatic spread it would also be necessary to use it as neoadjuvant strategy and eliminate tumoral cells that might already have migrated at the time of therapy administration. Therefore an association with a cytotoxic compound would be required.

3. Treatment of metastatic disease

Therapeutic approaches for metastatic disease are represented by systemic chemotherapy, and, since the disease might be limited to the liver surgery, by loco-regional treatments such as surgery and hepatic intra-arterial (i.a.) chemo/radiotherapy; few randomized trials had been reported, and treatment currently adopted are often based on the numerous non randomized studies that have been published (Pereira et al., 2013).

3.1 Loco-regional treatments

When metastatic spread is limited to the liver, in selected case with localized and reduced number, **surgery** is considered by numerous centers the best therapeutic option. Several studies have been published suggesting that that complete removal of liver metastasis improve the survival of high-selected patients (Aoyama et al., 2000; Frenkel et al., 2009; Mariani et al., 2009).

These works show a two fold increase in median overall survival in R0 resected patients. However these studies are non-randomized and might therefore contain selection bias as the patients who undergo surgery has limited disease and is likely to have better survival than patients not fulfilling the selection criteria. However the study from Mariani et al. shows that the variables “R0 resections” and “number of metastasis resected” correlated with prolonged survival independently from “absence of miliary disease” and “prolonged disease free interval from primary tumor

diagnosis" (Mariani et al., 2009); this suggest that the prolonged overall survival is also related to the surgical procedure. Indeed surgery at Curie regarded as the treatment of choice in cases with **slowly progressive disease** with **limited number of** lesions when **R0 resection** is possible.

Another treatment modality when the disease is limited to the liver is represented by **intra-arterial hepatic chemotherapy**; this technique implies the injection of the therapeutical compound directly into the liver through catheterisation of the hepatic arthery, allowing local treatment also when the disease is widespread into the organ and nodules are in locations of difficult access with surgery; a small study performed on 10 patients reports a median survival of 16 months of patients treated with hepatic arterial infusion of cisplatin, vinblastine and dacarbazine (Melichar et al., 2009); a large randomized EORTC trial on 117 patients compares hepatic i.a. fotemustine with systemic fotemustine, showing no improvement in overall survival with local treatment (median 14 months) but a benefit in progression free survival for the intra-hepatic arm (4.5 versus 3.5 months) (Leyvraz et al., 2014a).

The local injection of chemotherapeutics might be accompanied by infusion of chemical compounds (**chemo-embolization**). This technique allows to concentrate the drug in the liver and blocks temporarily the vascular supply to the tumor. Transarterial chemoembolization of liver metastasis with cisplatin followed by injection of polyvinyl particles have been described on a small series of 14 patients. 57% of patients achieved partial response and 29% had stable disease (SD), median survival for responders was 14.5 months (Huppert et al., 2010); however a more recent study on 19 patients testing hepatic i.a. infusion of cisplatin with or without polyvinyl sponge produced very modest results (Agarwala et al., 2004); another work, which studied fotemustine chemoembolization on 21 UM metastatic patients showed partial regression (PR) in 14% of patients and SD in 39% (Edelhauser et al., 2012) . Indeed all these studies were performed on small non-randomized series and are insufficient to prove any significant efficacy with these therapeutic procedures.

The same principle supports the use of **immuno-embolization**, a technique that consist in hepatic i.a. embolization followed by injection of granulocyte macrophage colony-stimulating factor (GM-CSF). Sato et al. describes a phase I study on 39

patients with surgical unresectable liver metastasis treated with immunoembolization with GM-CSF. On 31 assessable highly-selected UM patients 2 CR, 8 PR and 10 SD were recorded with a median intent-to-treat overall survival of 14.4 months (Sato et al., 2008). Another study comparing chemoembolization with Carmustine and Immunoembolization with GM-CSF in 53 patients favored Immunoembolization in better progression-free survival (PFS) (12.4 vs. 4.8 months) and prolonged OS (27.2 vs 9.9 months) in univariate analysis, which was confirmed in multivariate analysis for selected subgroups of patients (Yamamoto et al., 2009)

Radio-embolization with Yttrium-90, the intra-arterial local administration of microsphere containing this radioactive isotope, has more recently been proposed for liver metastasis of UM. Yttrium-90 is a beta emitter with limited tissue penetration and therefore allows selective irradiation with limited toxicity. A retrospective review on 11 patients treated with Yttrium-90 microspheres delivered via the hepatic artery showed responses in all patients and 1 complete response (CR) and 6 PR in 9 evaluable patients, with 1 year Overall Survival (OS) od 80% (Huppert et al., 2010). Another study on 22 patients who failed chemo or immunoembolization reports 1CR, clinical benefit in 62% of patients and a median OS of 10 months (Gonsalves et al., 2011)

Another reported options in local treatment are **stereotactic liver radiotherapy**, particularly in patients with few metastasis with favorable locations (Pereira et al., 2013) and **isolated liver perfusion**, which is considered in few specialized centers: Olofsson et al. from the university hospital of Goteborg, Sweden, reported on a series of 34 patients 12% of complete responses and 68% of overall radiological responses with this technique, with a median OS of 24 months (Olofsson et al., 2014a). A clinical trial had been started by the same insititution to prove a clinical benefit on a randomized trial basis (Olofsson et al., 2014b).

3.2 Systemic treatments

Systemic therapy represents the treatment of choice for multi-organ disease (when the tumor cells disseminate to other organs such as lungs and bones) and is often considered for diffuse liver disease .

Intravenous systemic treatment had been attempted with different chemotherapeutics. The compounds traditionally used have been initially chosen in analogy with treatments used for cutaneous melanoma. Single agent regimens proposed rely on the use of **alkylating** agents such as **dacarbazine**, **fotemustine** or **temozolomide**, **no proof**.

In the already cited study of Leyvraz et al. among 79 selected evaluable patients with disease limited to the liver who received i.v. injection of fotemustine median OS was 13,8 months with 20% survival at 2 years (Leyvraz et al., 2014). Another smaller study on i.v. fotemustine in metstatic UM reported 10% of PR and 44% SD (Spagnolo et al., 2013); a small phase II trial on 14 patients assessing the efficacy of oral administration of temozolomide reported no complete or partial responses (Bedikian et al., 2003). Another small phase II study on 11 patients with second line i.v. **bendamustine** showed no responses (Schmidt-Hieber et al., 2004). Similarly a study on weekly docosahexanoic acid-**paclitaxel** showed no Objective Responses and a limited OS (9.8 months) (Homsi et al., 2010). **Camptothecin** in monotherapy produced equivalent results (Ellerhorst et al., 2002).

Combinatorial approaches with conventional chemotherapies did not showed up to now any advantage in Overall Survival in comparison with monotherapies.

A randomized phase II trial on 48 patients testing the alkylating agent **treosulfan** alone and in combination with **gemcitabine** favored the combination with gemcitabine, with one patient out of with PR was reported for 1 patient out of 24 and 7 SD in the combination arm versus no objective responses and 3 SD in the monotherapy arm, however no difference in OS could be assessed (Schmittel et al., 2006) addition of **cisplatin** to the combination resulted in excessive hematologic toxicity without improvement in efficacy (Schmittel et al., 2005).

A multicenter study on a series of 24 patients reports the association of **bleomycin**, **vincristine**, **lomustine** and **dacarbazine** with **intereferon alpha** (Kivelä et al., 2003), again no objective response was observed and median OS was 10.6 months and the combination of **dacarabazine**, **carmustine**, **cisplatin** and **tamoxifen** were used in the study of Pereira et al. with unsatisfactory efficacy (Pereira et al., 2013).

The small number of studies, mostly consistent in small series, and the relative lack of prospective and randomized phase III trials, which is a consequence of the rarity of this tumor, explains the absence of a clear consensus on therapies for metastatic disease. Up to now no effective standard therapy had been defined; Augsburger et al. reviews 80 publications published between Jan 1, 1980 and June 30, 2008. Only 28% were prospective phase I/II or phase II trials, and the most promising results are issued from trials on highly selected patients; on the contrary the largest unselected study reported, the COMS study on 738 patients, shows the worst median OS (only 3.6 months) (Augsburger et al., 2009; Diener-West et al., 2005). Treatments are therefore usually decided according to the different expertise of the regional centers of reference for the disease.

But with the increasing molecular knowledge and availability of targeted therapies, clinicians and pharmaceutical companies have shown great interest in testing new molecules for the prevention and therapy of metastatic UM.

3.3 Molecular targeted therapy of metastatic UM

Targeted therapy allows, by the administration of compounds that interfere with specific cellular molecules, the inhibition of signaling pathways whose function is altered in tumors. No specific compound is known to target the mutated proteins GNAQ/11, EF1AX and SF3B1, which are recurrently mutated in UM, or to exert synthetic lethality with BAP1 loss. However numerous studies tried to assess the response of UM to the wide number of targeted compounds already available for preclinical and clinical studies.

a. Targeting neaongiogenesis and the escape from immune surveillance

Anti VEGF/VEGFR compounds had been tested quite early. A few preclinical reports attested in vivo inhibitory activity of **Bevacizumab**, an anti-VEGF-A antibody, in UM models (Sudaka et al., 2013; Yang et al., 2010); moreover, Bevacizumab was “already known “ in the field of UM since its use have been suggested for the

treatment of local complications of radiations on primary tumors (Mashayekhi et al., 2014).

However preclinical studies also suggest that alternative compensatory mechanism act upon Bevacizumab blockade of VEGF (Lattanzio et al., 2013; Logan et al., 2013) possibly undermining its efficacy. A clinical phase II study of bevacizumab combined with temozolomide on 35 patients showed a 6-month PFS rate of 20%, with durable SD in five patients (14%). Median PFS and OS were 12 weeks and 10 months respectively. (Piperno-Neumann et al., submitted 2014); combination of Bevacizumab with **Aflibercept** (a potent inhibitor of the action of VEGFR1 and VEGFR2) also showed limited efficacy in UM (Tarhini et al., 2011).

6 patients with metastatic UM were included in a pilot study testing low-dose **thalidomide**, an antineoplastic and antiangiogenic agent, in combination with interferon alpha2-b. The study failed to show any efficacy on UM patients (Solti et al., 2007).

Immunotherapy treatment with **Ipilimumab** is also reported. Retrospective series reported limited activity of the compound in metastatic UM patients with a range of OS form 5,2 to 9.6 (Danielli et al., 2012; Kelderman et al., 2013; Luke et al., 2013; Maio et al., 2013). **Anti-PDL1** antibodies, other molecules that increase immunitary response versus tumoral cells, have also been suggested to be effective in UM through in vitro studies on UM cell lines (Yang et al., 2008b), however no dedicated clinical study had yet been started.

b. Targeting alteration of cellular pathways of UM

As UM show **constitutive activation** of **MAPK pathway** (Babchia et al., 2008, 2010; Calipel et al., 2006; Weber et al., 2003), numerous preclinical studies have tested **MEK inhibitors** as a therapeutic approach for UM. Calipel et al. demonstrate effective inhibition of UM cell lines with the MEK inhibitor **UO126** independently of BRaf mutational status (Calipel et al., 2006). Studies on the potent and orally available non ATP-competitive MEK1 inhibitor **Selumetinib** (AZD6244) demonstrated a specificity for GNAQ and BRAF mutated lines (Ambrosini et al., 2012) and showed to downregulate not only MAPK signaling but to reduce phosphorylation of mTOR

effector p70S6K in GNAQ mutated cell line 92.1 (Ho et al., 2012b), confirming the possibility of interconnections between the two pathways already reported by Babchia et al. (Babchia et al., 2010).

With the identification of GNAQ and GNA11 mutations as drivers of UM, MEK inhibitors where shown to possess selectivity for mutated tumors and the validation of this class of molecules towards the clinical setting was pushed further. However the in vitro efficacy of MEK inhibition seems less important on GNAQ/11 mutated lines than on BRAF mutated ones as showed by the study of Mitsiades et al, suggesting a reduced efficacy of this class of compounds in UM compared to its cutaneous counterpart (Mitsiades et al., 2011).

A randomized phase I trial compared the efficacy of temozolomide vs. Selumetinib in120 first-line metastatic patients (Carvajal RD et al., 2014). Objective response rate was 15% for Selumetinib versus 0% with chemotherapy , stablilization was achieved in 50 vs 23% of the patients respectively; the median PFS was significantly improved in patients receiving Selumetinib: 16 versus 7 weeks; but not OS (11.8 months versus 9.1 months).

Sorafenib, another compound acting on the MAPK cascade, but upstream of MEK had been tested for activity in UM. Sorafenib is a small molecule inhibitor of RAF as well as PDGFR-B, VEGFR and Kit. Unfortunately clinical assessment of this strategy has failed to show any efficacy: a phase II trial of Sorafenib in combination with Paclitaxel and carboplatin (SWOG S0512) was terminated early because of absence of objective response with RECIST criteria (Bhatia et al., 2012). Indeed, recent studies in cutaneous melanoma showed that inhibition of BRaf in BRaf Wt tumors paradoxically activates MEK1/2, promoting neoplastic proliferation that suggest that single agent BRaf inhibition might be detrimental in UM patients (Infante and Swanton, 2014).

GNAQ and 11 mutations were reported to be oncogenic and to activate MAPK pathway through PLCB/PKC activation. Consequently, a blockade of PKC activity would represent an alternative strategy to inhibiting the MAPK cascade. Two PKC inhibitors, Enzastaurin (LY317615) and Sotrastaurin (AEB071), have been tested in UM cell lines (Wu et al., 2012b, 2012c). Both showed to selectively target GNAQ mutated cell lines with a reduction in cell viability correlated with inhibiton of PKC/ERK PKC/NFkB signaling activities. A clinical phase I trial had been launched to

confirm activity of Sotrastaurin in metastatic UM patients (NCT01430416). A preliminary report showed clinical benefit in about half of patients. Unfortunately, a limited number of objective responses were observed and the drug activity appeared more often correlated with disease stabilization (Piperno-Neumann et al., 2014b). Ancillary studies have therefore been focusing on the search of biomarker of PKC inhibitor efficacy in patients but with still no success (Piperno-Neumann et al., 2014a). A second phase Ib/II trial is ongoing, combining sotrastaurin (AEB071) and a MEK inhibitor (MEK 162) (NCT01801358).

A second pathway that was shown to be activated in UM is the **PI3K/mTOR** pathway (Abdel-Rahman et al., 2006; Ambrosini et al., 2013; Babchia et al., 2010a; Bao et al., 2012b; Musi et al., 2014a; Ye et al., 2008). Babchia et al. reports reducution in cell viability upon administration of the PI3K inhibitor LY294002 , and the result was confirmed on other cell lines by (Babchia et al., 2010b).Reports on AKT inhibitors activity is more controversial, Lefevre reports limited in vitro efficacy of AKT inhibition AKT inhibitors showed limited effects on UM cell lines in while more important effects were reported by Ambrosini et al. (Ambrosini et al., 2013; Lefevre et al., 2004). Interestingly, inhibition of the downstream AKT effector mTOR with Rapamycin, a selective inhibitor of the mTORC1 complex, had only minor efficacy on the tested cell lines in the study of Babchia (Babchia et al., 2010b). However, in another study the effects of the ATP competitive mTOR inhibitor AZD8055 were more pronounced than the effects of Selumetinib on a xenograft model of the GNAQ mutated cell line 92.1 (Ho et al., 2012a), supporting a potential role for mTOR driven signaling in UM growth. Even if preclinical work on mTOR signaling and activity in UM is still limited, a phase II clinical trial (NCT01252251) has already been launched to test the Rapamycin analogue **Everolimus** (RAD001) **in combination with** the somatostatin receptor inhibitor **Pasireotide** in metastatic UM. The outcomes of this trial are expected at the end of 2015. Another clinical trial (NCT01979523) is testing the **AKT inhbitor** GSK2141795 **in combination with** MEK **inhibitor** Trametinib, while no clinical assesment of PI3K inhibitors has yet been reported.

The activation of other signaling cascades which are suggested to converge to MAPK and PI3K cascades depends on signaling form **receptor tyrosine kinases** (RTKs) such as **C-Kit**, **IGF1R** and **MET**.

C-kit pathway has been shown to be activated in UM, with early studies demonstrated a good inhibition with Imatinib, a c-kit inhibitor, in UM cell lines (Lefevre et al., 2004). However, another study using tumor-derived UM cells reported only a weak activity of **Imatinib**, comparable to the effects achieved in cutaneous melanoma (Knight et al., 2006). In agreement with this finding, a phase II trial in UM assessing the efficacy of Imatinib in UM metastatic patients was stopped after 5 months because of absence of objective response in 13 patients (Penel et al., 2008). Similar conclusions were drawn from another study on 12 patients (Hofmann et al., 2009). A pilot study on 20 patients with **Sunitinib**, a multi kinase inhibitor that acts on c-KIT, PDGF and VEGF receptors, showed as well modest results: median OS and PFS were 8.2 and 4.2 months respectively, which is similar to the data presented for conventional therapies. Grade 3 and 4 toxicity was also frequently observed and led to dose reductions in 11 patients. Moreover no correlation of c-Kit expression with OS or PFS of patients was found (Mahipal et al., 2012). Finally a randomized multicenter trial on 74 comparing Dacarbazine with Sunitinib in advanced UM patients was stopped for futility (Sacco et al., 2013).

IGFR was suggested to be enriched in metastatic tumors (Economou et al., 2005). Inhbition of this receptor with Picropodophyllin resulted in reduced UM cell viability, diminished phosphorylation of ERK and AKT, induced apoptosis and caused tumor regression in OCM1 injected xenografts; in this model a reduced number of liver micrometastasis compared to controls was also observed (Economou et al., 2008; Girnita et al., 2006).

To date, no clinical trial with specific IGFR pathway inhibitors is ongoing. Indeed Pasireotide, a somatostatin analogue that has been shown to suppress IGF1R function (Patel et al., 2011) is being tested in metastatic UM patients, and somatostatin receptors were recently found expressed in about 50% of metastasis (Valsecchi et al., 2013),a notion that further supports the value of testing this compound.

Finally, inhibition of **MET** was suggested to have an impact on spreading and progression of UM in preclinical models. Met is the RTK for the hepatocyte growth factor, a soluble molecule produced in the liver which was suggested to contribute to

progression of UM and might possibly explain UM specific tropism. Surriga et al. tested the MET and ALK inhibitor Crizotinib in a xenograft model of UM metastasis (Surriga et al., 2013): the experimental group treated with Crizotinib presented a significant decrease in number and size of metastases compared to the control group. The same study reports that Crizotinib alone failed to induce significant antiproliferative and cytotoxic effects on already established tumors, showing that Crizotinib alone is probably insufficient to cure metastatic disease but might be more effective in adjuvant combination therapy.

Another class of compounds which might impact on UM metastasis are HDAC inhibitors. A preclinical study showed some proof of efficacy of HDAC inhibitors on primary and metastatic UM already in 2003 (Klisovic et al., 2003); this therapeutical strategy was then re-proposed by Landreville et al. . HDAC inhibitors were identified as a result of a bioinformatics screen of compounds able to revert the molecular class towards a low-risk profile and were then suggested to decrease the propensity of tumors to induce metastasis, however they resulted in limited reduction of cell viability in vitro and in vivo (Landreville et al., 2012). A clinical trial NCT01587352 is currently testing the efficacy of Vorinostat, an HDAC inhibitor, on metastatic UM patients , even if this class of compounds might be more useful in an adjuvant setting, as in the case of clinical trial NCT02068586, testing Valproic Acid, wich demonstrated activity in inhibiting HDAC, in high risk (non-metastatic) UM patients.

Another therapeutic strategy suggested by preclinical works imply the use of **HSP90 inhibitors**. Two compounds, 17-AAG and its analogue 17-DMAG, are very potent inhibitors of UM cell proliferation in vitro, and their specificity of action might rely on inhibition of HSP90 chaperone activity towards B-Raf or Cyclin D1 (Babchia et al., 2008). Moreover, a combination of 17-DMAG, an HSP90 inhibitor, with Imatinib has synergistic inhibitory effects on cell proliferation in UM cell lines, suggesting a possible therapeutic use of these compounds in combination (Babchia et al., 2008).

Finally two recent papers show the implication of the protein YAP in the proliferation and survival of GNAQ/11 mutated UM cell lines (Feng et al., 2014; Yu et al., 2014a). These papers showed that inhibition of YAP using the compound Verteporfin reduces tumor growth in UM xenografts. However further studies using more specific compounds in a wider range of UM models are required to confirm these preliminary

results. Importantly, the limited efficacy obtained with single drug therapy also suggests that drug combinations might be more effective in killing UM cell and reduce tumor growth in vivo.

c. Combination therapy

Single agent therapies proved limited efficacy in UM, moreover, the effectiveness of these agents tested on other type of cancer had been limited by the emergence of drug resistances. This pushed clinicians and researchers to test combinatorial therapies in order to obtain significant clinical benefit.

Combinations with compounds targeting the three main pathways that had been implicated in UM (MEK/ERK, PKC and PI3K/mTOR) have been studied in the preclinical setting.

Chen et al. tested the combination of **PKC inhibitor** Sotrastaurin and **MEK inhibitor** MEK162 on a 92.1 xenograft mouse model and showed tumor shrinkage with the combination which was not achieved with monotherapies (Chen et al., 2013a). In vitro assays with MEK inhibitor PD0325901 and Sotrastaurin showed a strong synergy and an increase in apoptosis. The two drugs were confirmed to target the same pathway, being MEK downstream of PKC, and to lead to a more complete dephosphorylation of ERK possibly preventing a negative feedback loop to MEK inhibition via PKC. A phase Ib/II clinical trial with AEBB071 and MEK162 in patients with metastatic UM is currently ongoing (NCT01801358).

The combination of **MEK inhibitor** and **PI3K inhibitor** was also reported to have a synergistic effect with induction of apoptosis in a GNAQ/11 dependent manner by Khalili et al. The effect is explained by a reverse correlation between MAPK or AKT phosphorylation and PI3K or MEK inhibition respectively (Khalili et al., 2012); this confirms the crosstalk between ERK and PI3K/MTOR pathway in UM already suggested by Babchia (Babchia et al., 2010).

A combination between MEK inhibitor Selumetinib and AKT inhibitor MK2206 was reported as synergistic in GNAQ mutated cell lines 92.1 and Omm1.3, while no synergy was observed in the BRAF mutated cell line OCM1 and the GNAQ/11 Wild type cell line Mel290. This study reported a selective induction of autophagy with the combination in GNAQ mutated cell lines. Finally an enhanced effect of the

combination was assessed in a xenograft model injected with 92.1 cells (Ambrosini et al., 2013). NCT01979523, a clinical trial with MEK inhibitor trametinib with or without AKT inhibitor GSK2141795 is currently testing the effects of this double inhibition in metastatic UM patients.

Ho et al. tested the association between **MEK inhibitor** Selumetinib and the ATP-competitive **mTOR inhibitor** AZD8055. Although this combination was synergistic in a GNAQ as well as in a BRAF mutated context, significant increase of apoptosis was shown for BRAF mutated cell lines only; *in vivo* experiments also confirmed an enhanced efficacy with tumor regression on a BRAF mutated model only, while the effect of the combination was not statistically different form mTOR inhibitor monotherapy in a GNAQ mutated context (Ho et al., 2012a).

The combination of a **PI3K inhibitor** with the **PKC inhibitor** Sotrastaurin had also been tested: Musi et. al. reported a synergistic effect of BYL719 with Sotrastaurin in GNAQ mutant cells, with induction of apoptosis. In vivo studies with injected 92.1 cells proved an increased inhibition of tumor growth compared to monotherapies (Musi et al., 2014b).

The possibility of targeting the PI3K/mTOR pathway in UM with a combination of **PI3K inhibitor** and an **mTOR inhibitor** had been reported by Babchia, who showed a synergistic interaction in 92.1 cell line (Babchia et al., 2010b).

Finally the idea of combining **MEK inhibition** with **MET inhibition** is suggested by Chattopadhyay, who showed a GNAQ-selective effect of the combination of MEK inhibitor Selumetinib and MET inhibitor MK8033, which resulted in an increase of apoptosis in GNAQ mutants only. On the contrary a reduction in cell migration was observed in GNAQ mutated as well as WT cells (Chattopadhyay et al., 2014).

VIII. REFERENCES

Aalto, Y., Eriksson, L., Seregard, S., Larsson, O., and Knuutila, S. (2001). Concomitant loss of chromosome 3 and whole arm losses and gains of chromosome 1, 6, or 8 in metastasizing primary uveal melanoma. Invest. Ophthalmol. Vis. Sci. *42*, 313–317.

Abdel-Rahman, M.H., Yang, Y., Zhou, X.-P., Craig, E.L., Davidorf, F.H., and Eng, C. (2006). High Frequency of Submicroscopic Hemizygous Deletion Is a Major Mechanism of Loss of Expression of PTEN in Uveal Melanoma. JCO *24*, 288–295.

Abdel-Rahman, M.H., Pilarski, R., Cebulla, C.M., Massengill, J.B., Christopher, B.N., Boru, G., Hovland, P., and Davidorf, F.H. (2011). Germline BAP1 mutation predisposes to uveal melanoma, lung adenocarcinoma, meningioma, and other cancers. J. Med. Genet. *48*, 856–859.

Agarwala, S.S., Panikkar, R., and Kirkwood, J.M. (2004). Phase I/II randomized trial of intrahepatic arterial infusion chemotherapy with cisplatin and chemoembolization with cisplatin and polyvinyl sponge in patients with ocular melanoma metastatic to the liver. Melanoma Res. *14*, 217–222.

Albert, D.M., and Polans, A. (2003). Ocular Oncology (CRC Press).

Albert, D.M., Ruzzo, M.A., McLaughlin, M.A., Robinson, N.L., Craft, J.L., and Epstein, J. (1984). Establishment of cell lines of uveal melanoma. Methodology and characteristics. IOVS *25*, 1284–1299.

Al-Jamal, R.T., and Kivelä, T. (2011). Prognostic associations of insulin-like growth factor-1 receptor in primary uveal melanoma. Can. J. Ophthalmol. *46*, 471–476.

All-Ericsson, C., Girnita, L., Seregard, S., Bartolazzi, A., Jager, M.J., and Larsson, O. (2002). Insulin-like growth factor-1 receptor in uveal melanoma: a predictor for metastatic disease and a potential therapeutic target. Invest. Ophthalmol. Vis. Sci. *43*, 1–8.

All-Ericsson, C., Girnita, L., Müller-Brunotte, A., Brodin, B., Seregard, S., Ostman, A., and Larsson, O. (2004). c-Kit-dependent growth of uveal melanoma cells: a potential therapeutic target? Invest. Ophthalmol. Vis. Sci. *45*, 2075–2082.

Ambrosini, G., Pratilas, C.A., Qin, L.-X., Tadi, M., Surriga, O., Carvajal, R.D., and Schwartz, G.K. (2012). Identification of Unique MEK-Dependent Genes in GNAQ Mutant Uveal Melanoma Involved in Cell Growth, Tumor Cell Invasion, and MEK Resistance. Clin Cancer Res *18*, 3552–3561.

Ambrosini, G., Musi, E., Ho, A.L., De Stanchina, E., and Schwartz, G.K. (2013). Inhibition of Mutant GNAQ Signaling in Uveal Melanoma Induces AMPK-Dependent Autophagic Cell Death. Mol. Cancer Ther.

Aoyama, T., Mastrangelo, M.J., Berd, D., Nathan, F.E., Shields, C.L., Shields, J.A., Rosato, E.L., Rosato, F.E., and Sato, T. (2000). Protracted survival after resection of metastatic uveal melanoma. Cancer *89*, 1561–1568.

Aubert, C., Rouge, F., Reillaudou, M., and Metge, P. (1993). Establishment and characterization of human ocular melanoma cell lines. Int. J. Cancer *54*, 784–792.

Augsburger, J.J., Gamel, J.W., and Shields, J.A. (1989). Cobalt plaque radiotherapy versus enucleation for posterior uveal melanoma: comparison of survival by prognostic index groups. Trans Am Ophthalmol Soc *87*, 348–359; discussion 359–361.

Augsburger, J.J., Gamel, J.W., Lauritzen, K., and Brady, L.W. (1990). Cobalt-60 plaque radiotherapy vs enucleation for posterior uveal melanoma. Am. J. Ophthalmol. *109*, 585–592.

Augsburger, J.J., Corrêa, Z.M., and Shaikh, A.H. (2009). Effectiveness of treatments for metastatic uveal melanoma. Am. J. Ophthalmol. *148*, 119–127.

Babchia, N., Calipel, A., Mouriaux, F., Faussat, A.-M., and Mascarelli, F. (2008). 17-AAG and 17-DMAG-induced inhibition of cell proliferation through B-Raf downregulation in WT B-Raf-expressing uveal melanoma cell lines. Invest. Ophthalmol. Vis. Sci. *49*, 2348–2356.

Babchia, N., Calipel, A., Mouriaux, F., Faussat, A.-M., and Mascarelli, F. (2010a). The PI3K/Akt and mTOR/P70S6K signaling pathways in human uveal melanoma cells: interaction with B-Raf/ERK. Invest. Ophthalmol. Vis. Sci. *51*, 421–429.

Babchia, N., Calipel, A., Mouriaux, F., Faussat, A.-M., and Mascarelli, F. (2010b). The PI3K/Akt and mTOR/P70S6K signaling pathways in human uveal melanoma cells: interaction with B-Raf/ERK. Invest. Ophthalmol. Vis. Sci. *51*, 421–429.

Bakalian, S., Marshall, J.-C., Logan, P., Faingold, D., Maloney, S., Cesare, S.D., Martins, C., Fernandes, B.F., and Burnier, M.N. (2008). Molecular Pathways Mediating Liver Metastasis in Patients with Uveal Melanoma. Clin Cancer Res *14*, 951–956.

Bao, X., Song, H., and Tang, X. (2012a). [Clinicopathological significance of expression of IGF-1R in uveal melanoma and its association with expression of p-AKT Thr308]. Zhonghua Yan Ke Za Zhi *48*, 413–416.

Bao, X., Song, H., and Tang, X. (2012b). [Clinicopathological significance of expression of IGF-1R in uveal melanoma and its association with expression of p-AKT Thr308]. Zhonghua Yan Ke Za Zhi *48*, 413–416.

Barbazetto, I.A., Lee, T.C., Rollins, I.S., Chang, S., and Abramson, D.H. (2003). Treatment of choroidal melanoma using photodynamic therapy. Am. J. Ophthalmol. *135*, 898–899.

Barishak, Y.R., Vanherick, W., and Yoneda, C. (1960). Tissue culture of uveal melanomas. Arch. Ophthalmol. *64*, 352–366.

Baserga, R. (1995). The Insulin-like Growth Factor I Receptor: A Key to Tumor Growth? Cancer Res *55*, 249–252.

Becher, R., Gibas, Z., Karakousis, C., and Sandberg, A.A. (1983). Nonrandom chromosome changes in malignant melanoma. Cancer Res. *43*, 5010–5016.

Bechrakis, N.E., Petousis, V., Willerding, G., Krause, L., Wachtlin, J., Stroux, A., and Foerster, M.H. (2010). Ten-year results of transscleral resection of large uveal melanomas: local tumour control and metastatic rate. Br J Ophthalmol *94*, 460–466.

Bedikian, A.Y., Papadopoulos, N., Plager, C., Eton, O., and Ring, S. (2003). Phase II evaluation of temozolomide in metastatic choroidal melanoma. Melanoma Res. *13*, 303–306.

Bhatia, S., Moon, J., Margolin, K.A., Weber, J.S., Lao, C.D., Othus, M., Aparicio, A.M., Ribas, A., and Sondak, V.K. (2012). Phase II trial of sorafenib in combination with carboplatin and paclitaxel in patients with metastatic uveal melanoma: SWOG S0512. PLoS ONE *7*, e48787.

Blanco, P.L., Marshall, J.C.A., Antecka, E., Callejo, S.A., Filho, J.P.S., Saraiva, V., and Burnier, M.N. (2005). Characterization of Ocular and Metastatic Uveal Melanoma in an Animal Model. IOVS *46*, 4376–4382.

Blasi, M.A., Roccella, F., Balestrazzi, E., Del Porto, G., De Felice, N., Roccella, M., Rota, R., and Grammatico, P. (1999). 3p13 region: a possible location of a tumor suppressor gene involved in uveal melanoma. Cancer Genet. Cytogenet. *108*, 81–83.

Borthwick, N.J., Thombs, J., Polak, M., Gabriel, F.G., Hungerford, J.L., Damato, B., Rennie, I.G., Jager, M.J., and Cree, I.A. (2011). The biology of micrometastases from uveal melanoma. Journal of Clinical Pathology *64*, 666–671.

Van den Bosch, T., Kilic, E., Paridaens, D., and De Klein, A. (2010). Genetics of uveal melanoma and cutaneous melanoma: two of a kind? Dermatol Res Pract *2010*, 360136.

Buecher, B., Gauthier-Villars, M., Desjardins, L., Lumbroso-Le Rouic, L., Levy, C., Pauw, A., Bombled, J., Tirapo, C., Houdayer, C., Bressac-de Paillerets, B., et al. (2010). Contribution of CDKN2A/P16 INK4A , P14 ARF , CDK4 and BRCA1/2 germline mutations in individuals with suspected genetic predisposition to uveal melanoma. Familial Cancer *9*, 663–667.

Calipel, A., Mouriaux, F., Glotin, A.-L., Malecaze, F., Faussat, A.-M., and Mascarelli, F. (2006). Extracellular Signal-regulated Kinase-dependent Proliferation Is Mediated through the Protein Kinase A/B-Raf Pathway in Human Uveal Melanoma Cells. J. Biol. Chem. *281*, 9238–9250.

Calipel, A., Abonnet, V., Nicole, O., Mascarelli, F., Coupland, S.E., Damato, B., and Mouriaux, F. (2011). Status of RASSF1A in Uveal Melanocytes and Melanoma Cells. Mol Cancer Res *9*, 1187–1198.

Campbell, W.G., and Pejnovic, T.M. (2012). Treatment of amelanotic choroidal melanoma with photodynamic therapy. Retina (Philadelphia, Pa.) *32*, 1356–1362.

Carbone, M., Yang, H., Pass, H.I., Krausz, T., Testa, J.R., and Gaudino, G. (2013). BAP1 and cancer. Nat. Rev. Cancer *13*, 153–159.

Carvajal RD, Sosman JA, Quevedo J, and Et al (2014). Effect of selumetinib vs chemotherapy on progression-free survival in uveal melanoma: A randomized clinical trial. JAMA *311*, 2397–2405.

Cassoux, N., Rodrigues, M.J., Plancher, C., Asselain, B., Levy-Gabriel, C., Lumbroso-Le Rouic, L., Piperno-Neumann, S., Dendale, R., Sastre, X., Desjardins, L., et al. (2014). Genome-wide profiling is a clinically relevant and affordable prognostic test in posterior uveal melanoma. Br J Ophthalmol *98*, 769–774.

Caujolle, J.-P., Paoli, V., Chamorey, E., Maschi, C., Baillif, S., Herault, J., Gastaud, P., and Hannoun-Levi, J.M. (2013). Local recurrence after uveal melanoma proton beam therapy: recurrence types and prognostic consequences. Int. J. Radiat. Oncol. Biol. Phys. *85*, 1218–1224.

Chattopadhyay, C., Grimm, E.A., and Woodman, S.E. (2014). Simultaneous inhibition of the HGF/MET and Erk1/2 pathways affect uveal melanoma cell growth and migration. PLoS ONE *9*, e83957.

Chen, X., Wang, J., Shen, H., Lu, J., Li, C., Hu, D.-N., Dong, X.D., Yan, D., and Tu, L. (2011). Epigenetics, MicroRNAs, and Carcinogenesis: Functional Role of MicroRNA-137 in Uveal Melanoma. IOVS *52*, 1193–1199.

Chen, X., Wu, Q., Tan, L., Porter, D., Jager, M.J., Emery, C., and Bastian, B.C. (2013a). Combined PKC and MEK inhibition in uveal melanoma with GNAQ and GNA11 mutations. Oncogene.

Chen, X., He, D., Dong, X.D., Dong, F., Wang, J., Wang, L., Tang, J., Hu, D.-N., Yan, D., and Tu, L. (2013b). MicroRNA-124a is epigenetically regulated and acts as a tumor suppressor by controlling multiple targets in uveal melanoma. Invest. Ophthalmol. Vis. Sci. *54*, 2248–2256.

Crosby, M.B., Yang, H., Gao, W., Zhang, L., and Grossniklaus, H.E. (2011). Serum vascular endothelial growth factor (VEGF) levels correlate with number and location of micrometastases in a murine model of uveal melanoma. Br J Ophthalmol *95*, 112–117.

Cross, N.A., Murray, A.K., Rennie, I.G., Ganesh, A., and Sisley, K. (2003). Instability of microsatellites is an infrequent event in uveal melanoma. Melanoma Res. *13*, 435–440.

De la Cruz, P.O., Specht, C.S., and McLean, I.W. (1990). Lymphocytic infiltration in uveal malignant melanoma. Cancer *65*, 112–115.

Damato, B., Dopierala, J., Klaasen, A., Van Dijk, M., Sibbring, J., and Coupland, S.E. (2009). Multiplex ligation-dependent probe amplification of uveal melanoma: correlation with metastatic death. Invest. Ophthalmol. Vis. Sci. *50*, 3048–3055.

Damato, B., Eleuteri, A., Taktak, A.F.G., and Coupland, S.E. (2011). Estimating prognosis for survival after treatment of choroidal melanoma. Progress in Retinal and Eye Research *30*, 285–295.

Damato, B., Kacperek, A., Errington, D., and Heimann, H. (2013). Proton beam radiotherapy of uveal melanoma. Saudi Journal of Ophthalmology *27*, 151–157.

Danielli, R., Ridolfi, R., Chiarion-Sileni, V., Queirolo, P., Testori, A., Plummer, R., Boitano, M., Calabrò, L., Rossi, C.D., Giacomo, A.M.D., et al. (2012). Ipilimumab in pretreated patients with metastatic uveal melanoma: safety and clinical efficacy. Cancer Immunol. Immunother. *61*, 41–48.

Daniels, A.B., Lee, J.-E., MacConaill, L.E., Palescandolo, E., Hummelen, P.V., Adams, S.M., DeAngelis, M.M., Hahn, W.C., Gragoudas, E.S., Harbour, J.W., et al. (2012). High Throughput Mass Spectrometry-Based Mutation Profiling of Primary Uveal Melanoma. IOVS *53*, 6991–6996.

Demicheli, R., Fornili, M., and Biganzoli, E. (2014). Bimodal mortality dynamics for uveal melanoma: a cue for metastasis development traits? BMC Cancer *14*, 392.

Dendale, R., Lumbroso-Le Rouic, L., Noel, G., Feuvret, L., Levy, C., Delacroix, S., Meyer, A., Nauraye, C., Mazal, A., Mammar, H., et al. (2006). Proton beam radiotherapy for uveal melanoma: results of Curie Institut-Orsay proton therapy center (ICPO). Int. J. Radiat. Oncol. Biol. Phys. *65*, 780–787.

Desjardins, L., Lumbroso, L., Levy, C., Mazal, A., Delacroix, S., Rosenwald, J.C., Dendale, R., Plancher, C., and Asselain, B. (2003). [Treatment of uveal melanoma with iodine 125 plaques or proton beam therapy: indications and comparison of local recurrence rates]. J Fr Ophtalmol *26*, 269–276.

Desjardins, L., Levy-Gabriel, C., Lumbroso-Lerouic, L., Sastre, X., Dendale, R., Couturier, J., Piperno-Neumann, S., Dorval, T., Mariani, P., Salmon, R., et al. (2006). [Prognostic factors for malignant uveal

melanoma. Retrospective study on 2,241 patients and recent contribution of monosomy-3 research]. J Fr Ophtalmol *29*, 741–749.

Desjardins, L., Lumbroso-Le Rouic, L., Levy-Gabriel, C., Cassoux, N., Dendale, R., Mazal, A., Delacroix, S., Sastre, X., Plancher, C., and Asselain, B. (2012). Treatment of uveal melanoma by accelerated proton beam. Dev Ophthalmol *49*, 41–57.

Diener-West, M., Hawkins, B.S., Markowitz, J.A., and Schachat, A.P. (1992). A review of mortality from choroidal melanoma. II. A meta-analysis of 5-year mortality rates following enucleation, 1966 through 1988. Arch. Ophthalmol. *110*, 245–250.

Diener-West, M., Earle, J.D., Fine, S.L., Hawkins, B.S., Moy, C.S., Reynolds, S.M., Schachat, A.P., Straatsma, B.R., and Collaborative Ocular Melanoma Study Group (2001). The COMS randomized trial of iodine 125 brachytherapy for choroidal melanoma, III: initial mortality findings. COMS Report No. 18. Arch. Ophthalmol. *119*, 969–982.

Diener-West, M., Reynolds, S.M., Agugliaro, D.J., Caldwell, R., Cumming, K., Earle, J.D., Green, D.L., Hawkins, B.S., Hayman, J., Jaiyesimi, I., et al. (2004). Screening for Metastasis From Choroidal Melanoma: The Collaborative Ocular Melanoma Study Group Report 23. JCO *22*, 2438–2444.

Diener-West, M., Reynolds, S.M., Agugliaro, D.J., Caldwell, R., Cumming, K., Earle, J.D., Hawkins, B.S., Hayman, J.A., Jaiyesimi, I., Jampol, L.M., et al. (2005). Development of metastatic disease after enrollment in the COMS trials for treatment of choroidal melanoma: Collaborative Ocular Melanoma Study Group Report No. 26. Arch. Ophthalmol. *123*, 1639–1643.

Dong, F., and Lou, D. (2012). MicroRNA-34b/c suppresses uveal melanoma cell proliferation and migration through multiple targets. Mol. Vis. *18*, 537–546.

Dono, M., Angelini, G., Cecconi, M., Amaro, A., Esposito, A.I., Mirisola, V., Maric, I., Lanza, F., Nasciuti, F., Viaggi, S., et al. (2014). Mutation frequencies of GNAQ, GNA11, BAP1, SF3B1, EIF1AX and TERT in uveal melanoma: detection of an activating mutation in the TERT gene promoter in a single case of uveal melanoma. Br J Cancer *110*, 1058–1065.

Dratviman-Storobinsky, O., Cohen, Y., Frenkel, S., Merhavi-Shoham, E., El, S.D.-B., Binkovsky, N., Pe'er, J., and Goldenberg-Cohen, N. (2012). The role of RASSF1A in uveal melanoma. Invest. Ophthalmol. Vis. Sci. *53*, 2611–2619.

Dunavoelgyi, R., Dieckmann, K., Gleiss, A., Sacu, S., Kircher, K., Georgopoulos, M., Georg, D., Zehetmayer, M., and Poetter, R. (2011). Local Tumor Control, Visual Acuity, and Survival After Hypofractionated Stereotactic Photon Radiotherapy of Choroidal Melanoma in 212 Patients Treated Between 1997 and 2007. International Journal of Radiation Oncology*Biology*Physics *81*, 199–205.

Dunavoelgyi, R., Dieckmann, K., Gleiss, A., Sacu, S., Kircher, K., Georgopoulos, M., Georg, D., Zehetmayer, M., and Poetter, R. (2012). Radiogenic side effects after hypofractionated stereotactic photon radiotherapy of choroidal melanoma in 212 patients treated between 1997 and 2007. Int. J. Radiat. Oncol. Biol. Phys. *83*, 121–128.

Economou, M.A., All-Ericsson, C., Bykov, V., Girnita, L., Bartolazzi, A., Larsson, O., and Seregard, S. (2005). Receptors for the liver synthesized growth factors IGF-1 and HGF/SF in uveal melanoma: intercorrelation and prognostic implications. Invest. Ophthalmol. Vis. Sci. *46*, 4372–4375.

Economou, M.A., Andersson, S., Vasilcanu, D., All-Ericsson, C., Menu, E., Girnita, A., Girnita, L., Axelson, M., Seregard, S., and Larsson, O. (2008). Oral picropodophyllin (PPP) is well tolerated in vivo and inhibits IGF-1R expression and growth of uveal melanoma. Acta Ophthalmol *86 Thesis 4*, 35–41.

Edelhauser, G., Schicher, N., Berzaczy, D., Beitzke, D., Höeller, C., Lammer, J., and Funovics, M. (2012). Fotemustine chemoembolization of hepatic metastases from uveal melanoma: a retrospective single-center analysis. AJR Am J Roentgenol *199*, 1387–1392.

Edmunds, S.C., Kelsell, D.P., Hungerford, J.L., and Cree, I.A. (2002). Mutational analysis of selected genes in the TGFbeta, Wnt, pRb, and p53 pathways in primary uveal melanoma. Invest. Ophthalmol. Vis. Sci. *43*, 2845–2851.

Edmunds, S.C., Cree, I.A., Dí Nícolantonío, F., Hungerford, J.L., Hurren, J.S., and Kelsell, D.P. (2003). Absence of BRAF gene mutations in uveal melanomas in contrast to cutaneous melanomas. Br J Cancer *88*, 1403–1405.

Ehlers, J.P., and Harbour, J.W. (2005). NBS1 expression as a prognostic marker in uveal melanoma. Clin. Cancer Res. *11*, 1849–1853.

Ehlers, J.P., Worley, L., Onken, M.D., and Harbour, J.W. (2005). DDEF1 is located in an amplified region of chromosome 8q and is overexpressed in uveal melanoma. Clin. Cancer Res. *11*, 3609–3613.

Ehlers, J.P., Worley, L., Onken, M.D., and Harbour, J.W. (2008). Integrative genomic analysis of aneuploidy in uveal melanoma. Clin. Cancer Res. *14*, 115–122.

Ellerhorst, J.A., Bedikian, A.Y., Smith, T.M., Papadopoulos, N.E., Plager, C., and Eton, O. (2002). Phase II trial of 9-nitrocamptothecin (RFS 2000) for patients with metastatic cutaneous or uveal melanoma. Anticancer Drugs *13*, 169–172.

Ewens, K.G., Kanetsky, P.A., Richards-Yutz, J.A., Purrazzella, J., Shields, C.L., Ganguly, T., and Ganguly, A. (2014). Chromosome 3 Status Combined with BAP1 and EIF1AX Mutation Profiles are Associated with Metastasis in Uveal Melanoma. Invest. Ophthalmol. Vis. Sci.

Feng, X., Degese, M.S., Iglesias-Bartolome, R., Vaque, J.P., Molinolo, A.A., Rodrigues, M., Zaidi, M.R., Ksander, B.R., Merlino, G., Sodhi, A., et al. (2014). Hippo-Independent Activation of YAP by the GNAQ Uveal Melanoma Oncogene through a Trio-Regulated Rho GTPase Signaling Circuitry. Cancer Cell *25*, 831–845.

Folberg, R., Rummelt, V., Parys-Van Ginderdeuren, R., Hwang, T., Woolson, R.F., Pe'er, J., and Gruman, L.M. (1993). The prognostic value of tumor blood vessel morphology in primary uveal melanoma. Ophthalmology *100*, 1389–1398.

Folberg, R., Kadkol, S.S., Frenkel, S., Valyi-Nagy, K., Jager, M.J., Pe'er, J., and Maniotis, A.J. (2008). Authenticating Cell Lines in Ophthalmic Research Laboratories. Investigative Ophthalmology & Visual Science *49*, 4697–4701.

Foster, W.J., Fuller, C.E., Perry, A., and Harbour, J.W. (2003). Status of the NF1 tumor suppressor locus in uveal melanoma. Arch. Ophthalmol. *121*, 1311–1315.

Frenkel, S., Nir, I., Hendler, K., Lotem, M., Eid, A., Jurim, O., and Pe'er, J. (2009). Long-term survival of uveal melanoma patients after surgery for liver metastases. Br J Ophthalmol *93*, 1042–1046.

Furney, S.J., Pedersen, M., Gentien, D., Dumont, A.G., Rapinat, A., Desjardins, L., Turajlic, S., Piperno-Neumann, S., De la Grange, P., Roman-Roman, S., et al. (2013). SF3B1 mutations are associated with alternative splicing in uveal melanoma. Cancer Discov.

Gamel, J.W., McLean, I.W., Greenberg, R.A., Zimmerman, L.E., and Lichtenstein, S.J. (1982). Computerized histologic assessment of malignant potential: a method for determining the prognosis of uveal melanomas. Hum. Pathol. *13*, 893–897.

Gass, J.D. (1985). Comparison of uveal melanoma growth rates with mitotic index and mortality. Arch. Ophthalmol. *103*, 924–931.

Gentien, D., Kosmider, O., Nguyen-Khac, F., Albaud, B., Rapinat, A., Dumont, A.G., Damm, F., Popova, T., Marais, R., Fontenay, M., et al. (2014). A common alternative splicing signature is associated with SF3B1 mutations in malignancies from different cell lineages. Leukemia *28*, 1355–1357.

Gill, H.S., and Char, D.H. (2012). Uveal melanoma prognostication: from lesion size and cell type to molecular class. Canadian Journal of Ophthalmology / Journal Canadien d'Ophtalmologie *47*, 246–253.

Girnita, A., All-Ericsson, C., Economou, M.A., Aström, K., Axelson, M., Seregard, S., Larsson, O., and Girnita, L. (2006). The insulin-like growth factor-I receptor inhibitor picropodophyllin causes tumor regression and attenuates mechanisms involved in invasion of uveal melanoma cells. Clin. Cancer Res. *12*, 1383–1391.

Goldstein, A.M. (2011). Germline BAP1 mutations and tumor susceptibility. Nat Genet *43*, 925–926.

Goldstein, A.M., Chan, M., Harland, M., Gillanders, E.M., Hayward, N.K., Avril, M.-F., Azizi, E., Bianchi-Scarra, G., Bishop, D.T., Paillerets, B.B., et al. (2006). High-risk Melanoma Susceptibility Genes and Pancreatic Cancer, Neural System Tumors, and Uveal Melanoma across GenoMEL. Cancer Res *66*, 9818–9828.

Gonsalves, C.F., Eschelman, D.J., Sullivan, K.L., Anne, P.R., Doyle, L., and Sato, T. (2011). Radioembolization as salvage therapy for hepatic metastasis of uveal melanoma: a single-institution experience. AJR Am J Roentgenol *196*, 468–473.

Gottlicher, M., Minucci, S., Zhu, P., Kramer, O.H., Schimpf, A., Giavara, S., Sleeman, J.P., Lo Coco, F., Nervi, C., Pelicci, P.G., et al. (2001). Valproic acid defines a novel class of HDAC inhibitors inducing differentiation of transformed cells. EMBO J *20*, 6969–6978.

Griewank, K.G., Yu, X., Khalili, J., Sozen, M.M., Stempke-Hale, K., Bernatchez, C., Wardell, S., Bastian, B.C., and Woodman, S.E. (2012). Genetic and molecular characterization of uveal melanoma cell lines. Pigment Cell Melanoma Res *25*, 182–187.

Griffin, C.A., Long, P.P., and Schachat, A.P. (1988). Trisomy 6p in an ocular melanoma. Cancer Genet. Cytogenet. *32*, 129–132.

Grossniklaus HE (2013). Progression of ocular melanoma metastasis to the liver: The 2012 zimmerman lecture. JAMA Ophthalmol *131*, 462–469.

Guénel, P., Laforest, L., Cyr, D., Févotte, J., Sabroe, S., Dufour, C., Lutz, J.M., and Lynge, E. (2001). Occupational risk factors, ultraviolet radiation, and ocular melanoma: a case-control study in France. Cancer Causes Control *12*, 451–459.

Haluska, F.G., Tsao, H., Wu, H., Haluska, F.S., Lazar, A., and Goel, V. (2006). Genetic alterations in signaling pathways in melanoma. Clin. Cancer Res. *12*, 2301s–2307s.

Harbour, J.W. (2012). The genetics of uveal melanoma: an emerging framework for targeted therapy. Pigment Cell Melanoma Res *25*, 171–181.

Harbour, J.W., and Chen, R. (2013). The DecisionDx-UM Gene Expression Profile Test Provides Risk Stratification and Individualized Patient Care in Uveal Melanoma. PLoS Currents.

Harbour, J.W., Brantley, M.A., Jr, Hollingsworth, H., and Gordon, M. (2004). Association between posterior uveal melanoma and iris freckles, iris naevi, and choroidal naevi. The British Journal of Ophthalmology *88*, 36.

Harbour, J.W., Onken, M.D., Roberson, E.D.O., Duan, S., Cao, L., Worley, L.A., Council, M.L., Matatall, K.A., Helms, C., and Bowcock, A.M. (2010). Frequent Mutation of BAP1 in Metastasizing Uveal Melanomas. Science *330*, 1410–1413.

Harbour, J.W., Roberson, E.D.O., Anbunathan, H., Onken, M.D., Worley, L.A., and Bowcock, A.M. (2013). Recurrent mutations at codon 625 of the splicing factor SF3B1 in uveal melanoma. Nat. Genet. *45*, 133–135.

Hendrix, M.J., Seftor, E.A., Seftor, R.E., Kirschmann, D.A., Gardner, L.M., Boldt, H.C., Meyer, M., Pe'er, J., and Folberg, R. (1998). Regulation of uveal melanoma interconverted phenotype by hepatocyte growth factor/scatter factor (HGF/SF). Am. J. Pathol. *152*, 855–863.

Henriquez, F., Janssen, C., Kemp, E.G., and Roberts, F. (2007). The T1799A BRAF Mutation Is Present in Iris Melanoma. IOVS *48*, 4897–4900.

Ho, A.L., Musi, E., Ambrosini, G., Nair, J.S., Deraje Vasudeva, S., De Stanchina, E., and Schwartz, G.K. (2012a). Impact of combined mTOR and MEK inhibition in uveal melanoma is driven by tumor genotype. PLoS ONE *7*, e40439.

Ho, A.L., Musi, E., Ambrosini, G., Nair, J.S., Deraje Vasudeva, S., De Stanchina, E., and Schwartz, G.K. (2012b). Impact of combined mTOR and MEK inhibition in uveal melanoma is driven by tumor genotype. PLoS ONE *7*, e40439.

Hodge, W.G., Duclos, A.J., Rocha, G., Antecka, E., Baines, M.G., Corriveau, C., Brownstein, S., and Deschenes, J. (1995). DNA index and S phase fraction in uveal malignant melanomas. Br J Ophthalmol *79*, 521–526.

Hofmann, U.B., Kauczok-Vetter, C.S., Houben, R., and Becker, J.C. (2009). Overexpression of the KIT/SCF in uveal melanoma does not translate into clinical efficacy of imatinib mesylate. Clin. Cancer Res. *15*, 324–329.

Homsi, J., Bedikian, A.Y., Papadopoulos, N.E., Kim, K.B., Hwu, W.-J., Mahoney, S.L., and Hwu, P. (2010). Phase 2 open-label study of weekly docosahexaenoic acid-paclitaxel in patients with metastatic uveal melanoma. Melanoma Res. *20*, 507–510.

Horsman, D.E., and White, V.A. (1993). Cytogenetic analysis of uveal melanoma. Consistent occurrence of monosomy 3 and trisomy 8q. Cancer *71*, 811–819.

Horsman, D.E., Sroka, H., Rootman, J., and White, V.A. (1990). Monosomy 3 and isochromosome 8q in a uveal melanoma. Cancer Genet. Cytogenet. *45*, 249–253.

Horsthemke, B., Prescher, G., Bornfeld, N., and Becher, R. (1992). Loss of chromosome 3 alleles and multiplication of chromosome 8 alleles in uveal melanoma. Genes Chromosomes Cancer *4*, 217–221.

Hu, D.-N., Yu, G.-P., McCormick, S.A., Schneider, S., and Finger, P.T. (2005). Population-based incidence of uveal melanoma in various races and ethnic groups. Am. J. Ophthalmol. *140*, 612–617.

Huntington, A., Haugan, P., Gamel, J., and McLean, I. (1989). A simple cytologic method for predicting the malignant potential of intraocular melanoma. Pathol. Res. Pract. *185*, 631–634.

Huppert, P.E., Fierlbeck, G., Pereira, P., Schanz, S., Duda, S.H., Wietholtz, H., Rozeik, C., and Claussen, C.D. (2010). Transarterial chemoembolization of liver metastases in patients with uveal melanoma. Eur J Radiol *74*, e38–44.

Infante, J.R., and Swanton, C. (2014). Combined inhibition of BRAF and MEK in melanoma patients. Lancet Oncol. *15*, 908–910.

Ismail, I.H., Davidson, R., Gagné, J.-P., Xu, Z.Z., Poirier, G.G., and Hendzel, M.J. (2014). Germline Mutations in BAP1 Impair Its Function in DNA Double-Strand Break Repair. Cancer Res.

Jensen, A.W., Petersen, I.A., Kline, R.W., Stafford, S.L., Schomberg, P.J., and Robertson, D.M. (2005). Radiation complications and tumor control after 125I plaque brachytherapy for ocular melanoma. International Journal of Radiation Oncology*Biology*Physics *63*, 101–108.

Jensen, D.E., Proctor, M., Marquis, S.T., Gardner, H.P., Ha, S.I., Chodosh, L.A., Ishov, A.M., Tommerup, N., Vissing, H., Sekido, Y., et al. (1998). BAP1: a novel ubiquitin hydrolase which binds to the BRCA1 RING finger and enhances BRCA1-mediated cell growth suppression. Oncogene *16*, 1097–1112.

Kalirai, H., Dodson, A., Faqir, S., Damato, B.E., and Coupland, S.E. (2014). Lack of BAP1 protein expression in uveal melanoma is associated with increased metastatic risk and has utility in routine prognostic testing. Br. J. Cancer.

Kan-Mitchell, J., Mitchell, M.S., Rao, N., and Liggett, P.E. (1989). Characterization of uveal melanoma cell lines that grow as xenografts in rabbit eyes. IOVS *30*, 829–834.

Karlsson, M., Boeryd, B., Carstensen, J., Frånlund, B., Gustafsson, B., Kågedal, B., Sun, X.-F., and Wingren, S. (1996). Correlations of Ki-67 and PCNA to DNA ploidy, S-phase fraction and survival in uveal melanoma. European Journal of Cancer *32*, 357–362.

Kelderman, S., Van der Kooij, M.K., Van den Eertwegh, A.J.M., Soetekouw, P.M.M.B., Jansen, R.L.H., Van den Brom, R.R.H., Hospers, G.A.P., Haanen, J.B.A.G., Kapiteijn, E., and Blank, C.U. (2013). Ipilimumab in pretreated metastastic uveal melanoma patients. Results of the Dutch Working group on Immunotherapy of Oncology (WIN-O). Acta Oncol *52*, 1786–1788.

Khalili, J.S., Yu, X., Wang, J., Hayes, B.C., Davies, M.A., Lizee, G., Esmaeli, B., and Woodman, S.E. (2012). Combination small molecule MEK and PI3K inhibition enhances uveal melanoma cell death in a mutant GNAQ- and GNA11-dependent manner. Clin. Cancer Res. *18*, 4345–4355.

Kilic, E., Naus, N.C., Van Gils, W., Klaver, C.C., Van Til, M.E., Verbiest, M.M., Stijnen, T., Mooy, C.M., Paridaens, D., Beverloo, H.B., et al. (2005). Concurrent loss of chromosome arm 1p and chromosome 3 predicts a decreased disease-free survival in uveal melanoma patients. Invest. Ophthalmol. Vis. Sci. *46*, 2253–2257.

Kilic, E., Van Gils, W., Lodder, E., Beverloo, H.B., Van Til, M.E., Mooy, C.M., Paridaens, D., De Klein, A., and Luyten, G.P.M. (2006). Clinical and cytogenetic analyses in uveal melanoma. Invest. Ophthalmol. Vis. Sci. *47*, 3703–3707.

Kirby, D.B. (1929). Tissue Culture in Ophthalmic Research. Trans Am Ophthalmol Soc *27*, 334–383.

Kishore, K., Ghazvini, S., Char, D.H., Kroll, S., and Selle, J. (1996). p53 gene and cell cycling in uveal melanoma. Am. J. Ophthalmol. *121*, 561–567.

Kivelä, T., Suciu, S., Hansson, J., Kruit, W.H.J., Vuoristo, M.-S., Kloke, O., Gore, M., Hahka-Kemppinen, M., Parvinen, L.-M., Kumpulainen, E., et al. (2003). Bleomycin, vincristine, lomustine and dacarbazine (BOLD) in combination with recombinant interferon alpha-2b for metastatic uveal melanoma. Eur. J. Cancer *39*, 1115–1120.

Klisovic, D.D., Katz, S.E., Effron, D., Klisovic, M.I., Wickham, J., Parthun, M.R., Guimond, M., and Marcucci, G. (2003). Depsipeptide (FR901228) inhibits proliferation and induces apoptosis in primary and metastatic human uveal melanoma cell lines. Invest. Ophthalmol. Vis. Sci. *44*, 2390–2398.

Knight, L.A., Di Nicolantonio, F., Whitehouse, P.A., Mercer, S.J., Sharma, S., Glaysher, S., Hungerford, J.L., Hurren, J., Lamont, A., and Cree, I.A. (2006). The effect of imatinib mesylate (Glivec) on human tumor-derived cells. Anticancer Drugs *17*, 649–655.

Konstantinidis, L., Roberts, D., Errington, R.D., Kacperek, A., and Damato, B. (2013). Whole anterior segment proton beam radiotherapy for diffuse iris melanoma. Br J Ophthalmol *97*, 471–474.

Koopmans, A.E., Vaarwater, J., Paridaens, D., Naus, N.C., Kilic, E., De Klein, A., and Rotterdam Ocular Melanoma Study group (2013). Patient survival in uveal melanoma is not affected by oncogenic mutations in GNAQ and GNA11. Br. J. Cancer *109*, 493–496.

Koopmans, A.E., Verdijk, R.M., Brouwer, R.W.W., Van den Bosch, T.P.P., Van den Berg, M.M.P., Vaarwater, J., Kockx, C.E.M., Paridaens, D., Naus, N.C., Nellist, M., et al. (2014). Clinical significance of immunohistochemistry for detection of BAP1 mutations in uveal melanoma. Mod. Pathol.

Kujala, E., Mäkitie, T., and Kivelä, T. (2003). Very long-term prognosis of patients with malignant uveal melanoma. Invest. Ophthalmol. Vis. Sci. *44*, 4651–4659.

Lamperska, K., Mackiewicz, K., Kaczmarek, A., Kwiatkowska, E., Starzycka, M., Romanowska, B., Heizman, J., Stachura, J., and Mackiewicz, A. (2002). Expression of p16 in sporadic primary uveal melanoma. Acta Biochim. Pol. *49*, 377–385.

Landreville, S., Agapova, O.A., Matatall, K.A., Kneass, Z.T., Onken, M.D., Lee, R.S., Bowcock, A.M., and Harbour, J.W. (2012). Histone deacetylase inhibitors induce growth arrest and differentiation in uveal melanoma. Clin. Cancer Res. *18*, 408–416.

Lane, A.M., Egan, K.M., Harmon, D., Holbrook, A., Munzenrider, J.E., and Gragoudas, E.S. (2009). Adjuvant interferon therapy for patients with uveal melanoma at high risk of metastasis. Ophthalmology *116*, 2206–2212.

Larsen, A.-C., Holst, L., Kaczkowski, B., Andersen, M.T., Manfé, V., Siersma, V.D., Kolko, M., Kiilgaard, J.F., Winther, O., Prause, J.U., et al. (2013). MicroRNA expression analysis and Multiplex ligation-dependent probe amplification in metastatic and non-metastatic uveal melanoma. Acta Ophthalmol.

Lattanzio, L., Tonissi, F., Torta, I., Gianello, L., Russi, E., Milano, G., Merlano, M., and Lo Nigro, C. (2013). Role of IL-8 induced angiogenesis in uveal melanoma. Invest New Drugs *31*, 1107–1114.

Lattman, J., Kroll, S., Char, D.H., Ghazvini, S., Frigillana, H., O'Brien, J.M., and Elbakri, H.R. (1995). Cell cycling and prognosis in uveal melanoma. Clin. Cancer Res. *1*, 41–47.

Laurent, C., Valet, F., Planque, N., Silveri, L., Maacha, S., Anezo, O., Hupe, P., Plancher, C., Reyes, C., Albaud, B., et al. (2011). High PTP4A3 Phosphatase Expression Correlates with Metastatic Risk in Uveal Melanoma Patients. Cancer Res *71*, 666–674.

Lefevre, G., Glotin, A.-L., Calipel, A., Mouriaux, F., Tran, T., Kherrouche, Z., Maurage, C.-A., Auclair, C., and Mascarelli, F. (2004). Roles of Stem Cell Factor/c-Kit and Effects of Glivec®/STI571 in Human Uveal Melanoma Cell Tumorigenesis. J. Biol. Chem. *279*, 31769–31779.

Leyvraz, S., Piperno-Neumann, S., Suciu, S., Baurain, J.F., Zdzienicki, M., Testori, A., Marshall, E., Scheulen, M., Jouary, T., Negrier, S., et al. (2014a). Hepatic intra-arterial versus intravenous fotemustine in patients with liver metastases from uveal melanoma (EORTC 18021): a multicentric randomized trial. Ann. Oncol. *25*, 742–746.

Leyvraz, S., Piperno-Neumann, S., Suciu, S., Baurain, J.F., Zdzienicki, M., Testori, A., Marshall, E., Scheulen, M., Jouary, T., Negrier, S., et al. (2014b). Hepatic intra-arterial versus intravenous fotemustine in patients with liver metastases from uveal melanoma (EORTC 18021): a multicentric randomized trial. Ann. Oncol. *25*, 742–746.

Liu, N., Sun, Q., Chen, J., Li, J., Zeng, Y., Zhai, S., Li, P., Wang, B., and Wang, X. (2012). MicroRNA-9 suppresses uveal melanoma cell migration and invasion through the NF-κB1 pathway. Oncol. Rep. *28*, 961–968.

Logan, P., Burnier, J., and Burnier, M.N. (2013). Vascular endothelial growth factor expression and inhibition in uveal melanoma cell lines. Ecancermedicalscience *7*, 336.

Luke, J.J., Callahan, M.K., Postow, M.A., Romano, E., Ramaiya, N., Bluth, M., Giobbie-Hurder, A., Lawrence, D.P., Ibrahim, N., Ott, P.A., et al. (2013). Clinical activity of ipilimumab for metastatic uveal melanoma: a retrospective review of the Dana-Farber Cancer Institute, Massachusetts General Hospital, Memorial Sloan-Kettering Cancer Center, and University Hospital of Lausanne experience. Cancer *119*, 3687–3695.

Lutz, J.-M., Cree, I., Sabroe, S., Kvist, T.K., Clausen, L.B., Afonso, N., Ahrens, W., Ballard, T.J., Bell, J., Cyr, D., et al. (2005). Occupational risks for uveal melanoma results from a case-control study in nine European countries. Cancer Causes Control *16*, 437–447.

Maat, W., Van der Velden, P.A., Out-Luiting, C., Plug, M., Dirks-Mulder, A., Jager, M.J., and Gruis, N.A. (2007). Epigenetic inactivation of RASSF1a in uveal melanoma. Invest. Ophthalmol. Vis. Sci. *48*, 486–490.

Maat, W., Kilic, E., Luyten, G.P.M., Klein, A. de, Jager, M.J., Gruis, N.A., and Velden, P.A.V. der (2008a). Pyrophosphorolysis Detects B-RAF Mutations in Primary Uveal Melanoma. IOVS *49*, 23–27.

Maat, W., Beiboer, S.H.W., Jager, M.J., Luyten, G.P.M., Gruis, N.A., and Velden, P.A. van der (2008b). Epigenetic Regulation Identifies RASEF as a Tumor-Suppressor Gene in Uveal Melanoma. IOVS *49*, 1291–1298.

Mahipal, A., Tijani, L., Chan, K., Laudadio, M., Mastrangelo, M.J., and Sato, T. (2012). A pilot study of sunitinib malate in patients with metastatic uveal melanoma. Melanoma Res. *22*, 440–446.

Maio, M., Danielli, R., Chiarion-Sileni, V., Pigozzo, J., Parmiani, G., Ridolfi, R., De Rosa, F., Del Vecchio, M., Di Guardo, L., Queirolo, P., et al. (2013). Efficacy and safety of ipilimumab in patients with pre-treated, uveal melanoma. Ann. Oncol. *24*, 2911–2915.

Malaponte, G., Libra, M., Gangemi, P., Bevelacqua, V., Mangano, K., D'Amico, F., Mazzarino, M.C., Stivala, F., McCubrey, J.A., and Travali, S. (2006). Detection of BRAF gene mutation in primary choroidal melanoma tissue. Cancer Biol. Ther. *5*, 225–227.

Mallikarjuna, K., Pushparaj, V., Biswas, J., and Krishnakumar, S. (2006). Expression of insulin-like growth factor receptor (IGF-1R), c-Fos, and c-Jun in uveal melanoma: an immunohistochemical study. Curr. Eye Res. *31*, 875–883.

Mallikarjuna, K., Pushparaj, V., Biswas, J., and Krishnakumar, S. (2007). Expression of epidermal growth factor receptor, ezrin, hepatocyte growth factor, and c-Met in uveal melanoma: an immunohistochemical study. Curr. Eye Res. *32*, 281–290.

Mariani, P., Piperno-Neumann, S., Servois, V., Berry, M.G., Dorval, T., Plancher, C., Couturier, J., Levy-Gabriel, C., Lumbroso-Le Rouic, L., Desjardins, L., et al. (2009). Surgical management of liver metastases from uveal melanoma: 16 years' experience at the Institut Curie. Eur J Surg Oncol *35*, 1192–1197.

Martin, M., Maßhöfer, L., Temming, P., Rahmann, S., Metz, C., Bornfeld, N., Van de Nes, J., Klein-Hitpass, L., Hinnebusch, A.G., Horsthemke, B., et al. (2013a). Exome sequencing identifies recurrent somatic mutations in EIF1AX and SF3B1 in uveal melanoma with disomy 3. Nat. Genet.

Martin, M., Maßhöfer, L., Temming, P., Rahmann, S., Metz, C., Bornfeld, N., Van de Nes, J., Klein-Hitpass, L., Hinnebusch, A.G., Horsthemke, B., et al. (2013b). Exome sequencing identifies recurrent somatic mutations in EIF1AX and SF3B1 in uveal melanoma with disomy 3. Nat Genet *45*, 933–936.

Mashayekhi, A., Rojanaporn, D., Al-Dahmash, S., Shields, C.L., and Shields, J.A. (2014). Monthly intravitreal bevacizumab for macular edema after iodine-125 plaque radiotherapy of uveal melanoma. Eur J Ophthalmol *24*, 228–234.

Matatall, K.A., Agapova, O.A., Onken, M.D., Worley, L.A., Bowcock, A.M., and Harbour, J.W. (2013). BAP1 deficiency causes loss of melanocytic cell identity in uveal melanoma. BMC Cancer *13*, 371.

McCannel TA, Burgess BL, Rao NP, Nelson SF, and Straatsma BR (2010). IDentification of candidate tumor oncogenes by integrative molecular analysis of choroidal melanoma fine-needle aspiration biopsy specimens. Arch Ophthalmol *128*, 1170–1177.

McLean, I.W., Foster, W.D., Zimmerman, L.E., and Gamel, J.W. (1983). Modifications of Callender's classification of uveal melanoma at the Armed Forces Institute of Pathology. Am. J. Ophthalmol. *96*, 502–509.

McLean, I.W., Keefe, K.S., and Burnier, M.N. (1997). Uveal melanoma. Comparison of the prognostic value of fibrovascular loops, mean of the ten largest nucleoli, cell type, and tumor size. Ophthalmology *104*, 777–780.

McLean, I.W., Saraiva, V.S., and Burnier, M.N. (2004). Pathological and prognostic features of uveal melanomas. Can. J. Ophthalmol. *39*, 343–350.

Melichar, B., Voboril, Z., Lojík, M., and Krajina, A. (2009). Liver metastases from uveal melanoma: clinical experience of hepatic arterial infusion of cisplatin, vinblastine and dacarbazine. Hepatogastroenterology *56*, 1157–1162.

Merbs, S.L., and Sidransky, D. (1999). Analysis of p16 (CDKN2/MTS-1/INK4A) alterations in primary sporadic uveal melanoma. Invest. Ophthalmol. Vis. Sci. *40*, 779–783.

Merhavi, E., Cohen, Y., Avraham, B.C.R., Frenkel, S., Chowers, I., Pe'er, J., and Goldenberg-Cohen, N. (2007). Promoter methylation status of multiple genes in uveal melanoma. Invest. Ophthalmol. Vis. Sci. *48*, 4403–4406.

Mitsiades, N., Chew, S.A., He, B., Riechardt, A.I., Karadedou, T., Kotoula, V., and Poulaki, V. (2011). Genotype-Dependent Sensitivity of Uveal Melanoma Cell Lines to Inhibition of B-Raf, MEK, and Akt Kinases: Rationale for Personalized Therapy. Investigative Ophthalmology & Visual Science *52*, 7248–7255.

Mooy, C.M., Van der Helm, M.J., Van der Kwast, T.H., De Jong, P.T., Ruiter, D.J., and Zwarthoff, E.C. (1991). No N-ras mutations in human uveal melanoma: the role of ultraviolet light revisited. Br. J. Cancer *64*, 411–413.

Mooy, C.M., Luyten, G.P., De Jong, P.T., Luider, T.M., Stijnen, T., Van de Ham, F., Van Vroonhoven, C.C., and Bosman, F.T. (1995). Immunohistochemical and prognostic analysis of apoptosis and proliferation in uveal melanoma. Am. J. Pathol. *147*, 1097–1104.

Moulin, A.P., Clément, G., Bosman, F.T., Zografos, L., and Benhattar, J. (2008). Methylation of CpG island promoters in uveal melanoma. Br J Ophthalmol *92*, 281–285.

Mouratova (2012). Epidemiology of Ocular Tumors in Children and Adults (JP Medical Ltd).

Mouriaux, F., Kherrouche, Z., Maurage, C.-A., Demailly, F.-X., Labalette, P., and Saule, S. (2003). Expression of the c-kit receptor in choroidal melanomas. Melanoma Res. *13*, 161–166.

Munzenrider, J.E., Verhey, L.J., Gragoudas, E.S., Seddon, J.M., Urie, M., Gentry, R., Birnbaum, S., Ruotolo, D.M., Crowell, C., and McManus, P. (1989). Conservative treatment of uveal melanoma: local recurrence after proton beam therapy. Int. J. Radiat. Oncol. Biol. Phys. *17*, 493–498.

Murali, R., Wiesner, T., and Scolyer, R.A. (2013). Tumours associated with BAP1 mutations. Pathology *45*, 116–126.

Musi, E., Ambrosini, G., Stanchina, E.D., and Schwartz, G.K. (2014a). The Phosphoinositide 3-Kinaseα Selective Inhibitor, BYL19, Enhances the Effect of the Protein Kinase C Inhibitor, AEB071, in GNAQ/GNA11 Mutant Uveal Melanoma Cells. Mol Cancer Ther molcanther.0550.2013.

Musi, E., Ambrosini, G., De Stanchina, E., and Schwartz, G.K. (2014b). The phosphoinositide 3-kinase α selective inhibitor BYL719 enhances the effect of the protein kinase C inhibitor AEB071 in GNAQ/GNA11-mutant uveal melanoma cells. Mol. Cancer Ther. *13*, 1044–1053.

Nelson, M.A., Radmacher, M.D., Simon, R., Aickin, M., Yang, J., Panda, L., Emerson, J., Roe, D., Adair, L., Thompson, F., et al. (2000). Chromosome abnormalities in malignant melanoma: clinical significance of nonrandom chromosome abnormalities in 206 cases. Cancer Genet. Cytogenet. *122*, 101–109.

Neumann, L.C., Weinhäusel, A., Thomas, S., Horsthemke, B., Lohmann, D.R., and Zeschnigk, M. (2011). EFS shows biallelic methylation in uveal melanoma with poor prognosis as well as tissue-specific methylation. BMC Cancer *11*, 380.

O'Hayre, M., Vázquez-Prado, J., Kufareva, I., Stawiski, E.W., Handel, T.M., Seshagiri, S., and Gutkind, J.S. (2013). The emerging mutational landscape of G proteins and G-protein-coupled receptors in cancer. Nat Rev Cancer *advance online publication*.

Olofsson, R., Cahlin, C., All-Ericsson, C., Hashimi, F., Mattsson, J., Rizell, M., and Lindnér, P. (2014a). Isolated hepatic perfusion for ocular melanoma metastasis: registry data suggests a survival benefit. Ann. Surg. Oncol. *21*, 466–472.

Olofsson, R., Ny, L., Eilard, M.S., Rizell, M., Cahlin, C., Stierner, U., Lönn, U., Hansson, J., Ljuslinder, I., Lundgren, L., et al. (2014b). Isolated hepatic perfusion as a treatment for uveal melanoma liver metastases (the SCANDIUM trial): study protocol for a randomized controlled trial. Trials *15*, 317.

Onken, M.D., Worley, L.A., Ehlers, J.P., and Harbour, J.W. (2004). Gene expression profiling in uveal melanoma reveals two molecular classes and predicts metastatic death. Cancer Res. *64*, 7205–7209.

Onken, M.D., Worley, L.A., Person, E., Char, D.H., Bowcock, A.M., and Harbour, J.W. (2007). Loss of heterozygosity of chromosome 3 detected with single nucleotide polymorphisms is superior to monosomy 3 for predicting metastasis in uveal melanoma. Clin. Cancer Res. *13*, 2923–2927.

Onken, M.D., Worley, L.A., and Harbour, J.W. (2008a). A metastasis modifier locus on human chromosome 8p in uveal melanoma identified by integrative genomic analysis. Clin. Cancer Res. *14*, 3737–3745.

Onken, M.D., Worley, L.A., Long, M.D., Duan, S., Council, M.L., Bowcock, A.M., and Harbour, J.W. (2008b). Oncogenic mutations in GNAQ occur early in uveal melanoma. Invest. Ophthalmol. Vis. Sci. *49*, 5230–5234.

Onken, M.D., Worley, L.A., Tuscan, M.D., and Harbour, J.W. (2010). An accurate, clinically feasible multi-gene expression assay for predicting metastasis in uveal melanoma. J Mol Diagn *12*, 461–468.

Onken, M.D., Worley, L.A., Char, D.H., Augsburger, J.J., Correa, Z.M., Nudleman, E., Aaberg, T.M., Altaweel, M.M., Bardenstein, D.S., Finger, P.T., et al. (2012). Collaborative Ocular Oncology Group report number 1: prospective validation of a multi-gene prognostic assay in uveal melanoma. Ophthalmology *119*, 1596–1603.

Pache, M., Glatz, K., Bösch, D., Dirnhofer, S., Mirlacher, M., Simon, R., Schraml, P., Rufle, A., Flammer, J., Sauter, G., et al. (2003). Sequence analysis and high-throughput immunohistochemical profiling of KIT (CD 117) expression in uveal melanoma using tissue microarrays. Virchows Arch. *443*, 741–744.

Papadopoulos, S., Benter, T., Anastassiou, G., Pape, M., Gerhard, S., Bornfeld, N., Ludwig, W.-D., and Dörken, B. (2002). Assessment of genomic instability in breast cancer and uveal melanoma by random amplified polymorphic DNA analysis. Int. J. Cancer *99*, 193–200.

Papaemmanuil, E., Cazzola, M., Boultwood, J., Malcovati, L., Vyas, P., Bowen, D., Pellagatti, A., Wainscoat, J.S., Hellstrom-Lindberg, E., Gambacorti-Passerini, C., et al. (2011). Somatic SF3B1 mutation in myelodysplasia with ring sideroblasts. N. Engl. J. Med. *365*, 1384–1395.

Papastefanou, V.P., and Cohen, V.M.L. (2011). Uveal melanoma. J Skin Cancer *2011*, 573974.

Parrella, P., Sidransky, D., and Merbs, S.L. (1999). Allelotype of posterior uveal melanoma: implications for a bifurcated tumor progression pathway. Cancer Res. *59*, 3032–3037.

Parrella, P., Fazio, V.M., Gallo, A.P., Sidransky, D., and Merbs, S.L. (2003). Fine mapping of chromosome 3 in uveal melanoma: identification of a minimal region of deletion on chromosomal arm 3p25.1-p25.2. Cancer Res. *63*, 8507–8510.

Patel, M., Smyth, E., Chapman, P.B., Wolchok, J.D., Schwartz, G.K., Abramson, D.H., and Carvajal, R.D. (2011). Therapeutic implications of the emerging molecular biology of uveal melanoma. Clin. Cancer Res. *17*, 2087–2100.

Peña-Llopis, S., Vega-Rubín-de-Celis, S., Liao, A., Leng, N., Pavía-Jiménez, A., Wang, S., Yamasaki, T., Zhrebker, L., Sivanand, S., Spence, P., et al. (2012). BAP1 loss defines a new class of renal cell carcinoma. Nat. Genet. *44*, 751–759.

Penel, N., Delcambre, C., Durando, X., Clisant, S., Hebbar, M., Negrier, S., Fournier, C., Isambert, N., Mascarelli, F., and Mouriaux, F. (2008). O-Mel-Inib: a Cancéro-pôle Nord-Ouest multicenter phase II trial of high-dose imatinib mesylate in metastatic uveal melanoma. Invest New Drugs *26*, 561–565.

Pereira, P.R., Odashiro, A.N., Marshall, J.C., Correa, Z.M., Belfort, R., and Burnier, M.N. (2005). The role of c-kit and imatinib mesylate in uveal melanoma. J Carcinog *4*, 19.

Pereira, P.R., Odashiro, A.N., Lim, L.-A., Miyamoto, C., Blanco, P.L., Odashiro, M., Maloney, S., De Souza, D.F., and Burnier, M.N. (2013). Current and emerging treatment options for uveal melanoma. Clin Ophthalmol *7*, 1669–1682.

Pestova, T.V., Borukhov, S.I., and Hellen, C.U. (1998). Eukaryotic ribosomes require initiation factors 1 and 1A to locate initiation codons. Nature *394*, 854–859.

Piperno-Neumann, S. (2012). A randomized multicentric phase III ongoing study of adjuvant fotemustine versus observation in high risk uveal melanoma patients (FOTEADJ). Acta Ophthalmologica *90*, 0–0.

Piperno-Neumann, S., Servois, V., Bidard, F.-C., Mariani, P., Plancher, C., Diallo, A., Vago-Ady, N., and Desjardins, L. (2013). BEVATEM: Phase II study of bevacizumab (B) in combination with temozolomide (T) in patients (pts) with first-line metastatic uveal melanoma (MUM): Final results. J. Clin. Oncol. *31*.

Piperno-Neumann, S., Kapiteijn, E., Larkin, J.M.G., Carvajal, R.D., Luke, J.J., Seifert, H., Roozen, I., Zoubir, M., Ramkumar, T., Emery, C., et al. (2014a). Landscape of genetic alterations in patients with metastatic uveal melanoma. J. Clin. Oncol. *32:5s*.

Piperno-Neumann, S., Kapiteijn, E., Larkin, J.M.G., Carvajal, R.D., Luke, J.J., Seifert, H., Roozen, I., Zoubir, M., Yang, L., Choudhury, S., et al. (2014b). Phase I dose-escalation study of the protein kinase C (PKC) inhibitor AEB071 in patients with metastatic uveal melanoma. J. Clin. Oncol. *32:5s*.

Prescher, G., Bornfeld, N., and Becher, R. (1990). Nonrandom chromosomal abnormalities in primary uveal melanoma. J. Natl. Cancer Inst. *82*, 1765–1769.

Prescher, G., Bornfeld, N., and Becher, R. (1994). Two subclones in a case of uveal melanoma. Relevance of monosomy 3 and multiplication of chromosome 8q. Cancer Genet. Cytogenet. *77*, 144–146.

Prescher, G., Bornfeld, N., Friedrichs, W., Seeber, S., and Becher, R. (1995). Cytogenetics of twelve cases of uveal melanoma and patterns of nonrandom anomalies and isochromosome formation. Cancer Genet. Cytogenet. *80*, 40–46.

Puusaari, I., Heikkonen, J., and Kivelä, T. (2004a). Effect of radiation dose on ocular complications after iodine brachytherapy for large uveal melanoma: empirical data and simulation of collimating plaques. Invest. Ophthalmol. Vis. Sci. *45*, 3425–3434.

Puusaari, I., Heikkonen, J., and Kivelä, T. (2004b). Ocular complications after iodine brachytherapy for large uveal melanomas. Ophthalmology *111*, 1768–1777.

Quesada, V., Conde, L., Villamor, N., Ordóñez, G.R., Jares, P., Bassaganyas, L., Ramsay, A.J., Beà, S., Pinyol, M., Martínez-Trillos, A., et al. (2012). Exome sequencing identifies recurrent mutations of the splicing factor SF3B1 gene in chronic lymphocytic leukemia. Nat. Genet. *44*, 47–52.

Van Raamsdonk, C.D., Fitch, K.R., Fuchs, H., De Angelis, M.H., and Barsh, G.S. (2004). Effects of G-protein mutations on skin color. Nat Genet *36*, 961–968.

Van Raamsdonk, C.D., Bezrookove, V., Green, G., Bauer, J., Gaugler, L., O'Brien, J.M., Simpson, E.M., Barsh, G.S., and Bastian, B.C. (2008). Frequent somatic mutations of GNAQ in uveal melanoma and blue naevi. Nature *457*, 599–602.

Van Raamsdonk, C.D., Griewank, K.G., Crosby, M.B., Garrido, M.C., Vemula, S., Wiesner, T., Obenauf, A.C., Wackernagel, W., Green, G., Bouvier, N., et al. (2010). Mutations in GNA11 in uveal melanoma. N. Engl. J. Med. *363*, 2191–2199.

Rennie, I.G., Rees, R.C., Parsons, M.A., Lawry, J., and Cottam, D. (1989). Estimation of DNA content in uveal melanomas by flow cytometry. Eye (Lond) *3 (Pt 5)*, 611–617.

Rietschel, P., Panageas, K.S., Hanlon, C., Patel, A., Abramson, D.H., and Chapman, P.B. (2005). Variates of survival in metastatic uveal melanoma. J. Clin. Oncol. *23*, 8076–8080.

Rossi, D., Bruscaggin, A., Spina, V., Rasi, S., Khiabanian, H., Messina, M., Fangazio, M., Vaisitti, T., Monti, S., Chiaretti, S., et al. (2011). Mutations of the SF3B1 splicing factor in chronic lymphocytic leukemia: association with progression and fludarabine-refractoriness. Blood *118*, 6904–6908.

Rossi, D., Spina, V., Bomben, R., Rasi, S., Dal-Bo, M., Bruscaggin, A., Rossi, F.M., Monti, S., Degan, M., Ciardullo, C., et al. (2013). Association between molecular lesions and specific B-cell receptor subsets in chronic lymphocytic leukemia. Blood *121*, 4902–4905.

Sacco, J.J., Nathan, P.D., Danson, S., Lorigan, P., Nicholson, S., Ottensmeier, C., Corrie, P., Steven, N., Goodman, A., Larkin, J.M.G., et al. (2013). Sunitinib versus dacarbazine as first-line treatment in patients with metastatic uveal melanoma. J. Clin. Oncol. *31*.

Sanke, R.F., Collin, J.R., Garner, A., and Packard, R.B. (1981). Local recurrence of choroidal malignant melanoma following enucleation. Br J Ophthalmol *65*, 846–849.

Saraiva, V.S., Caissie, A.L., Segal, L., Edelstein, C., and Burnier, M.N., Jr (2005). Immunohistochemical expression of phospho-Akt in uveal melanoma. Melanoma Res. *15*, 245–250.

Sato, T., Eschelman, D.J., Gonsalves, C.F., Terai, M., Chervoneva, I., McCue, P.A., Shields, J.A., Shields, C.L., Yamamoto, A., Berd, D., et al. (2008). Immunoembolization of Malignant Liver Tumors, Including Uveal Melanoma, Using Granulocyte-Macrophage Colony-Stimulating Factor. JCO *26*, 5436–5442.

Schiffner, S., Braunger, B.M., De Jel, M.M., Coupland, S.E., Tamm, E.R., and Bosserhoff, A.K. (2014). Tg(Grm1) transgenic mice: A murine model that mimics spontaneous uveal melanoma in humans? Experimental Eye Research *127*, 59–68.

Schmidt-Hieber, M., Schmittel, A., Thiel, E., and Keilholz, U. (2004). A phase II study of bendamustine chemotherapy as second-line treatment in metastatic uveal melanoma. Melanoma Res. *14*, 439–442.

Schmittel, A., Scheulen, M.E., Bechrakis, N.E., Strumberg, D., Baumgart, J., Bornfeld, N., Foerster, M.H., Thiel, E., and Keilholz, U. (2005). Phase II trial of cisplatin, gemcitabine and treosulfan in patients with metastatic uveal melanoma. Melanoma Res. *15*, 205–207.

Schmittel, A., Schmidt-Hieber, M., Martus, P., Bechrakis, N.E., Schuster, R., Siehl, J.M., Foerster, M.H., Thiel, E., and Keilholz, U. (2006). A randomized phase II trial of gemcitabine plus treosulfan versus treosulfan alone in patients with metastatic uveal melanoma. Ann. Oncol. *17*, 1826–1829.

Scholes, A.G., Liloglou, T., Maloney, P., Hagan, S., Nunn, J., Hiscott, P., Damato, B.E., Grierson, I., and Field, J.K. (2001). Loss of heterozygosity on chromosomes 3, 9, 13, and 17, including the retinoblastoma locus, in uveal melanoma. Invest. Ophthalmol. Vis. Sci. *42*, 2472–2477.

Scott, L.M., and Rebel, V.I. (2013). Acquired mutations that affect pre-mRNA splicing in hematologic malignancies and solid tumors. J. Natl. Cancer Inst. *105*, 1540–1549.

Seddon, J.M., Albert, D.M., Lavin, P.T., and Robinson, N. (1983). A prognostic factor study of disease-free interval and survival following enucleation for uveal melanoma. Arch. Ophthalmol. *101*, 1894–1899.

Seregard, S. (1999). Long-term survival after ruthenium plaque radiotherapy for uveal melanoma. A meta-analysis of studies including 1,066 patients. Acta Ophthalmol Scand *77*, 414–417.

Shah, A.A., Bourne, T.D., and Murali, R. (2013). BAP1 protein loss by immunohistochemistry: a potentially useful tool for prognostic prediction in patients with uveal melanoma. Pathology *45*, 651–656.

Shields, C.L., and Shields, J.A. (2004). Recent developments in the management of choroidal melanoma. Curr Opin Ophthalmol *15*, 244–251.

Shields, J.A., and Shields, C.L. (1993). Current management of posterior uveal melanoma. Mayo Clin. Proc. *68*, 1196–1200.

Shields, J.A., and Shields, C.L. (2008). Intraocular Tumors: An Atlas and Textbook (Lippincott Williams & Wilkins).

Shields, C.L., Naseripour, M., Cater, J., Shields, J.A., Demirci, H., Youseff, A., and Freire, J. (2002). Plaque radiotherapy for large posterior uveal melanomas (> or =8-mm thick) in 354 consecutive patients. Ophthalmology *109*, 1838–1849.

Shields, C.L., Furuta, M., Thangappan, A., Nagori, S., Mashayekhi, A., Lally, D.R., Kelly, C.C., Rudich, D.S., Nagori, A.V., Wakade, O.A., et al. (2009). Metastasis of uveal melanoma millimeter-by-millimeter in 8033 consecutive eyes. Arch. Ophthalmol. *127*, 989–998.

Singh, A.D., and Borden, E.C. (2005). Metastatic uveal melanoma. Ophthalmol Clin North Am *18*, 143–150, ix.

Singh, A.D., and Topham, A. (2003). Incidence of uveal melanoma in the United States: 1973-1997. Ophthalmology *110*, 956–961.

Singh, A.D., Boghosian-Sell, L., Wary, K.K., Shields, C.L., De Potter, P., Donoso, L.A., Shields, J.A., and Cannizzaro, L.A. (1994). Cytogenetic findings in primary uveal melanoma. Cancer Genet. Cytogenet. *72*, 109–115.

Singh, A.D., Shields, C.L., De Potter, P., Shields, J.A., Trock, B., Cater, J., and Pastore, D. (1996). Familial uveal melanoma. Clinical observations on 56 patients. Arch. Ophthalmol. *114*, 392–399.

Singh, A.D., De Potter, P., Fijal, B.A., Shields, C.L., Shields, J.A., and Elston, R.C. (1998). Lifetime prevalence of uveal melanoma in white patients with oculo(dermal) melanocytosis. Ophthalmology *105*, 195–198.

Singh, A.D., Rennie, I.G., Seregard, S., Giblin, M., and McKenzie, J. (2004). Sunlight exposure and pathogenesis of uveal melanoma. Surv Ophthalmol *49*, 419–428.

Singh, A.D., Kalyani, P., and Topham, A. (2005a). Estimating the risk of malignant transformation of a choroidal nevus. Ophthalmology *112*, 1784–1789.

Singh, A.D., Bergman, L., and Seregard, S. (2005b). Uveal melanoma: epidemiologic aspects. Ophthalmol Clin North Am *18*, 75–84, viii.

Singh, A.D., Kivelä, T., Seregard, S., Robertson, D., and Bena, J.F. (2008). Primary transpupillary thermotherapy of “small” choroidal melanoma: is it safe? Br J Ophthalmol *92*, 727–728.

Singh, A.D., Tubbs, R., Biscotti, C., Schoenfield, L., and Trizzoi, P. (2009). Chromosomal 3 and 8 Status Within Hepatic Metastasis of Uveal Melanoma. Archives of Pathology & Laboratory Medicine *133*, 1223–1227.

Singh, A.D., Turell, M.E., and Topham, A.K. (2011). Uveal Melanoma: Trends in Incidence, Treatment, and Survival. Ophthalmology *118*, 1881–1885.

Sisley, K., Cottam, D.W., Rennie, I.G., Parsons, M.A., Potter, A.M., Potter, C.W., and Rees, R.C. (1992). Non-random abnormalities of chromosomes 3, 6, and 8 associated with posterior uveal melanoma. Genes Chromosomes Cancer *5*, 197–200.

Sisley, K., Curtis, D., Rennie, I.G., and Rees, R.C. (1993). Loss of heterozygosity of the thyroid hormone receptor B in posterior uveal melanoma. Melanoma Res. *3*, 457–461.

Sisley, K., Rennie, I.G., Parsons, M.A., Jacques, R., Hammond, D.W., Bell, S.M., Potter, A.M., and Rees, R.C. (1997). Abnormalities of chromosomes 3 and 8 in posterior uveal melanoma correlate with prognosis. Genes Chromosomes Cancer *19*, 22–28.

Sisley, K., Parsons, M.A., Garnham, J., Potter, A.M., Curtis, D., Rees, R.C., and Rennie, I.G. (2000). Association of specific chromosome alterations with tumour phenotype in posterior uveal melanoma. Br. J. Cancer *82*, 330–338.

Smith, J.H., Padnick-Silver, L., Newlin, A., Rhodes, K., and Rubinstein, W.S. (2007). Genetic study of familial uveal melanoma: association of uveal and cutaneous melanoma with cutaneous and ocular nevi. Ophthalmology *114*, 774–779.

Solti, M., Berd, D., Mastrangelo, M.J., and Sato, T. (2007). A pilot study of low-dose thalidomide and interferon alpha-2b in patients with metastatic melanoma who failed prior treatment. Melanoma Res. *17*, 225–231.

Soparker, C.N., O'Brien, J.M., and Albert, D.M. (1993). Investigation of the role of the ras protooncogene point mutation in human uveal melanomas. Invest. Ophthalmol. Vis. Sci. *34*, 2203–2209.

Soufir, N., Bressac-de Paillerets, B., Desjardins, L., Lévy, C., Bombled, J., Gorin, I., Schlienger, P., and Stoppa-Lyonnet, D. (2000). Individuals with presumably hereditary uveal melanoma do not harbour germline mutations in the coding regions of either the P16INK4A, P14ARF or cdk4 genes. Br. J. Cancer *82*, 818–822.

Spagnolo, F., Grosso, M., Picasso, V., Tornari, E., Pesce, M., and Queirolo, P. (2013). Treatment of metastatic uveal melanoma with intravenous fotemustine. Melanoma Res. *23*, 196–198.

Sudaka, A., Susini, A., Lo Nigro, C., Fischel, J.-L., Toussan, N., Formento, P., Tonissi, F., Lattanzio, L., Russi, E., Etienne-Grimaldi, M.-C., et al. (2013). Combination of bevacizumab and irradiation on uveal melanoma: an in vitro and in vivo preclinical study. Invest New Drugs *31*, 59–65.

Suesskind, D., Scheiderbauer, J., Buchgeister, M., Partsch, M., Budach, W., Bartz-Schmidt, K.U., Ritz, R., Grisanti, S., and Paulsen, F. (2013). Retrospective evaluation of patients with uveal melanoma treated by stereotactic radiosurgery with and without tumor resection. JAMA Ophthalmol *131*, 630–637.

Surriga, O., Rajasekhar, V.K., Ambrosini, G., Dogan, Y., Huang, R., and Schwartz, G.K. (2013a). Crizotinib, a c-Met Inhibitor, Prevents Metastasis in a Metastatic Uveal Melanoma Model. Mol Cancer Ther *12*, 2817–2826.

Surriga, O., Rajasekhar, V.K., Ambrosini, G., Dogan, Y., Huang, R., and Schwartz, G.K. (2013b). Crizotinib, a c-Met Inhibitor, Prevents Metastasis in a Metastatic Uveal Melanoma Model. Mol Cancer Ther *12*, 2817–2826.

Tarhini, A.A., Frankel, P., Margolin, K.A., Christensen, S., Ruel, C., Shipe-Spotloe, J., Gandara, D.R., Chen, A., and Kirkwood, J.M. (2011). Aflibercept (VEGF Trap) in inoperable stage III or stage iv melanoma of cutaneous or uveal origin. Clin. Cancer Res. *17*, 6574–6581.

Testa, J.R., Cheung, M., Pei, J., Below, J.E., Tan, Y., Sementino, E., Cox, N.J., Dogan, A.U., Pass, H.I., Trusa, S., et al. (2011). Germline BAP1 mutations predispose to malignant mesothelioma. Nat Genet *43*, 1022–1025.

Topcu-Yilmaz, P., Kiratli, H., Saglam, A., Söylemezoglu, F., and Hascelik, G. (2010). Correlation of clinicopathological parameters with HGF, c-Met, EGFR, and IGF-1R expression in uveal melanoma. Melanoma Res. *20*, 126–132.

Trolet, J., Hupé, P., Huon, I., Lebigot, I., Decraene, C., Delattre, O., Sastre-Garau, X., Saule, S., Thiéry, J.-P., Plancher, C., et al. (2009). Genomic profiling and identification of high-risk uveal melanoma by array CGH analysis of primary tumors and liver metastases. Invest. Ophthalmol. Vis. Sci. *50*, 2572–2580.

Tschentscher, F., Prescher, G., Horsman, D.E., White, V.A., Rieder, H., Anastassiou, G., Schilling, H., Bornfeld, N., Bartz-Schmidt, K.U., Horsthemke, B., et al. (2001). Partial deletions of the long and short

arm of chromosome 3 point to two tumor suppressor genes in uveal melanoma. Cancer Res. *61*, 3439–3442.

Tschentscher, F., Hüsing, J., Hölter, T., Kruse, E., Dresen, I.G., Jöckel, K.-H., Anastassiou, G., Schilling, H., Bornfeld, N., Horsthemke, B., et al. (2003). Tumor Classification Based on Gene Expression Profiling Shows That Uveal Melanomas with and without Monosomy 3 Represent Two Distinct Entities. Cancer Res *63*, 2578–2584.

Valsecchi, M.E., Coronel, M., Intenzo, C.M., Kim, S.M., Witkiewicz, A.K., and Sato, T. (2013). Somatostatin receptor scintigraphy in patients with metastatic uveal melanoma. Melanoma Res. *23*, 33–39.

van, J.G.M., Koopmans, A.E., Verdijk, R.M., Naus, N.C., de, A., and Kilic, E. (2013). Diagnosis, Histopathologic and Genetic Classification of Uveal Melanoma. In Melanoma - From Early Detection to Treatment, H. Duc, ed. (InTech),.

Vaqué, J.P., Dorsam, R.T., Feng, X., Iglesias-Bartolome, R., Forsthoefel, D.J., Chen, Q., Debant, A., Seeger, M.A., Ksander, B.R., Teramoto, H., et al. (2013). A Genome-wide RNAi Screen Reveals a Trio-Regulated Rho GTPase Circuitry Transducing Mitogenic Signals Initiated by G Protein-Coupled Receptors. Molecular Cell *49*, 94–108.

Van der Velden, P.A., Metzelaar-Blok, J.A., Bergman, W., Monique, H., Hurks, H., Frants, R.R., Gruis, N.A., and Jager, M.J. (2001). Promoter hypermethylation: a common cause of reduced p16(INK4a) expression in uveal melanoma. Cancer Res. *61*, 5303–5306.

Van der Velden, P.A., Zuidervaart, W., Hurks, M.H.M.H., Pavey, S., Ksander, B.R., Krijgsman, E., Frants, R.R., Tensen, C.P., Willemze, R., Jager, M.J., et al. (2003). Expression profiling reveals that methylation of TIMP3 is involved in uveal melanoma development. Int. J. Cancer *106*, 472–479.

Virgili, G., Gatta, G., Ciccolallo, L., Capocaccia, R., Biggeri, A., Crocetti, E., Lutz, J.-M., Paci, E., and EUROCARE Working Group (2007). Incidence of uveal melanoma in Europe. Ophthalmology *114*, 2309–2315.

Voelter, V., Schalenbourg, A., Pampallona, S., Peters, S., Halkic, N., Denys, A., Goitein, G., Zografos, L., and Leyvraz, S. (2008). Adjuvant intra-arterial hepatic fotemustine for high-risk uveal melanoma patients. Melanoma Res. *18*, 220–224.

Vrabec, F. (1948). Quatre cas de mélanoblastome de la choroïde humaine cultivés in vitro. Ophthalmologica *115*, 129–140.

De Waard-Siebinga, I., Blom, D.J., Griffioen, M., Schrier, P.I., Hoogendoorn, E., Beverstock, G., Danen, E.H., and Jager, M.J. (1995). Establishment and characterization of an uveal-melanoma cell line. Int. J. Cancer *62*, 155–161.

Wang, L., Lawrence, M.S., Wan, Y., Stojanov, P., Sougnez, C., Stevenson, K., Werner, L., Sivachenko, A., DeLuca, D.S., Zhang, L., et al. (2011). SF3B1 and other novel cancer genes in chronic lymphocytic leukemia. N. Engl. J. Med. *365*, 2497–2506.

Wang, X., Egan, K.M., Gragoudas, E.S., and Kelsey, K.T. (1996). Constitutional alterations in p16 in patients with uveal melanoma. Melanoma Res. *6*, 405–410.

Wang, Z., Nabhan, M., Schild, S.E., Stafford, S.L., Petersen, I.A., Foote, R.L., and Murad, M.H. (2013). Charged particle radiation therapy for uveal melanoma: a systematic review and meta-analysis. Int. J. Radiat. Oncol. Biol. Phys. *86*, 18–26.

Weber, A., Hengge, U.R., Urbanik, D., Markwart, A., Mirmohammadsaegh, A., Reichel, M.B., Wittekind, C., Wiedemann, P., and Tannapfel, A. (2003). Absence of mutations of the BRAF gene and constitutive activation of extracellular-regulated kinase in malignant melanomas of the uvea. Lab. Invest. *83*, 1771–1776.

Weis E, Shah CP, Lajous M, Shields JA, and Shields CL (2006). The association between host susceptibility factors and uveal melanoma: A meta-analysis. Arch Ophthalmol *124*, 54–60.

Whelchel, J.C., Farah, S.E., McLean, I.W., and Burnier, M.N. (1993). Immunohistochemistry of infiltrating lymphocytes in uveal malignant melanoma. Invest. Ophthalmol. Vis. Sci. *34*, 2603–2606.

Wiesner, T., Obenauf, A.C., Murali, R., Fried, I., Griewank, K.G., Ulz, P., Windpassinger, C., Wackernagel, W., Loy, S., Wolf, I., et al. (2011). Germline mutations in BAP1 predispose to melanocytic tumors. Nat Genet *43*, 1018–1021.

Wiesner, T., Murali, R., Fried, I., Cerroni, L., Busam, K., Kutzner, H., and Bastian, B.C. (2012). A distinct subset of atypical Spitz tumors is characterized by BRAF mutation and loss of BAP1 expression. Am. J. Surg. Pathol. *36*, 818–830.

Wilson, M.W., and Hungerford, J.L. (1999). Comparison of episcleral plaque and proton beam radiation therapy for the treatment of choroidal melanoma. Ophthalmology *106*, 1579–1587.

Wiltshire, R.N., Elner, V.M., Dennis, T., Vine, A.K., and Trent, J.M. (1993). Cytogenetic analysis of posterior uveal melanoma. Cancer Genet. Cytogenet. *66*, 47–53.

Woodman, S.E. (2012). Metastatic uveal melanoma: biology and emerging treatments. Cancer J *18*, 148–152.

Worley, L.A., Onken, M.D., Person, E., Robirds, D., Branson, J., Char, D.H., Perry, A., and Harbour, J.W. (2007). Transcriptomic versus Chromosomal Prognostic Markers and Clinical Outcome in Uveal Melanoma. Clin Cancer Res *13*, 1466–1471.

Worley, L.A., Long, M.D., Onken, M.D., and Harbour, J.W. (2008). Micro-RNAs associated with metastasis in uveal melanoma identified by multiplexed microarray profiling. Melanoma Res. *18*, 184–190.

Wu, X., Zhou, J., Rogers, A.M., Jänne, P.A., Benedettini, E., Loda, M., and Hodi, F.S. (2012a). c-Met, epidermal growth factor receptor, and insulin-like growth factor-1 receptor are important for growth in uveal melanoma and independently contribute to migration and metastatic potential. Melanoma Res. *22*, 123–132.

Wu, X., Zhu, M., Fletcher, J.A., Giobbie-Hurder, A., and Hodi, F.S. (2012b). The protein kinase C inhibitor enzastaurin exhibits antitumor activity against uveal melanoma. PLoS ONE *7*, e29622.

Wu, X., Li, J., Zhu, M., Fletcher, J.A., and Hodi, F.S. (2012c). Protein kinase C inhibitor AEB071 targets ocular melanoma harboring GNAQ mutations via effects on the PKC/Erk1/2 and PKC/NF-κB pathways. Mol. Cancer Ther. *11*, 1905–1914.

Yamamoto, A., Chervoneva, I., Sullivan, K.L., Eschelman, D.J., Gonsalves, C.F., Mastrangelo, M.J., Berd, D., Shields, J.A., Shields, C.L., Terai, M., et al. (2009). High-dose immunoembolization: survival benefit in patients with hepatic metastases from uveal melanoma. Radiology *252*, 290–298.

Yan, D., Zhou, X., Chen, X., Hu, D.-N., Dong, X.D., Wang, J., Lu, F., Tu, L., and Qu, J. (2009). MicroRNA-34a inhibits uveal melanoma cell proliferation and migration through downregulation of c-Met. Invest. Ophthalmol. Vis. Sci. *50*, 1559–1565.

Yan, D., Dong, X.D., Chen, X., Yao, S., Wang, L., Wang, J., Wang, C., Hu, D.-N., Qu, J., and Tu, L. (2012). Role of microRNA-182 in posterior uveal melanoma: regulation of tumor development through MITF, BCL2 and cyclin D2. PLoS ONE *7*, e40967.

Yang, C., and Wei, W. (2011). The miRNA expression profile of the uveal melanoma. Sci. China Life Sci. *54*, 351–358.

Yang, H., Fang, G., Huang, X., Yu, J., Hsieh, C.-L., and Grossniklaus, H.E. (2008a). In-vivo xenograft murine human uveal melanoma model develops hepatic micrometastases. Melanoma Res. *18*, 95–103.

Yang, H., Jager, M.J., and Grossniklaus, H.E. (2010). Bevacizumab suppression of establishment of micrometastases in experimental ocular melanoma. Invest. Ophthalmol. Vis. Sci. *51*, 2835–2842.

Yang, W., Chen, P.W., Li, H., Alizadeh, H., and Niederkorn, J.Y. (2008b). PD-L1: PD-1 interaction contributes to the functional suppression of T-cell responses to human uveal melanoma cells in vitro. Invest. Ophthalmol. Vis. Sci. *49*, 2518–2525.

Yarovoy, A.A., Magaramov, D.A., and Bulgakova, E.S. (2012). The comparison of ruthenium brachytherapy and simultaneous transpupillary thermotherapy of choroidal melanoma with brachytherapy alone. Brachytherapy *11*, 224–229.

Ye, M., Hu, D., Tu, L., Zhou, X., Lu, F., Wen, B., Wu, W., Lin, Y., Zhou, Z., and Qu, J. (2008). Involvement of PI3K/Akt Signaling Pathway in Hepatocyte Growth Factor–Induced Migration of Uveal Melanoma Cells. IOVS *49*, 497–504.

Yoshida, K., Sanada, M., Shiraishi, Y., Nowak, D., Nagata, Y., Yamamoto, R., Sato, Y., Sato-Otsubo, A., Kon, A., Nagasaki, M., et al. (2011). Frequent pathway mutations of splicing machinery in myelodysplasia. Nature *478*, 64–69.

Yoshida, M., Selvan, S., McCue, P.A., DeAngelis, T., Baserga, R., Fujii, A., Rui, H., Mastrangelo, M.J., and Sato, T. (2014). Expression of insulin-like growth factor-1 receptor in metastatic uveal melanoma and implications for potential autocrine and paracrine tumor cell growth. Pigment Cell Melanoma Res *27*, 297–308.

Yoshikawa, Y., Sato, A., Tsujimura, T., Emi, M., Morinaga, T., Fukuoka, K., Yamada, S., Murakami, A., Kondo, N., Matsumoto, S., et al. (2012). Frequent inactivation of the BAP1 gene in epithelioid-type malignant mesothelioma. Cancer Sci. *103*, 868–874.

Yu, F.-X., Luo, J., Mo, J.-S., Liu, G., Kim, Y.C., Meng, Z., Zhao, L., Peyman, G., Ouyang, H., Jiang, W., et al. (2014a). Mutant Gq/11 Promote Uveal Melanoma Tumorigenesis by Activating YAP. Cancer Cell *25*, 822–830.

Yu, H., Mashtalir, N., Daou, S., Hammond-Martel, I., Ross, J., Sui, G., Hart, G.W., Rauscher, F.J., Drobetsky, E., Milot, E., et al. (2010). The ubiquitin carboxyl hydrolase BAP1 forms a ternary complex with YY1 and HCF-1 and is a critical regulator of gene expression. Mol. Cell. Biol. *30*, 5071–5085.

Yu, H., Pak, H., Hammond-Martel, I., Ghram, M., Rodrigue, A., Daou, S., Barbour, H., Corbeil, L., Hébert, J., Drobetsky, E., et al. (2014b). Tumor suppressor and deubiquitinase BAP1 promotes DNA double-strand break repair. Proc. Natl. Acad. Sci. U.S.A. *111*, 285–290.

Zeschnigk, M., Tschentscher, F., Lich, C., Brandt, B., Horsthemke, B., and Lohmann, D.R. (2003). Methylation Analysis of Several Tumour Suppressor Genes Shows a Low Frequency of Methylation of *CDKN2A* and *RARB* in Uveal Melanomas. International Journal of Genomics *4*, 329–336.

Zimmerman, L.E., McLean, I.W., and Foster, W.D. (1978). Does enucleation of the eye containing a malignant melanoma prevent or accelerate the dissemination of tumour cells. Br J Ophthalmol *62*, 420–425.

(1998). The Collaborative Ocular Melanoma Study (COMS) randomized trial of pre-enucleation radiation of large choroidal melanoma II: initial mortality findings. COMS report no. 10. Am. J. Ophthalmol. *125*, 779–796.

Objectives

Uveal Melanoma patients lack of effective therapy for metastatic disease. New understanding of the molecular pathology of the disease is fueling the interest in testing new therapeutic strategies with targeted compounds as well as drug combinations.

The abundance of the molecules requiring efficacy assessment compared to the low incidence of the disease, as well as the enormous number of different possible associations (in number and time-schedules) of promising compounds require a systematic preclinical testing.

Unfortunately the preclinical models widely used for the preclinical assessment of therapeutic options in UM do not satisfy our current knowledge on the pathobiology of the disease.

These models do not display BAP1 mutations, a marker of aggressive and metastatic disease, and they present in some cases BRAF mutations , which are not found in UM patients. Moreover these cell lines have been strongly selected by long term passages in culture and possibly subjected to contamination with other UM cell lines because of the lack of availability of certified batches from institutional cell banks.

During my PhD I aimed to establish UM cell lines derived from patients or from Patient-derived xenografts and representing the genetic landscape of the disease in order to use them for the assessment of the efficacy of different therapeutic strategies. I also aimed to develop a rapid and effective pipeline for the discovery of synergistic interactions in 2 drug combinations exerting a selective cytotoxic or cytostatic effect on UM cell lines in order to enhance the in vivo discovery of effective combination strategies.

RESULTS

Establishment of novel cell lines recapitulating the genetic landscape of uveal melanoma and preclinical validation of mTOR as a therapeutic target

Nabil Amirouchene-Angelozzi[a]*, Fariba Nemati[b]*, David Gentien[c], André Nicolas[d], Amaury Dumont[e], Guillaume Carita[b], Jacques Camonis[e], Laurence Desjardins[f], Nathalie Cassoux[f], Sophie Piperno-Neumann[g], Pascale Mariani[h], Xavier Sastre[d], Didier Decaudin[b]° and Sergio Roman-Roman[i]°

***° equally contributed**

Authors' Affiliations:

[a]Biophenics Laboratory, Translational Research Department, Institut Curie, 26 rue d'Ulm 75005, Paris; [b]Laboratory of Preclinical Investigation, Translational Research Department, Institut Curie, 26, rue d'Ulm 75005, Paris; [c]Genomics Platform, Translational Research Department, Institut Curie, 26 rue d'Ulm 75005, Paris; [d]Department of Tumor Biology, Institut Curie, 26 rue d'Ulm 75005, Paris; [e]Institut Curie, INSERM U830; [f]Department of Ophthalmological Oncology, Institut Curie, 26 rue d'Ulm 75005, Paris; [g]Department of Medical Oncology, Institut Curie, 26 rue d'Ulm 75005, Paris; [h]Department of Surgery, Institut Curie, 26 rue d'Ulm 75005, Paris; [i]Translational Research Department, Institut Curie, 26 rue d'Ulm 75005, Paris;

E-mails: nabil.amirouchene-angelozzi@curie.fr; Fariba.Nemati@curie.fr; David.gentien@curie.fr; andre.nicolas@curie.fr; Amaury.Dumont @curie.fr; Guillaume.Carita@curie.fr; Jacques.Camonis@curie.fr; Laurance.desjardins@curie.net; Nathalie.Cassoux@curie.net; Sophie.Piperno-Neumann@curie.net; Pascale.Mariani @curie.net; Xavier.Sastre@curie.net; Didier.Decaudin@curie.net; Sergio.Roman-Roman@curie.fr.

Corresponding Author: Sergio Roman-Roman, Institut Curie, Translational Research Department, 26 rue Ulm 75005 Paris, France
Phone: +33 153197411 Fax +33153194130 E-mail: Sergio.Roman-Roman@curie.fr.

Highlights:

- A panel of UM cell lines including BAP1-deficient cells has been established
- mTOR pathway is a potential therapeutic target in UM
- Everolimus displays therapeutical efficacy in vivo

Keywords: uveal melanoma, BAP1, Everolimus, mTOR, cell lines, patients-derived tumor xenografts

Grant Support: This project is supported by French national cancer Institute (INCa).

Disclosure of Potential Conflicts of Interest: No potential conflicts of interest were disclosed.

Abstract

Uveal melanoma (UM) is the most common primary tumor of the eye in adults. There is no standard adjuvant treatment to prevent metastasis and no effective therapy in the metastatic setting. We have established a unique panel of 7 UM cell lines from either patient's tumors or patient-derived tumor xenografts (PDXs). This panel recapitulates the molecular landscape of the disease in terms of genetic alterations and mutations. All the cell lines display GNAQ or GNA11 activating mutations, and importantly four of them display BAP1 (BRCA1 associated protein-1) deficiency, a hallmark of aggressive disease. mTOR pathway was shown to be activated in most of the cell lines in the absence of AKT signaling upregulation. mTOR inhibitor Everolimus reduced the viability of UM cell lines and significantly delayed tumor growth in 4 PDXs. Our data suggest that mTOR inhibition with Everolimus, most probably in combination with other agents, may be considered as a therapeutic option for the management of uveal melanoma.

I. Introduction

Uveal melanoma (UM) is the most frequent and aggressive ocular primary tumor in adults with approximately 5 new cases per million per year in the United States and in Europe (Mallone et al., 2012)(Singh et al., 2011). Even if local control rate with photon radiotherapy exceeds 90% at 10 years (Dunavoelgyi et al., 2011) enucleation remains the treatment of choice for large tumors (Singh and Topham, 2003; Singh et al., 2011). Up to 50% of patients develop metastasis, which occur only *via* hematogenous spread because of the absence of lymphatic drainage of the eye and are rarely detected at the time of initial diagnosis (2-4% of the patients)(Harbour and Chen, 2013). In 90% of cases, metastatic spread involves the liver usually leading to death within a few months despite medical treatment (Gragoudas et al., 1991). Currently, no effective adjuvant therapy is available to prevent metastases, neither there is any effective treatment once metastases have developed.

Genome-wide techniques of genetic analysis (Trolet et al., 2009) and expression profiling (Onken et al., 2004) divide UM in two subgroups according to the risk of metastatic spreading. UM at high risk for metastasis are associated to monosomy of chromosome 3, loss of 6q and gain of 8q (Trolet et al., 2009). Although occurring in the same cell lineage uveal and skin melanomas represent different diseases: we have recently demonstrated that uveal melanomas display a remarkably low mutation burden with ~2000 predicted somatic single nucleotide variants per tumor and low levels of aneuploidy. Moreover no ultraviolet radiation DNA-damage signature has been found in UM (Furney et al., 2013) and BRAF or NRAS mutations commonly found in cutaneous melanoma are not observed in UM (Cohen et al., 2003; Cruz et al., 2003; Edmunds et al., 2003; Kiliç et al., 2004; Rimoldi et al., 2003; Weber et al., 2003). Mutually exclusive mutations in the *GNAQ*/*11* genes activating the MAP kinase pathway have been described in the majority of UM (Van Raamsdonk et al., 2010, 2008). Although *GNAQ*/*11* mutational status is not correlated with disease-free survival, these mutations are considered oncogenic drivers and consequently potential good targets for therapeutic intervention. Inactivating mutations of the tumor suppressor *BAP1* occur in ~85% of aggressive tumors and are associated with metastatic disease (Harbour et al., 2010). Recently exome and whole genome sequencing of uveal melanomas identified recurrent mutations in *SF3B1* (Furney et al., 2013; Harbour et al., 2013; Martin et al., 2013), which encodes a component of the spliceosome, and

in the translation initiation factor *EIF1AX* (Martin et al., 2013). *SF3B1* and *EIF1AX* mutations are inversely correlated with chromosome 3 monosomy and associated with good prognosis (Furney et al., 2013; Harbour et al., 2013; Martin et al., 2013).

The currently available UM cell lines do not completely reflect the genetic alterations recurrently found in UM (Griewank et al., 2012). Some cell lines display BRAF mutations, which are not found in UM samples and to our knowledge no UM cell line harboring BAP1 mutations, which represent a hallmark of aggressive UM, have been described so far. The first goal of our study was to develop cellular models of UM covering the genetic landscape (genetic alterations and mutations) of this disease, to provide a good model for assessing the efficacy of new drugs and drug combinations. Next we looked at the activation status of PI3K/mTOR signaling pathway and assessed the effect of Everolimus on cell viability. We have finally examined the effect of mTOR inhibition in vivo using several previously described patient-derived UM xenografts (Némati et al., 2010).

II. Materials and Methods

1. Tumor samples.

Eighty-seven tumor samples were obtained either from patients (60 from primary tumors and 13 from metastasis) or from 14 patient-derived xenografts (PDXs), which were established as described in (Némati et al., 2010). All patients had previously given their informed consent for experimental research on residual tumor tissue available after histopathologic and cytogenetic analyses.

2. Establishment of uveal melanoma cell lines.

Fresh or DMSO frozen tumor samples obtained from pathologists were mechanically fragmented, passed in a 40 µM Nylon filter and resuspended in RPMI 1640 (Gibco, France), supplemented with 20% (vol/vol) fetal bovine serum (FBS, Invitrogen, France), 100 U/ml penicillin and 100 µg/ml streptomycin (P/S, Invitrogen, France).

Once cell lines showed unlimited proliferation and were cultured for more than 40 passages were considered as established. Optic microscopy images were taken with a Leica DM IL microscope and a Nikon DS-L1 camera.

3. Cell culture.

92.1(De Waard-Siebinga et al., 1995), Mel202(Ksander et al., 1991), were purchased from The European Searchable Tumour Line Database (Tubingen University, Germany). OMM1, OMM2.5 (Luyten et al., 1996)(Chen et al., 1997) were kindly provided by P.A. Van Der Velden (Leiden University, The Netherlands). All cell lines were cultured in RPMI1640 supplemented with 20% FBS (Life Technologies), Penicillin 100U/ml –Streptomycin 100µg/ml (Life Technologies). All cell lines were tested for Mycoplasma and proved to be Mycoplasma free. Cell lines were maintained in a humidified atmosphere (5% CO2) at 37°C. All cell lines were genotyped: Short Tandem repeat Polymorphism (STR) profiles of 92.1, Mel202, OMM1, OMM2.5 matched at 100% those presented in reference (Griewank et al., 2012).

4. Chemicals.

mTOR inhibitor Everolimus/Rad001, MEK inhibitor GSK1120212, and AKT inhibitor KRX-0401 were supplied by Euromedex (France) and dissolved in DMSO (Rad001,GSK1120212) or ethanol (KRX0401) at 10mM and stored at −20°C.

5. Cell viability assays.

We determined cell viability using a colorimetric assay based on 3-(4,5-dimethylthiazol-2-yl)-2,5 diphenyltetrazolium bromide (MTT; M-2128, Sigma) as explained in (Marty et al., 2008). Cells were seeded at appropriate concentration in 96-well plates at day 0 (MM28:3500 cells/well; MP38:8000 cells/well; MP41:1500; MP46:6000 cells/well; MP65:8000 cells/well; MM66:6000 cells/well; 92.1; Mel202:4000 cells/well; OMM1:1500 cells/well; OMM2.5:3500 cells/well); drug was

added to the medium at day 2 and cell viability tested by MTT assay at day 7. Results are expressed as relative percentages of metabolically active cells compared with untreated controls. Drug sensitivity curves were calculated using GraphPad Prism 4.

6. Genomic analysis.

The DNA was extracted from cell pellets using a standard phenol/chloroform procedure. The total RNA was isolated from cell pellets using a miRNeasy mini kit (Qiagen, Courtaboeuf, France) and cDNA synthesis was performed with MuLV Reverse Transcriptase in accordance with the manufacturers' instructions (Invitrogen, Cergy-Pontoise, France), with quality assessments performed on an Agilent 2100 bioanalyzer. For Sanger sequencing, gDNA was amplified by PCR and the products were sequenced using dye-terminator chemistry as previously described (16). Primer sequences for *BAP1*, *GNAQ*, *GNQ11*, *SF3B1* and *EIF1AX* are available upon request. Sequences were visualized using Sequencher software. To perform Loss of heterozygosity and copy number values analysis and to detect other abnormalities, genetic analyses of the cell lines were done using Affymetrix Genome-Wide SNP Arrays 6.0. or Cytoscan HD (Affymetrix, High Wycombe, UK). DNA was used to perform Affymetrix Human mapping SNP 6.0 assay as described in (Tuefferd et al., 2008) or Cytoscan assay according to the manufacturer’s protocol at the Institut Curie microarray core facility. Genetic profiles were compared to the profiles of the corresponding tumors and PDXs by Chromosome Analysis Suite (Affymetrix). To perform Short Tandem repeat Polymorphism (STR) analysis GenePrint 10 system kit (Promega, France) was used according to manufacturer’s instructions.

7. Cytopathologic analysis.

Cells were fixed in a 4% formalin solution and embedded in paraffin. 4 µm sections were cut from the embedded blocks, and then dewaxed for immunostaining. Heat-induced epitope retrieval was performed at 97° for 20 min in EDTA buffer pH 9.0 (Dako S2367). Mouse antihuman BAP1 antibody (monoclonal mouse anti BAP1 (C4) Santa Cruz Biotechnology, Inc, Santa Cruz, CA) was applied for 1 hour at a concentration of 1:200. For antibody revelation polymer HRP (DAKO Envision,

Denmark) was used followed by application of di-aminobenzidin (DAB) for 5 minutes. The immunostaining was performed on a Dako Autostainer Platform. A brown coloration of nuclear localization of strong intensity was observed in the presence of the protein. Cell nuclei were counterstained with Herris' Hematoxylin. Epithelial cells of normal breast glands were used as positive control for BAP1.

8. Western blotting.

Tissue lysates were loaded onto gels, transferred to nitrocellulose and revealed as described in (Marty et al., 2008). Quantification was performed using a LAS-3000 Luminescent Image analyzer and Image Gauge software (Fuji, FSVT, Courbevoie, France). Actin was used for normalization between samples and detected using anti-beta-actin primary antibodies at the dilution of 1:5000 (Sigma-Aldrich, Saint Quentin Fallavier, France). AKT, phospho-AKT (S473), phospho-AKT (T308), S6, phospho-S6 (Ser 235/236) (Cell Signaling Technology, Ozyme, Saint Quentin en Yveline, France) and BAP1 (C4) (Santa Cruz Biotechnologies) antibodies were used at 1:1000 dilution.

9. *In vivo* antitumor efficacy of mTOR inhibitor.

Female SCID mice were grafted with a tumor fragment of 15 mm^3. Mice bearing tumors with a volume of 40 to 200 mm^3 were individually identified and randomly assigned to the control or treatment groups (6-10 animals per group). Number of mice used were respectively: for PDXs MP34: 8 mice for the control group, 8 for the treatment group; for PDXs MP41: 10 mice for controls and 9 for the treatment group; for PDX MP55: 10 mice for the control group and 8 mice for the treatment group; for PDX MP46: 8 mice for the control group and 6 for the treatment group. Mice were weighed twice a week. Tumor volumes were calculated by measuring two perpendicular diameters with calipers. Xenografted mice were sacrificed at the end of treatment or when their tumor reached a volume of 2,000 mm^3. Each tumor volume (V) was calculated according to the following formula: $V = a \times b^2 / 2$, where a and b are the largest and smallest perpendicular tumor diameters. Relative tumor volumes (RTV) were

calculated with the following formula: RTV = (V_x/V_1), where V_x is the tumor volume on day *x* and V_1 is the tumor volume on the first day of treatment. Growth curves were obtained by plotting the mean values of RTV on the *Y* axis against time (*X* axis, expressed as days of treatment). Antitumor activity was evaluated according to tumor growth inhibition (TGI), calculated with the following formula: percent TGI = 100 − (RTVt / RTVc × 100), where RTVt is the median RTV for a treatment group and RTVc is the median RTV for its control group at the end of the therapy. mTOR inhibitor (Everolimus) was reconstituted in PEG300/HPBCD/Glucose 5% (10/10/80), and administered PO at a dose of 2mg/kg 3 times a week, for 4 to 6 weeks. In all *in vivo* experiments, mice of the control groups received 0.2 ml of the drug-formulating vehicle with the same schedule as the treated animals. The experimental protocol and animal housing were in accordance with institutional guidelines as put forth by the French Ethical Committee (Agreement C75-05 - 18, France), and the ethics committee of the Institut Curie that approved this project.

10. Expression of tumor-specific antigens

Expression of tumor-specific antigens was assessed by reverse transcription-PCR on RNA extracted from cellular culture as described in (Némati et al., 2010).

11. Assessment of Synergy in drug combination experiments

Synergy computed as excess over Bliss (Straussman et al., 2012) was assessed by calculation, for each combination of doses tested, of its fractional inhibition value (1-fraction of viable cells compared to controls) and by successive subtraction of the fractional inhibition value calculated according to the Bliss independence model. Therefore Excess over Bliss= c- (a+b-2*a*b) where a is the fractional inhibition obtained with a x concentration of drug A, B is the fractional inhibition obtained with an y conscentration of drug B and c is the fractional inhibition obtained with x concentration of drug A combined with y concentration of drug B. Synergy calculated as Combination Index was obtained using Chu and Talalay median-effect equation (Chou, 2006) with the software Compusyn ComboSyn, Inc., Paramus, NJ. USA, 2005 (Chou, 2010).

12. Statistical methods.

For *in vitro* experiments 95% Confidence Intervals on 3 independent replicates were calculated to assess statistical significance for synergic effects of drug combinations. For *in vivo* experiments the statistical significance of the difference between calculated RTVs for treatments groups versus its control groups was calculated by the two-tailed Student's *t* test.

III. Results

1. Establishment of UM cell lines

We have established 7 UM cell lines: 2 of them, MP38 and MP65, were obtained directly from human primary tumors (success rate of 3%), 3 cell lines derived from PDX models (Némati et al., 2010) of liver (MM28 and MM66) or skin (MM33) metastasis, while MP41 and MP46 derived from PDX models of primary tumors (See Table 1). MP38 and MP65 display a fusiform morphology, MP41 shows a predominant epithelioid appearance while MP46, MM28, MM33 and MM66 have a mixed morphology (see Figure 1). All the cell lines grow adherent to the flask with MM66 having a minor component growing in suspension. Estimated doubling times (shown in Table 1) ranged between 40 and 120 hours.

2. Characterization of UM cell lines

Copy number and SNP profiles were generated for each cell line and compared to the profiles obtained from the tumors of origin (patients or PDXs). DNA arrays profiles are represented in supplementary figure 1. Genotype analysis by Affymetrix mapping SNPs arrays confirmed the overall conservation of chromosome alterations between cell lines and corresponding tumor specimens, in particular for chromosomes 1, 3, 6, 8 and 16 whose status are known to have an impact on classification and prognosis of the disease (Couturier and Saule, 2012; Harbour, 2012). Six cell lines display loss or LOH of 1p and gain of 1q; five cell lines display chromosome 3 monosomy or

Model	Origin	Morphology	Doubling time	Status of chromosomes 1;3;6;8 and 16	LOH of chromosome 3	BAP1 Mutations	BAP1 Protein Expression	GNAQ	GNA11	SF3B1 Mutations	EIF1AX
MP38 CL	Primary Tumor	S	80h	L3q;G8;L16q	Yes[1]	c.68-9_72del	No	c.626 a>T	–	–	–
MP41 CL	PDX established from Primary Tumor	E	41h	L1p;G1q;L3;G6p;L6q;L8p;G8q;L16	Yes[2]	–	Yes	–	c.626 a>A/T	–	–
MP46 CL	PDX established from Primary Tumor	M	110h	G1q;G6p;L6q;L8p;G8q;L16q	Yes	–	No	c.626 a>T	–	–	–
MP65 CL	Primary Tumor	S	120h	G1q;G6p;G8	Yes	c.1717del	No	–	c.626 A>T	–	–
MM28 CL	PDX established from Liver Metastasis	M	109h	L1p;G1q;L3q;G6p;L6q;L8p;G8q;L16	Yes[1]	c.1881C>A	No	–	c.626 A>T	–	–
MM33 CL	PDX established from Skin Metastasis	M	91h	G1;G6p;G8;G16	No		Yes	c.626 a>C	–	–	c.22G/A
MM66 CL	PDX established from Liver Metastasis	M	80h	G1q;L6q;G8	No	–	Yes	–	c.626 A>T	–	–
92.1 CL	Primary tumor	M	38h	der(X) t(X ;6)(q28 ;p11),+8[5]	ND	ND	Yes	c.626 a>T [4]	–	–	c.17G/A
Mel202 CL	Primary tumor	M	43h	ND	ND	ND	Yes	c.629 G>A [4]	–	c.1793c>T	–
OMM1 CL	Subcutis Metastasis	M	34h	der(1)t(1 ;3)(p31 ;p13),+3[50%], add(8)p11),add(16)(p12) [6]	ND	ND	Yes	–	626 A>T [4]	–	–
0MM2.5 CL	Liver Metastasis	M	50h	ND	ND	ND	Yes	c.626 a>C [4]	–	–	–
MP34 X	Primary tumor	E	7d	L1p ;L6q	Yes[1]	–	Yes	–	c.626 A>T	c.1793c>T	–
MP41 X	Primary tumor	E	15d	L1p ;G1q.L6q;L8p;G8q;G16p;L16q	No	–	Yes	–	626 a>A/T	–	–
MP55 X	Primary tumor	E	8d	L3;G6p;Lq;G8p;G8q;	Yes	c.516C > G	No	–	c.626 A>T	–	–
MP46 X	Primary tumor	M	11d	G1q ;L3 ;G6p ; L8p ; G8q ;L16q	Yes	–	No	c.626 a>T	–	–	–

Table 1. Characteristics of UM cell lines and Xenografts used in this study.

Model: CL, cell line; X, Xenograft; Morphology: S, spindle cell; M, mixed; E, Epithelioid.; Doubling time. h: hours; d:days. ND: not determined.

[1]Uniparental disomy of 3q; [2] Uniparental disomy of chromosome 3; [3] as determined by Western Blot and Immunocytochemistry; [4]92.1 and Mel202 were tested for GNAQ 626A>C, GNAQ 626A>T, GNA11 626A>T the other data on GNA mutations were issued from (Griewank et al., 2012); [5](De Waard-Siebinga et al., 1995); [6](Luyten et al., 1996).

Copy number variations and LOH refers to chromosomes 1, 3, 6, 8 and 16 (G:gain; L:loss).

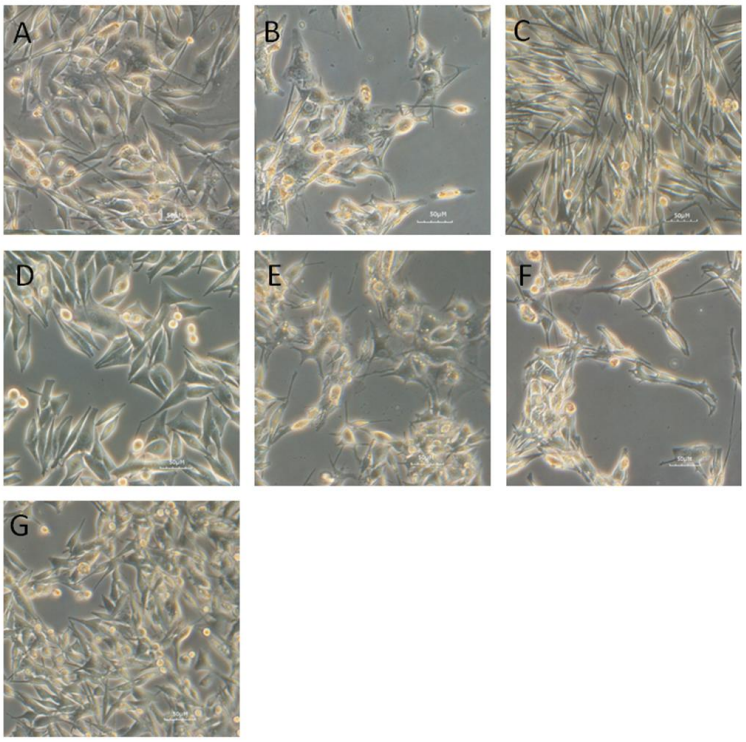

Figure 1. Morphological analysis of established uveal melanoma cell lines. Light microscopy image of UM cell lines showing predominant epithelioid (MP41) spindle (MP38; MP65) or mixed morphology (MM28; MM33; MP46; MM66). MM28 (A), MM33 (B), MP38 (C), MP41 (D), MP46 (E), MP65 (F), MM66 (G).

isodisomy. Five cell lines show gain of 6p and loss or LOH of 6q and one shows loss of 6q only. A gain of 8q was observed in six cell lines except for MP38, with three showing also 8p loss. Loss of 16q was found in four cell lines.

As shown in table 1 all cell lines harbor mutually exclusive mutations in either GNAQ or GNA11 as occurred in the corresponding tumor of origin: *GNAQ* c.626A>C; p.Gln209Pro in MM33 and *GNAQ* c.626A>T p.Gln209Pro in MP46 and MP38, while MP41, MP65, MM28 and MM66 bear *GNA11* mutations (GNA11 c.626 a>T; p.Gln209Leu). Three cell lines display loss of function mutations of the *BAP1* gene associated with a LOH of chromosome 3. MP38 harbors a deletion of 14 pb (c.68-9_72del) leading eventually to the loss of a splice site. MP65 displays a frame-shift deletion of 1pb (c.1717del; p.Leu573TrpfsX3) and MM28 harbors a *BAP1* point mutation (c.1881C>A; p.Y627). Western blot showed expression of BAP1 in MP41,

MM33 and MM66 cell lines and absence of the protein in the 3 *BAP1* mutated cells and in MP46 (Figure 2). The expression of BAP1 was also checked by immunocytochemistry (data not shown) confirming nuclear localization of BAP1 in MP41 M33 and MM66 lines, and absence of nuclear staining in the remaining cell lines. A strong BAP1 nuclear staining was observed as well in a series of previously described UM cell lines including 92.1, Mel202, , OMM1,, and OMM2.5 (Griewank et al., 2012).

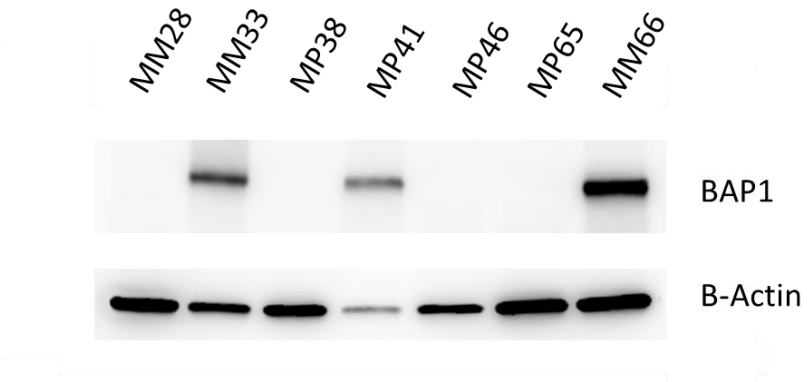

Figure 2. Western blot analysis of BAP1 protein expression in UM cell lines. Immunostaining on cell lines MM33, MP41 and MM66 reveals presence of the protein BAP1 while MP28 MP46 and MP65 show loss of BAP1 protein expression.

All the cell lines established in this study as well as cell lines received from other laboratories were tested for known *SF3B1* mutations. Only Mel202 proved to be mutated for *SF3B1* (c.1793c>T; p.Arg625Gly). *EIF1AX* gene were also tested at exons 1 and 2 and proved mutated in cell lines MM33 (c.22G/A; p.Gly8Arg) and 92**.**1 (c.17G/A; p.Gly6Asp). Short Tandem repeat Polymorphism (STR) genotyping was performed and results are reported in Supplementary table 1.

The expression of 12 tumor-specific antigens (i.e., MAGE1, MAGE2, MAGE3, MAGE4, MAGE6, MAGE10, MAGE-C2, LAGE1, LAGE2, NA17, tyrosinase, and Melan-A) was assessed on cell lines;data are shown in Supplementary table 2. All the cell lines except MM33 showed a strong expression of Tyrosinase and NA-17. Expression of MAGE and LAGE antigens was found to be negative or very low in our cell lines except MP46 which exhibits a 20% and 100% expression of MAGE2 and

MAGE3 respectively). This expression pattern corresponds to what has been already described for the original models and patients (Némati et al., 2010).

3. Activation of mTOR pathway and effect of Everolimus on UM cell lines

UM cells have been reported to display activation of the PKC, MEK-ERK and PI3K/mTOR pathways (Abdel-Rahman et al., 2006; Khalili et al., 2012; Pópulo et al., 2011, 2010; Saraiva et al., 2005) . Clinical trials with PKC and MEK inhibitors are in progress. The MEK inhibitor Selumetinib has been shown to increase progression free survival compared to standard of care, but failed to demonstrate a statistically significant increase in overall survival (Carvajal et al.,2013). No clinical data concerning the use of PI3K/mTOR inhibitors in UM have been reported so far. Some in vitro studies have addressed the effect of these inhibitors using UM cell lines but in a BAP1-proficient context and sometimes with cell lines displaying activating B-RAF mutations (Babchia et al., 2010; Ho et al., 2012; Khalili et al., 2012). We therefore decided to assess the activation status of PI3K/mTOR pathway on our panel of cell lines which recapitulate the genetic features of the disease.

First, we tested the activation of the pathway on 2 BAP1 mutated (MP38 and MP65) and 2 BAP1 wild-type cell lines (MP41 and MM66). BT20, a cell line displaying a PI3KCA mutation conferring a constitutive activity to the kinase, was used as control for the activation of PI3K/mTOR pathway. Analysis of the phosphorylation of mTOR downstream target S6 ribosomal protein (El-Hashemite et al., 2003) showed an activation of mTOR pathway comparable to that of BT20, with evidence of

phosphorylation of the protein also after 24h of serum starvation in 3 out of 4 uveal melanoma cell lines (Figure 3). Phospho-AKT was barely detectable on western blot, and the ratio between phospho AKT and total AKT was found dramatically low as compared to BT20 (Figure 3). This suggests that mTOR activation of UM cell lines is not dependent of AKT phosphorylation. In agreement with this hypothesis, the AKT inhibitor Perifosine did not significantly alter cell proliferation of UM cell lines (supplementary Figure 2).

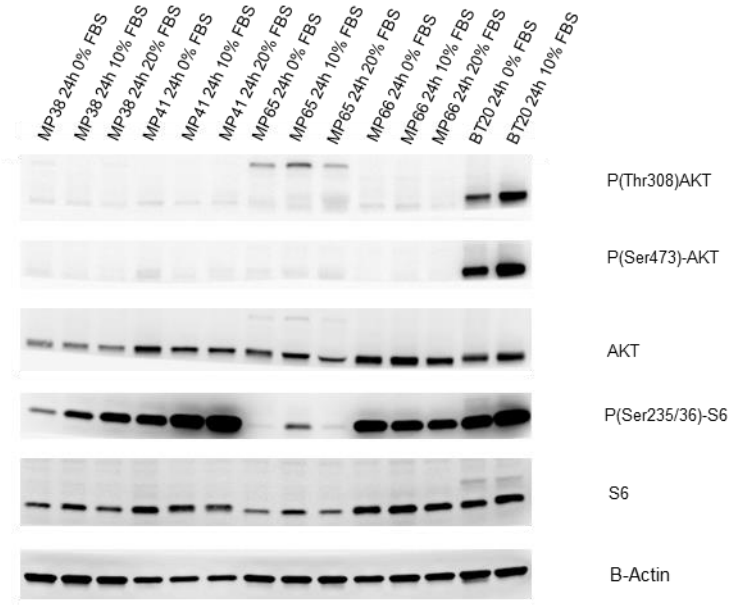

Figure 3. Analysis of mTOR and AKT signaling pathway in UM cell. UM cell lines were cultured for 24h at different serum concentrations. P(Ser473)-AKT, P(Thr308)-AKT, AKT, P(Ser235/236)-S6, S6 and B-Actin were evaluated on cellular lysates by Western blot analysis.

Viability of 10 UM cell lines (MM28, MP38, MP41, MP46, MP56 and MM66, 92.1, Mel202, OMM1 and OMM2.5) was significant affected by Everolimus at relative low doses even if a full inhibition of cellular viability was not reached (Figure 4A). The slopes of curves obtained with Everolimus suggest a cytostatic rather than cytotoxic effect. As depicted in Figure 4B, a dramatic reduction in S6 phosphorylation could be observed in 6 different UM cell lines treated with Everolimus at 1 nM. The most sensitive cell lines in terms of cellular viability (MM66, OMM1 and OMM2.5) display the higher reduction in S6 phosphorylation, whereas MP65 and MP41 are the more resistant to Everolimus in terms of both cell viability and S6 phosphorylation. However a statistically significant correlation between the effect of Everolimus on S6 phosphorylation and cellular viability in the different cell lines could not be demonstrated. Altogether our data demonstrate that UM cell lines display mTOR signaling activation and that Everolimus significantly affects cell proliferation at doses at which it inhibits mTOR downstream signaling.

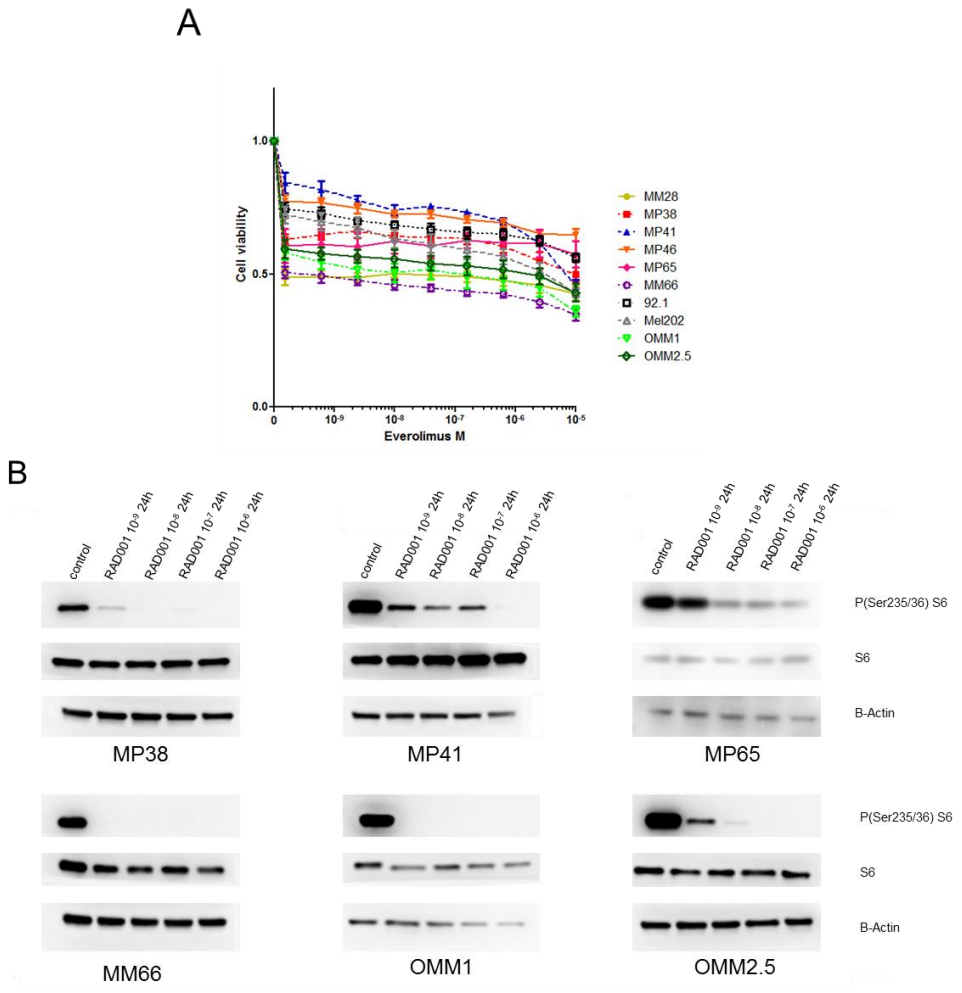

Figure 4. Sensitivity of a representative panel of uveal melanoma cell lines to mTOR inhibitor Everolimus and effect of Everolimus on UM cell lines viability. A. UM cell lines were treated for 24 hours with different concentrations of Everolimus and P(Ser235/236)-S6, S6 and B-Actin assessed by Western blot analysis. **B.** MM28 (GNAQ 11 mutated, BAP1 deficient) Mp38 (GNAQ mutated, BAP1 deficient), MP41 (GNA11 mutated), MP46 (GNAQ mutated, BAP1 deficient) MP65 (GNA11 mutated, BAP1 deficient), MM66 (GNA11 mutated), 92.1 (GNAQ mutated, EIF1AX mutated), Mel202 (GNAQ mutated, SF3B1 mutated), OMM1 (GNA11 mutated), OMM2.5 (GNAQ mutated) were seeded at adequate concentration and left in contact with the drugs for 5 days. Cell viability was quantified with MTT assay. Results are expressed as mean of at least 3 separate experiments. Error bars represent standard errors of the mean.

4. Everolimus effects in vivo

We then decided to test in vivo the effect of Everolimus using our UM PDX panel previously characterized (Laurent et al., 2013; Némati et al., 2010) and representing the genetic landscape of UM. Four models were tested for this purpose: MP34, MP41, MP55, and MP46. We did not succeed in establishing cell lines from MP34 and MP55 PDXs. MP34 displays a mutation in GNAQ and the others harbor GNA11

mutations. Two of them (MP46 and MP55) do not express BAP1 protein as assessed by immunohistochemistry (Laurent et al., 2013). MP34 harbors an *SF3B1* mutation. Mice were treated with Everolimus per os at 2mg/kg 3 times per week for 4 to 6 weeks. As depicted in Figure 5, treatment with the mTOR inhibitor resulted in a significant tumor growth delay in the models MP41, MP55 and MP34, with a Tumor Growth Inhibition (TGI) of 57%, 51% and 47 % respectively, and a moderate effect in MP46 with a TGI of 38%. Taken together, our results show that Everolimus significantly reduced tumor growth of uveal melanoma in vivo.

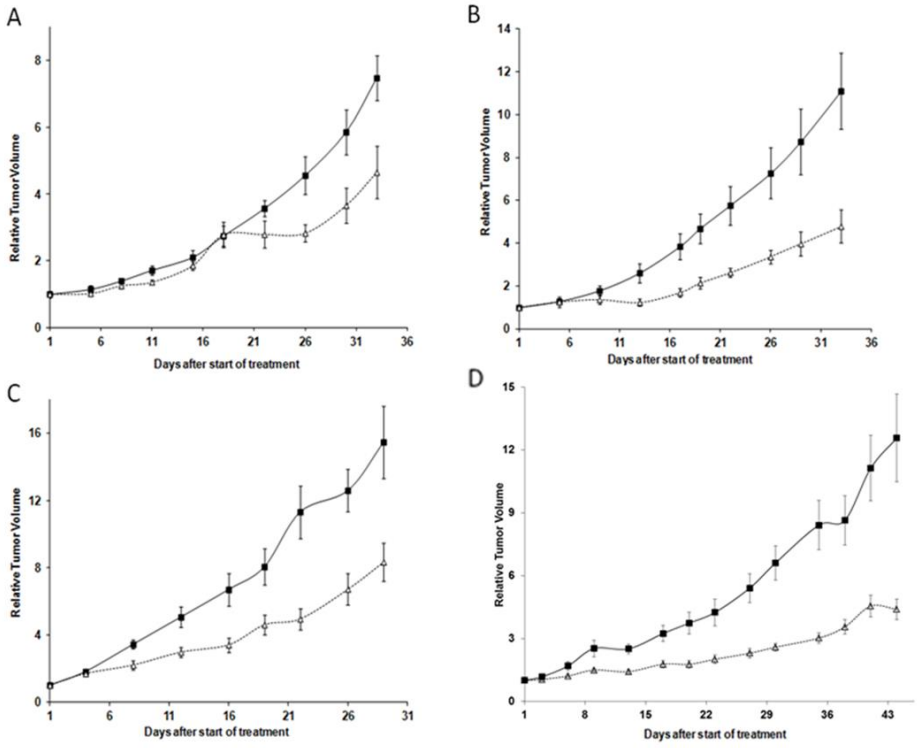

Figure 5. Effects of mTOR inhibitor Everolimus in the growth of four UM PDXs in vivo. Growth curves of four human uveal melanoma xenografts: MP46 (A), MP55 (B), MP34(C), and MP41(D), treated with Everolimus (Δ) per os at 2 mg/kg 3 times a week, or receiving vehicle (■) with the same schedule as the treated animals for 4 (MP46, MP55, MP34) to 6 (MP41) weeks. Tumor volume and RTV were calculated as described in Materials and Methods. Growth curves were obtained by plotting mean RTV against time. Bars, SD. For the treated groups *n* = 6-8 mice; for the control groups *n* = 8-10 mice. P values calculated at the end of the treatment were < 0.05 for the four models.

5. Effect of combined MEK inhibitor and Everolimus on UM cell proliferation

Given that tumor regression was not achieved with Everolimus alone and since mTOR inhibitors have been reported to have a rather cytostatic than cytotoxic effect (Weigelt et al., 2011), combinatorial approaches need to be addressed to implement efficient therapeutic schedules. MAPK inhibitors clearly represent good candidates to be tested in combination with Everolimus given that *GNAQ*/*11* activating mutations result in MAPK upregulated activity. Interestingly the MEK inhibitor Trametinib has shown in our hands to display the lowest IC_{50} among a panel of compounds tested on UM cell lines (data not shown). Moreover recent data encouraged further testing MEK inhibitors in uveal melanoma metastatic patients (Carvajal et al. 2013) . We therefore tested on the already described panel of 10 UM cell lines whether the MEK inhibitor GSK1120212 (Trametinib) could enhance the in vitro efficacy of Everolimus. Figure 6A-C shows the effect of single drug and of the combination on the 10 different cell lines. Analysis of synergism was performed according to two different models: Bliss independence (Keith et al., 2005) and combination Index described by Chou and Talalay (reference). Although both analyses gave roughly the same results the first method was more reproducible in our hands and therefore only the data generated with it are shown in Supplementary Figure 3. Importantly, the majority of UM cell lines exhibited low to moderate synergy between Everolimus and Trametinib suggesting that combinatorial approaches with agents targeting MEK and mTOR pathways could be promising for treatment of UM patients. This needs to be addressed in preclinical in vivo models. Under our in vitro experimental conditions combination of Everolimus and Trametinib did not result in induction of apoptosis (examining cleaved PARP by Western blot) in UM cell lines with the exception of 92.1 cells in which Everolimus was shown to increase the apoptosis induced by Trametinib (data not shown). Furher investigations will be necessary to better understand the molecular mechanisms resulting in the observed synergy of these two compounds.

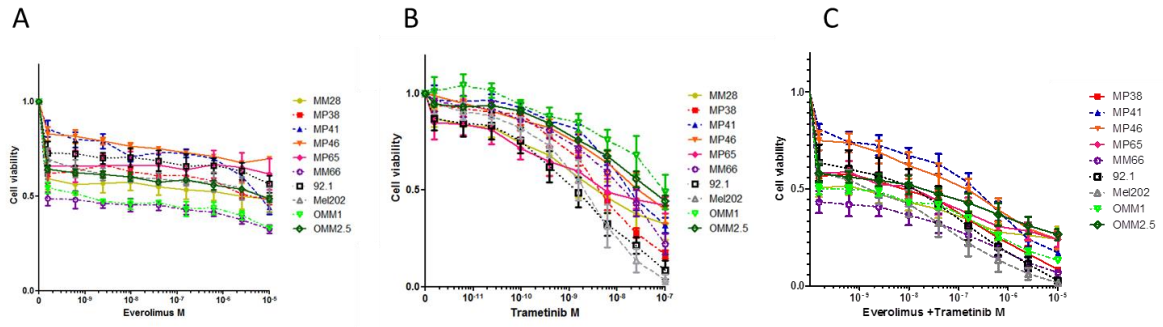

Figure 6. Effect of the combination of MEK inhibitor Trametinib and mTOR inhibitor Everolimus on the viability of a panel of 10 UM cell lines. Cell lines were treated at the indicated doses of inhibitors for 5 days and cell viability was determined by MTT as described in Material and Methods. Drug concentration is expressed as Molarity; Drug concentration in (C) is expressed as sum of the concentration of each drug . A and B: single drug curves for Everolimus and Trametinib, C: combination. Drug concentrations for the combination had been selected maintaining a constant ratio between the two drugs in order to facilitate synergy evaluation.

IV. Discussion

An efficient management of UM patients requires a better understanding of genetic and molecular abnormalities implicated in development and progression of this disease. With the emergence of an armamentarium of targeted drugs it is mandatory having at your disposal relevant *in vitro* and *in vivo* preclinical models for testing new drugs and drug combinations in order to rationally set up clinical trials. We have recently described a panel of patient-derived UM PDXs which recapitulates the genetic features of primary human UMs and exhibit genetic stability over the course of their *in vivo* maintenance (Laurent et al., 2013; Némati et al., 2010). Although this panel represents a useful preclinical tool for both pharmacologic and biological assessments, it is preferable for some functional studies to have access to a panel of well-characterized tumor cell lines. Unfortunately obtaining UM cell lines from patients is not easy and the cell lines reported to be of uveal origin do not always display the genetic alterations described in UM. Actually some UM cell lines described in the literature have activating mutations in BRAF (Calipel et al., 2003; Griewank et al., 2012) despite the absence of these mutations in UM tissues, and no UM cell line harboring BAP1 mutations, a hallmark of metastasizing UM, has been reported. In this paper we have established and characterized 7 new human UM cell

lines. Five of them were obtained from PDXs models and the other two directly from human primary tumors. This suggests that the success in establishing UM cell lines could be significantly improved by previously engrafting the UM samples in immunodeficient mice as already reported for colorectal tumors (Dangles-Marie et al., 2007). We are still working to develop UM cell lines from our entire collection of PDX and hope to expand our cell lines panel in the future. The UM cell lines described here match the genotype of the tumors of origin. All of them harbor mutually exclusive activating mutation in either *GNAQ* or *GNA11*. Importantly we have established 4 BAP1-deficient UM cell lines. Interestingly we could not demonstrate any BAP1 mutation in the BAP1 deficient model MP46, which display a LOH with isodisomy of chromosome 3. For all the cell lines established, the absence of nuclear BAP1 totally correlated with LOH of chromosome 3. The 7 cell lines were found to be wild type for *SF3B1* while one was found mutated in the *EIF1AX* gene. These two mutations are associated with good prognosis (Furney et al., 2013; Harbour et al., 2013; Martin et al., 2013).

We have shown that Everolimus significantly affects the cell growth of our UM cell line panel and other UM cell lines previously described. It has been reported that Everolimus very slightly affects cell proliferation of two UM cell lines (92.1 and Mel270) at doses at which it entirely inhibit mTOR downstream signaling (Babchia et al., 2010). Interestingly, the cell lines displaying the highest sensitivity to Everolimus in terms of cell viability exhibited a more pronounced reduction in the phosphorylation S6 ribosomal protein and viceversa. We have also shown that mTOR signaling seems activated in the absence of significant activation of AKT. The activation of mTOR can be a consequence of MAPK activation resulting from *GNAQ*/*11* activating mutations present in 84% of UM. In a recent study the PI3K inhibitor GSK2126458 showed a reduced efficacy on *GNAQ* or *GNA11* mutated UM cell lines compared to wild type uveal melanoma cells (Khalili et al., 2012). Interestingly in the same study RPPA analysis showed a reduced phosphorylation of pS473-AKT in *GNAQ* mutated cells compared to *GNAQ* wild type. Basal P-4EBP and basal P-S6 were on the contrary higher in the *GNAQ* mutated cell lines, suggesting a key role of the pathway downstream of mTOR in *GNAQ* mutant cells. This is in line with the observation that in our cellular models phosphorylation of AKT was very weak in comparison with a cell line (BT20) displaying a constitutive active PI3K/AKT pathway. On the contrary,

phosphorylation of S6 in our cellular models and in BT20 cell line was similar. Interestingly MP41 and MM66 showed significant phosphorylation of S6 even after 24h serum starvation at the same levels of the controls, suggesting a constitutive activation of the pathway.

Inhibiting PI3K axis alone or in combination with mTOR inhibition has been proposed as a therapeutic strategy for UM (Babchia et al., 2010). These studies have shown that PI3K inhibition by LY294002 is more effective than mTOR inhibition by Everolimus but these differences were significant only in a *GNAQ/11* wild type context.

Few studies have addressed the effect of PI3K/mTOR pathway *in vivo* and results were non-conclusive or conducted with cell lines not perfectly representing the genetic landscape of UM (Ho et al., 2012). Here we show that the mTOR inhibitor Everolimus significantly delayed tumor growth in 4 different UM PDX models. In vivo effect of Everolimus does not seem to be dependent of the BAP1 status but the reduced number of PDX models (2 BAP1 proficient and 2 BAP1 deficient) cannot allow concluding about a potential influence of BAP status on the response to this agent. In vitro data suggest that genetic differences and specifically BAP1 mutations does not influence the response to Everolimus. Although cell lines established from UM metastases were at least as sensitive to Everolimus as cell lines established from primary tumors, it is important to note that the four UM PDX models used in this work were established from primary tumors. In the absence of a comprehensive study addressing the genetic landscape of metastatic UM we need to be cautious in the conclusions about potential effects of Everolimus on metastatic UM patients.

Given that treatment with Everolimus did not result in tumor regression, combination strategies need to be addressed in vitro and in vivo. Actually, the effect of Everolimus alone is probably cytostatic and it might benefit from combination with MEK inhibitors or low doses of dual mTOR/PI3K inhibitors as suggested in recent studies (Mitsiades et al., 2011; Nyfeler et al., 2012).

Everolimus has already indications in oncology and a clinical phase 2 trial is currently ongoing at Sloan-Kettering cancer center with the aim of assessing its efficacy in combination with a somatostatin receptor inhibitor Pasireotide on patients with metastatic UM (clinicaltrial.gov identifier NCT01252251). Our preliminary data

indicates a synergy of Everolimus and the MEK inhibitor Trametinib. It would be necessary to evaluate the synergy displayed by other combinations of currently available inhibitors of PI3K/mTOR and MEK-ERK pathways across a heterogeneous panel of UM cell lines and then to assess their efficacy in vivo . We believe our approach using *in vitro* and *in vivo* models will help to orientate in the future innovative clinical trials in uveal melanoma patients.

V. Conclusions

We have established 7 UM cell lines from either patient surgical specimens or patient-derived xenografts (PDXs). This panel of cell lines has been fully characterized in terms of genetic alterations and recurrent mutations and recapitulates together with our previously described panel of PDXs (Laurent et al., 2013; Némati et al., 2010) the diversity of UM genetic landscape. Moreover we have demonstrated in our UM cellular models the activation of mTOR pathway in the absence of significant AKT phosphorylation. Treatment with the mTOR inhibitor Everolimus resulted in the reduction of cell viability of all the studied UM cell lines and significantly delayed in vivo tumor growth of 4 independent UM PDXs. Although efficient therapeutic combinations need to be carefully evaluated, our data suggest that Everolimus could be considered as a therapeutic option for managing UM.

VI. References

Abdel-Rahman, M.H., Yang, Y., Zhou, X.-P., Craig, E.L., Davidorf, F.H., Eng, C., 2006. High Frequency of Submicroscopic Hemizygous Deletion Is a Major Mechanism of Loss of Expression of PTEN in Uveal Melanoma. JCO 24, 288–295.

Babchia, N., Calipel, A., Mouriaux, F., Faussat, A.-M., Mascarelli, F., 2010. The PI3K/Akt and mTOR/P70S6K signaling pathways in human uveal melanoma cells: interaction with B-Raf/ERK. Invest. Ophthalmol. Vis. Sci. 51, 421–429.

Calipel, A., Lefevre, G., Pouponnot, C., Mouriaux, F., Eychène, A., Mascarelli, F., 2003. Mutation of B-Raf in Human Choroidal Melanoma Cells Mediates Cell Proliferation and Transformation through the MEK/ERK Pathway. J. Biol. Chem. 278, 42409–42418.

Carvajal, R.D., Sosman, J.A., Quevedo, F., Milhem, M.M., Joshua, A.M., Kudchadkar, R.R., Linette, G.P., Gajewski, T., Lutzky, J., Lawson, D.H., Lao, C.D., Flynn, P.J., Albertini, M.R., Sato, T., Paucar, D., Panageas, K.S., Dickson, M.A., Wolchok, J.D., Chapman, P.B., Schwartz, D.K., 2013. Phase II study of selumetinib (sel) versus temozolomide (TMZ) in gnaq/Gna11 (Gq/11) mutant (mut) uveal melanoma (UM). J. Clin. Oncol. 31, 2013 ASCO annual Meeting Abstracts.

Chen, P.W., Murray, T.G., Uno, T., Salgaller, M.L., Reddy, R., Ksander, B.R., 1997. Expression of MAGE genes in ocular melanoma during progression from primary to metastatic disease. Clin. Exp. Metastasis 15, 509–518.

Chou, T.-C., 2006. Theoretical Basis, Experimental Design, and Computerized Simulation of Synergism and Antagonism in Drug Combination Studies. Pharmacol Rev 58, 621–681.

Chou, T.-C., 2010. Drug Combination Studies and Their Synergy Quantification Using the Chou-Talalay Method. Cancer Res 70, 440–446.

Cohen, Y., Goldenberg-Cohen, N., Parrella, P., Chowers, I., Merbs, S.L., Pe'er, J., Sidransky, D., 2003. Lack of BRAF Mutation in Primary Uveal Melanoma. IOVS 44, 2876–2878.

Couturier, J., Saule, S., 2012. Genetic determinants of uveal melanoma. Dev Ophthalmol 49, 150–165.

Cruz, F., Rubin, B.P., Wilson, D., Town, A., Schroeder, A., Haley, A., Bainbridge, T., Heinrich, M.C., Corless, C.L., 2003. Absence of BRAF and NRAS Mutations in Uveal Melanoma. Cancer Res 63, 5761–5766.

Dangles-Marie, V., Pocard, M., Richon, S., Weiswald, L.-B., Assayag, F., Saulnier, P., Judde, J.-G., Janneau, J.-L., Auger, N., Validire, P., Dutrillaux, B., Praz, F., Bellet, D., Poupon, M.-F., 2007. Establishment of human colon cancer cell lines from fresh tumors versus xenografts: comparison of success rate and cell line features. Cancer Res. 67, 398–407.

De Waard-Siebinga, I., Blom, D.J., Griffioen, M., Schrier, P.I., Hoogendoorn, E., Beverstock, G., Danen, E.H., Jager, M.J., 1995. Establishment and characterization of an uveal-melanoma cell line. Int. J. Cancer 62, 155–161.

Dunavoelgyi, R., Dieckmann, K., Gleiss, A., Sacu, S., Kircher, K., Georgopoulos, M., Georg, D., Zehetmayer, M., Poetter, R., 2011. Local Tumor Control, Visual Acuity, and Survival After Hypofractionated Stereotactic Photon Radiotherapy of Choroidal Melanoma in 212 Patients Treated Between 1997 and 2007. International Journal of Radiation Oncology*Biology*Physics 81, 199–205.

Edmunds, S.C., Cree, I.A., Dí Nícolantonío, F., Hungerford, J.L., Hurren, J.S., Kelsell, D.P., 2003. Absence of BRAF gene mutations in uveal melanomas in contrast to cutaneous melanomas. Br J Cancer 88, 1403–1405.

El-Hashemite, N., Zhang, H., Henske, E.P., Kwiatkowski, D.J., 2003. Mutation in TSC2 and activation of mammalian target of rapamycin signalling pathway in renal angiomyolipoma. The Lancet 361, 1348–1349.

Furney, S.J., Pedersen, M., Gentien, D., Dumont, A.G., Rapinat, A., Desjardins, L., Turajlic, S., Piperno-Neumann, S., De la Grange, P., Roman-Roman, S., Stern, M.-H., Marais, R., 2013. SF3B1 mutations are associated with alternative splicing in uveal melanoma. Cancer Discov.

Gragoudas, E.S., Egan, K.M., Seddon, J.M., Glynn, R.J., Walsh, S.M., Finn, S.M., Munzenrider, J.E., Spar, M.D., 1991. Survival of patients with metastases from uveal melanoma. Ophthalmology 98, 383–389; discussion 390.

Griewank, K.G., Yu, X., Khalili, J., Sozen, M.M., Stempke-Hale, K., Bernatchez, C., Wardell, S., Bastian, B.C., Woodman, S.E., 2012. Genetic and molecular characterization of uveal melanoma cell lines. Pigment Cell Melanoma Res 25, 182–187.

Harbour, J.W., 2012. The genetics of uveal melanoma: an emerging framework for targeted therapy. Pigment Cell Melanoma Res 25, 171–181.

Harbour, J.W., Chen, R., 2013. The DecisionDx-UM Gene Expression Profile Test Provides Risk Stratification and Individualized Patient Care in Uveal Melanoma. PLoS Currents.

Harbour, J.W., Onken, M.D., Roberson, E.D.O., Duan, S., Cao, L., Worley, L.A., Council, M.L., Matatall, K.A., Helms, C., Bowcock, A.M., 2010. Frequent Mutation of BAP1 in Metastasizing Uveal Melanomas. Science 330, 1410–1413.

Harbour, J.W., Roberson, E.D.O., Anbunathan, H., Onken, M.D., Worley, L.A., Bowcock, A.M., 2013. Recurrent mutations at codon 625 of the splicing factor SF3B1 in uveal melanoma. Nat. Genet. 45, 133–135.

Ho, A.L., Musi, E., Ambrosini, G., Nair, J.S., Deraje Vasudeva, S., De Stanchina, E., Schwartz, G.K., 2012. Impact of combined mTOR and MEK inhibition in uveal melanoma is driven by tumor genotype. PLoS ONE 7, e40439.

Keith, C.T., Borisy, A.A., Stockwell, B.R., 2005. Multicomponent therapeutics for networked systems. Nat Rev Drug Discov 4, 71–78.

Khalili, J.S., Yu, X., Wang, J., Hayes, B.C., Davies, M.A., Lizee, G., Esmaeli, B., Woodman, S.E., 2012. Combination small molecule MEK and PI3K inhibition enhances uveal melanoma cell death in a mutant GNAQ- and GNA11-dependent manner. Clin. Cancer Res. 18, 4345–4355.

Kiliç, E., Brüggenwirth, H.T., Verbiest, M.M.P.J., Zwarthoff, E.C., Mooy, N.M., Luyten, G.P.M., De Klein, A., 2004. The RAS-BRAF kinase pathway is not involved in uveal melanoma. Melanoma Res. 14, 203–205.

Ksander, B.R., Rubsamen, P.E., Olsen, K.R., Cousins, S.W., Streilein, J.W., 1991. Studies of tumor-infiltrating lymphocytes from a human choroidal melanoma. Invest. Ophthalmol. Vis. Sci. 32, 3198–3208.

Laurent, C., Gentien, D., Piperno-Neumann, S., Némati, F., Nicolas, A., Tesson, B., Desjardins, L., Mariani, P., Rapinat, A., Sastre-Garau, X., Couturier, J., Hupé, P., De Koning, L., Dubois, T., Roman-Roman, S., Stern, M.-H., Barillot, E., Harbour, J.W., Saule, S., Decaudin, D., 2013. Patient-derived xenografts recapitulate molecular features of human uveal melanomas. Mol Oncol 7, 625–636.

Luyten, G.P., Naus, N.C., Mooy, C.M., Hagemeijer, A., Kan-Mitchell, J., Van Drunen, E., Vuzevski, V., De Jong, P.T., Luider, T.M., 1996. Establishment and characterization of primary and metastatic uveal melanoma cell lines. Int. J. Cancer 66, 380–387.

Mallone, S., De Vries, E., Guzzo, M., Midena, E., Verne, J., Coebergh, J.W., Marcos-Gragera, R., Ardanaz, E., Martinez, R., Chirlaque, M.D., Navarro, C., Virgili, G., 2012. Descriptive epidemiology of malignant mucosal and uveal melanomas and adnexal skin carcinomas in Europe. European Journal of Cancer 48, 1167–1175.

Martin, M., Maßhöfer, L., Temming, P., Rahmann, S., Metz, C., Bornfeld, N., Van de Nes, J., Klein-Hitpass, L., Hinnebusch, A.G., Horsthemke, B., Lohmann, D.R., Zeschnigk, M., 2013. Exome sequencing identifies recurrent somatic mutations in EIF1AX and SF3B1 in uveal melanoma with disomy 3. Nat. Genet.

Marty, B., Maire, V., Gravier, E., Rigaill, G., Vincent-Salomon, A., Kappler, M., Lebigot, I., Djelti, F., Tourdès, A., Gestraud, P., Hupé, P., Barillot, E., Cruzalegui, F., Tucker, G.C., Stern, M.-H., Thiery, J.-P., Hickman, J.A., Dubois, T., 2008. Frequent PTEN genomic alterations and activated phosphatidylinositol 3-kinase pathway in basal-like breast cancer cells. Breast Cancer Res. 10, R101.

Mitsiades, N., Chew, S.A., He, B., Riechardt, A.I., Karadedou, T., Kotoula, V., Poulaki, V., 2011. Genotype-Dependent Sensitivity of Uveal Melanoma Cell Lines to Inhibition of B-Raf, MEK, and Akt Kinases: Rationale for Personalized Therapy. Investigative Ophthalmology & Visual Science 52, 7248–7255.

Némati, F., Sastre-Garau, X., Laurent, C., Couturier, J., Mariani, P., Desjardins, L., Piperno-Neumann, S., Lantz, O., Asselain, B., Plancher, C., Robert, D., Péguillet, I., Donnadieu, M.-H., Dahmani, A., Bessard, M.-A., Gentien, D., Reyes, C., Saule, S., Barillot, E., Roman-Roman, S., Decaudin, D., 2010. Establishment and Characterization of a Panel of Human Uveal Melanoma Xenografts Derived from Primary and/or Metastatic Tumors. Clin Cancer Res 16, 2352–2362.

Nyfeler, B., Chen, Y., Li, X., Pinzon-Ortiz, M., Wang, Z., Reddy, A., Pradhan, E., Das, R., Lehár, J., Schlegel, R., Finan, P.M., Cao, Z.A., Murphy, L.O., Huang, A., 2012. RAD001 Enhances the Potency of BEZ235 to Inhibit mTOR Signaling and Tumor Growth. PLoS ONE 7, e48548.

Onken, M.D., Worley, L.A., Ehlers, J.P., Harbour, J.W., 2004. Gene expression profiling in uveal melanoma reveals two molecular classes and predicts metastatic death. Cancer Res. 64, 7205–7209.

Pópulo, H., Soares, P., Faustino, A., Rocha, A.S., Silva, P., Azevedo, F., Lopes, J.M., 2011. mTOR pathway activation in cutaneous melanoma is associated with poorer prognosis characteristics. Pigment Cell & Melanoma Research 24, 254–257.

Pópulo, H., Soares, P., Rocha, A.S., Silva, P., Lopes, J.M., 2010. Evaluation of the mTOR pathway in ocular (uvea and conjunctiva) melanoma. Melanoma Res. 20, 107–117.

Rimoldi, D., Salvi, S., Liénard, D., Lejeune, F.J., Speiser, D., Zografos, L., Cerottini, J.-C., 2003. Lack of BRAF Mutations in Uveal Melanoma. Cancer Res 63, 5712–5715.

Saraiva, V.S., Caissie, A.L., Segal, L., Edelstein, C., Burnier, M.N., Jr, 2005. Immunohistochemical expression of phospho-Akt in uveal melanoma. Melanoma Res. 15, 245–250.

Selumetinib Shows Promise in Metastatic Uveal Melanoma, 2013. . Cancer Discovery 3, OF8–OF8.

Singh, A.D., Topham, A., 2003. Survival rates with uveal melanoma in the United States: 1973-1997. Ophthalmology 110, 962–965.

Singh, A.D., Turell, M.E., Topham, A.K., 2011. Uveal Melanoma: Trends in Incidence, Treatment, and Survival. Ophthalmology 118, 1881–1885.

Straussman, R., Morikawa, T., Shee, K., Barzily-Rokni, M., Qian, Z.R., Du, J., Davis, A., Mongare, M.M., Gould, J., Frederick, D.T., Cooper, Z.A., Chapman, P.B., Solit, D.B., Ribas, A., Lo, R.S., Flaherty, K.T., Ogino, S., Wargo, J.A., Golub, T.R., 2012. Tumour micro-environment elicits innate resistance to RAF inhibitors through HGF secretion. Nature advance online publication.

Trolet, J., Hupé, P., Huon, I., Lebigot, I., Decraene, C., Delattre, O., Sastre-Garau, X., Saule, S., Thiéry, J.-P., Plancher, C., Asselain, B., Desjardins, L., Mariani, P., Piperno-Neumann, S., Barillot, E., Couturier, J., 2009. Genomic profiling and identification of high-risk uveal melanoma by array CGH analysis of primary tumors and liver metastases. Invest. Ophthalmol. Vis. Sci. 50, 2572–2580.

Tuefferd, M., De Bondt, A., Van Den Wyngaert, I., Talloen, W., Verbeke, T., Carvalho, B., Clevert, D.-A., Alifano, M., Raghavan, N., Amaratunga, D., Göhlmann, H., Broët, P., Camilleri-Broët, S., 2008. Genome-wide copy number alterations detection in fresh frozen and matched FFPE samples using SNP 6.0 arrays. Genes, Chromosomes and Cancer 47, 957–964.

Van Raamsdonk, C.D., Bezrookove, V., Green, G., Bauer, J., Gaugler, L., O'Brien, J.M., Simpson, E.M., Barsh, G.S., Bastian, B.C., 2008. Frequent somatic mutations of GNAQ in uveal melanoma and blue naevi. Nature 457, 599–602.

Van Raamsdonk, C.D., Griewank, K.G., Crosby, M.B., Garrido, M.C., Vemula, S., Wiesner, T., Obenauf, A.C., Wackernagel, W., Green, G., Bouvier, N., Sozen, M.M., Baimukanova, G., Roy, R., Heguy, A., Dolgalev, I., Khanin, R., Busam, K., Speicher, M.R., O'Brien, J., Bastian, B.C., 2010. Mutations in GNA11 in uveal melanoma. N. Engl. J. Med. 363, 2191–2199.

Weber, A., Hengge, U.R., Urbanik, D., Markwart, A., Mirmohammadsaegh, A., Reichel, M.B., Wittekind, C., Wiedemann, P., Tannapfel, A., 2003. Absence of mutations of the BRAF gene

and constitutive activation of extracellular-regulated kinase in malignant melanomas of the uvea. Lab. Invest. 83, 1771–1776.
Weigelt, B., Warne, P.H., Downward, J., 2011. PIK3CA mutation, but not PTEN loss of function, determines the sensitivity of breast cancer cells to mTOR inhibitory drugs. Oncogene 30, 3222–3233.

Supplementary Figure Legends

Supplementary Figure S1. DNA microarray analysis of the 7 Uveal Melanoma cell lines. Allele ratio (top) copy number values (middle), and Log2ratio (bottom) for MM28 (A), MM33 (B), MP38 (C), MP41 (D), MP46 (E), MP65 (F), MM66 (G); red line:LOH.

Supplementary figure S2. Sensitivity of a representative panel of uveal melanoma cell lines to AKT inhibitor Perifosine. MM28 (GNAQ 11 mutated, BAP1 deficient) MP38 (GNAQ mutated, BAP1 deficient), MP41 (GNA11 mutated), MP46 (GNAQ mutated, BAP1 deficient) MP65 (GNA11 mutated, BAP1 deficient), MM66 (GNA11 mutated), 92.1 (GNAQ mutated, EIF1AX mutated), Mel202 (GNAQ mutated, SF3B1 mutated), OMM1 (GNA11 mutated), OMM2.5 (GNAQ mutated) were seeded at adequate concentration and left in contact with the drugs for 5 days. Cell viability was quantified with MTT assay. Results are expressed as mean of at least 3 separate experiments. Error bars represent standard errors of the mean.

Supplementary figure S3. Synergy by excess over Bliss (A) and corresponding normalised cell viability fractions (B) for the combination of Everolimus and Trametinib on a panel of 10 UM cell lines. Fractional inhibition calculated for Trametinib and Everolimus used as single agent and in combination were used to assess synergy as explained in paragraph 2.11. Results from 3 independent experiments were used to calculate 95% confidence intervals. **A** shows synergy values as mean of three separate experiments, values that resulted significantly > 0 with a p value <0.05 are colored in red (synergy), values that resulted significantly < 0 with a p value <0.05 are colored in blue (antagnism), values that produced synergy values not significantly different from 0 are colored in white

(antagonism). **B.** express the corresponding percentage of fractional inhibition for each condition tested.

Supplementary Figure 1

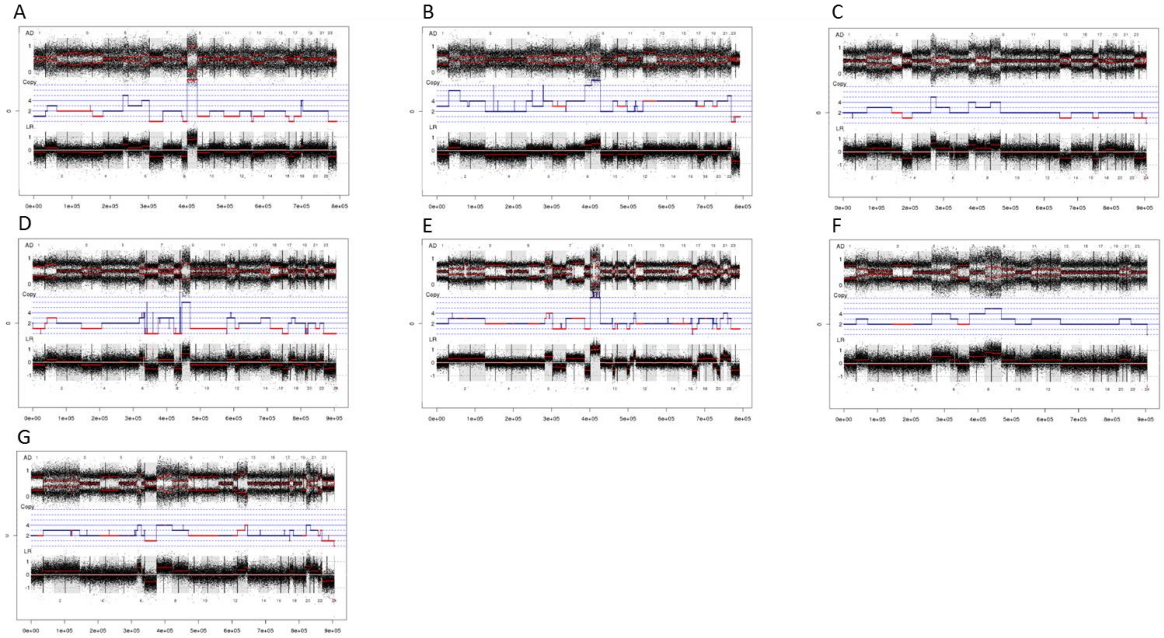

Supplementary Figure 2

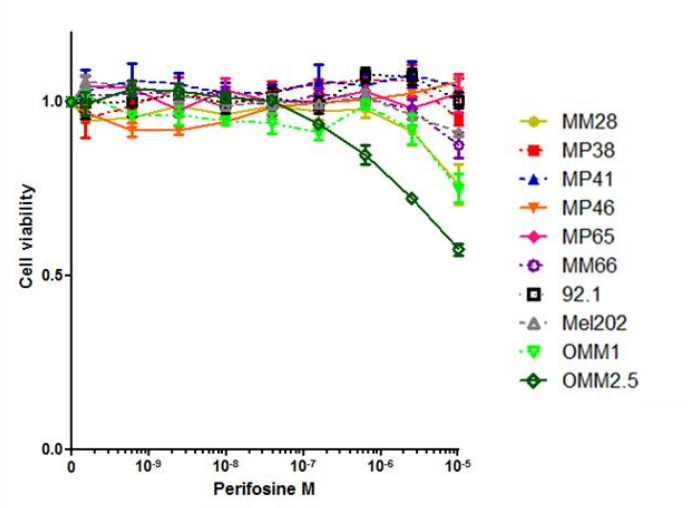

Supplementary Figure 3

A

Rad001	Trametinib	MM28	MP38	MP41	MP46	MP65	MM66	92.1	Mel202	OMM1	OMM2.5
10µM	100nM	-7	0	-3	4	3	1	3	1	3	-5
2,5µM	25nM	-7	-2	4	5	2	5	7	2	9	-1
625nM	6,25nM	-3	1	8	6	3	5	3	6	7	1
156nM	1,56nM	-3	6	7	5	1	5	4	10	2	2
39,1nM	0,391nM	-2	3	1	6	0	5	2	11	-1	1
9,7nM	0,1nM	0	7	0	4	-3	3	2	7	0	3
2,4nM	0,02nM	0	6	5	3	3	2	4	7	-1	3
0,6nM	0,006nM	-5	1	4	4	-3	4	3	5	4	2
0,02nM	0,002nM	2	2	4	7	-1	4	2	8	6	3

B

Rad001	Trametinib	MP38	MP41	MP46	MP65	MM28	MM66	92.1	Mel202	OMM1	OMM2.5
10µM	100nM	92	83	76	76	76	93	97	98	87	74
2,5µM	25nM	83	76	70	72	74	88	89	94	82	69
625nM	6,25nM	75	62	61	69	72	81	80	87	74	63
156nM	1,56nM	66	47	51	63	66	74	69	78	65	57
39,1nM	0,391nM	56	37	44	56	60	68	58	68	58	53
9,7nM	0,1nM	51	33	38	49	57	64	48	58	57	48
2,4nM	0,02nM	46	28	31	48	53	59	43	53	51	46
0,6nM	0,006nM	42	26	26	41	48	58	40	46	50	44
0,02nM	0,002nM	44	19	25	42	50	57	37	42	50	42

Supplementary Table S1. Short tandem repeats profiles of uveal melanoma cell lines.

CELL LINE	**Amelogenin**	**CSF1PO**	**D13S317**	**D16S539**	**D5S818**	**D7S820**	**THO1**	**TPOX**	**vWA**	**D21S11**
MM28	x;y	11	8;11	10;12	11	8;10	7;9,3	11	17;18	28;29
MM33	x	10;12	8	11;12	11:12	10;11	6;8	11	15	31,2;32,2
MP38	x	11	12	9	12	10;12	7;9	8	14;17	31;31,2
MP41	x	9;10	11;14	13	10;13	9;10	6;7	8;11	15;18	30,2;31,2
MP46	x	11	10;12	12	12	11	9	11	16;17	30;31
MP65	x	10	8;13	11	12	8;11	7;9,3	8;12	14;18	30;30,2
MM66	x	12	12;14	11;13	12;13	10	6;7	8;11	14;18	28;31
92.1	x	10;11	11.12	12	9;11	10;11	9;9,3	8;9	16	30
MEL 202	x	10;11	11;13	11;12	11;12	11;12	6;7	8	18;19	30,2;31,2
OMM1	x	10;12	12	9	11	13	7	8;9	19	30;30,2
OMM2.5	x;y	11	12	12	12	8 ;9	6;9	10	17;18	28 ;29

Supplementary Table S2. Expression of tumoral antigens relative to maximal expression

	MM33	MP46	MP65	MM66	Mel285	MM28	MP38	MP41
Actine	+/-	++	+++	+++	+++	+++	+++	+++
NA17	+/-	+++	+++	+++	0	+++	+++	+++
Tyrosinase	+	+	+++	++++	0	+++	+	++++
Melan-A	+	+++	++++	++++	0	++++	++++	++++
MAGE-1	0	+	0	0	0	+/-	0	+/-
MAGE-2	0	++	0	0	0	+/-	+/-	+/-
MAGE-3	0	++	0	0	0	+/-	++	+/-
MAGE-4	0	0	0	0	0	0	0	0
MAGE-6	0	+	0	0	0	+	+	+/-
MAGE-10	0	0	0	0	0	0	0	0
LAGE-1	0	+/-	0	0	0	0	0	0
LAGE-2	+/-	+	0	0	0	0	0	0
MAGE-C2	0	0	0	0	0	0	0	0

+/-: <= 4%; +: 4-20%; ++: 20-100%; +++: 100%; ++++: > 100%.

Identification of strong combination activity between PIK3 and mTOR inhibitors in uveal melanoma cell lines

Nabil Amirouchene-Angelozzi[a], **Marie Schoumacher**[b], **Guillaume Carita**[c], **Ahmed Dahmani**[c], **David Gentien**[d] , **Fariba Nemati**[b], **Didier Decaudin**[c] **and Sergio Roman-Roman**[b]

Authors' Affiliations:

[a]Biophenics Laboratory, Translational Research Department, Institut Curie, 26 rue d'Ulm 75005, Paris; ; [b]Translational Research Department, Institut Curie, 26 rue d'Ulm 75005, Paris; [c]Laboratory of Preclinical Investigation, Translational Research Department, Institut Curie, 26, rue d'Ulm 75005, Paris; [d]Genomics Platform, Translational Research Department, Institut Curie, 26 rue d'Ulm 75005, Paris;

Corresponding Author: Sergio Roman-Roman, Institut Curie, Translational Research Department, 26 rue Ulm 75005 Paris, France
Phone: +33 153197411 Fax +33153194130 E-mail: Sergio.Roman-Roman@curie.fr.

Highlights:

- A panel of UM cell lines including BAP1-deficient cells has been used for in vitro synergy assays.
- A pipeline for fast and systematic assessment of synergy in 2-drugs combinations has been developed.
- Everolimus and PI3K inhibitor GDC0941 are highly synergistic in vitro and strongly induce apoptosis in UM cell lines.

Keywords: uveal melanoma, cell lines, BAP1, Everolimus, mTOR, GDC0941, PI3K, synergy, apoptosis.

Grant Support: This project is supported by French national cancer Institute (INCa).

Disclosure of Potential Conflicts of Interest: No potential conflicts of interest were disclosed.

ABSTRACT

Uveal Melanoma (UM) is the most frequent primary ocular tumor. About a half of the patients develop metastatic disease, for which no treatment has proved effective. We have developed a fast pipeline to screen 2 drug combinations for synergy. We applied this method to a panel of UM cell lines representative of the molecular background of the disease. We tested 7 targeted agents for which promising preclinical results have been reported, assessing all the possible 2-drugs combinations. We selected the most synergistic associations for further in vitro evaluation. Among them the most promising is the association of mTOR inhibitor Everolimus and PI3K inhibitor GDC0941, which resulted in a strong increase of apoptosis compared to monotherapies in several UM cell lines. This efficient combination is therefore very promising for in vivo studies.

I. INTRODUCTION

Uveal Melanoma (UM) is the most common primary ocular tumor in adults, with an average incidence of 5 cases per million (Singh and Topham, 2003). Up to 50% of patients with UM develop metastatic disease, to the liver in 90%. The median survival of metastatic UM patients is 6 months (Gragoudas et al., 1991). All therapeutic approaches have up to now failed in proving an advantage in patient survival.

A series of preclinical studies have been conducted in the last years with the goal of identifying efficient therapeutic strategies. The most promising results have been obtained with Selumetinib and Sotrastaurin, two molecules targeting respectively the MAPK and the PKC pathways. However, no improvement in overall survival has been demonstrated in clinical trials with the administration of these compounds (Carvajal RD et al., 2014; Piperno-Neumann et al., 2014).

In a previous work we have shown the efficacy of Everolimus, a selective inhibitor of mTOR pathway, on relevant models of UM (Amirouchene-Angelozzi et al., 2014). Even if a significant growth inhibition was demonstrated both *in vitro* and *in vivo*, Everolimus failed to induce apoptosis of UM cells and it did not induce tumor regression in vivo. mTOR acts as downstream effector of PI3K and AKT, two key proteins of the PI3K/mTOR pathway which have been suggested to be potential therapeutic targets following combinatorial strategies in UM (Khalili et al., 2012a; Musi et al., 2014a).

We have recently described the establishment of a panel of relevant UM cell lines. Importantly, four cell lines display a BAP-1 deficiency, a marker of high risk tumors strongly associated with tumor progression and metastasis (Amirouchene-Angelozzi et al., 2014). To our knowledge no preclinical study systematically comparing drug combinations in a large panel of relevant UM cell lines has been conducted.

In this study we have performed a screening on UM cell lines to identify synergistic combinations that could overcome the low efficacy observed in vitro and in vivo with monotherapies. Seven compounds targeting the key effectors of the MAPK/PKC and PI3K/mTOR pathways were evaluated in two-drug regimens in vitro. The most promising associations were tested for their effects on cell cycle and apoptosis on

two selected cell models. Finally we validated our results on the full panel of UM cell lines.

II. MATERIALS AND METHODS

1. Cell culture.

MM28, MP38, MP41, MP46, MP65 and MM66 were established in our laboratory as described in (Amirouchene-Angelozzi et al., 2014). 92.1 (De Waard-Siebinga et al., 1995), Mel202 (Ksander et al., 1991), were purchased from The European Searchable Tumour Line Database (Tubingen University, Germany). OMM1, OMM2.5 (Luyten et al., 1996)(Chen et al., 1997) were kindly provided by P.A. Van Der Velden (Leiden University, The Netherlands). All cell lines were cultured in RPMI1640 supplemented with 10% (92.1, Mel202, OMM1, OMM2.5) or 20% (MM28, MP38, MP41, MP46, MP65, MM66) FBS (Life Technologies), Penicillin 100U/ml –Streptomycin 100µg/ml (Life Technologies). All cell lines were tested for Mycoplasma and proved to be Mycoplasma free. Cell lines were maintained in a humidified atmosphere (5% CO2) at 37°C. All cell lines were genotyped: Short Tandem repeat Polymorphism (STR) profiles of 92.1, Mel202, OMM1, OMM2.5 matched at 100% those presented in reference (Griewank et al., 2012).

2. Chemicals.

MEK inhibitor AZD6244 (Selumetinib), MEK inhibitor GSK1120212 (Trametinib), PKC inhibitor AEB071 (Sotrastaurin), PI3K inhibitor GDC0941, mTOR inhibitor Rad001 (Everolimus), PI3K/mTOR inhibitor BEZ235, and AKT inhibitor KRX-0401 (Perifosine) were supplied by Euromedex (France) and dissolved in DMSO (AZD6244, GSK1120212, AEB071, GDC0941, BEZ235) or ethanol (KRX0401) at 10mM and stored at −20°C.

3. Drug combination cell viability assays.

Cells were seeded in 200µL of culture medium, at appropriate concentration, in 96-well plates at day 0 (MM28: 3500 cells/well; MP38: 8000 cells/well; MP41: 1500 cells/well; MP46: 6000 cells/well; MP65: 8000 cells/well; MM66: 6000 cells/well; 92.1: 2000 cells/well; Mel202: 4000 cells/well; OMM1: 1500 cells/well; OMM2.5: 3500 cells/well); drugs were added to the medium at day 2 and cell viability tested at day 7 by MTT (M-2128, Sigma) assay as explained in (Marty et al., 2008). A spectrophotometer Infinite M200 (Tecan) was used to read colorimetric results of the MTT test. Results are expressed as relative percentages of metabolically active cells compared with untreated controls. Cell viability was calculated as fraction of viable cells for a given concentration of compound compared to the corresponding control wells. Drug sensitivity curves were calculated using GraphPad Prism 4.

4. Procedure for drug combination in cell viability assays.

At day 2 a master plate (2ml DeepWell 96 well plates; STARLAB) with serial dilutions of Drug A, drug B and DMSO was prepared. Drugs were diluted in culture medium in the first well of the series (first column), at the desired concentration, and the DMSO adjusted at 0,1% in the first well (fig 1A). From the first well medium containing drugs or DMSO only was iteratively diluted 1:4 for 8 times; wells in position 6 were left with medium only and acted as control wells (fig 1B). The highest drug concentration for each serial dilution was decided so that the final concentrations of the 2 drugs produced a comparable effect on cell lines and exerted their full efficacy in monotherapy within the first half of dilutions. For each compound these “starting concentrations“ were extrapolated on the basis of previous experiments on MP41 and MP38 cell lines or from the literature. Finally medium was aspirated form the culture plate and replaced with 170 µL of fresh medium and: 30 µL of medium containing dilutions of Drug A + 30µL of medium containing dilutions of DMSO (row B-C); 30 µL of medium containing dilutions of Drug A + 30µL of medium containing dilutions of Drug B (row D-E), 30 µL of medium containing dilutions of Drug B + 30µL of medium containing dilutions of DMSO (row F-G) (fig 1 D). Concentrations of DMSO up to 0,3% were tested on the cell lines and did not resulted toxic.

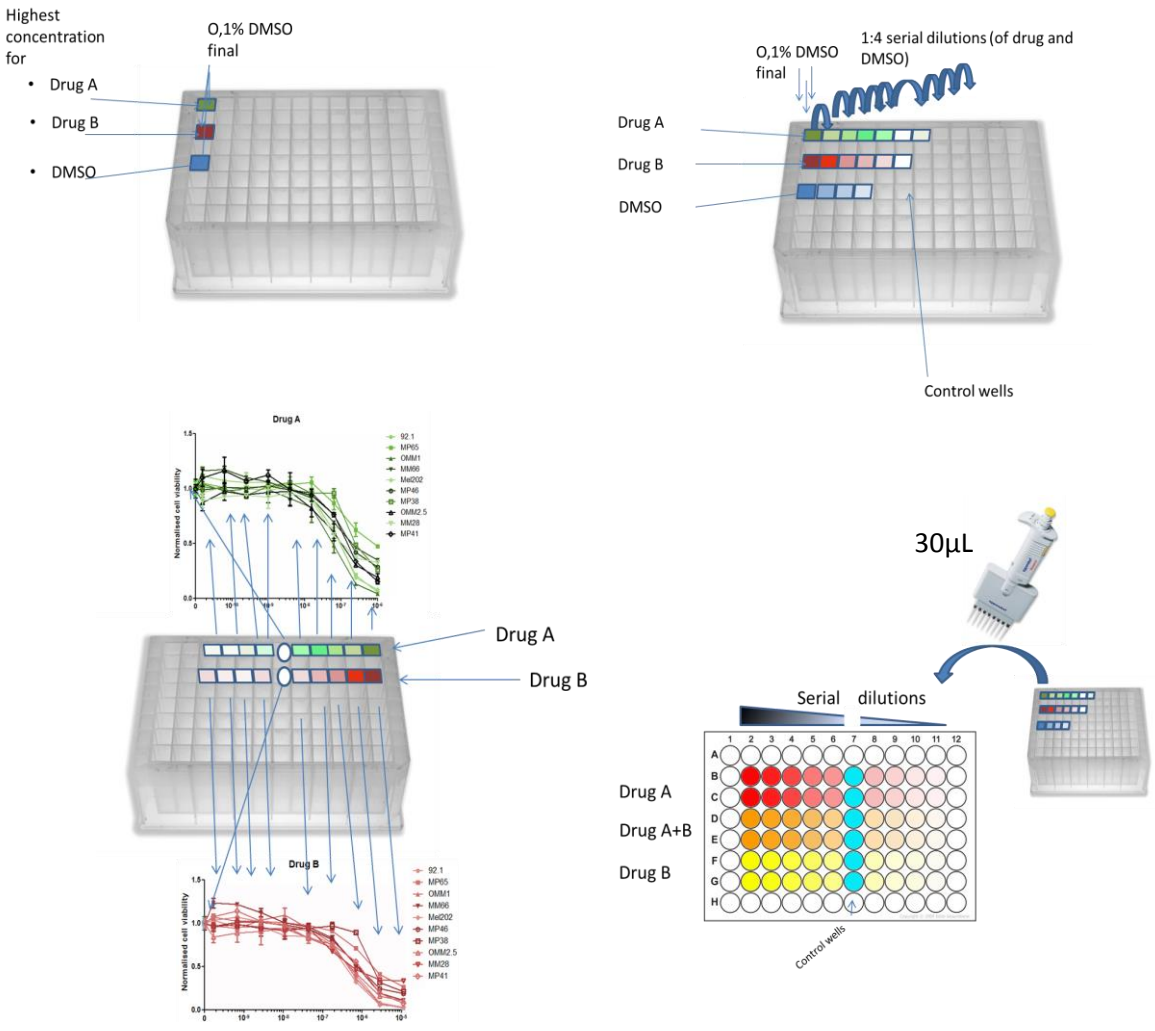

Figure 1. Drugging procedure for combination assays. A:Drugs and DMSO were diluted in medium in master plates at the desired concentration; B:Drugs and DMSO were dilutioned iteratively (ratio 1:4) in the master plates C: concentration in the master plate was defined in order to have a final drug concentration in single drug dilutions that exerted its full activity in the first half of the wells of the series; D: 30µL of the serially diluted drug or DMSO from the masterplate were added to seeded 96 well plates to produce a duplicate of dilutions for drug A, for drug B and for the combination of the two.

Each 96 well plate contained in the end, in duplicate, 9 serial dilutions 1:4 of 2 single drugs and 9 two drugs dilutions corresponding to the combination of the first dilution of first drug with the first dilution of second drug and so on (Fig.2).

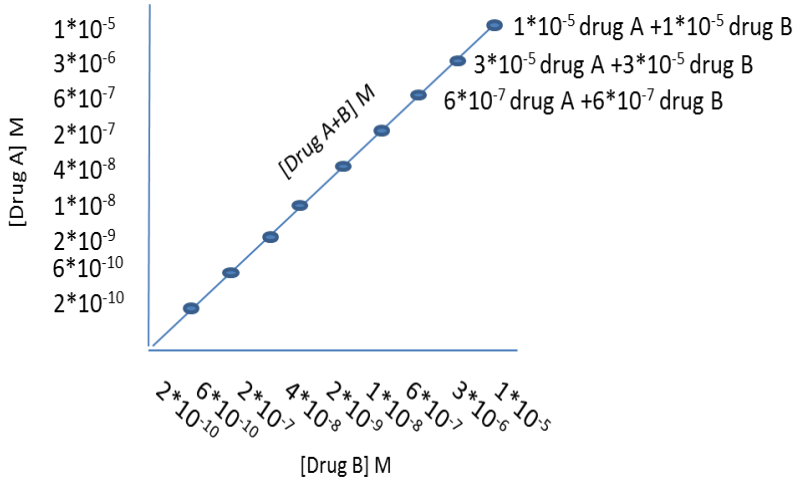

Figure 2. Drug combination data. For each combination tested the information correspondent to drug association is represented by cell viability upon serial (1:4) dilutions of the 2 drugs combined at a costant ratio.

Three different combinations were tested on the whole panel of cell lines for each experimental procedure, the tests were repeated until at least an independent triplicate for each drug combination was obtained.

5. Calculation of the Synergy.

To assess drug synergy we recalculated the cell viability for the association of the 2 drugs from single drug viability data, according to Bliss independence definition.

Bliss assumes that the effect of 2 drugs acting independently on a given system will result in an effect equal to the effect of drug A + the effect of drug B – the products of the effects of drug A and B. Thus if a given amount of drug kills half of the cells of a well compared to controls and the drug B exerts the same effect, if the two compounds act independently, they will kill 50%+50%-25% =75 % of the cells, or from another point of view Drug A will kill 50% and drug B the 50% of the remaining cells (50%+25%=75%). The effect of a drug on a viability is by definition 1-viability, which means that if cell viability of a certain drug concentration is 40% (or 0,4) the effect of the drug is 100%-40%=60% (or Fa=0,6). This effect following Bliss independence hypothesis is termed additivism.

$$\text{Bliss ratio} = \frac{\text{Viability}_{\text{Drug A+B}}}{\text{Viability}_{\text{Bliss Idependence}}} = \frac{1\text{-Fa}_{\text{Drug A+B}}}{1\text{-}(\text{Fa}_{\text{Drug A}} + \text{Fa}_{\text{Drug B}} - \text{Fa}_{\text{Drug A}} * \text{Fa}_{\text{Drug B}})}$$

$$\text{Fa} = 1 - \frac{\text{Number of cells in treated wells}}{\text{Number of cells in control wells}}$$

This simple algorithm can be applied for all the screened concentrations of a 2 drug combination assay in order to calculate values of a sensitivity curve representative of independence, or additive effect.

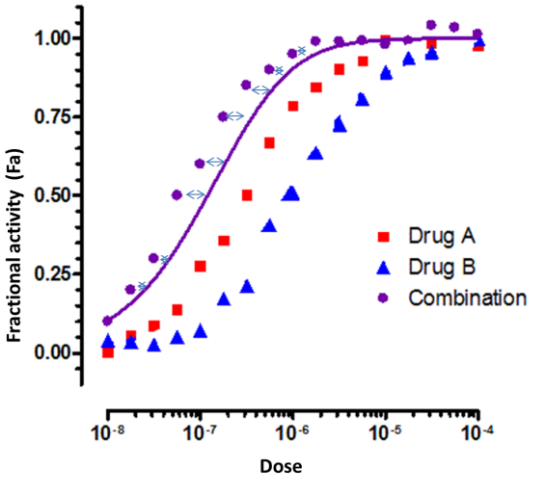

Figure 3. Bliss additivism. The effects of a drug combination in the case of independence (additive effects) can be calculated on the basis of single drug effects (purple line). Purple dots represent the effects experimentally assessed with drug combination. The ratio between assessed and calculated effects with the combination (two-headed arrows) represents the synergy (or antagonism) of the combination.

If the effect of a combination is more important than what calculated in case of independence this effect is synergistic, and if it is less important the behavior of the two drugs is antagonistic. When no significant synergy or antagonism is assessed the drugs have additive effect (fig.3).

To estimate the magnitude of the effect we defined a Bliss ratio index, defined as the ratio between normalized cell viability obtained with drug combination and normalized cell viability calculated in case of independence. Bliss ratio greater than 1 indicates synergy, an index smaller than 1 antagonism while a ratio of 1 indicates additivism. Values are given as average of at least 3 replicates and defined as synergistic or antagonistic if 95% C.I. did not include 1; Synergy tables were colored accordingly to statistical significance (fig. 4)

Bliss ratio >1 : Synergy
Bliss ratio =1 : Addittivity
Bliss ratio <1 : Antagonism

An Average Synergy Score was calculated for each combination as mean of the highest Bliss ratios obtained for every cell line.

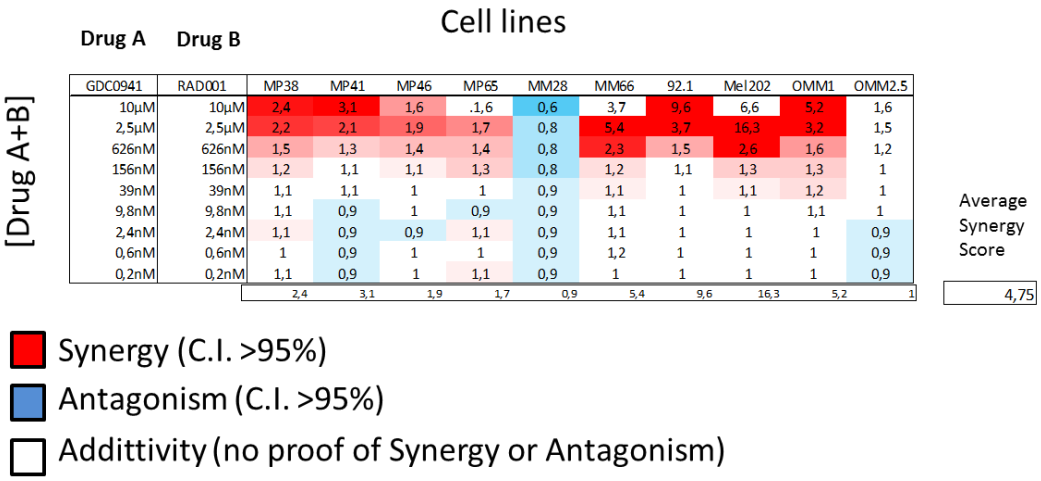

Figure 4. Synergy table. Bliss ratio values are calculated for each of the 9 tested dilutions of a drug association (columns). The first and second columns indicate the concentrations at which Drug A and Drug B are associated. Each column represents a cell line. Results from 3 independent experiments were used to calculate 95% confidence intervals; bliss ratio values are expressed as mean of three separate experiments, values that resulted significantly > 0 with a p value <0.05 are colored in red (synergy), values that resulted significantly < 0 with a p value <0.05 are colored in blue (antagnism), values that produced synergy values not significantly different from 0 are colored in white (antagonism). An Average Synergy score was calculated as mean of the highest Bliss ratio for every cell line.

6. Cell cycle analysis by Flow cytometry.

We collected floating and detached (after trypsinization) treated and control cells. Then, we washed them once with PBS and then with PBS containing 0.5% BSA. We fixed the cells in cold 70% ethanol with gentle vortexing. After fixation, we incubated the cells in PBS containing 10 µg/ml propidium iodide (PI; P3566, Invitrogen) and 200 µg/ml RNase A (Pure Link™ RNase A, Invitrogen) for 30 min at RT. We collected the samples using FACScalibur (Becton Dickinson) and we analyzed a minimum of 20,000 cells per sample using CellQuest software (Becton Dickinson). We quantified DNA content by using FlowJo Software (Milteny Biotec) and we expressed results as a distribution of cells in each cell-cycle phase. Statistical significance on 3

independent experiments was assessed with two-ways ANOVA with Bonferroni post-test using the Software GraphPad Prism.

7. Apoptosis evaluation.

Following drug treatments, we harvested cells at 72h and we detected apoptosis using the following assays:

Detection of PARP cleavage: We performed immunoblot (see corresponding paragraph above) using whole protein lysates of floating plus adherent cells to visualize the cleavages of PARP and, which serve as markers of cells undergoing apoptosis.

Annexin V assay: we determined the proportion of apoptotic cells by using the annexin-V-FLUOS staining kit (Roche) according to the manufacturer's instructions. After sequential staining by annexin V and PI, we performed flow cytometry analyses on a LSRII Instrument (Becton Dickinson). Using FlowJo software, we analyzed a minimum of 20,000 cells per sample and we evaluated the percentage of living cells with low annexin V and low PI staining, apoptotic cells with high annexin V and low PI staining and necrotic cells with high annexin V and high PI staining.

8. Western blotting.

Tissue lysates were loaded onto gels, transferred to nitrocellulose and revealed as described in (Marty et al., 2008). Quantification was performed using a LAS-3000 Luminescent Image analyzer and Image Gauge software (Fuji, FSVT, Courbevoie, France). Actin was used for normalization between samples and detected using anti-beta-actin primary antibodies at the dilution of 1:5000 (Sigma-Aldrich, Saint Quentin Fallavier, France). Cleaved PARP Cleaved PARP (Asp214) Rabbit mAb (Cell Signalling) was used at 1:1000 dilution.

III. RESULTS

1. Set up of a pipeline to study two-drug regimen synergy

We chose a small series of compounds targeting some of the pathways recognized to be deregulated in UM: the MEK/ERK, the PKC and the PI3K/mTOR pathways.

The compounds tested were: mTOR inhibitor Rad001 (Everolimus), PI3K inhibitor GDC0941, the dual PI3K/mTOR inhibitor BEZ235, AKT inhibitor Perifosine, PKC inhibitor AEB071 (Sotrastaurin), MEK inhibitors GSK1120212 (Trametinib) and AZD6224 (Selumetinib).

We set up a simple pipeline to be able to reliably test major effects of synergy between every couple of drugs in a relevant panel of 10 UM cell lines. This panel is representative of the genetic landscape of the disease (see Table1). Five cell lines harbor GNAQ mutations, while the other five are mutated in GNA11. Four cell lines are BAP-1-deficient. One cell line display a SF3B1 mutation and another one an EIF1AX mutation. Each drug was tested in combination with all the others except for the two MEK inhibitors, Selumetinib and Trametinib,

Cell line	MP38	MP41	MP46	MP65	MM28	MM66	92.1	Mel202	OMM1	OMM2.5
Origin	Primary	Primary	Primary	Primary	Metastasis	Metastasis	Primary	Primary	Metastasis	Metastasis
GNAQ Mutations	c.626 a>T		c.626 a>T				c.626 a>T	c.629 G>A		c.626 a>C
GNA11 Mutations		c.626 a>A/T		c.626 a>A/T	c.626 a>A/T	c.626 a>A/T			c.626 a>A/T	
BAP1 Mutation	c.68-9_72del			c.1717del	c.1881C>A					
BAP1 loss	Yes		Yes	Yes	Yes					
SF3B1 Mutations								c.1793c>T		
EIF1AX Mutations							c.17G/A			

Table 1 : Cell lines used for the synergy screening with their respective origin (Primary or Metastasis), Mutational status of GNAQ/11, BAP1, SF3B1 and ELF1AX and expression of BAP1 as assessed by Immunohistochemistry.

2. Synergistic combinations

Among the associations evaluated the most synergistic were the combination of mTOR inhibitor Everolimus and PI3K inhibitor GDC0941 (overall synergy score: 4,75); followed by the combination of Everolimus with dual mTOR/PI3K inhibitor BEZ235 (Synergy score: 3,1), the combination of GDC0941 and MEK inhibitor Selumetinib (Synergy score: 2,17), the combination of GDC0941 and Sotrasturin PKC inhibitor (Synergy score 2,14), the combination of BEZ235 and Selumetinib (Synergy score: 2,04). All the other combinations scored less than 2 (see Figure 5).

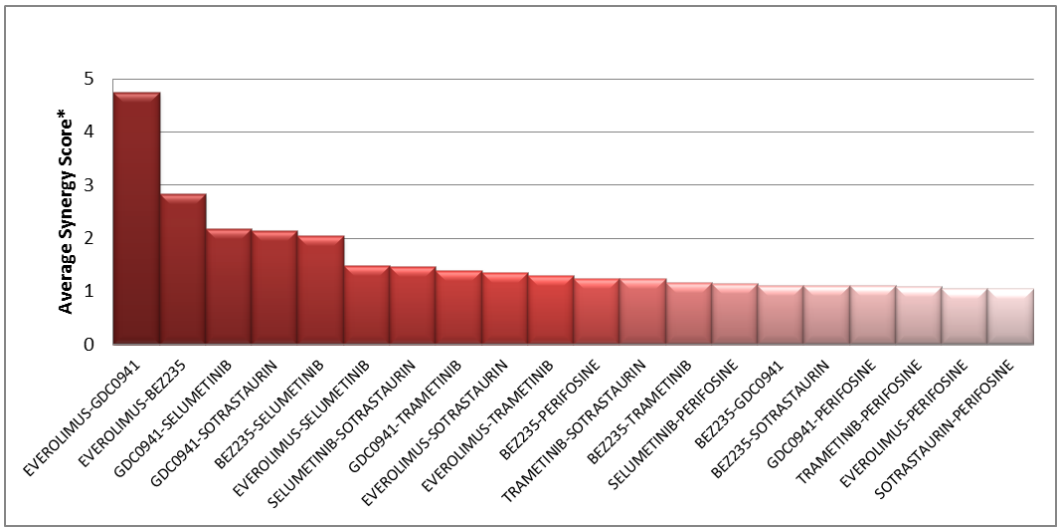

Figure 5. Average synergy score for all the tested combinations.

3. Analysis of the effects of drug combination

Among the combinations displaying an average bliss score higher than 2 we selected three for further studies: GDC0941 PI3K inhibitor combined to mTOR inhibitor Everolimus, GDC0941 combined to MEK inhibitor Selumetinib, and the association of Everolimus and Selumetinib. We excluded the combination of PI3K and BEZ from further testing because it did not show superiority compared to PI3K-Everolimus combination.BEZ235 is a dual PI3K/mTOR inhibitor and the comparable effect of the two combinations suggests that the synergy is likely to be due to PI3K inhibition in

both associations. For the same reason we did not further analyze BEZ235-Selumetinib combination. We did not further test Sotrastaurin-GDC0941 given that PI3K inhibitor synergy with Sotrastaurin has been already described (Musi et al., 2014). We decided to include in further evaluation the combination of Everolimus with Selumetinib as comparative control because the compounds are in the other 2 combinations and it shows a modest synergy (Synergy Score: 1,48). Full Synergy data for the 3 selected combinations are depicted in Fig.6; the complete data for all the combination tested are presented in supplementary Fig.1).

In order to study the nature of the synergistic interactions of these three combinations of drugs we selected two cell lines: Mel202 and MM28. The former displayed the highest bliss ratio score for the combination of GDC0941 with Everolimus as well as for the combination of Everolimus with Selumetinib, while it was the third most synergistic cell line in Selumetinib and GDC0941 combination. MM28 showed a slight antagonism for the three combinations at the doses resulting in the highest synergy in Mel202 (Fig. 6).

Cell cycle analysis was performed for the three combinations on Mel202 and MM28 after 72h of contact with the drugs, at concentrations at which bliss ratio was the highest. Single treatments did not significantly affect cell cycle in Mel202 or MM28 while a significant increase in G1 resulted in Mel202 with the combination of Everolimus and Selumetinib (G1=79+/-1%; $p<0,01$) and with the combination of Everolimus and GDC0941 (G1=86+/-8%; $p<0,05$) compared to untreated cells (G1=77+/-3%). The only combination that affected significantly cell cycle on MM28 was Everolimus with GDC0941 (G1=86+/-8%; $p<0,05$) compared to untreated control (G1=77+/-3%) (Fig.7A).

GDC0941	Everolimus	MP38	MP41	MP46	MP65	MM28	MM66	92.1	Mel202	OMM1	OMM2.5
10µM	10µM	2,4	3,1	1,6	.1,6	0,6	3,7	9,6	6,6	5,2	1,6
2,5µM	2,5µM	2,2	2,1	1,9	1,7	0,8	5,4	3,7	16,3	3,2	1,5
626nM	626nM	1,5	1,3	1,4	1,4	0,8	2,3	1,5	2,6	1,6	1,2
156nM	156nM	1,2	1,1	1,1	1,3	0,8	1,2	1,1	1,3	1,3	1
39nM	39nM	1,1	1,1	1	1	0,9	1,1	1	1,1	1,2	1
9,8nM	9,8nM	1,1	0,9	1	0,9	0,9	1,1	1	1	1,1	1
2,4nM	2,4nM	1,1	0,9	0,9	1,1	0,9	1,1	1	1	1	0,9
0,6nM	0,6nM	1	0,9	1	1	0,9	1,2	1	1	1	0,9
0,2nM	0,2nM	1,1	0,9	1	1,1	0,9	1	1	1	1	0,9

Average Synergy Score

4,75

Selumetinib	GDC0941	MP38	MP41	MP46	MP65	MM28	MM66	92.1	Mel202	OMM1	OMM2.5
1µM	10µM	2,2	3,6	1,4	.1,8	0,7	NA	.10,4	NA	1,1	1,3
250nM	2,5µM	2	2,2	1,4	.1,2	0,9	2,7	4,1	2,9	.1,1	1,4
63nM	626nM	.1,4	1,2	1,2	.1,4	.1,1	1,2	1,6	1,4	1,1	1,2
16nM	156nM	1,1	0,9	.1,1	1	1	.1,1	.1,2	.1,1	1	.1,1
4nM	39nM	.1,1	.1	1	1,2	.1,1	1,1	.1,1	0,9	1	.1,1
1nM	9,8nM	1	0,9	.1	1,2	.1	1	.1,1	.1	1	.1,1
0,1nM	2,4nM	.1,1	.1,1	.1	.1,1	1,1	1	.1	.1	1,1	1,1
0,06nM	0,6nM	1	.1	1	.1,2	1,1	.1,1	1,1	.1	.1	1,1
0,02nM	0,2nM	1,1	0,9	1,1	.1,4	.1,1	.1	1,2	1	1	.1

2,17

Selumetinib	Everolimus	MP38	MP41	MP46	MP65	MM28	MM66	92.1	Mel202	OMM1	OMM2.5
1µM	10µM	1,4	1,4	1,4	1,1	0,7	1,8	2,1	1,9	1,3	1
250nM	2,5µM	1,4	1,5	1,4	1,7	0,8	1,9	1,5	2,5	1,4	1,2
63nM	626nM	1,3	1,5	1,3	2,3	1	1,8	1,3	1,8	1,2	1,2
16nM	156nM	1,2	1,2	1,2	1,6	1	1,4	1,1	1,4	1	1,2
4nM	39nM	1,1	1,1	1,2	1,3	1	1,2	1,1	1,2	1,1	1,1
1nM	9,8nM	1	1,1	1,1	1,1	1	1,2	1,1	1,1	1	1
0,1nM	2,4nM	1,1	1,1	1,1	1,2	0,9	1,1	1,1	1	1,1	1,1
0,06nM	0,6nM	0,9	1	1,1	1,1	0,9	1,1	1,1	1,1	1,1	1
0,02nM	0,2nM	0,9	1	1,1	1	0,9	1	1	1,1	1,1	1,1

1,48

Synergy (C.I. >95%)
Antagonism (C.I. >95%)
Additivity (no proof of Synergy or Antagonism)

Figure 6. Synergy Table for the 3 selected combinations: Everolimus+GDCO0941, GDC0941+ Selumetinib, Everolimus+Selumetinib. Results from 3 independent experiments were used to calculate 95% confidence intervals; bliss ratio values are expressed as mean of three separate experiments, values that resulted significantly > 0 with a p value <0.05 are colored in red (synergy), values that resulted significantly < 0 with a p value <0.05 are colored in blue (antagnism), values that produced synergy values not significantly different from 0 are colored in white (antagonism). Average Synergy score for each combination are depicted aside. NA: non applicable.

Analysis of cell cycle profiles revealed also a strong subG1 peak in Mel202 samples treated with the combination of Everolimus and GDC0941. A smaller subG1 peak was also visible in Mel202 samples treated with GDC0941 and Selumetinib combination, while for Everolimus and Selumetinib combination subG1 population was very reduced. No subG1 peak was observed in MM28 samples with either single or combination treatments (Supplementary figure 2)

The analysis of apoptosis, performed by Annexin V staining, revealed a significant increase in apoptotic (Q3= 12+/-2%; p>0,01) and late apoptotic cells (Q2=25+/-1%; p<0,001) with Everolimus and GDC0941 combination compared to controls (Q3=2+/-

0,1%; Q2= 2,+/-1%). Selumetinib and GDC0941 combination did not significantly increased apoptotic cells (Q3=8+/-1%) or late apoptotic cells (Q2= 8+/-1%). A slight non-significant increase in apoptotic cells (Q3=5+/-0,3%) and a significant increase in late apoptotic cells (Q2= 9+/-2%) was found with Selumetinib and Everolimus combination (Fig. 7B).

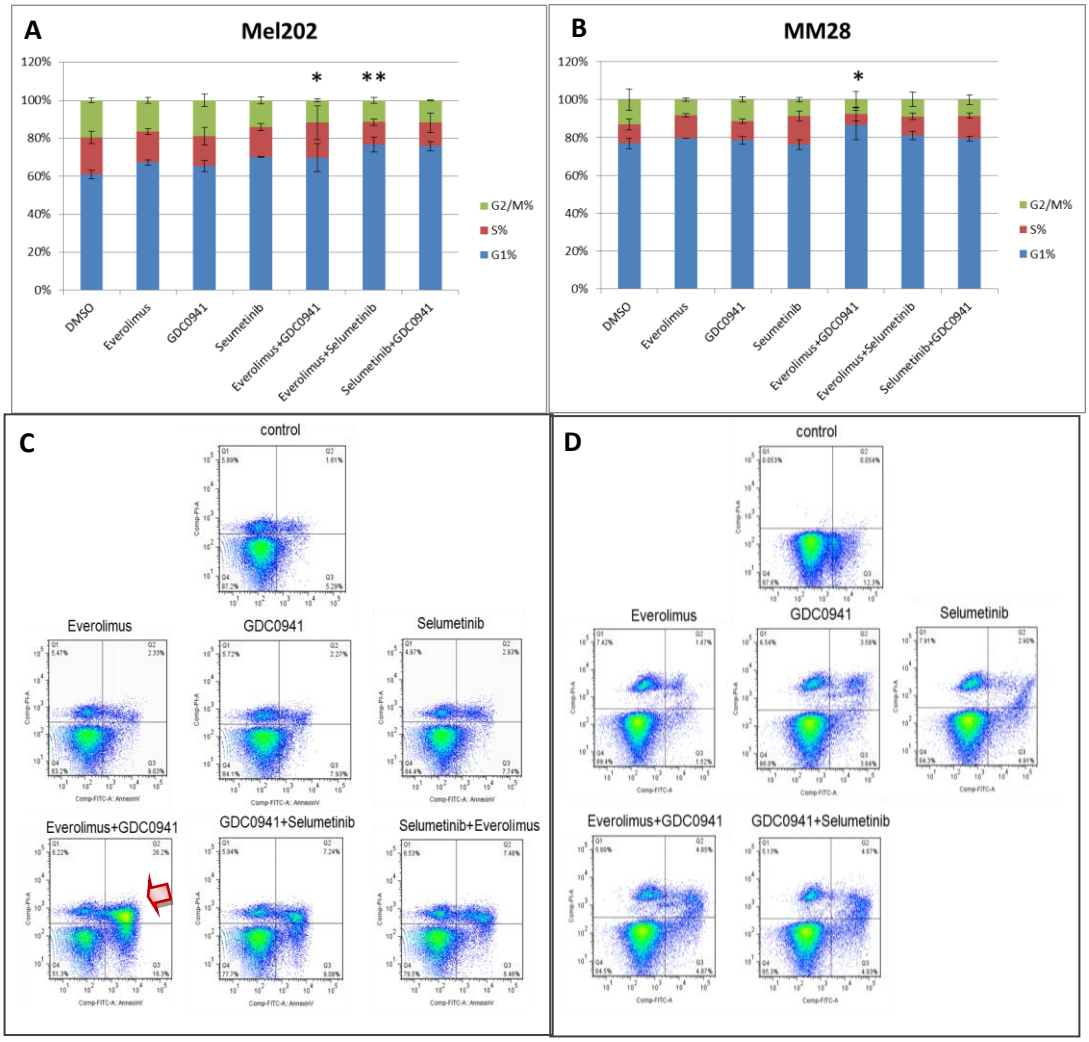

Figure 7. Cell cycle and apoptosis analysis of single drug treatments and combination of: GDC0941; Everolimus; Selumetinib. Mel202 (A,C) and MM28 (B,D) were incubated for 72h with 0,25µM Selumetinib, 2,5µM Everolimus, 2,5µM GDC0941 single drug or combination as indicated for each experimental condition. **A,B : Cell cycle analysis**. Bars represent the mean and variability is expressed as Standard Error of the Mean. Statistical Significance was assessed with two ways ANOVA with Bonferroni post-test correction. *=p>0,05 **=p<0,01. **C,D : .Annexin V test for Apoptosis.** The arrow indicates the strong increase in apoptosis with the combination of Everolimu and GDC0941 in Mel202 only. Pictures are representative of a duplicate.

On the basis of the highest synergy score and of the strongest effects on induction of apoptosis on cell line Mel202 we selected Everolimus and GDC0941 combination for validation of pro-apoptotic effects using the entire panel of UM cell lines. MP38, MP41, MP46, MP65, MM28, MM66, 92.1, Mel202, OMM1, and OMM2.5 were tested by Western Blot analysis of cleaved PARP in the same experimental condition previously used to test apoptosis in Mel202 cells. A strong induction of cleaved PARP was found with the GDC0941/Everolimus combination compared to single treatments in Mel202, 92.1, MM66, MP65 and OMM2.5.In OMM1 combination did not result in an increase of the apoptosis induced by single agents. In the remaining cell lines no apoptotic effects of either single of combination treatments were observed. Importantly, no synergy could be detected in Mel285, a GNAQ, GNA11 wild type uveal melanoma cell line and Melan3, a primary uveal melanocyte cell line (Fig.8).

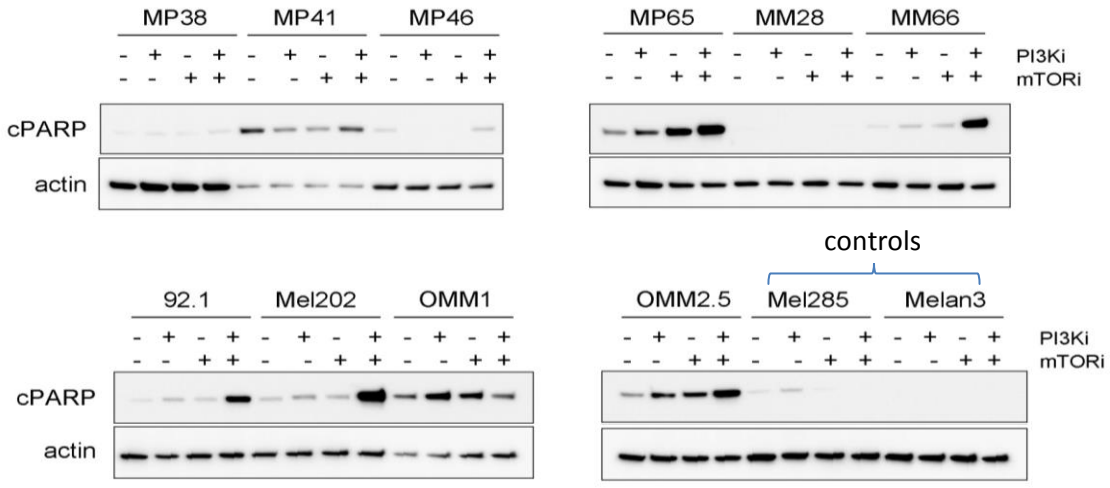

Figure 8. Assesment of apoptosis induced by the association of GDC0941 and Everolimus. **Lysates of** MP38,MP41,MP46,MP65,MM28,MP66,92.1, Mel202,OMM1,OMM2.5 were assessed for cleaved PARP by immunoblotting after 72h exposure to 2,5µM GDC0941, 2,5µM Everolimus or the association of the two. Mel285, an uM cell line wild type for GNAQ/11 and Melan3 (a primary line of human uveal melanocytes) were used as control.

IV. DISCUSSION

In this study we have used a simple pipeline to assess drug synergy in cell lines in order to identify potential effective combination strategies for UM patients. We have included seven drugs affecting signaling pathways recognized to be deregulated in UM patients. The experimental procedure in our screening combines 2 drugs at a fix and constant ratio, at concentrations at which the single drugs display comparable efficacy. This allows the evaluation of the synergistic effects of two-drugs regimens in vitro. In order to screen a relevant number of combinations on a panel of 10 lines we decided to test the drugs simultaneously. Our data show that the mTOR inhibitor Everolimus and the PI3K inhibitor GDC0941 synergistically induce a strong apoptotic effect in a half of the tested cell lines.

Some previous studies have addressed the in vitro (and some cases in vivo) efficacy of this drugs mainly in monotherapy regimens.

MEK inhibitors Trametinib and Selumetinib as well as PKC inhibitor Sotrastaurin have demonstrated a selective activity on GNAQ GNA11 mutated UM (Khalili et al., 2012b; Mitsiades et al., 2011; Wu et al., 2012). A clinical trial has proved an improvement in progression free survival in patients treated with Selumetinib compared to a control group treated with Temozolomide (Carvajal RD et al., 2014) but without impact on overall survival. Clinical trials with PKC inhibitor Sotrastaurin (NCT01430416) and MEK inhibitor Trametinib (NCT01979523) are ongoing (Piperno-Neumann et al., 2014).

The PI3K/AKT/mTOR pathway has been suggested to play a key role in UM (Ambrosini et al., 2013a; Abdel-Rahman et al., 2006; Babchia et al., 2010a; Bao et al., 2012; Ye et al., 2008; Musi et al., 2014b). The effect of PI3K inhibitors on UM cell lines has been addressed by testing LY294002, GSK2126458, and BYL791; the last two compounds were shown to be more potent on GNAQ/11 mutated cell lines compared to wild type counterparts (Babchia et al., 2010a; Khalili et al., 2012b; Musi et al., 2014b).

Lefevre et al. (Lefevre et al., 2004) have reported a rather limited effect of AKT inhibiton on UM cell lines, while MK2206 AKT inhibitor has been demonstrated to selectively reduced viability in GNAQ/11 mutated models (Ambrosini et al., 2013b; Babchia et al., 2010b). In our hands, the AKT inhibitor Perifosine showed a limited effect on UM cell line viability.

mTOR inhibition with Rapamycin on UM cell lines has been described by Babchia et al., who reported limited activity of the compound but efficacy of the combination with LY94002 on one GNAQ mutated cell line (Babchia et al., 2010b). The efficacy of the ATP competitive mTOR inhibitor AZD8055 in a xenograft model, without evidence of apoptotic effects in vitro, has been also reported (Ho et al., 2012). The PI3K inhibitor we decided to test is GDC0941 a potent PI3K inhibitor highly selective for α/δ with a modest effect on p110β and p110γ. We also selected for evaluation an agent targeting PI3K/mTOR pathway on a wider range of targets: BEZ235 a p110α/γ/δ/β and mTOR inhibitor, which targets with a lower affinity ATR and show a poor inhibitory effect of Akt and PDK1. Everolimus was selected for our screening based on the significant tumor growth inhibitory effects on 4 UM PDXs (Amirouchene-Angelozzi et al., 2014). In vitro analysis showed that Everolimus displays cytostatic effects, and therefore drug combination seems necessary to improve its efficacy. Clinical trials with Selumetinib and Sotrastaurin showed as well a limited response: Selumetinib slightly increased disease free survival but did not affect overall survival (Carvajal RD et al., 2014). Sotrastaurin has been shown to display a limited efficiency in patients and combination with the MEK inhibitor MEK162 is being tested in a clinical trial (NCT01801358). AKT inhibitor GSK2141795 is also being tested in association with Trametinib.

Among the most synergistic combinations that we selected for further in vitro characterization two of them associate Everolimus, a cytostatic inhibitor of mTOR. The effect of Everolimus is relatively constant for a wide range of concentrations, as previously seen from sensitivity curves (Amirouchene-Angelozzi et al., 2014). On the contrary treatment with the other compounds tested resulted in sigmoidal shaped sensitivity curves with a narrower efficacy window. On the basis of our experimental pipeline effective concentrations of the second drugs were associated with high doses of Everolimus, even if lower doses of this compound have been proved to be

effective. Therefore, we decided to validate our results using a matrix of doses with the goal of investigating the minimal doses at which the synergy is effective and evaluating the possible dependency of the synergy on specific ratios of concentrations between the two compounds.

We have used a panel of 10 lines repre sentative of the disease in terms of somatic mutations. Half of them are mutated for GNAQ and the other half for GNA11. 4 cell lines have a loss of expression of BAP1, while two presented either an SF3B1 or an EIF1AX mutation. Half of the cell lines were issued directly from patients and the other half from PDXs, and finally half of them were derived from primary tumors and the other half from metastasis. Even if the number of cell lines could not allow performing statistical analysis with stratification for the different variables no correlation could be observed between response to the different combinations and mutational status.

Interestingly MM28, a BAP1 mutated, GNA11 mutated cell line, presented a profile of widespread antagonism. MM28 are slow cycling cells (doubling time: 109h). Although this might contribute to the phenotype observed another slow cycling BAP1 mutated GNA mutated cell line, MP65 (doubling time 120h) display a completely different behavior, suggesting that doubling times cannot explain this results. A comparative pathway activation analysis by RNA or proteomic analysis comparing MM28 cell line with the others could be very informative.

The combination of PI3K and Everolimus as well as the combination of PI3K and BEZ235 resulted in the highest average bliss ratio synergy scores. GDC0941 targets selectively PI3K subunits α/δ , BEZ 235 on the contrary also targets γ/β PI3K subunits and mTOR and it is capable of inhibiting both TORC1 and TORC2 complexes. Combination of Everolimus and GDC0941 resulted in synergistic effects very similar to those found with Everolimus and BEZ235 association. This suggests that the synergy derives from the effect of either GDC0941 or BEZ235 on PI3K subunits α/δ and that inhibition of TORC2 does not contributes to the synergy. For these reasons the combination with BEZ235 was not validated further

The combination of Everolimus and GDC0941 resulted in a strong increase of apoptosis on half of the cell lines tested. Babchia et al. have shown that the

synergistic effects of LY294002 and Rapamycin on 92.1 are related to the inhibition of the feedback of mTOR on AKT (Babchia et al., 2010b). We have previously reported (Amirouchene-Angelozzi et al., 2014) that on the tested cell lines AKT phosphorylation is low compared to tumor cell lines that have constitutive activation of AKT. The resistance of the UM cell lines to the AKT inhibitor Perifosine suggests that a rebound of mTOR inhibition on AKT phosphorylation is not the principal mechanism explaining the synergy. However this may seem to be in contradiction with the efficacy of GDC0941. Understanding the molecular basis of the synergy between Everolimus and GDC0941 would require wide unbiased analysis using transcriptomic or proteomic approaches.

Although the combination of PI3K inhibitors with Selumetinib was also found synergistic the bliss scores and apoptotic fractions were lower than those obtained with the combination with GDC0941 and Everolimus. Khalili et al showed a very strong increase of apoptosis on cell line Mel202 with the combination of GSK2126458 PI3K/mTOR inhibitor and Trametinib (Khalili et al., 2012b). A large inhibition of PI3K/mTOR pathway could explain the effect of this combination. In our hands combination of BEZ235 and Trametinib did not show a significant synergy, and the synergistic effects of GDC0941 and Trametinib were lower than what found with Selumetinib. Moreover the PI3K inhibitor used by Khalili might affect other targets than those affected by BEZ235. It would be interesting to evaluate the induction of apoptosis with combinations of all these compounds. The combination of Selumetinib and Everolimus resulted in a modest increase in apoptosis. This is in line with the results of Ho et al. showing a modest increase of SubG1 fraction with the same combination. These authors show a modest (10 to 15%) increase of apoptosis with the combination of Selumetinib with an ATP competitive inhibitor AZD8055 (Ho et al., 2012). However the model tested, OCM1, is a BRAF mutated cell line. Other combinations reported as synergistic include PKC/MEK inhibitors and PKC/PI3K inhibitors. The PKC inhibitor Sotrastaurin has been tested by Chen et al. with MEK inhibitors MEK162 or PD0325901. These combinations were shown to be synergistic on GNAQ/11 mutated cell lines and resulted in tumor regression in a 92.1 xenograft mouse model (Chen et al., 2013). In our study the combination of Sotrastaurin with either Selumetinib or Trametinib resulted in modest synergies. This suggests that the

effects might be compound dependent. Sotrastaurin and BYL719 in the study of Musi et al. showed an increase in apoptosis but the effect is modest (maximum with 92.1 with 9% of SubG1 fraction with the combination) (Musi et al., 2014b).

Obviously the next step of this work will be to evaluate in vivo the most promising combinations identified in our screening and specially the combination Everolimus and GDC0941. For this purpose we have access to a unique panel of UM PDXs. Confirmation of our in vitro data in relevant in vivo models will hopefully allow the implementation of clinical trials using rational combination of drugs.

V. REFERENCES

Abdel-Rahman, M.H., Yang, Y., Zhou, X.-P., Craig, E.L., Davidorf, F.H., Eng, C., 2006. High Frequency of Submicroscopic Hemizygous Deletion Is a Major Mechanism of Loss of Expression of PTEN in Uveal Melanoma. JCO 24, 288–295.

Ambrosini, G., Musi, E., Ho, A.L., De Stanchina, E., Schwartz, G.K., 2013a. Inhibition of Mutant GNAQ Signaling in Uveal Melanoma Induces AMPK-Dependent Autophagic Cell Death. Mol. Cancer Ther.

Ambrosini, G., Musi, E., Ho, A.L., Stanchina, E. de, Schwartz, G.K., 2013b. Inhibition of Mutant GNAQ Signaling in Uveal Melanoma Induces AMPK-Dependent Autophagic Cell Death. Mol Cancer Ther.

Amirouchene-Angelozzi, N., Nemati, F., Gentien, D., Nicolas, A., Dumont, A., Carita, G., Camonis, J., Desjardins, L., Cassoux, N., Piperno-Neumann, S., Mariani, P., Sastre, X., Decaudin, D., Roman-Roman, S., 2014. Establishment of novel cell lines recapitulating the genetic landscape of uveal melanoma and preclinical validation of mTOR as a therapeutic target. Mol Oncol.

Babchia, N., Calipel, A., Mouriaux, F., Faussat, A.-M., Mascarelli, F., 2010a. The PI3K/Akt and mTOR/P70S6K signaling pathways in human uveal melanoma cells: interaction with B-Raf/ERK. Invest. Ophthalmol. Vis. Sci. 51, 421–429.

Babchia, N., Calipel, A., Mouriaux, F., Faussat, A.-M., Mascarelli, F., 2010b. The PI3K/Akt and mTOR/P70S6K signaling pathways in human uveal melanoma cells: interaction with B-Raf/ERK. Invest. Ophthalmol. Vis. Sci. 51, 421–429.

Bao, X., Song, H., Tang, X., 2012. [Clinicopathological significance of expression of IGF-1R in uveal melanoma and its association with expression of p-AKT Thr308]. Zhonghua Yan Ke Za Zhi 48, 413–416.

Carvajal RD, Sosman JA, Quevedo J, Et al, 2014. Effect of selumetinib vs chemotherapy on progression-free survival in uveal melanoma: A randomized clinical trial. JAMA 311, 2397–2405.

Chen, P.W., Murray, T.G., Uno, T., Salgaller, M.L., Reddy, R., Ksander, B.R., 1997. Expression of MAGE genes in ocular melanoma during progression from primary to metastatic disease. Clin. Exp. Metastasis 15, 509–518.

Chen, X., Wu, Q., Tan, L., Porter, D., Jager, M.J., Emery, C., Bastian, B.C., 2013. Combined PKC and MEK inhibition in uveal melanoma with GNAQ and GNA11 mutations. Oncogene.

De Waard-Siebinga, I., Blom, D.J., Griffioen, M., Schrier, P.I., Hoogendoorn, E., Beverstock, G., Danen, E.H., Jager, M.J., 1995. Establishment and characterization of an uveal-melanoma cell line. Int. J. Cancer 62, 155–161.

Gragoudas, E.S., Egan, K.M., Seddon, J.M., Glynn, R.J., Walsh, S.M., Finn, S.M., Munzenrider, J.E., Spar, M.D., 1991. Survival of patients with metastases from uveal melanoma. Ophthalmology 98, 383–389; discussion 390.

Griewank, K.G., Yu, X., Khalili, J., Sozen, M.M., Stempke-Hale, K., Bernatchez, C., Wardell, S., Bastian, B.C., Woodman, S.E., 2012. Genetic and molecular characterization of uveal melanoma cell lines. Pigment Cell Melanoma Res 25, 182–187.

Ho, A.L., Musi, E., Ambrosini, G., Nair, J.S., Deraje Vasudeva, S., De Stanchina, E., Schwartz, G.K., 2012. Impact of combined mTOR and MEK inhibition in uveal melanoma is driven by tumor genotype. PLoS ONE 7, e40439.

Khalili, J.S., Yu, X., Wang, J., Hayes, B.C., Davies, M.A., Lizee, G., Esmaeli, B., Woodman, S.E., 2012a. Combination small molecule MEK and PI3K inhibition enhances uveal melanoma cell death in a mutant GNAQ- and GNA11-dependent manner. Clin. Cancer Res. 18, 4345–4355.

Khalili, J.S., Yu, X., Wang, J., Hayes, B.C., Davies, M.A., Lizee, G., Esmaeli, B., Woodman, S.E., 2012b. Combination small molecule MEK and PI3K inhibition enhances uveal melanoma cell death in a mutant GNAQ- and GNA11-dependent manner. Clin. Cancer Res. 18, 4345–4355.

Ksander, B.R., Rubsamen, P.E., Olsen, K.R., Cousins, S.W., Streilein, J.W., 1991. Studies of tumor-infiltrating lymphocytes from a human choroidal melanoma. Invest. Ophthalmol. Vis. Sci. 32, 3198–3208.

Lefevre, G., Glotin, A.-L., Calipel, A., Mouriaux, F., Tran, T., Kherrouche, Z., Maurage, C.-A., Auclair, C., Mascarelli, F., 2004. Roles of Stem Cell Factor/c-Kit and Effects of Glivec®/STI571 in Human Uveal Melanoma Cell Tumorigenesis. J. Biol. Chem. 279, 31769–31779.

Luyten, G.P., Naus, N.C., Mooy, C.M., Hagemeijer, A., Kan-Mitchell, J., Van Drunen, E., Vuzevski, V., De Jong, P.T., Luider, T.M., 1996. Establishment and characterization of primary and metastatic uveal melanoma cell lines. Int. J. Cancer 66, 380–387.

Marty, B., Maire, V., Gravier, E., Rigaill, G., Vincent-Salomon, A., Kappler, M., Lebigot, I., Djelti, F., Tourdès, A., Gestraud, P., Hupé, P., Barillot, E., Cruzalegui, F., Tucker, G.C., Stern, M.-H., Thiery, J.-P., Hickman, J.A., Dubois, T., 2008. Frequent PTEN genomic alterations and activated phosphatidylinositol 3-kinase pathway in basal-like breast cancer cells. Breast Cancer Res. 10, R101.

Mitsiades, N., Chew, S.A., He, B., Riechardt, A.I., Karadedou, T., Kotoula, V., Poulaki, V., 2011. Genotype-Dependent Sensitivity of Uveal Melanoma Cell Lines to Inhibition of B-Raf, MEK, and Akt Kinases: Rationale for Personalized Therapy. Investigative Ophthalmology & Visual Science 52, 7248–7255.

Musi, E., Ambrosini, G., De Stanchina, E., Schwartz, G.K., 2014a. The phosphoinositide 3-kinase α selective inhibitor BYL719 enhances the effect of the protein kinase C inhibitor AEB071 in GNAQ/GNA11-mutant uveal melanoma cells. Mol. Cancer Ther. 13, 1044–1053.

Musi, E., Ambrosini, G., Stanchina, E.D., Schwartz, G.K., 2014b. The Phosphoinositide 3-Kinaseα Selective Inhibitor, BYL19, Enhances the Effect of the Protein Kinase C Inhibitor, AEB071, in GNAQ/GNA11 Mutant Uveal Melanoma Cells. Mol Cancer Ther molcanther.0550.2013.

Piperno-Neumann, S., Kapiteijn, E., Larkin, J.M.G., Carvajal, R.D., Luke, J.J., Seifert, H., Roozen, I., Zoubir, M., Yang, L., Choudhury, S., Yerramilli-Rao, P., Hodi, F.S., Schwartz, G.K., 2014. Phase I dose-escalation study of the protein kinase C (PKC) inhibitor AEB071 in patients with metastatic uveal melanoma. J. Clin. Oncol. 32:5s.

Singh, A.D., Topham, A., 2003. Incidence of uveal melanoma in the United States: 1973-1997. Ophthalmology 110, 956–961.

Wu, X., Li, J., Zhu, M., Fletcher, J.A., Hodi, F.S., 2012. Protein kinase C inhibitor AEB071 targets ocular melanoma harboring GNAQ mutations via effects on the PKC/Erk1/2 and PKC/NF-κB pathways. Mol. Cancer Ther. 11, 1905–1914.
Ye, M., Hu, D., Tu, L., Zhou, X., Lu, F., Wen, B., Wu, W., Lin, Y., Zhou, Z., Qu, J., 2008. Involvement of PI3K/Akt Signaling Pathway in Hepatocyte Growth Factor–Induced Migration of Uveal Melanoma Cells. IOVS 49, 497–504.

Supplementary Materials

Supplementary Figure 1. Synergy table for the 20 drug associations tested.

Supplementary Figure 2. Representative profiles of cell cycle analysis after 72h incubation with Everolimus, GDC0941, Selumetinib or 2 drugs combinations of those compounds. Cell cycle profiles are representative of 3 independent experiments. Mean and Standard Error of the Mean are showed within each graph. Arrows indicates subG1 peaks.

Supplementary Figure 1

GDC0941	Everolimus	MP38	MP41	MP46	MP65	MM28	MM66	92.1	Mel202	OMM1	OMM2.5
1,0E-05	1,0E-05	2,4	3,1	1,6	.1,6	0,6	.3,7	9,6	.6,6	5,2	.1,6
2,5E-06	2,5E-06	2,2	2,1	1,9	1,7	0,8	5,4	3,7	16,3	3,2	.1,5
6,3E-07	6,3E-07	1,5	1,3	1,4	1,4	0,8	2,3	1,5	2,6	1,6	.1,2
1,6E-07	1,6E-07	1,2	.1,1	1,1	1,3	0,8	1,2	.1,1	1,3	1,3	.1
3,9E-08	3,9E-08	.1,1	.1,1	1	.1	0,9	1,1	.1	1,1	1,2	.1
9,8E-09	9,8E-09	.1,1	0,9	1	0,9	0,9	.1,1	.1	1	.1,1	1
2,4E-09	2,4E-09	1,1	0,9	0,9	1,1	0,9	.1,1	.1	.1	.1	0,9
6,1E-10	6,1E-10	.1	0,9	1	1	0,9	.1,2	1	.1	1	0,9
1,5E-10	1,5E-10	.1,1	0,9	.1	1,1	0,9	.1	.1	.1	1	0,9

BEZ235	Everolilmus	MP38	MP41	MP64	MP65	MM28	MM66	92.1	Mel202	OMM1	OMM2.5
1,0E-06	1,0E-05	0,8		1	.1,4	0,5					0,7
2,5E-07	2,5E-06	.1,1	1,9	1,3	1,6	0,7	.1,4				0,9
6,3E-08	6,3E-07	2,2	2,7	1,9	1,8	0,9	.3,7	6,2		4,6	1,4
1,6E-08	1,6E-07	2	.1,8	1,5	1,4	1,2	.2,4	2,6	5,2	3,9	1,5
3,9E-09	3,9E-08	1,4	.1,2	1,1	1,2	.1,1	.1,5	.1,3	2,1	1,8	1,2
9,8E-10	9,8E-09	1,2	.1,1	1,1	1,1	1	.1,2	.1,1	1,3	1,4	1,1
2,4E-10	2,4E-09	1,1	1,1	.1	1,1	1	.1,2	1,1	1,2	1,2	1,1
6,1E-11	6,1E-10	.1,1		.1	.1	0,9	1,1	.1	.1,1	1,1	.1
1,5E-11	1,5E-10	.1		.1	.1	1	.1,1	.1,1	1,2	.1,1	1,1

Selumetinib	GDC0941 PI3	MP38	MP41	MP46	MP65	MM28	MM66	92.1	Mel202	OMM1	OMM2.5
1,0E-06	1,0E-05	2,2	3,6	1,4	.1,8	0,7	NA	.10,4	NA	1,1	1,3
2,5E-07	2,5E-06	2	2,2	1,4	.1,2	0,9	2,7	4,1	2,9	.1,1	1,4
6,3E-08	6,3E-07	.1,4	1,2	1,2	.1,4	.1,1	1,2	1,6	1,4	1,1	1,2
1,6E-08	1,6E-07	1,1	0,9	.1,1	1	1	.1,1	.1,2	.1,1	1	.1,1
3,9E-09	3,9E-08	.1,1	.1	1	1,2	.1,1	1,1	.1,1	0,9	1	.1,1
9,8E-10	9,8E-09	1	0,9	.1	1,2	.1	1	.1,1	.1	1	.1,1
2,4E-10	2,4E-09	.1,1	.1,1	.1	.1,1	1,1	1	.1	.1	1,1	1,1
6,1E-11	6,1E-10	1	.1	1	.1,2	1,1	.1,1	1,1	.1	.1	1,1
1,5E-11	1,5E-10	1,1	0,9	1,1	.1,4	.1,1	.1	1,2	1	1	.1

GDC0941	Sotrastaurin	MP38	MP41	MP46	MP65	MM28	MM66	92.1	Mel202	OMM1	OMM2.5
1,0E-05	1,0E-05	0,8	.2	0,9	0,6	0,7	.1,4	.2,8	NA	.1,4	1,5
2,5E-06	2,5E-06	1,2	3,1	1,7	1,6	0,8	2,3	3,8	.1,9	.1,3	1,8
6,3E-07	6,3E-07	1,1	2,1	1,9	1,8	.1,1	3,1	.2,6	2,6	1	1,4
1,6E-07	1,6E-07	.1	.1,2	1,1	1	1,1	1,4	.1,2	.1,3	.1	1,2
3,9E-08	3,9E-08	.1	1	1	.1	.1	.1	1	.1	1	1
9,8E-09	9,8E-09	1	0,9	1	1	.1	1	.1	.1	1	1,1
2,4E-09	2,4E-09	1,1	.1	.1	.1	.1	1	.1	1	1	.1
6,1E-10	6,1E-10	1	.1	.1	.1	1,1	1	0,9	.1	1	0,9
1,5E-10	1,5E-10	1	1	.1	.1	.1	1	.1	.1,1	1	.1

Selumetinib	BEZ235	MP38	MP41	MP46	MP65	MM28	MM66	92.1	Mel202	OMM1	OMM2.5
1,0E-06	1,0E-06	1,2	1,6	1,3	6,5	0,8	2	1,6	0	2,3	1
2,5E-07	2,5E-07	1,1	1,8	1,4	3,1	0,9	1,5	1,2	1,2	1,4	1
6,3E-08	6,3E-08	1,2	1,2	1,1	1,4	1,2	1,4	1	1,3	1,2	1,1
1,6E-08	1,6E-08	1,1	1	1	0,9	1,2	1,1	1	0,9	1	1,1
3,9E-09	3,9E-09	1	1	1	1	1,1	1	1	0,9	1	1
9,8E-10	9,8E-10	1	1	0,9	0,9	0,9	1,1	0,9	0,8	1	1,1
2,4E-10	2,4E-10	1	1	0,9	0,9	1	1	1	0,8	1	1,1
6,1E-11	6,1E-11	1	1,1	1	0,9	1,1	0,9	0,9	0,7	1	1
1,5E-11	1,5E-11	1	1,1	1	1	1	0,9	0,9	0,8	1	1,1

Selumetinib	Everolimus	MP38	MP41	MP46	MP65	MM28	MM66	92.1	Mel202	OMM1	OMM2.5
1,0E-06	1,0E-05	1,4	1,4	1,4	.1,1	0,7	1,8	.2,1	.1,9	1,3	1
2,5E-07	2,5E-06	1,4	1,5	1,4	.1,7	0,8	1,9	1,5	2,5	1,4	1,2
6,3E-08	6,3E-07	1,3	1,5	1,3	.2,3	.1	1,8	1,3	1,8	1,2	1,2
1,6E-08	1,6E-07	1,2	1,2	1,2	.1,6	1	1,4	.1,1	1,4	1	1,2
3,9E-09	3,9E-08	1,1	1,1	1,2	.1,3	.1	1,2	1,1	1,2	1,1	1,1
9,8E-10	9,8E-09	1	1,1	1,1	.1,1	1	.1,2	1,1	1,1	.1	1
2,4E-10	2,4E-09	.1,1	1,1	.1,1	.1,2	0,9	.1,1	.1,1	.1	.1,1	.1,1
6,1E-11	6,1E-10	0,9	1	1,1	.1,1	0,9	.1,1	.1,1	.1,1	.1,1	.1
1,5E-11	1,5E-10	0,9	.1	1,1	.1	0,9	.1	1	.1,1	.1,1	.1,1

Selumetinib	Sotrastaurin	MP38	MP41	MP46	MP65	MM28	MM66	92.1	Mel202	OMM1	OMM2.5
1,0E-06	1,0E-05	0,9	0,8	0,9	0,7	0,7	,1,2	0,9	0,5	1,8	0,6
2,5E-07	2,5E-06	1,2	,1,3	,1,1	0,6	0,9	,1,5	0,8	,1,2	2,3	0,7
6,3E-08	6,3E-07	1,6	1,5	1,4	1	1	1,7	1,7	,4,9	,1,2	0,8
1,6E-08	1,6E-07	1,3	1,1	,1,2	1,2	,1	1,4	1,1	,1,5	0,9	1,2
3,9E-09	3,9E-08	,1,1	1	,1	1,2	1,1	1	1	1	1	,1,1
9,8E-10	9,8E-09	,1	,1	1	,1	1	1	1	,1	0,9	,1,1
2,4E-10	2,4E-09	1	,1	1	1,1	1	1	,1	1	,1	,1
6,1E-11	6,1E-10	1	,1	,1	0,9	1,1	1	0,9	,1	0,9	,1,1
1,5E-11	1,5E-10	1	1,1	,1	1,1	,1	,1	,1	1	1	1

Trametinib	GDC0941	MP38	MP41	MP46	MP65	MM28	MM66	92.1	Mel202	OMM1	OMM2.5
1,0E-07	1,0E-05	,1,1	1,7	0,7	,1,2	0,3	0,7	0,7	0	0,7	0,9
2,5E-08	2,5E-06	1,8	2,0	,1,1	,1,2	0,4	2,8	,1,9	0,3	1	,1,1
6,3E-09	6,3E-07	1,6	2,1	1,5	,1,1	0,8	,2,6	0	0	,1,1	,1,2
1,6E-09	1,6E-07	1,3	1,2	1,4	,1	0,9	,1,2	,1,6	,1,7	,1	,1,1
3,9E-10	3,9E-08	,1,1	1,0	,1,2	1	1	,1,1	,1,2	,1,1	1	0,9
9,8E-11	9,8E-09	,1	0,9	,1,1	,1	1	,1	,1,1	,1	,1	1,0
2,4E-11	2,4E-09	1	0,9	,1	1	1	,1	,1,1	1	1	0,9
6,1E-12	6,1E-10	,1	0,9	1,1	,1	1	0,9	,1	,1	1	0,9
1,5E-12	1,5E-10	,1	0,7	1,2	1	,1	,1	,1	,1	1	,1

Sotrastaurin	Everolimus	MP38	MP41	MP46 p20	MP65	MM28	MM66	92.1	Mel202	omm1	omm2.5
1,0E-05	1,0E-05	0,8	0,9	1	0,8	0,5	1	,1,2	0,7	1,4	0,8
2,5E-06	2,5E-06	1,3	1,1	1,2	,1,1	0,6	,1,2	,1,1	0,9	1,8	0,8
6,3E-07	6,3E-07	1,2	1,1	1,4	1,4	0,8	,1,5	1,5	1,6	1,3	1,1
1,6E-07	1,6E-07	1,1	1	1,1	,1,1	1	1,2	1,1	1,2	,1	1,2
3,9E-08	3,9E-08	1	1	,1	,1	1	,1,1	,1	1	,1	,1,1
9,8E-09	9,8E-09	,1	0,9	1	,1,1	1	1,1	1	,1	0,9	,1
2,4E-09	2,4E-09	,1	0,9	,1	1	,1	1,1	1	,1,1	1	,1
6,1E-10	6,1E-10	,1	,1	,1	1	,1	1,1	1	,1,1	1	1
1,5E-10	1,5E-10	1	1	,1	1	,1	,1,1	1	1,1	1,1	,1

Everolimus	Trametinib	MP38	MP41	MP46	MP65	MM28	MM66	92.1	Mel202	OMM1	OMM2.5
1,0E-05	1,0E-07	1	0,8	1,2	,1,1	0,6	,1	2	0,7	1,2	0,8
2,5E-06	2,5E-08	0,9	1,2	1,2	,1	0,7	1,4	,2	,1,2	1,5	1
6,3E-07	6,3E-09	,1	1,2	1,2	,1,1	0,9	1,3	,1,1	,1,5	1,3	,1
1,6E-07	1,6E-09	1,2	,1,1	1,1	,1	0,9	1,2	,1,1	1,5	,1	,1
3,9E-08	3,9E-10	,1,1	,1	,1,1	1	0,9	1,2	,1,1	1,4	1	,1
9,8E-09	9,8E-11	1,1	,1	,1,1	0,9	1	1,1	,1	1,2	,1	,1,1
2,4E-09	2,4E-11	1,1	,1,1	,1,1	,1	1	,1,1	,1,1	,1,2	1	,1,1
6,1E-10	6,1E-12	,1	,1,1	,1,1	0,9	0,9	1,1	,1	,1,1	1,1	,1
1,5E-10	1,5E-12	,1	,1	1,1	0,9	,1	1,1	,1	,1,1	,1,1	,1,1

BEZ235	Perifosine	MP38	MP41	MP46	MP65	MM28	MM66	92.1	Mel202	OMM1	OMM2.5
1,0E-05	1,0E-05	1,2	0,9	1,1	1,1	0,7	0,9	1,7	1,7	0,9	0,9
2,5E-06	2,5E-06	1	1	1	1,1	0,8	1	1,3	1,1	1,3	1,1
6,3E-07	6,3E-07	1	1	1	1	0,8	1,1	1,2	1,1	1,2	1
1,6E-07	1,6E-07	1,1	1,1	1	1	0,9	1	1,1	1,1	1,1	1
3,9E-08	3,9E-08	0,9	1,1	1	1	0,9	1	1,1	1	1,1	0,9
9,8E-09	9,8E-09	1,1	1	1	0,9	1	0,9	1,1	1,1	1,1	1
2,4E-09	2,4E-09	1	0,9	1	0,9	1	1	1,1	1,1	1	1
6,1E-10	6,1E-10	1	1	1	0,8	1	0,9	1,1	1,2	1	1
1,5E-10	1,5E-10	1	0,9	1	0,7	1	1	1	1	1	1

Trametinib	sotrastaurin	MP38	MP41	MP46	MP65	MP28	MM66	92.1	MEl202	OMM1	OMM2.5
1,0E-07	1,0E-05	0,3	0,2	0,5	0,5	0,5	0,3	0,1	0,1	0,5	0,4
2,5E-08	2,5E-06	0,7	0,3	0,7	0,6	0,5	0,8	0,3	0	0,8	0,4
6,3E-09	6,3E-07	,1,2	1,3	1,3	0,7	0,7	1,4	,1,3	0	1,4	0,6
1,6E-09	1,6E-07	,1,4	2,0	,1,3	1	,1	1,1	,1,5	,1,9	1	,1
3,9E-10	3,9E-08	,1,2	1,1	,1	0,9	1,1	1,0	,1,2	,1,2	0,9	0,9
9,8E-11	9,8E-09	,1,1	0,9	,1	1	,1	1,0	,1,1	,1	1	0,9
2,4E-11	2,4E-09	,1	1,0	1	1	,1	1,0	,1	1,1	0,9	0,9
6,1E-12	6,1E-10	,1	1,0	1	0,9	0,9	1,0	,1	1	1	0,9
1,5E-12	1,5E-10	1	0,9	,1	0,9	1	1,0	1,1	1	0,8	0,9

BEZ235	Trametinib	MP38	MP41	MP46	MP65	MM28	MM66	92.1	Mel202	OMM1	OMM2.5
1,0E-06	1,0E-07	1,8	1,1	0,6	0,7	0,3	0,4	0,2	0,1	0,4	0,9
2,5E-07	2,5E-08	0,7	0,9	0,8	.1,4	0,4	0,3	0,8	0	0,5	0,7
6,3E-08	6,3E-09	0,9	1,4	1,3	1,1	0,6	0,9	1	.1	.1	1,0
1,6E-08	1,6E-09	1	1,1	.1,1	.1,1	0,9	.1,1	1	.1,1	0,8	1,0
3,9E-09	3,9E-10	.1	.1,1	1	1	.1	0,9	0,9	1	0,9	1,0
9,8E-10	9,8E-11	.1,1	.1	1	1	.1,1	1	0,9	0,9	0,9	0,9
2,4E-10	2,4E-11	1	.1	1	0,9	1	0,9	.1	1	0,9	0,9
6,1E-11	6,1E-12	0,9	0,9	1	1	.1	0,9	1	0,9	0,9	1,0
1,5E-11	1,5E-12	0,9	1	0,9	0,9	.1,1	0,9	1	1	0,8	1,0

Selumetinib	Perifosine	MP38	MP41	MP46	MP65	MM28	MM66	92.1	Mel202	OMM1	OMM2.5
1,0E-06	1,0E-05	1,2	1	.1	0,9	1	1	1,2	1,7	1,2	.1
2,5E-07	2,5E-06	.1,2	.1	.1	1	1,1	1	.1	1,3	.1,1	.1
6,3E-08	6,3E-07	.1,1	1	.1	1	.1,1	0,9	1	1,3	1	1
1,6E-08	1,6E-07	.1	1	1	1	.1	0,9	0,9	1,1	.1	1
3,9E-09	3,9E-08	1	1	.1,1	1	1	0,9	.1	.1	1	1
9,8E-10	9,8E-09	1	.1	1	1	.1	0,9	0,9	1,1	1	1
2,4E-10	2,4E-09	1	1	1	.1	.1	1	0,9	1,1	.1	1
6,1E-11	6,1E-10	.1	.1	.1	1	1	0,9	0,9	1	.1,1	1
1,5E-11	1,5E-10	.1,1	1,1	.1	1	.1,1	1	0,9	.1,1	.1	.1

GDC0941	Everolimus	MP38	MP41	MP46	MP65	MM28	MM66	92.1	Mel202	OMM1	OMM2.5
1,0E-05	1,0E-05	0,5	0,7	0,6	0,8	0,3	0,9	0,7	0,2	0,6	0,7
2,5E-06	2,5E-06	.1,1	.1,2	0,9	1	0,4	1,4	1	0,8	1,3	.1,1
6,3E-07	6,3E-07	.1,1	.1,1	.1,1	.1	0,8	1,3	1,4	.1,6	.1,2	.1,1
1,6E-07	1,6E-07	.1	.1	1	.1,1	.1,1	1,1	.1	1,1	.1	1
3,9E-08	3,9E-08	.1	.1	1	.1	.1	.1	.1	.1,1	.1	.1,1
9,8E-09	9,8E-09	1	.1	1	1	1	1	1	.1,1	1	1
2,4E-09	2,4E-09	1	.1	1	1	1	1	0,9	.1	1	.1
6,1E-10	6,1E-10	1	.1	1	1	.1	.1	0,9	1	.1	.1,1
1,5E-10	1,5E-10	0,9	0,9	.1	1	1	.1,1	0,9	0,9	1	.1

Sotrasturin	BEZ235	MP38	MP41	MP46	MP65	MM28	MM66	92.1	Mel202	OMM1	OMM2.5
1,0E-05	1,0E-06	0,7	0,3	0,9	0,2	0,6	0,6	0,3	0,5	0,5	0,9
2,5E-06	2,5E-07	.1	#NOMBRE!	1,2	.1	0,5	0,4	0,3	0,4	.1,3	0,9
6,3E-07	6,3E-08	1,2	.1,5	1,5	.1,4	0,8	.1,5	1,4	.1,1	.1,1	1,3
1,6E-07	1,6E-08	1	.1,1	.1,1	.1	.1	.1	1,1	1,1	1	1,2
3,9E-08	3,9E-09	1	0,9	1,1	0,9	.1	.1,3	.1	.1,1	1	1,1
9,8E-09	9,8E-10	.1	.1,1	1	0,9	1,1	.1,2	1	.1	0,9	1,1
2,4E-09	2,4E-10	1	1	.1	1	1	.1,1	1,1	.1	1	.1
6,1E-10	6,1E-11	.1	1,1	1	1	.1	.1,2	.1	.1	0,9	1
1,5E-10	1,5E-11	.1	1,1	1	1	1	0,8	1,1	.1	0,9	0,9

GDC0914	Everolimus	MP38	MP41	MP46	MP65	MM28	MM66	92.1	Mel202	OMM1
1,0E-05	1,0E-05	1	0,8	1	0,8	1	.1,1	1,6	0	0,9
2,5E-06	2,5E-06	.1	0,8	0,9	0,9	1	0,9	1,2	1	.1,1
6,3E-07	6,3E-07	1	0,9	1	0,9	.1,1	1	1	1,1	.1,1
1,6E-07	1,6E-07	0,9	0,9	.1	1	.1	.1,1	1	.1	.1
3,9E-08	3,9E-08	0,9	.1	.1	1	.1	.1,1	1	1	0,9
9,8E-09	9,8E-09	1	1	.1	1	1	.1	0,8	1,1	0,9
2,4E-09	2,4E-09	.1	1,2	.1	1	1	1	0,9	1,2	1,1
6,1E-10	6,1E-10	.1	.1,1	1,1	1	1,1	0,9	1	.1	1
1,5E-10	1,5E-10	.1	1,2	1,1	1	.1	0,9	1,2	1,1	1,1

Perifosine	Trametinib	MP38	MP41	MP46	MP65	MM28	MM66	92.1	Mel202	OMM1	OMM2.5
1,0E-05	1,0E-07	.1,2	.1	.1,1	1	1	.1,4	.1,7	0,5	1,5	0,9
2,5E-06	2,5E-08	1	0,9	.1	.1	.1	0,9	.17979	0,8	1,2	0,9
6,3E-07	6,3E-09	.1	0,8	.1	1	.1,1	.1	.1	1,1	.1,1	1
1,6E-07	1,6E-09	1	0,9	1	1	1	1	0,9	.1	.1	0,9
3,9E-08	3,9E-10	0,9	.1	0,9	1	1	1,1	0,8	0,9	1	1
9,8E-09	9,8E-11	1	0,9	0,9	.1	1	.1	0,9	1	.1	1
2,4E-09	2,4E-11	.1,1	0,9	0,9	1	1	1	1	1	1,1	1
6,1E-10	6,1E-12	.1	.1	0,9	1	1	1	0,9	.1	.1,1	.1
1,5E-10	1,5E-12	.1,1	0,9	0,9	1	1	0,9	0,9	.1	.1,1	1

Everolimus	Perifosine	MP38	MP41	MP46	MP65	MM28	MM66	92.1	Mel202	OMM1	OMM2.5
1,0E-05	1,0E-05	.1,1	1	1,1	0,9	0,9	0,9	1,1	.1,1	1,2	1,1
2,5E-06	2,5E-06	.1,1	0,9	1,1	1	0,9	.1	1	1,1	.1	1
6,3E-07	6,3E-07	.1,2	1	1,1	.1	0,9	.1,1	1	.1,1	.1	0,9
1,6E-07	1,6E-07	.1,1	1,2	1,1	0,9	0,9	.1	1	1	.1	1
3,9E-08	3,9E-08	.1,1	1	1,1	0,9	1	.1	1	.1	1,1	0,9
9,8E-09	9,8E-09	.1,1	1	1	.1	1	1	1	1,1	1	0,9
2,4E-09	2,4E-09	.1,1	1,1	1	1	.1	0,9	1	1,1	1,1	1
6,1E-10	6,1E-10	.1,1	1	1	.1	1	0,9	1	.1	.1,1	0,9
1,5E-10	1,5E-10	.1,2	1,1	1,1	1	1	0,8	1,1	.1,1	.1,1	1

Perifosine	Sotrastaurin	MP38	MP41	MP46	MP65	MM28	MM66	92.1	Mel202	OMM1	OMM2.5
1,0E-05	1,0E-05	.1	.1,2	0,9	.1,1	.1	1	.1,1	.1	.1	0,7
2,5E-06	2,5E-06	1	.1,1	0,9	1,1	1	1	1	1	1,2	0,8
6,3E-07	6,3E-07	.1,1	1,1	1	.1	.1	1	.1,1	.1,1	.1	0,9
1,6E-07	1,6E-07	.1	1	0,9	.1	.1,1	1,1	1	.1	.1	0,9
3,9E-08	3,9E-08	.1,1	1	1	1	.1,1	.1	1	0,9	.1	1
9,8E-09	9,8E-09	1	.1	0,9	1	.1	.1	0,9	0,8	1	.1
2,4E-09	2,4E-09	1	.1,1	0,9	.1	.1	.1	1	1	.1	1
6,1E-10	6,1E-10	1	.1	0,9	.1,1	1	1	.1	0,9	.1,1	0,9
1,5E-10	1,5E-10	1	.1,1	1	1,1	1	.1,1	.1	0,9	1,1	1

Supplementary Figure 2

Mel202

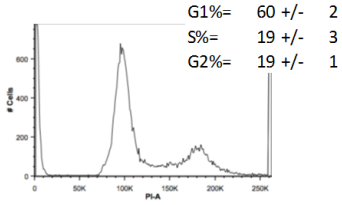

CONTROL

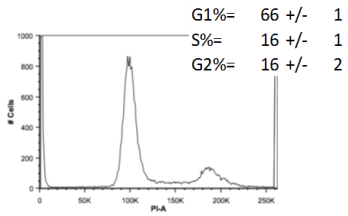

Everolimus 2,5 µM

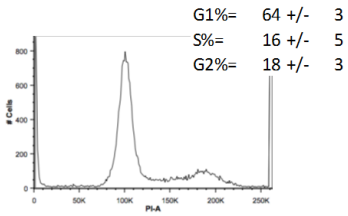

GDC0941 2,5µM

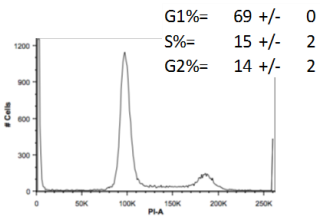

Selumetinib 0,25 µM

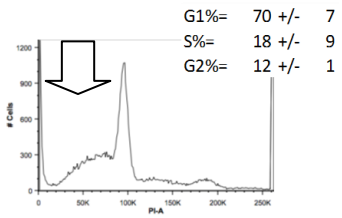

Everolimus 2,5 µM + GDC0941 2,5µM

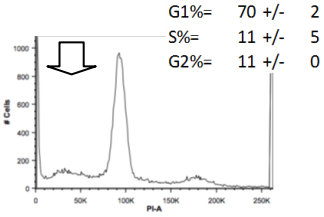

Selumetinib 0,25 µM + GDC0941 2,5µM

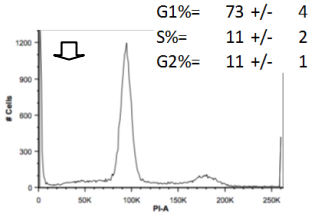

Everolimus 2,5µM + Selumetinib 0,25 µM

MM28

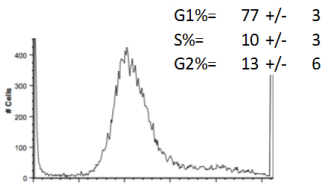

CONTROL

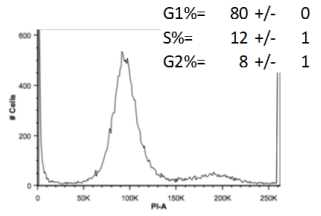

Everolimus 2,5 µM

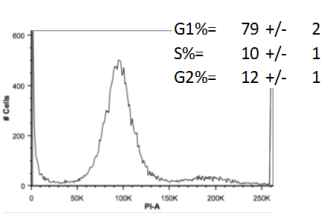

GDC0941 2,5µM

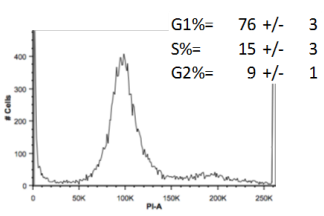

Selumetinib 0,25 µM

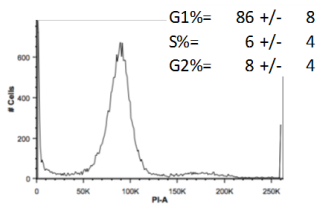

Everolimus 2,5 µM + GDC0941 2,5µM

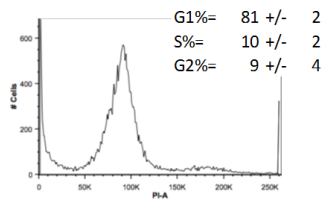

Selumetinib 0,25 µM + GDC0941 2,5µM

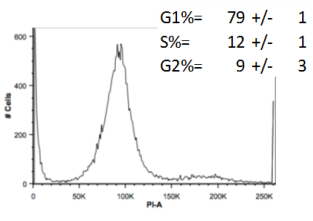

GDC0941 2,5µM + Selumetinib 0,25 µM

CONCLUSIONS AND PERSPECTIVES

CONCLUSIONS AND PERSPECTIVES

We have established a panel of 7 human UM cell lines representative of the genetic landscape of the disease. This panel has been used as a tool to discover effective therapeutic strategies for UM. First, we have focused our interest on the PI3K/mTOR pathway and we have assessed the effects of the mTOR inhibitor Everolimus on UM cell viability.

Interestingly we obtained significant tumor growth delay in vivo by using 4 different UM PDX models. Given the relative resistance of these tumors these data are promising and could justify the assessment of Everolimus in clinical trials. Everolimus is already approved by FDA and EMEA for renal cell carcinoma after failure of anti VEGF therapy, for Advanced ER+, Her2- breast cancer in combination with Exemestane, and for progressive PNETs; the set-up of a clinical study on Everolimus would be therefore less challenging than for other inhibitors of the PI3K/mTOR pathway. We have recently found one PDX model completely resistant to Everolimus and this gives the opportunity to investigate and identify potential biomarkers predicting the response to this drug.

The promising in vitro data showing that Everolimus and a MEK inhibitor synergistically affected the viability of some UM cells led us to proceed to a drug combination screening by using inhibitors targeting the major pathways deregulated in UM. This screening is based on the concept of synergy, or increase of the effect of a drug by its combination with a second one, and it lays on the hypothesis that this drug have already a good efficacy in the disease. If two drugs of a combination display already selectivity on their own it is highly probable that the synergy will be also specific. On the contrary it might be even higher on normal cells thus resulting in potential side effects. In this way, the use of control cells (GNAQ/11 wild type, normal melanocytes) may help in assessing specific effects. However melanocytes grow very slowly and other physiologic cell lineages might possess activated pathways that could make them even more susceptible to active targeted drugs, and even more susceptible to the synergy.

Testing in these combinatorial assays drugs that are already proved as promising in vivo or in clinical trials increases the chances of finding non-toxic, effective combinations. We performed our combination screening on a small non-automated way. Indeed the pipeline we propose has shown to be quite effective and the same principle could be applied on a wider scale with a robotic approach.

We have found that half of the models tested in vitro are highly susceptible to undergo apoptosis when PI3K inhibitor GDC0941 is added to Everolimus. The molecular mechanism of this effect has not been assessed yet, although preliminary results suggest that a feedback on AKT is not responsible for the synergy. The variability in apoptotic effects on our cell lines suggest that different classes of UM might exhibit variable susceptibility to the combination. It is therefore crucial to investigate the molecular basis of Everolimus-GDC0941 synergy. Finally *in vivo* tests conducted in our panel of UM PDX models are necessary to further evaluate the efficacy of the combination.

4 of our established cell lines are BAP1 deficient. These cell lines are to date the only in vitro models of UM to display this phenotype. Since BAP1 is lost in about 80% of metastasizing tumors, and as a consequence in a similar percentage of UM metastasis, selective targeting of these cell lines could represent an effective strategy for the therapy of metastatic UM. Ashworth et al. have shown the possibility to target the loss of tumor suppressor genes with synthetic lethality. Cancer cell harboring homozygous inactivation of either BRCA1 or BRCA2 genes are selectively killed by PARP inhibitors (Farmer et al., 2005). The same strategy could be applied in UM. High Throughput siRNA or drug screening could identify a genetic or molecular target whose function is necessary for cell viability in the absence of BAP1 but whose inactivation could be tolerable in cells with wild type BAP1. Such a strategy could spare toxicity in normal cells, while specifically targeting cells with BAP1 loss.

Having “naturally mutated” cell lines with BAP1 loss is essential, and an attempt to artificially modulate BAP1 expression in wild type cells is unlikely to serve in this purpose. In our experience we did not observed an evident morphological difference in BAP1 mutated cell lines, as might be suggested by studies on knock down of BAP1 UM cells. Harbour et al. describes upon RNA interference mediated

knockdown of BAP1 on 92.1 the development of “a rounded epithelioid morphology, and cell growing as multicellular non-adherent spheroids” (Harbour et al., 2010). We did not observe such characteristics in BAP1 mutated cells compared to wild type. Moreover the knock down of BAP1 in wild type cells is reported to block cell cycle in cell lines infected stably with specific short-hairpin RNA (Matatall et al., 2013). We have observed the same phenomenon in our laboratory. Moreover Matatall reports the overcome of cell cycle block in 4 weeks, which might suggest that the protein is re-expressed at least at low levels or that other mutations allow to compensate for the loss. This might add another element of artificiality and preclude any comparison between manipulated cells and their wild type counterparts.

A trend towards longer doubling times in the BAP1-loss subgroup is observed in our cellular models. This would go against the intuitive idea that a more aggressive tumor cycles faster. Interestingly we could not observe fast growing BAP1 mutated PDXs, in comparison with wild type PDXs (personal communication of Dr. Nemati). An histopathological study on cell cycle markers as Ki67 or estimators of cell cycle distribution (Yanagita et al., 2012) could address this question in the clinical setting. Indeed this could be a possibly explanation for the chemoresistance showed by UM metastasis treated with classical alkylating agents.

In our drug study no pattern of response was clearly found to be related to BAP1 status. But 4 models are not sufficient for effective statistical comparisons. Therefore more BAP1 models have to be established for solid statistical inference on in vitro tests.

Interestingly one of the cell lines displaying BAP1 protein loss, MP46, does not show any mutation of BAP1. BAP1 mutations were identified in patient DNA with an a heteroduplex detection method (Laurent et al., 2013). Deep sequencing can increase the odds of finding an undetected mutation, however it is possible that alterations in non-coding regions or epigenetic alterations could be responsible for the phenotype. The percentage of UM displaying BAP1 loss without a known mutation in the BAP1 gene is still unknown, although it is probably a quite rare phenomenon (Koopmans et al., 2014). A report on clear cell carcinoma indicates a

similar situation in clear cell renal cancer with BAP1 loss. A study on 25 samples with negative BAP immunohistochemistry resulted in only 22 tumors with assessed BAP1 mutation. Tracking back BAP1 expression in MP46 (BAP1 mRNA, activation status of the promoter) could offer new insights on the possibility of alternative mechanism of BAP1 silencing.

Our BAP1-deficient cell lines are a valuable tool to study BAP1 functions in UM. The difference in the phenotypical expression of BAP1 deficiency in different pathologic contexts (hereditary tumor syndrome with germ-line mutations of BAP1, aggressive UM and clear cell carcinoma, BAP1 mutated mouse models of Myelodysplastic syndrome) indicates that the functions and possibly the players interacting with BAP1 are different in different cells. Our cell lines represent the perfect instrument to investigate the functions of BAP1 in the specific context of aggressive UM. Indeed the putative functions of BAP1 in tumor progression and tumor invasivity would find in our model the perfect ground for in vitro experimentation.

In our study we could assess only 2 SF3B1 mutated cell lines and only one which bears a mutation of EF1AX. Two of those cell lines have been developed by other laboratories several years ago. No other cell lines bearing SF3B1 or EF1AX mutations is known, and targeted sequencing of all the available UM cell lines could increase the possibilities of assembling panels of cell lines which allow to discriminate SF3B1 or EIF1AX dependent phenotypes as well.

In conclusion we have provided the scientific community of an indispensable tool for the study of UM and BAP1, we have proposed a highly effective pipeline for the study of drug synergy in vitro and we have identified Everolimus, alone and in combination with PI3K inhibitor GDC0941 as a promising strategy in the treatment of advanced UM.

REFERENCES

Farmer, H., McCabe, N., Lord, C.J., Tutt, A.N.J., Johnson, D.A., Richardson, T.B., Santarosa, M., Dillon, K.J., Hickson, I., Knights, C., Martin, N.M.B., Jackson, S.P., Smith, G.C.M., Ashworth, A., 2005. Targeting the DNA repair defect in BRCA mutant cells as a therapeutic strategy. Nature 434, 917–921.

Harbour, J.W., Onken, M.D., Roberson, E.D.O., Duan, S., Cao, L., Worley, L.A., Council, M.L., Matatall, K.A., Helms, C., Bowcock, A.M., 2010. Frequent Mutation of BAP1 in Metastasizing Uveal Melanomas. Science 330, 1410–1413.

Koopmans, A.E., Verdijk, R.M., Brouwer, R.W.W., Van den Bosch, T.P.P., Van den Berg, M.M.P., Vaarwater, J., Kockx, C.E.M., Paridaens, D., Naus, N.C., Nellist, M., Van Ijcken, W.F.J., Kiliç, E., De Klein, A., 2014. Clinical significance of immunohistochemistry for detection of BAP1 mutations in uveal melanoma. Mod. Pathol.

Laurent, C., Gentien, D., Piperno-Neumann, S., Némati, F., Nicolas, A., Tesson, B., Desjardins, L., Mariani, P., Rapinat, A., Sastre-Garau, X., Couturier, J., Hupé, P., De Koning, L., Dubois, T., Roman-Roman, S., Stern, M.-H., Barillot, E., Harbour, J.W., Saule, S., Decaudin, D., 2013. Patient-derived xenografts recapitulate molecular features of human uveal melanomas. Mol Oncol 7, 625–636.

Matatall, K.A., Agapova, O.A., Onken, M.D., Worley, L.A., Bowcock, A.M., Harbour, J.W., 2013. BAP1 deficiency causes loss of melanocytic cell identity in uveal melanoma. BMC Cancer 13, 371.

Yanagita, E., Kamoshida, S., Imagawa, N., Itoh, T., 2012. Immunohistochemistry-based cell cycle detection (iCCD): a novel system to visualize cell kinetics on formalin-fixed paraffin-embedded tissues. Am. J. Surg. Pathol. 36, 769–773.

APPENDIX

MOLECULAR ONCOLOGY 8 (2014) 1508–1520

available at www.sciencedirect.com

ScienceDirect

www.elsevier.com/locate/molonc

Establishment of novel cell lines recapitulating the genetic landscape of uveal melanoma and preclinical validation of mTOR as a therapeutic target

Nabil Amirouchene-Angelozzi[a,1], Fariba Nemati[b,1], David Gentien[c], André Nicolas[d], Amaury Dumont[e], Guillaume Carita[b], Jacques Camonis[e], Laurence Desjardins[f], Nathalie Cassoux[f], Sophie Piperno-Neumann[g], Pascale Mariani[h], Xavier Sastre[d], Didier Decaudin[b,1], Sergio Roman-Roman[i,*,1]

[a]Biophenics Laboratory, Translational Research Department, Institut Curie, 26 rue d'Ulm, 75005 Paris, France
[b]Laboratory of Preclinical Investigation, Translational Research Department, Institut Curie, 26, rue d'Ulm, 75005 Paris, France
[c]Genomics Platform, Translational Research Department, Institut Curie, 26, rue d'Ulm, 75005 Paris, France
[d]Department of Tumor Biology, Institut Curie, 26, rue d'Ulm, 75005 Paris, France
[e]Institut Curie, INSERM U830, France
[f]Department of Ophthalmological Oncology, Institut Curie, 26, rue d'Ulm, 75005 Paris, France
[g]Department of Medical Oncology, Institut Curie, 26, rue d'Ulm, 75005 Paris, France
[h]Department of Surgery, Institut Curie, 26, rue d'Ulm, 75005 Paris, France
[i]Translational Research Department, Institut Curie, 26, rue d'Ulm, 75005 Paris, France

ARTICLE INFO

Article history:
Received 10 February 2014
Received in revised form
5 April 2014
Accepted 4 June 2014
Available online 13 June 2014

Keywords:
Uveal melanoma

ABSTRACT

Uveal melanoma (UM) is the most common primary tumor of the eye in adults. There is no standard adjuvant treatment to prevent metastasis and no effective therapy in the metastatic setting. We have established a unique panel of 7 UM cell lines from either patient's tumors or patient-derived tumor xenografts (PDXs). This panel recapitulates the molecular landscape of the disease in terms of genetic alterations and mutations. All the cell lines display GNAQ or GNA11 activating mutations, and importantly four of them display BAP1 (BRCA1 associated protein-1) deficiency, a hallmark of aggressive disease. The mTOR pathway was shown to be activated in most of the cell lines independent of AKT signaling. mTOR inhibitor Everolimus reduced the viability of UM cell lines and significantly delayed tumor growth in 4 PDXs. Our data suggest that mTOR inhibition with

* *Corresponding author*. Tel.: +33 153197411; fax: +33153194130.
E-mail addresses: Nabil.Amirouchene-Angelozzi@curie.fr (N. Amirouchene-Angelozzi), Fariba.Nemati@curie.fr (F. Nemati), David.Gentien@curie.fr (D. Gentien), Andre.Nicolas@curie.fr (A. Nicolas), Amaury.Dumont@curie.fr (A. Dumont), Guillaume.Carita@curie.fr (G. Carita), Jacques.Camonis@curie.fr (J. Camonis), Laurance.Desjardins@curie.net (L. Desjardins), Nathalie.Cassoux@curie.net (N. Cassoux), Sophie.Piperno-Neumann@curie.net (S. Piperno-Neumann), Pascale.Mariani@curie.net (P. Mariani), Xavier.Sastre@curie.net (X. Sastre), Didier.Decaudin@curie.net (D. Decaudin), Sergio.Roman-Roman@curie.fr (S. Roman-Roman).
[1] Equally contributed.
http://dx.doi.org/10.1016/j.molonc.2014.06.004

BAP1
Everolimus
mTOR
Cell lines
Patients-derived tumor xenografts

Everolimus, possibly in combination with other agents, may be considered as a therapeutic option for the management of uveal melanoma.

1. Introduction

Uveal melanoma (UM) is the most frequent and aggressive ocular primary tumor in adults with approximately 5 new cases per million per year in the United States and in Europe (Mallone et al., 2012; Singh et al., 2011). Even if local control rate with photon radiotherapy exceeds 90% at 10 years (Dunavoelgyi et al., 2011) enucleation remains the treatment of choice for large tumors (Singh and Topham, 2003; Singh et al., 2011). Up to 50% of patients develop metastasis, which occur only *via* hematogenous spread because of the absence of lymphatic drainage of the eye and are rarely detected at the time of initial diagnosis (2–4% of the patients)(Harbour and Chen, 2013). In 90% of cases, metastatic spread involves the liver usually leading to death within a few months despite medical treatment (Gragoudas et al., 1991). Currently, no effective adjuvant therapy is available to prevent metastases, neither is there any effective treatment once metastases have developed.

Genome-wide genetic analysis (Trolet et al., 2009) and expression profiling (Onken et al., 2004) divide UM in two subgroups according to the risk of metastatic spreading. UM at high risk for metastasis are associated with monosomy of chromosome 3, loss of 6q and gain of 8q (Trolet et al., 2009). Although occurring in the same cell lineage, uveal and skin melanomas represent different diseases: we have recently demonstrated that uveal melanomas display a remarkably low mutation burden with ~2000 predicted somatic single nucleotide variants per tumor and low levels of aneuploidy. Moreover, no ultraviolet radiation DNA-damage signature has been found in UM (Furney et al., 2013) and BRAF or NRAS mutations commonly found in cutaneous melanoma are not observed in UM (Cohen et al., 2003; Cruz et al., 2003; Edmunds et al., 2003; Kiliç et al., 2004; Rimoldi et al., 2003; Weber et al., 2003). Mutually exclusive mutations in the *GNAQ/11* genes activating the MAP kinase pathway have been described in the majority of UM (Van Raamsdonk et al., 2010, 2008). Although *GNAQ/11* mutational status is not correlated with disease-free survival, these mutations are considered oncogenic drivers and consequently potential good targets for therapeutic intervention. Inactivating mutations of the tumor suppressor *BAP1* occur in ~85% of aggressive tumors and are associated with metastatic disease (Harbour et al., 2010). Recently, exome and whole genome sequencing of uveal melanomas identified recurrent mutations in *SF3B1* (Furney et al., 2013; Harbour et al., 2013; Martin et al., 2013), which encodes a component of the spliceosome, and in the translation initiation factor *EIF1AX* (Martin et al., 2013). *SF3B1* and *EIF1AX* mutations are inversely correlated with chromosome 3 monosomy and associated with good prognosis (Furney et al., 2013; Harbour et al., 2013; Martin et al., 2013).

The currently available UM cell lines do not completely reflect the genetic alterations recurrently found in UM (Griewank et al., 2012). Some cell lines display BRAF mutations, which are not found in UM samples and to our knowledge no UM cell line harboring BAP1 mutations, which represent a hallmark of aggressive UM, have been described so far. The first goal of our study was to develop cellular models of UM representing the genetic landscape (genetic alterations and mutations) of this disease, to provide a good model for assessing the efficacy of new drugs and drug combinations. Next we looked at the activation status of PI3K/mTOR signaling pathway and assessed the effect of Everolimus on cell viability. Last, to provide *in vivo* data, we examined the effect of mTOR inhibition using several previously described patient-derived UM xenografts (Némati et al., 2010).

2. Material and methods

2.1. Tumor samples

Eighty-seven tumor samples were obtained either from patients (60 from primary tumors and 13 from metastasis) or from 14 patient-derived xenografts (PDXs), which were established as described (Némati et al., 2010). All patients had previously given their informed consent for experimental research on residual tumor tissue available after histopathologic and cytogenetic analyses.

2.2. Establishment of uveal melanoma cell lines

Fresh or DMSO frozen tumor samples obtained from pathologists were mechanically fragmented, passed in a 40 μM Nylon filter and resuspended in RPMI 1640 (Gibco, France), supplemented with 20% (vol/vol) fetal bovine serum (FBS, Invitrogen, France), 100 U/ml penicillin and 100 μg/ml streptomycin (P/S, Invitrogen, France). Once cell lines showed unlimited proliferation and were cultured for more than 40 passages, they were considered established. Optic microscopy images were taken with a Leica DM IL microscope and a Nikon DS-L1 camera.

2.3. Cell culture

92.1 (De Waard-Siebinga et al., 1995), Mel202 (Ksander et al., 1991), were purchased from The European Searchable Tumour Line Database (Tubingen University, Germany). OMM1, OMM2.5 (Luyten et al., 1996; Chen et al., 1997) were kindly

provided by P.A. Van Der Velden (Leiden University, The Netherlands). Cell lines were cultured in RPMI-1640 supplemented with 20% (MM28, MM33, MP46, MP41, MP65, and MM66) or 10% (Mel202, OMM1, and OMM2.5) FBS (Life Technologies), Penicillin 100 U/ml – Streptomycin 100 μg/ml (Life Technologies). All cell lines were tested for Mycoplasma and proved to be Mycoplasma free. Cell lines were maintained in a humidified atmosphere (5% CO_2) at 37 °C. All cell lines were genotyped: Short Tandem repeat Polymorphism (STR) profiles of 92.1, Mel202, OMM1, OMM2.5 matched at 100% those presented in reference (Griewank et al., 2012).

2.4. Chemicals

mTOR inhibitor Everolimus/Rad001, MEK inhibitor GSK1120212, and AKT inhibitor KRX-0401 were supplied by Euromedex (France) and dissolved in DMSO (Rad001,GSK1120212) or ethanol (KRX0401) at 10 mM and stored at −20 °C.

2.5. Cell viability assays

We determined cell viability using a colorimetric assay based on 3-(4,5-dimethylthiazol-2-yl)-2,5 diphenyltetrazolium bromide (MTT; M-2128, Sigma) as explained previously (Marty et al., 2008). Cells were seeded at appropriate concentration in 96-well plates at day 0 (MM28:3500 cells/well; MP38:8000 cells/well; MP41:1500; MP46:6000 cells/well; MP65:8000 cells/well; MM66:6000 cells/well; 92.1; Mel202:4000 cells/well; OMM1:1500 cells/well; OMM2.5:3500 cells/well); drug was added to the medium at day 2 and cell viability tested by MTT assay at day 7. Results are expressed as relative percentages of metabolically active cells compared with untreated controls. Drug sensitivity curves were calculated using GraphPad Prism 4.

2.6. Genomic analysis

The DNA was extracted from cell pellets using a standard phenol/chloroform procedure. The total RNA was isolated from cell pellets using a miRNeasy mini kit (Qiagen, Courtaboeuf, France).cDNA synthesis was performed with MuLV Reverse Transcriptase in accordance with the manufacturers' instructions (Invitrogen, Cergy-Pontoise, France) and quality verified on an Agilent 2100 bioanalyzer. For Sanger sequencing, gDNA was amplified by PCR and the products were sequenced using dye-terminator chemistry as previously described (16). Primer sequences for *BAP1*, *GNAQ*, *GNQ11*, *SF3B1* and *EIF1AX* are available upon request. Sequences were visualized using Sequencher software. To perform Loss of heterozygosity and copy number analysis and to detect other abnormalities, genetic analyses of the cell lines were done using Affymetrix Genome-Wide SNP Arrays 6.0. or Cytoscan HD (Affymetrix, High Wycombe, UK). DNA was used to perform Affymetrix Human mapping SNP 6.0 assay as described in (Tuefferd et al., 2008) or Cytoscan assay according to the manufacturer's protocol at the Institut Curie microarray core facility. Genetic profiles were compared to the profiles of the corresponding tumors and PDXs by Chromosome Analysis Suite (Affymetrix). To perform Short Tandem repeat Polymorphism (STR) analysis GenePrint 10 system kit (Promega, France) was used according to manufacturer's instructions.

2.7. Cytopathologic analysis

Cells were fixed in a 4% formalin solution and embedded in paraffin. 4 μm sections were cut from the embedded blocks, and then dewaxed for immunostaining. Heat-induced epitope retrieval was performed at 97° for 20 min in EDTA buffer pH 9.0 (Dako S2367). Mouse antihuman BAP1 antibody (monoclonal mouse anti BAP1 (C4) Santa Cruz Biotechnology, Inc, Santa Cruz, CA) was applied for 1 h at a concentration of 1:200. For antibody revelation polymer HRP (DAKO Envision, Denmark) was used followed by application of di-aminobenzidin (DAB) for 5 min. The immunostaining was performed on a Dako Autostainer Platform. A brown coloration of nuclear localization of strong intensity was observed in the presence of the protein. Cell nuclei were counterstained with Herris' Hematoxylin. Epithelial cells of normal breast glands were used as positive control for BAP1.

2.8. Western blotting

Tissue lysates were loaded onto gels, transferred to nitrocellulose and revealed as described (Marty et al., 2008). Quantification was performed using a LAS-3000 Luminescent Image analyzer and Image Gauge software (Fuji, FSVT, Courbevoie, France). Beta-Actin was used for normalization between samples and detected using anti-beta-actin primary antibodies at the dilution of 1:5000 (Sigma–Aldrich, Saint Quentin Fallavier, France). AKT, phospho-AKT (S473), phospho-AKT (T308), S6, phospho-S6 (Ser 235/236) (Cell Signaling Technology, Ozyme, Saint Quentin en Yveline, France) and BAP1 (C4) (Santa Cruz Biotechnologies) antibodies were used at 1:1000 dilution.

2.9. In vivo antitumor efficacy of an mTOR inhibitor

Female SCID mice were grafted with a tumor fragment of 15 mm^3. Mice bearing tumors with a volume of 40–200 mm^3 were individually identified and randomly assigned to the control or treatment groups (6–10 animals per group). Number of mice used were respectively: for PDXs MP34: 8 mice for the control group, 8 for the treatment group; for PDXs MP41: 10 mice for controls and 9 for the treatment group; for PDX MP55: 10 mice for the control group and 8 mice for the treatment group; for PDX MP46: 8 mice for the control group and 6 for the treatment group. Mice were weighed twice a week. Tumor volumes were calculated by measuring two perpendicular diameters with calipers. Xenografted mice were sacrificed at the end of treatment or when their tumor reached a volume of 2000 mm^3. Each tumor volume (V) was calculated according to the following formula: $V = a \times b^2/2$, where a and b are the largest and smallest perpendicular tumor diameters. Relative tumor volumes (RTV) were calculated with the following formula: $RTV = (V_x/V_1)$, where V_x is the tumor volume on day x and V_1 is the tumor volume on the first day of treatment. Growth curves were obtained by plotting the mean values of RTV on the Y axis against time (X axis, expressed as days of treatment). Antitumor activity was evaluated according to tumor growth inhibition (TGI), calculated

with the following formula: percent TGI = 100 − (RTVt/RTVc × 100), where RTVt is the median RTV for a treatment group and RTVc is the median RTV for its control group at the end of the therapy. mTOR inhibitor (Everolimus) was reconstituted in PEG300/HPBCD/Glucose 5% (10/10/80), and administered PO at a dose of 2 mg/kg 3 times a week, for 4–6 weeks. In all *in vivo* experiments, mice of the control groups received 0.2 ml of the drug-formulating vehicle with the same schedule as the treated animals. The experimental protocol and animal housing were in accordance with institutional guidelines as put forth by the French Ethical Committee (Agreement C75-05 − 18, France), and the ethics committee of the Institut Curie that approved this project.

2.10. Expression of tumor-specific antigens

Expression of tumor-specific antigens was assessed by reverse transcription-PCR on RNA extracted from cellular culture as described (Némati et al., 2010).

2.11. Assessment of synergy in drug combination experiments

Synergy computed as excess over Bliss (Straussman et al., 2012) was assessed by calculation, for each combination of doses tested, of its fractional inhibition value (1 − fraction of viable cells compared to controls) and by successive subtraction of the fractional inhibition value calculated according to the Bliss independence model. Therefore Excess over Bliss = $c - (a + b - 2^*a^*b)$ where a is the fractional inhibition obtained with an *x* concentration of drug A, *b* is the fractional inhibition obtained with an y concentration of drug B and *c* is the fractional inhibition obtained with x concentration of drug A combined with y concentration of drug B. Synergy calculated as Combination Index was obtained using Chu and Talalay median-effect equation (Chou, 2006) with the software Compusyn ComboSyn, Inc., Paramus, NJ. USA, 2005 (Chou, 2010).

2.12. Statistical methods

For in vitro experiments 95% Confidence Intervals on 3 independent replicates were calculated to assess statistical significance for synergic effects of drug combinations. For *in vivo* experiments the statistical significance of the difference between calculated RTVs for treatments versus control groups was calculated by the two-tailed Student's *t* test.

3. Results

3.1. Establishment of UM cell lines

We have established 7 UM cell lines: 2 of them, MP38 and MP65, were obtained directly from human primary tumors (success rate of 3%), 3 cell lines derived from PDX models (Némati et al., 2010) of liver (MM28 and MM66) or skin (MM33) metastasis, while MP41 and MP46 derived from PDX models of primary tumors (See Table 1). MP38 and MP65 display a fusiform morphology, MP41 shows a predominant epithelioid appearance while MP46, MM28, MM33 and MM66 have a mixed morphology (see Figure 1). All the cell lines are adherent with MM66 having a minor component growing in suspension. Estimated doubling times (shown in Table 1) ranged between 40 and 120 h.

3.2. Characterization of UM cell lines

Copy number and SNP profiles were generated for each cell line and compared to the profiles obtained from the tumors of origin (patients or PDXs). DNA arrays profiles are represented in Supplementary Figure 1. Genotype analysis by Affymetrix mapping SNPs arrays confirmed the overall conservation of chromosome alterations between cell lines and corresponding tumor specimens, in particular for chromosomes 1, 3, 6, 8 and 16 whose status are known to have an impact on classification and prognosis of the disease (Couturier and Saule, 2012; Harbour, 2012). Six cell lines display loss or LOH of 1p or gain of 1q; five cell lines display chromosome 3 monosomy or isodisomy. Five cell lines show gain of 6p and loss or LOH of 6q and one shows loss of 6q only. A gain of 8q was observed in six cell lines except for MP38, with three showing also 8p loss. Loss of 16q was found in four cell lines.

As shown in Table 1 all cell lines harbor mutually exclusive mutations in either GNAQ or GNA11 as occurred in the corresponding tumor of origin: *GNAQ* c.626A > C; p.Gln209Pro in MM33 and *GNAQ* c.626A > T p.Gln209Pro in MP46 and MP38, while MP41, MP65, MM28 and MM66 bear *GNA11* mutations (GNA11 c.626 a > T; p.Gln209Leu). MP38, MP65, and MM28 display loss of function mutations of the *BAP1* gene associated with LOH of chromosome 3 as follows: MP38 harbors a deletion of 14 bp (c.68-9_72del) leading eventually to the loss of a splice site. MP65 displays a frame-shift deletion of 1 pb (c.1717del; p.Leu573TrpfsX3) and MM28 harbors a *BAP1* point mutation (c.1881C > A; p.Y627). Western blot showed expression of BAP1 in MP41, MM33 and MM66 cell lines and absence of the protein in the 3 *BAP1* mutated cells and in MP46 (Figure 2). The expression of BAP1 was also checked by immunocytochemistry (data not shown) confirming nuclear localization of BAP1 in MP41 M33 and MM66 lines, and absence of nuclear staining in the remaining cell lines. A strong BAP1 nuclear staining was observed as well in a series of previously described UM cell lines including 92.1, Mel202, OMM1, and OMM2.5 (Griewank et al., 2012).

All the cell lines established in this study as well as cell lines received from other laboratories were tested for known *SF3B1* mutations. Only Mel202 proved to be mutated for *SF3B1* (c.1793c > T; p.Arg625Gly). *EIF1AX* gene were also tested at exons 1 and 2 and proved mutated in cell lines MM33 (c.22G/A; p.Gly8Arg) and 92.1 (c.17G/A; p.Gly6Asp). Short Tandem repeat Polymorphism (STR) genotyping was performed and results are reported in Supplementary Table 1.

The expression of 12 tumor-specific antigens (i.e., MAGE1, MAGE2, MAGE3, MAGE4, MAGE6, MAGE10, MAGE-C2, LAGE1, LAGE2, NA17, tyrosinase, and Melan-A) was assessed on cell lines; data are shown in Supplementary Table 2. All the cell lines except MM33 showed a strong expression of Tyrosinase, NA-17 or both. Expression of MAGE and LAGE antigens was found to be negative or very low in our cell lines except

Table 1 – Characteristics of UM cell lines and Xenografts used in this study.

Model	Origin	Morphology	Doubling time	Status of chromosomes 1; 3;6; 8 and 16	LOH of chromosome 3	BAP1 mutations	BAP1 protein expression	GNAQ mutations	GNA11 mutations	SF3B1 mutations	EIF1AX mutations
MP38 CL	Primary Tumor	S	80 h	L3q; G8; L16q	Yes[a]	c.68-9_72del	No	c.626 a > T	_	_	_
MP41 CL	PDX established from Primary Tumor	M	41 h	L1p; G1q; L3; G6P; L6q; L8p; G8q; L16	Yes[b]	_	Yes	_	c.626 a > A/T	_	_
MP46 CL	PDX established from Primary Tumor	M	110 h	G1q; G6p; L6q; L8p; G8q; L16q	Yes	_	No	c.626 a > T	_	_	_
MP65 CL	Primary Tumor	S	120 h	G1q; G6p; G8	Yes	c.1717del	No	_	c.626A > T	_	_
MM28 CL	PDX established from Liver Metastasis	M	109 h	L1p; G1q; L3q; G6p; L6q; L8p; G8q; L16	Yes[a]	c.1881C > A	No	_	c.626A > T	_	_
MM33 CL	PDX established from Skin Metastasis	S	91 h	G1; G6p; L6q; G8; G16	No		Yes	c.626 a > C	_	_	c.22G/A
MM66 CL	PDX established from Liver Metastasis	M	80 h	G1q; L6q; G8	No	_	Yes	_	c.626A > T	_	_
92.1 CL	Primary tumor	M	38 h	der (X) t (X; 6)(q28; p11),+8[d]	ND	ND	Yes	c.626 a > T[c]	_	–	c.17G/A
Mel202 CL	Primary tumor	M	43 h	ND	ND	ND	Yes	c.629 G > A[c]	_	c.1793c > T	_
OMM1 CL	Subcutis Metastasis	M	34 h	der(1)t (1; 3)(p31; p13),+3[50%], add (8) p11),add (16)(p12)[e]	ND	ND	Yes	_	626A > T[c]	_	_
0MM2.5 CL	Liver Metastasis	M	50 h	ND	ND	ND	Yes	c.626 a > C[c]	_	_	_
MP34 X	Primary tumor	E	7 d	L1p; L6q	Yes[a]	_	Yes	_	c.626A > T	c.1793c > T	_
MP41 X	Primary tumor	E	15 d	L1p; G1q.L6q; L8p; G8q; G16p; L16q	No	_	Yes	_	626 a > A/T	_	_
MP55 X	Primary tumor	E	8 d	L3; G6p; Lq; G8p; G8q;	Yes	c.516C > G	No	_	c.626A > T	_	_
MP46 X	Primary tumor	M	11 d	G1q; L3; G6p; L8p; G8q; L16q	Yes	_	No	c.626 a > T	_	_	_

Model: CL, cell line; X, Xenograft.
Morphology: S, spindle cell; M, mixed; E, Epithelioid.
Doubling time. h: hours; d: days.
ND: not determined.
[3] As determined by Western Blot and Immunocytochemistry.
a Uniparental disomy of 3q.
b Uniparental disomy of chromosome 3.
c 92.1 and Mel202 were tested for GNAQ 626A > C, GNAQ 626A > T, GNA11 626A > T; the other data on GNA mutations were issued from (Griewank et al., 2012).
d (De Waard-Siebinga et al., 1995).
e (Luyten et al., 1996).

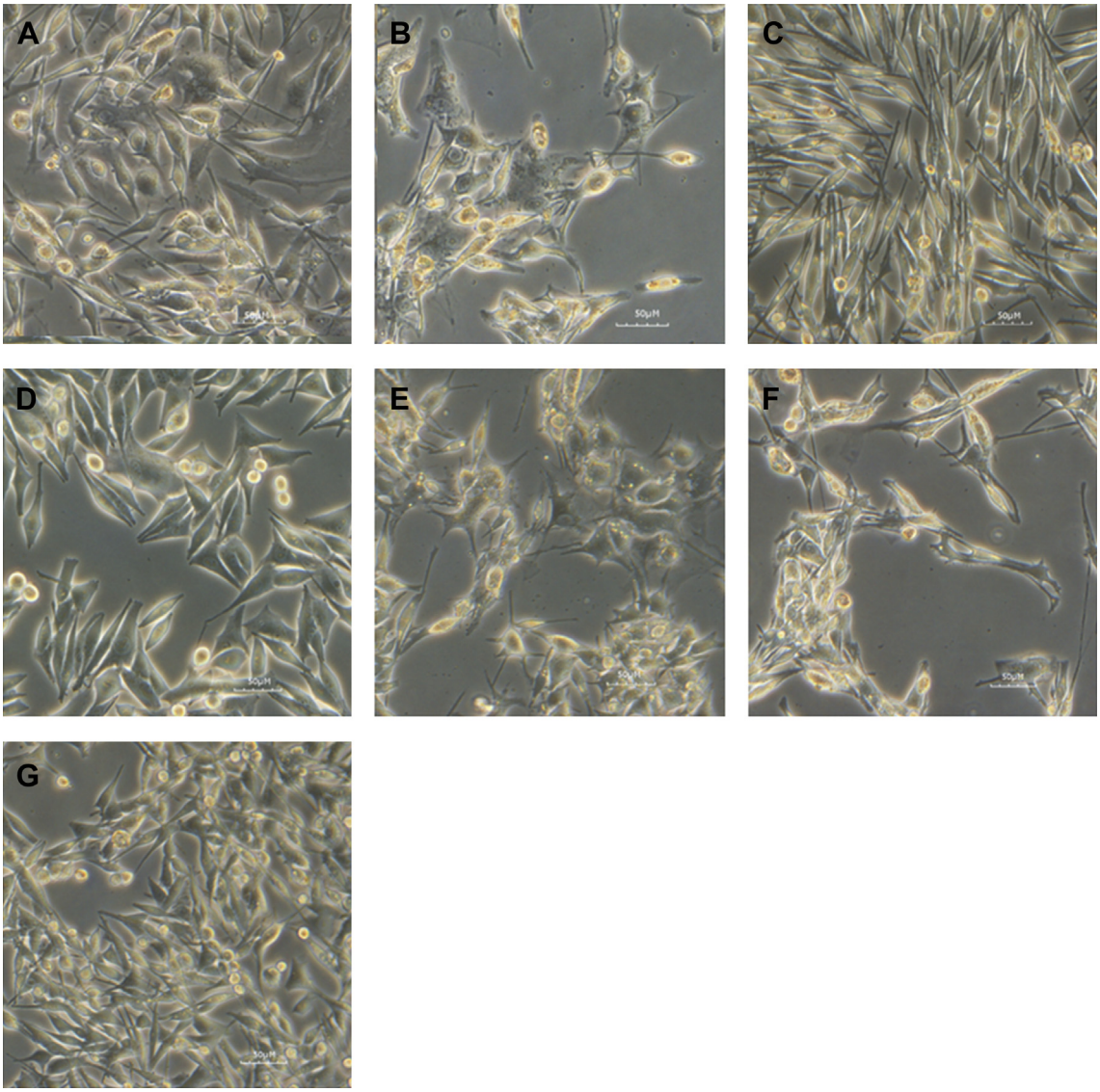

Figure 1 – Morphological analysis of established uveal melanoma cell lines. Light microscopy image of UM cell lines showing predominant epithelioid (MP41) spindle (MP38; MP65) or mixed morphology (MM28; MM33; MP46; MM66). MM28 (A), MM33 (B), MP38 (C), MP41 (D), MP46 (E), MP65 (F), MM66 (G).

MP46 which exhibits a 20% and 100% expression of MAGE2 and MAGE3 respectively). This expression pattern corresponds to what has been already described for the original models and patients (Némati et al., 2010).

3.3. *Activation of mTOR pathway and effect of Everolimus on UM cell lines*

UM cells have been reported to display activation of the PKC, MEK-ERK and PI3K/mTOR pathways (Abdel-Rahman et al., 2006; Khalili et al., 2012; Pópulo et al., 2011, 2010; Saraiva et al., 2005). Clinical trials with PKC and MEK inhibitors are in progress. The MEK inhibitor Selumetinib has been shown to increase progression free survival compared to standard of care, but failed to demonstrate a statistically significant increase in overall survival (Carvajal et al., 2013). No clinical data concerning the use of PI3K/mTOR inhibitors in UM have been reported so far. Some in vitro studies have addressed the effect of these inhibitors using UM cell lines but in a BAP1-proficient context and sometimes with cell lines displaying activating B-RAF mutations (Babchia et al., 2010; Ho et al., 2012; Khalili et al., 2012). We therefore decided to assess the activation status of PI3K/mTOR pathway on our panel of cell lines, which recapitulate the genetic features of the disease.

First, we tested the activation of the pathway on 2 BAP1 mutated (MP38 and MP65) and 2 BAP1 wild-type cell lines (MP41 and MM66). BT20, a cell line displaying a PI3KCA mutation conferring a constitutive activity to the kinase, was used as control for the activation of PI3K/mTOR pathway. Analysis

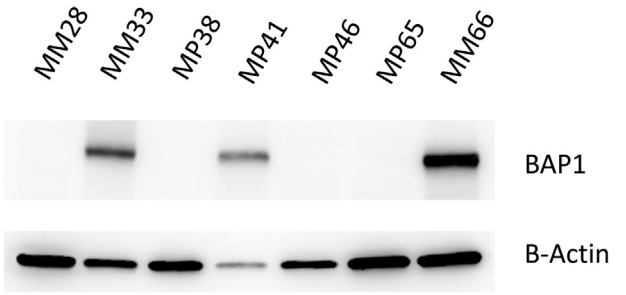

Figure 2 – Western blot analysis of BAP1 protein expression in UM cell lines. Immunostaining on cell lines MM33, MP41 and MM66 reveals presence of the protein BAP1 while MP28, MP38, MP46 and MP65 show loss of BAP1 protein expression.

of the phosphorylation of mTOR downstream target S6 ribosomal protein (El-Hashemite et al., 2003) showed an activation of mTOR pathway comparable to that of BT20, with evidence of phosphorylation of the protein also after 24 h of serum starvation in 3 out of 4 uveal melanoma cell lines (Figure 3). Phospho-AKT was barely detectable on western blot, and the ratio between phospho AKT and total AKT was found dramatically low as compared to BT20 (Figure 3). This suggests that mTOR activation of UM cell lines is not dependent of AKT phosphorylation. In agreement with this hypothesis, the AKT inhibitor Perifosine did not significantly alter cell proliferation of UM cell lines (supplementary Figure 2). Viability of 10 UM cell lines (MM28, MP38, MP41, MP46, MP56 and MM66, 92.1, Mel202, OMM1 and OMM2.5) was significant affected by Everolimus at relative low doses even if a full inhibition of cellular viability was not reached (Figure 4A). The slopes of curves obtained with Everolimus

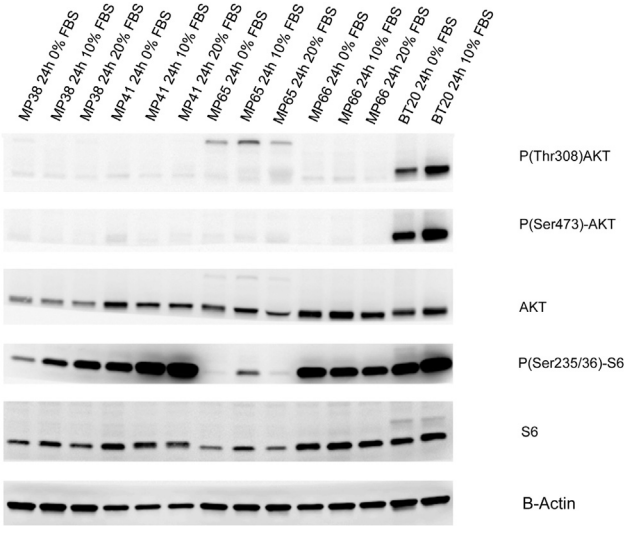

Figure 3 – Analysis of mTOR and AKT signaling pathway in UM cell. UM cell lines were cultured for 24 h at different serum concentrations. P(Ser473)-AKT, P(Thr308)-AKT, AKT, P(Ser235/236)-S6, S6 and B-Actin were evaluated on cellular lysates by Western blot analysis.

suggest a cytostatic rather than cytotoxic effect. As depicted in Figure 4B, a dramatic reduction in S6 phosphorylation could be observed in 6 different UM cell lines treated with Everolimus at 1 nM. The most sensitive cell lines in terms of cellular viability (MM66, OMM1 and OMM2.5) display the higher reduction in S6 phosphorylation, whereas MP65 and MP41 are the more resistant to Everolimus in terms of both cell viability and S6 phosphorylation. However a statistically significant correlation between the effect of Everolimus on S6 phosphorylation and cellular viability in the different cell lines could not be demonstrated. Altogether our data demonstrate that UM cell lines display mTOR signaling activation and that Everolimus significantly affects cell proliferation at doses at which it inhibits mTOR downstream signaling.

3.4. *Everolimus effects in vivo*

We then tested the effect of Everolimus *in vivo* using our UM PDX panel previously characterized (Laurent et al., 2013; Némati et al., 2010) that represents the genetic landscape of UM as described above. Four models were tested for this purpose: MP34, MP41, MP55, and MP46. Of note, we did not succeed in establishing cell lines from MP34 and MP55 PDXs. MP34 displays a mutation in GNAQ and MP41, MP55, and MP46 harbor GNA11 mutations. Two of them (MP46 and MP55) do not express BAP1 protein as assessed by immunohistochemistry (Laurent et al., 2013). MP34 harbors an *SF3B1* mutation. Mice were treated with Everolimus per os at 2 mg/kg 3 times per week for 4–6 weeks. As depicted in Figure 5, treatment with the mTOR inhibitor resulted in a significant tumor growth delay in the models MP41, MP55 and MP34, with a Tumor Growth Inhibition (TGI) of 57%, 51% and 47% respectively, and a moderate effect in MP46 with a TGI of 38%. Taken together, our results show that Everolimus significantly reduced tumor growth of uveal melanoma *in vivo*.

3.5. *Effect of combined MEK inhibitor and Everolimus on UM cell proliferation*

Given that tumor regression was not achieved with Everolimus alone and since mTOR inhibitors have been reported to have a rather cytostatic than cytotoxic effect (Weigelt et al., 2011), combinatorial approaches need to be addressed to implement efficient therapeutic schedules. MAPK inhibitors clearly represent good candidates to be tested in combination with Everolimus in UM given that *GNAQ/11* activating mutations result in MAPK upregulated activity and this gene is mutated in >85% of UM patients. Our data argue that the MEK inhibitor Trametinib displays the lowest IC_{50} among a panel of compounds tested on UM cell lines (data not shown). Moreover, recent data testing MEK inhibitors in uveal melanoma metastatic patients were promising (Carvajal et al., 2013). We, therefore, tested whether the MEK inhibitor GSK1120212 (Trametinib) on the already described panel of 10 UM cell lines could enhance the in vitro efficacy of Everolimus. Figure 6 shows the effect of single drug and of the combination on the 10 different cell lines. Analysis of synergism was performed according to two different models: Bliss

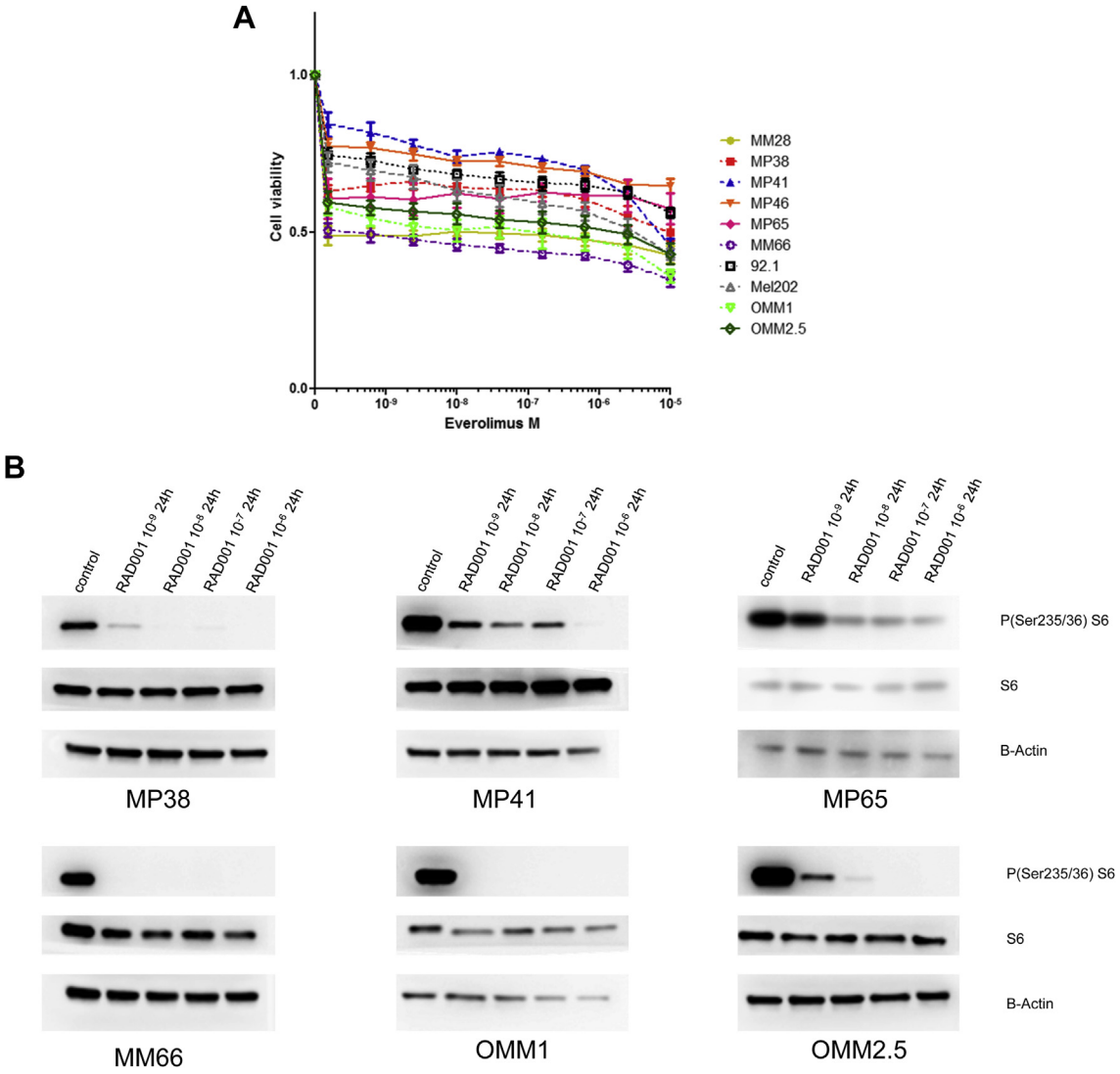

Figure 4 – Sensitivity of a representative panel of uveal melanoma cell lines to mTOR inhibitor Everolimus and effect of Everolimus on UM cell lines viability. A. UM cell lines were treated for 24 h with different concentrations of Everolimus and P(Ser235/236)-S6, S6 and B-Actin assessed by Western blot analysis. B. MM28 (GNAQ_11 mutated, BAP1 deficient) MP38 (GNAQ_mutated, BAP1 deficient), MP41 (GNA11 mutated), MP46 (GNAQ_mutated, BAP1 deficient) MP65 (GNA11 mutated, BAP1 deficient), MM66 (GNA11 mutated), 92.1 (GNAQ_mutated, EIF1AX mutated), Mel202 (GNAQ_mutated, SF3B1 mutated), OMM1 (GNA11 mutated), OMM2.5 (GNAQ_mutated) were seeded at adequate concentration and incubated with the drugs for 5 days. Cell viability was quantified with the MTT assay. Results are expressed as the mean of at least 3 separate experiments. Error bars represent standard errors of the mean.

independence (Keith et al., 2005) and combination Index described by Chu (2006). Although both analyses gave roughly the same results, the first method was more reproducible in our hands and therefore only the data generated with it are shown in Supplementary Figure 3. A significant fraction of UM cell lines exhibited moderate synergy between Everolimus and Trametinib supporting the development of combinatorial approaches with agents targeting MEK and mTOR pathways in UM patients. This needs to be addressed in preclinical *in vivo* models. Under our in vitro experimental conditions, the combination of Everolimus and Trametinib did not result in induction of apoptosis (examining cleaved PARP by Western blot) in UM cell lines with the exception of 92.1 cells in which Everolimus was shown to increase the apoptosis induced by Trametinib (data not shown). Further investigation is necessary to better understand the molecular mechanisms resulting in the observed synergy of these two compounds.

4. Discussion

Efficient management of UM patients requires a better understanding of the genetic and molecular abnormalities implicated in the development and progression of this disease. With the emergence of an armamentarium of targeted drugs,

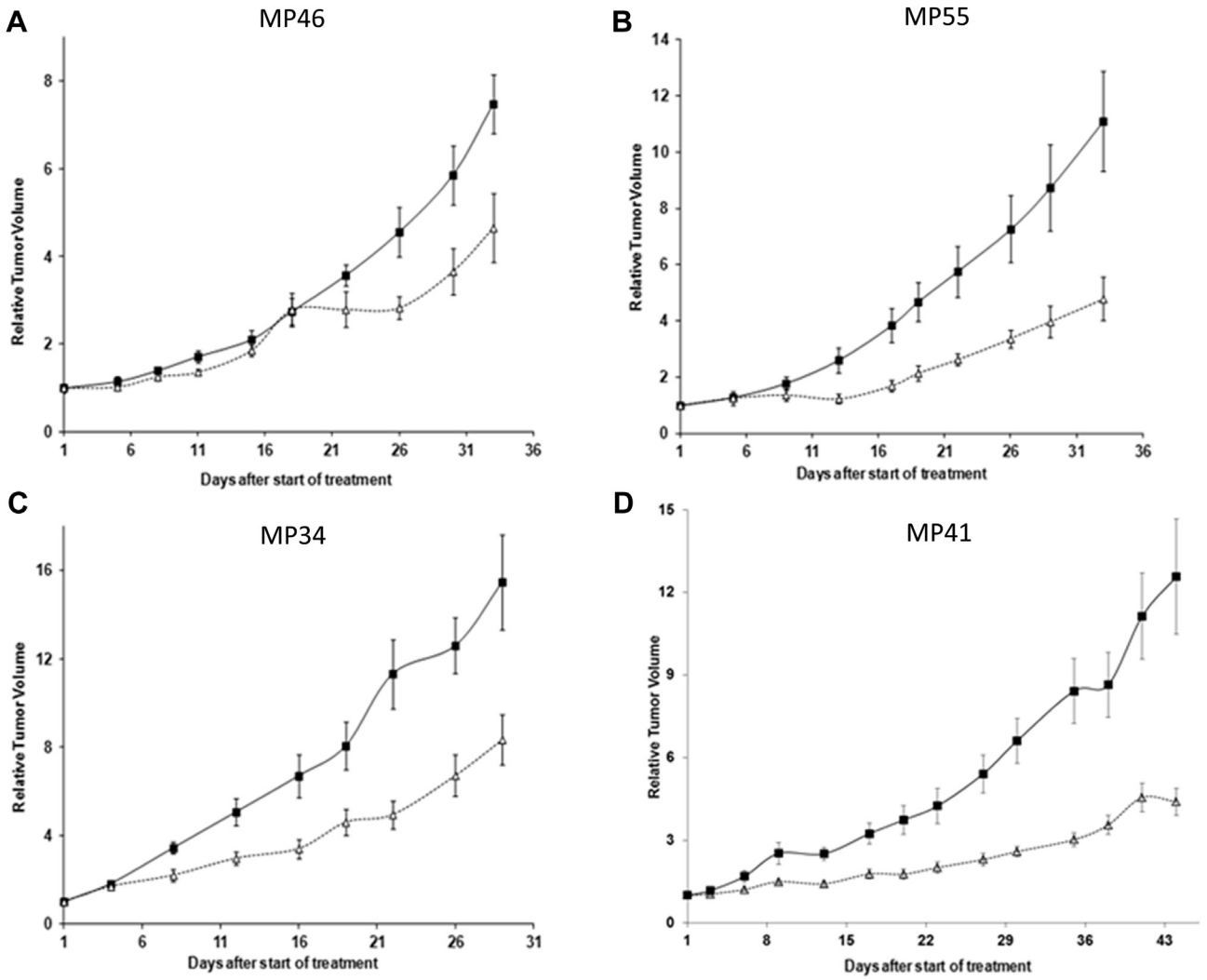

Figure 5 – Effects of mTOR inhibitor Everolimus in the growth of four UM PDXs in vivo. Growth curves of four human uveal melanoma xenografts: MP46 (A), MP55 (B), MP34(C), and MP41(D), treated with Everolimus (Δ) per os at 2 mg/kg 3 times a week, or receiving vehicle (■) with the same schedule as the treated animals for 4 (MP46, MP55, MP34) to 6 (MP41) weeks. Tumor volume and RTV were calculated as described in Materials and Methods. Growth curves were obtained by plotting mean RTV against time. Bars, SD. For the treated groups $n = 6–8$ mice; for the control groups $n = 8–10$ mice. P values calculated at the end of the treatment were < 0.05 for the four models.

in vitro and *in vivo* preclinical models for testing new drugs and drug combinations is mandatory to rationally set up clinical trials. We have recently described a panel of patient-derived UM PDXs, which recapitulates the genetic features of primary human UMs and exhibit genetic stability over the course of their *in vivo* maintenance (Laurent et al., 2013; Némati et al., 2010). Although this panel represents a powerful preclinical tool for both pharmacologic and biological analyses, it is useful for functional studies to have access to a panel of well-characterized tumor cell lines. Unfortunately, obtaining UM cell lines from patients is not easy and the cell lines reported to be of uveal origin do not always display the genetic alterations described in UM. For example, some UM cell lines described in the literature have activating mutations in BRAF (Calipel et al., 2003; Griewank et al., 2012) despite the absence of these mutations in UM tissues. Moreover no UM cell line harboring BAP1 mutations, a hallmark of metastasizing UM, has been reported. In this paper, we have established and characterized 7 new human UM cell lines. Five of them were obtained from PDXs models and the other two directly from human primary tumors. This suggests that the success in establishing UM cell lines could be significantly improved by previously engrafting the UM samples in immunodeficient mice as already reported for colorectal tumors (Dangles-Marie et al., 2007). We are continuing to develop UM cell lines from our entire collection of PDX and aim to expand our cell lines panel in the future. The UM cell lines described here match the genotype of the tumors of origin. All of them harbor mutually exclusive activating mutation in either *GNAQ* or *GNA11*. In addition, we have established 4 unprecedented BAP1-deficient UM cell lines. we could not demonstrate any BAP1 mutation in the BAP1 deficient model

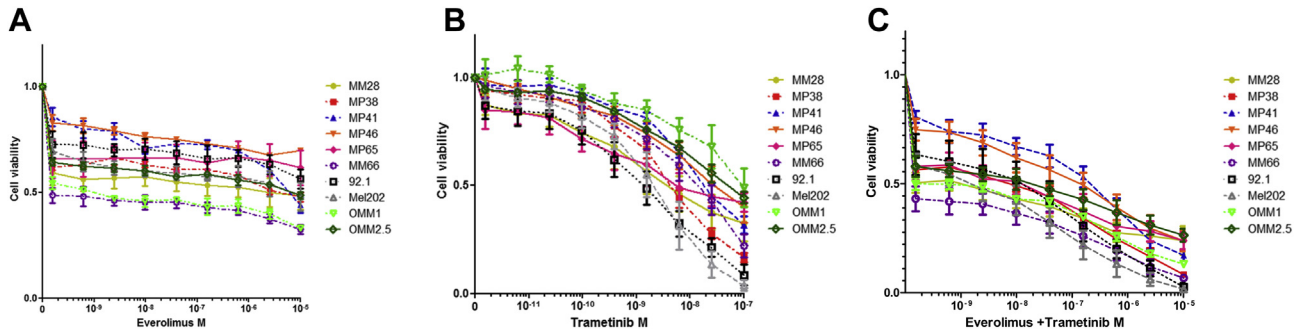

Figure 6 – Effect of the combination of MEK inhibitor Trametinib and mTOR inhibitor Everolimus on the viability of a panel of 10 UM cell lines. Cell lines were treated at the indicated doses of inhibitors for 5 days and cell viability was determined by MTT as described in Material and Methods. Drug concentration is expressed as Molarity; Drug concentration in (C) is expressed as sum of the concentration of each drug. A and B: single drug curves for Everolimus and Trametinib, C: combination. Drug concentrations for the combination had been selected maintaining a constant ratio between the two drugs in order to facilitate synergy evaluation.

MP46, which display a LOH with isodisomy of chromosome 3. For all the cell lines established, the absence of nuclear BAP1 correlated with LOH of chromosome 3. The 7 cell lines were found to be wild type for *SF3B1* while one was found mutated in the *EIF1AX* gene. Together, this describes the genetic landscape of our UM cell lines.

We show that Everolimus significantly affects the cell growth of our UM cell line panel and other UM cell lines previously described. It has been reported that Everolimus very slightly affects cell proliferation of two UM cell lines (92.1 and Mel270) at doses at which it entirely inhibit mTOR downstream signaling (Babchia et al., 2010). Interestingly, the cell lines displaying the highest sensitivity to Everolimus in terms of cell viability exhibited a more pronounced reduction in the phosphorylation S6 ribosomal protein, a target of mTOR. We also show that mTOR signaling is activated in the absence of significant AKT upregulation. The activation of mTOR can be a consequence of MAPK activation resulting from *GNAQ/11* activating mutations present in >85% of UM. In a recent study the PI3K inhibitor GSK2126458 showed a reduced efficacy on *GNAQ* or *GNA11* mutated UM cell lines compared to wild type uveal melanoma cells (Khalili et al., 2012). In the same study RPPA analysis showed a reduced phosphorylation of AKT in *GNAQ* mutated cells compared to *GNAQ* wild type, thus supporting our findings. In contrast, basal P-4EBP and basal P-S6 were higher in the *GNAQ* mutated cell lines, suggesting a key role of the pathway downstream of mTOR in *GNAQ* mutant cells. This is supported by the observation that in our cellular models phosphorylation of AKT was very weak in comparison with a cell line (BT20) displaying a constitutive active PI3K/AKT pathway. On the contrary, phosphorylation of S6 in our cellular models and in BT20 cell line was similar. Interestingly MP41 and MM66 showed significant phosphorylation of S6 even after 24 h serum starvation at the same levels of the controls, suggesting a constitutive activation of the pathway.

Inhibiting PI3K axis alone or in combination with mTOR inhibition has been proposed as a therapeutic strategy for UM (Babchia et al., 2010). This study showed that PI3K inhibition by LY294002 is more effective than mTOR inhibition by Everolimus, but these differences were significant only in a *GNAQ/11* wild-type context.

Few studies have addressed the effect of PI3K/mTOR pathway *in vivo*. Results were non-conclusive or conducted with cell lines not perfectly representing the genetic landscape of UM (Ho et al., 2012). Here we show that the mTOR inhibitor Everolimus significantly delayed tumor growth in 4 different UM PDX models. The *in vivo* effect of Everolimus is not dependent on BAP1 status. However, since this conclusion is based on four PDX models, it is possible that this finding is due to small sampling size. Our in vitro data also suggest that genetic differences and, specifically, BAP1 mutations does not influence the response to Everolimus.

Although cell lines established from UM metastases were at least as sensitive to Everolimus as cell lines established from primary tumors, it is important to note that the four UM PDX models used in this work were established from primary tumors and not metastatic lesions. In the absence of a comprehensive study using metastatic tissue in UM, caution is required in making conclusions about potential effects of Everolimus on metastatic UM patients.

Given that treatment with Everolimus did not result in tumor regression, combination strategies need to be addressed in vitro and *in vivo*. Our data supports the cytostatic effect of Everolimus alone, which would benefit from combination with MEK inhibitors or low doses of dual mTOR/PI3K inhibitors as others have argued (Mitsiades et al., 2011; Nyfeler et al., 2012).

Everolimus has indications in oncology and a clinical phase 2 trial is currently ongoing at Sloan-Kettering cancer center with the aim of assessing its efficacy in combination with a somatostatin receptor inhibitor Pasireotide on patients with metastatic UM (clinicaltrial.gov identifier NCT01252251). Our preliminary data indicates a synergy of Everolimus and the MEK inhibitor Trametinib. It would be of future interest to evaluate the synergy displayed by other combinations of currently available inhibitors of PI3K/mTOR and MEK-ERK pathways across a heterogeneous panel of UM cell lines and

then to assess their efficacy *in vivo*. We believe our approach using in vitro and *in vivo* models will help orient future innovative clinical trials in uveal melanoma patients.

5. Conclusions

We have established 7 UM cell lines from either patient surgical specimens or patient-derived xenografts (PDXs). This panel of cell lines has been fully characterized in terms of genetic alterations and recurrent mutations and recapitulates together with our previously described panel of PDXs (Laurent et al., 2013; Némati et al., 2010) the diversity of the UM genetic landscape. Moreover we have demonstrated in our UM cellular models the activation of mTOR pathway in the absence of significant AKT phosphorylation. Treatment with the mTOR inhibitor Everolimus resulted in the reduction of cell viability of all the studied UM cell lines and significantly delayed *in vivo* tumor growth of 4 independent UM PDXs. Although efficient therapeutic combinations need to be carefully evaluated, our data suggest that Everolimus could be considered as a therapeutic option for managing UM.

Grant support

This project is supported by French national cancer Institute (INCa).

Disclosure of potential conflicts of interest

No potential conflicts of interest were, disclosed.

Database linking

MM28, MM33, MP38, MP41, MP46, MP65, MM66 cell lines Affimetrix SNP Arrays 6.0 and Cytoscan HD Arrays are available at http://microarrays.curie.fr/publications/recherche_translationnelle/uveal_melanoma/.

Acknowledgments

The authors wish to thank Delphine Lequin, Julie Gayet, Sandrine Arrufat and Jordan Madic for technical help, Marika Pla, Isabelle Grandjean and colleagues for animal facilities support, Virginie Maire and the team of Thierry Dubois for useful technical advices, Olivier Lantz for helpful discussions, and Ronald Lebofsky for carefully reading the manuscript.

Appendix A. Supplementary data

Supplementary data related to this article can be found at http://dx.doi.org/10.1016/j.molonc.2014.06.004.

REFERENCES

Abdel-Rahman, M.H., Yang, Y., Zhou, X.-P., Craig, E.L., Davidorf, F.H., Eng, C., 2006. High frequency of submicroscopic hemizygous deletion is a major mechanism of loss of expression of PTEN in uveal melanoma. JCO 24, 288–295.

Babchia, N., Calipel, A., Mouriaux, F., Faussat, A.-M., Mascarelli, F., 2010. The PI3K/Akt and mTOR/P70S6K signaling pathways in human uveal melanoma cells: interaction with B-Raf/ERK. Invest. Ophthalmol. Vis. Sci. 51, 421–429.

Calipel, A., Lefevre, G., Pouponnot, C., Mouriaux, F., Eychène, A., Mascarelli, F., 2003. Mutation of B-Raf in human choroidal melanoma cells mediates cell proliferation and transformation through the MEK/ERK pathway. J. Biol. Chem. 278, 42409–42418.

Carvajal, R.D., Sosman, J.A., Quevedo, F., Milhem, M.M., Joshua, A.M., Kudchadkar, R.R., Linette, G.P., Gajewski, T., Lutzky, J., Lawson, D.H., Lao, C.D., Flynn, P.J., Albertini, M.R., Sato, T., Paucar, D., Panageas, K.S., Dickson, M.A., Wolchok, J.D., Chapman, P.B., Schwartz, D.K., 2013. Phase II study of selumetinib (sel) versus temozolomide (TMZ) in gnaq/Gna11 (Gq/11) mutant (mut) uveal melanoma (UM). J. Clin. Oncol. 31 (ASCO annual Meeting Abstracts).

Chen, P.W., Murray, T.G., Uno, T., Salgaller, M.L., Reddy, R., Ksander, B.R., 1997. Expression of MAGE genes in ocular melanoma during progression from primary to metastatic disease. Clin. Exp. Metastasis 15, 509–518.

Chou, T.-C., 2006. Theoretical basis, experimental design, and computerized simulation of synergism and antagonism in drug combination studies. Pharmacol. Rev. 58, 621–681.

Chou, T.-C., 2010. Drug combination studies and their synergy quantification using the Chou–Talalay method. Cancer Res. 70, 440–446.

Cohen, Y., Goldenberg-Cohen, N., Parrella, P., Chowers, I., Merbs, S.L., Pe'er, J., Sidransky, D., 2003. Lack of BRAF mutation in primary uveal melanoma. IOVS 44, 2876–2878.

Couturier, J., Saule, S., 2012. Genetic determinants of uveal melanoma. Dev. Ophthalmol. 49, 150–165.

Cruz, F., Rubin, B.P., Wilson, D., Town, A., Schroeder, A., Haley, A., Bainbridge, T., Heinrich, M.C., Corless, C.L., 2003. Absence of BRAF and NRAS mutations in uveal melanoma. Cancer Res. 63, 5761–5766.

Dangles-Marie, V., Pocard, M., Richon, S., Weiswald, L.-B., Assayag, F., Saulnier, P., Judde, J.-G., Janneau, J.-L., Auger, N., Validire, P., Dutrillaux, B., Praz, F., Bellet, D., Poupon, M.-F., 2007. Establishment of human colon cancer cell lines from fresh tumors versus xenografts: comparison of success rate and cell line features. Cancer Res. 67, 398–407.

De Waard-Siebinga, I., Blom, D.J., Griffioen, M., Schrier, P.I., Hoogendoorn, E., Beverstock, G., Danen, E.H., Jager, M.J., 1995. Establishment and characterization of an uveal-melanoma cell line. Int. J. Cancer 62, 155–161.

Dunavoelgyi, R., Dieckmann, K., Gleiss, A., Sacu, S., Kircher, K., Georgopoulos, M., Georg, D., Zehetmayer, M., Poetter, R., 2011. Local tumor control, visual acuity, and survival after hypofractionated stereotactic photon radiotherapy of choroidal melanoma in 212 patients treated between 1997 and 2007. Int. J. Radiat. Oncol. Biol. Phys. 81, 199–205.

Edmunds, S.C., Cree, I.A., Dí Nícolantonío, F., Hungerford, J.L., Hurren, J.S., Kelsell, D.P., 2003. Absence of BRAF gene mutations in uveal melanomas in contrast to cutaneous melanomas. Br. J. Cancer 88, 1403–1405.

El-Hashemite, N., Zhang, H., Henske, E.P., Kwiatkowski, D.J., 2003. Mutation in TSC2 and activation of mammalian target of rapamycin signalling pathway in renal angiomyolipoma. The Lancet 361, 1348–1349.

Furney, S.J., Pedersen, M., Gentien, D., Dumont, A.G., Rapinat, A., Desjardins, L., Turajlic, S., Piperno-Neumann, S., De la Grange, P., Roman-Roman, S., Stern, M.-H., Marais, R., 2013. SF3B1 mutations are associated with alternative splicing in uveal melanoma. Cancer Discov. 3, 1122–1129.

Gragoudas, E.S., Egan, K.M., Seddon, J.M., Glynn, R.J., Walsh, S.M., Finn, S.M., Munzenrider, J.E., Spar, M.D., 1991. Survival of patients with metastases from uveal melanoma. Ophthalmology 98, 383–390.

Griewank, K.G., Yu, X., Khalili, J., Sozen, M.M., Stempke-Hale, K., Bernatchez, C., Wardell, S., Bastian, B.C., Woodman, S.E., 2012. Genetic and molecular characterization of uveal melanoma cell lines. Pigment Cell Melanoma Res. 25, 182–187.

Harbour, J.W., 2012. The genetics of uveal melanoma: an emerging framework for targeted therapy. Pigment Cell Melanoma Res. 25, 171–181.

Harbour, J.W., Chen, R., 2013. The DecisionDx-UM gene expression profile test provides risk stratification and individualized patient care in uveal melanoma. PLoS Curr. 5.

Harbour, J.W., Onken, M.D., Roberson, E.D.O., Duan, S., Cao, L., Worley, L.A., Council, M.L., Matatall, K.A., Helms, C., Bowcock, A.M., 2010. Frequent mutation of BAP1 in metastasizing uveal melanomas. Science 330, 1410–1413.

Harbour, J.W., Roberson, E.D.O., Anbunathan, H., Onken, M.D., Worley, L.A., Bowcock, A.M., 2013. Recurrent mutations at codon 625 of the splicing factor SF3B1 in uveal melanoma. Nat. Genet. 45, 133–135.

Ho, A.L., Musi, E., Ambrosini, G., Nair, J.S., Deraje Vasudeva, S., De Stanchina, E., Schwartz, G.K., 2012. Impact of combined mTOR and MEK inhibition in uveal melanoma is driven by tumor genotype. PLoS One 7, e40439.

Keith, C.T., Borisy, A.A., Stockwell, B.R., 2005. Multicomponent therapeutics for networked systems. Nat. Rev. Drug Discov. 4, 71–78.

Khalili, J.S., Yu, X., Wang, J., Hayes, B.C., Davies, M.A., Lizee, G., Esmaeli, B., Woodman, S.E., 2012. Combination small molecule MEK and PI3K inhibition enhances uveal melanoma cell death in a mutant GNAQ- and GNA11-dependent manner. Clin. Cancer Res. 18, 4345–4355.

Kiliç, E., Brüggenwirth, H.T., Verbiest, M.M.P.J., Zwarthoff, E.C., Mooy, N.M., Luyten, G.P.M., De Klein, A., 2004. The RAS-BRAF kinase pathway is not involved in uveal melanoma. Melanoma Res. 14, 203–205.

Ksander, B.R., Rubsamen, P.E., Olsen, K.R., Cousins, S.W., Streilein, J.W., 1991. Studies of tumor-infiltrating lymphocytes from a human choroidal melanoma. Invest. Ophthalmol. Vis. Sci. 32, 3198–3208.

Laurent, C., Gentien, D., Piperno-Neumann, S., Némati, F., Nicolas, A., Tesson, B., Desjardins, L., Mariani, P., Rapinat, A., Sastre-Garau, X., Couturier, J., Hupé, P., De Koning, L., Dubois, T., Roman-Roman, S., Stern, M.-H., Barillot, E., Harbour, J.W., Saule, S., Decaudin, D., 2013. Patient-derived xenografts recapitulate molecular features of human uveal melanomas. Mol. Oncol. 7, 625–636.

Luyten, G.P., Naus, N.C., Mooy, C.M., Hagemeijer, A., Kan-Mitchell, J., Van Drunen, E., Vuzevski, V., De Jong, P.T., Luider, T.M., 1996. Establishment and characterization of primary and metastatic uveal melanoma cell lines. Int. J. Cancer 66, 380–387.

Mallone, S., De Vries, E., Guzzo, M., Midena, E., Verne, J., Coebergh, J.W., Marcos-Gragera, R., Ardanaz, E., Martinez, R., Chirlaque, M.D., Navarro, C., Virgili, G., 2012. Descriptive epidemiology of malignant mucosal and uveal melanomas and adnexal skin carcinomas in Europe. Eur. J. Cancer 48, 1167–1175.

Martin, M., Maßhöfer, L., Temming, P., Rahmann, S., Metz, C., Bornfeld, N., Van de Nes, J., Klein-Hitpass, L., Hinnebusch, A.G., Horsthemke, B., Lohmann, D.R., Zeschnigk, M., 2013. Exome sequencing identifies recurrent somatic mutations in EIF1AX and SF3B1 in uveal melanoma with disomy 3. Nat. Genet. 45, 933–936.

Marty, B., Maire, V., Gravier, E., Rigaill, G., Vincent-Salomon, A., Kappler, M., Lebigot, I., Djelti, F., Tourdès, A., Gestraud, P., Hupé, P., Barillot, E., Cruzalegui, F., Tucker, G.C., Stern, M.-H., Thiery, J.-P., Hickman, J.A., Dubois, T., 2008. Frequent PTEN genomic alterations and activated phosphatidylinositol 3-kinase pathway in basal-like breast cancer cells. Breast Cancer Res. 10, R101.

Mitsiades, N., Chew, S.A., He, B., Riechardt, A.I., Karadedou, T., Kotoula, V., Poulaki, V., 2011. Genotype-dependent sensitivity of uveal melanoma cell lines to inhibition of b-Raf, MEK, and Akt kinases: rationale for personalized therapy. Invest. Ophthalmol. Vis. Sci. 52, 7248–7255.

Némati, F., Sastre-Garau, X., Laurent, C., Couturier, J., Mariani, P., Desjardins, L., Piperno-Neumann, S., Lantz, O., Asselain, B., Plancher, C., Robert, D., Péguillet, I., Donnadieu, M.-H., Dahmani, A., Bessard, M.-A., Gentien, D., Reyes, C., Saule, S., Barillot, E., Roman-Roman, S., Decaudin, D., 2010. Establishment and characterization of a panel of human uveal melanoma xenografts derived from primary and/or metastatic tumors. Clin. Cancer Res. 16, 2352–2362.

Nyfeler, B., Chen, Y., Li, X., Pinzon-Ortiz, M., Wang, Z., Reddy, A., Pradhan, E., Das, R., Lehár, J., Schlegel, R., Finan, P.M., Cao, Z.A., Murphy, L.O., Huang, A., 2012. RAD001 enhances the potency of BEZ235 to inhibit mTOR signaling and tumor growth. PLoS One 7, e48548.

Onken, M.D., Worley, L.A., Ehlers, J.P., Harbour, J.W., 2004. Gene expression profiling in uveal melanoma reveals two molecular classes and predicts metastatic death. Cancer Res. 64, 7205–7209.

Pópulo, H., Soares, P., Faustino, A., Rocha, A.S., Silva, P., Azevedo, F., Lopes, J.M., 2011. mTOR pathway activation in cutaneous melanoma is associated with poorer prognosis characteristics. Pigment Cell Melanoma Res. 24, 254–257.

Pópulo, H., Soares, P., Rocha, A.S., Silva, P., Lopes, J.M., 2010. Evaluation of the mTOR pathway in ocular (uvea and conjunctiva) melanoma. Melanoma Res. 20, 107–117.

Rimoldi, D., Salvi, S., Liénard, D., Lejeune, F.J., Speiser, D., Zografos, L., Cerottini, J.-C., 2003. Lack of BRAF mutations in uveal melanoma. Cancer Res. 63, 5712–5715.

Saraiva, V.S., Caissie, A.L., Segal, L., Edelstein, C., Burnier Jr., M.N., 2005. Immunohistochemical expression of phospho-Akt in uveal melanoma. Melanoma Res. 15, 245–250.

Singh, A.D., Topham, A., 2003. Survival rates with uveal melanoma in the United States: 1973–1997. Ophthalmology 110, 962–965.

Singh, A.D., Turell, M.E., Topham, A.K., 2011. Uveal melanoma: trends in incidence, treatment, and survival. Ophthalmology 118, 1881–1885.

Straussman, R., Morikawa, T., Shee, K., Barzily-Rokni, M., Qian, Z.R., Du, J., Davis, A., Mongare, M.M., Gould, J., Frederick, D.T., Cooper, Z.A., Chapman, P.B., Solit, D.B., Ribas, A., Lo, R.S., Flaherty, K.T., Ogino, S., Wargo, J.A., Golub, T.R., 2012. Tumour micro-environment elicits innate resistance to RAF inhibitors through HGF secretion. Nature 487, 500–504.

Trolet, J., Hupé, P., Huon, I., Lebigot, I., Decraene, C., Delattre, O., Sastre-Garau, X., Saule, S., Thiéry, J.-P., Plancher, C., Asselain, B., Desjardins, L., Mariani, P., Piperno-Neumann, S., Barillot, E., Couturier, J., 2009. Genomic profiling and identification of high-risk uveal melanoma by array CGH analysis of primary tumors and liver metastases. Invest. Ophthalmol. Vis. Sci. 50, 2572–2580.

Tuefferd, M., De Bondt, A., Van Den Wyngaert, I., Talloen, W., Verbeke, T., Carvalho, B., Clevert, D.-A., Alifano, M.,

Raghavan, N., Amaratunga, D., Göhlmann, H., Broët, P., Camilleri-Broët, S., 2008. Genome-wide copy number alterations detection in fresh frozen and matched FFPE samples using SNP 6.0 arrays. Genes Chrom. Cancer 47, 957–964.

Van Raamsdonk, C.D., Bezrookove, V., Green, G., Bauer, J., Gaugler, L., O'Brien, J.M., Simpson, E.M., Barsh, G.S., Bastian, B.C., 2008. Frequent somatic mutations of GNAQ in uveal melanoma and blue naevi. Nature 457, 599–602.

Van Raamsdonk, C.D., Griewank, K.G., Crosby, M.B., Garrido, M.C., Vemula, S., Wiesner, T., Obenauf, A.C., Wackernagel, W., Green, G., Bouvier, N., Sozen, M.M., Baimukanova, G., Roy, R., Heguy, A., Dolgalev, I., Khanin, R., Busam, K., Speicher, M.R., O'Brien, J., Bastian, B.C., 2010. Mutations in GNA11 in uveal melanoma. N. Engl. J. Med. 363, 2191–2199.

Weber, A., Hengge, U.R., Urbanik, D., Markwart, A., Mirmohammadsaegh, A., Reichel, M.B., Wittekind, C., Wiedemann, P., Tannapfel, A., 2003. Absence of mutations of the BRAF gene and constitutive activation of extracellular-regulated kinase in malignant melanomas of the uvea. Lab. Invest 83, 1771–1776.

Weigelt, B., Warne, P.H., Downward, J., 2011. PIK3CA mutation, but not PTEN loss of function, determines the sensitivity of breast cancer cells to mTOR inhibitory drugs. Oncogene 30, 3222–3233.